DESIGNING AND PROCESSING OF POROUS Ti6Al4V CAGES FOR SPINAL SURGERY

A Thesis Submitted to the
Graduate School of Engineering and Sciences of Izmir Institute of
Technology in Partial Fulfillment of the
Requirements for the Degree of

MASTER OF SCIENCE

In Mechanical Engineering

by
Alpay HIZAL

August 2007
İZMİR

We approve the thesis of **Alpay HIZAL**

Date of Signature

....

17 August 2007

Prof.Dr. Mustafa GÜDEN
Supervisor
Department of Mechanical Engineering
Izmir Institute of Technology

....

17 August 2007

Assoc. Prof. Dr. Hasan YILDIZ
Department of Mechanical Engineering
Ege University

....

17 August 2007

Assist. Prof. Dr. Serhan ÖZDEMİR
Departmant of Mechanical Engineering
Izmir Institute of Technology

....

17 August 2007

Assoc. Prof. Dr. Metin TANOĞLU
Head of Department
Izmir Institute of Technology

....

Prof. Dr. M. Barış ÖZERDEM
Head of the Graduate School

ACKNOWLEDGEMENTS

ABSTRACT

DESIGNING AND PROCESSING OF POROUS
Ti6Al4V CAGES FOR SPINAL SURGERY

Ti6Al6V foam materials were prepared with spherical particles in range of 20-90μm. Average porosity under various compaction pressure (200 MPa, 400 MPa, 500MPa, 600MPa, 700MPa), sintering temperature (1000°C-1400°C) and time (4h-6h) was observed in the range of 52%-72%.

It was observed that sintered Ti6Al4V foam material can be potentially used for the spinal surgery. Furthermore, strength of the Ti6Al4V foam material in the porosity level of 40% is comparable with the human cortical bone.

And also 2^{2} Design of Experiment methods were used to investigate the major affective parameters during the processing of Ti6Al4V spinal cages. According to this investigation, sintering temperature, particle diameter and compaction pressure are the most affective parameters control the over all process of foam production.

In the design process, protection case also designed for the foam material to put them inside of it. The reason of producing protection case is that eliminating the particle loosing from the sharp edges of the Ti6Al4V foam material.

ÖZET

SPİNAL CERRAHİDE KULLANILMAK ÜZERE GÖZENEKLİ Ti6Al4V KAFESLERİN TASARLANMASI VE HAZIRLANMASI

Sinterlenmiş Ti6Al4V toz alaşım köpükler, %52-72 gözenek aralığında, küresel tozlar kullanılarak hazırlanmıştır. Gözenek oranını arttırmak için boşluk yapıcı madde kullanılmıştır. Küresel toz köpükler (200-700 MPa) basınçlarda soğuk preslenmiş ve 1200 °C – 1400 °C de 2, 4 ve 6 saat süresince sinterlenmiştir. Sinterlenmiş köpüklerin gözenek miktarları ve ortalama gözenek boyutları uygulanan presleme basıncı ve sinterleme sürelerine göre tespit edilmiştir.

Köpüklerin ortalama gözenek boyutları 94 ve 148 µm aralığında, kullanılan tozun ortalama tane boyutu ve presleme basıncına bağlı olarak değişim göstermiştir.

Sinterlenmiş köpüklerin mukavemetinin, süngersi kemiğin yerine geçmesi için yeterli olduğunu göstermiştir. Bunun yanında, %40 ve/veya daha düşük gözenek oranına sahip tabletlerin mukavemetlerinin insan kortikal kemiğinin mukavemetiyle kıyaslanabilir olduğu belirlenmiştir.

Ti6Al4V spinal kafeslerin üretim parametrelerinin etkileride bu çalışmada incelenmiş olup; araştırmalarda 2^2 deneysel dizayn yöntemi üretimde en etkili parametreleri ön görmek için kullanılmıştır. Bu method ışığında sinterleme sıcaklığı, basma basıncı ve kullanılan tanecik boyutu üretim üzerinde en etkili parametreler olduğu tespit edilmiştir.

Dizayn aşamasında Ti6Al4V spinal kafeslerin üzerine koruyucu gömlek tasarlanmıştır. Bu sayede malzemede keskin kenarlarda oluşması muhtemel tozlaşma (parçacık kopması) probleminin önüne geçilmiş olup; ekstra basma mukavemeti kazandırılmıştır.

TABLE OF CONTENTS

LIST OF FIGURES

LIST OF TABLES

CHAPTER 1

INTRODUCTION

Biocompatible materials are intended to interface with biological systems to evaluate, treat, augment or replace any tissue, organ or function of the body. Biomaterials are usually non-viable, but may also be viable.

Metals have a particular importance among the biomaterials since they have superior mechanical properties combined with relatively easy production routes and lower costs. Many metals, including even copper which is known as a toxic material for human body, have been used in biomedical applications since ancient times. Cobalt (Co) based alloys, stainless steels and titanium (Ti) and its alloys are three major metallic materials widely used in biomedical applications.

Ti and its alloys have been known to show good corrosion resistance and fatigue behavior and excellent biocompatibility to human body. These properties made Ti and its alloys one of the most important class of materials in orthopedic and dental implant applications. Similar to the most bulk metallic implant materials currently used in orthopedic applications, Ti and its alloys suffer from the problems of interfacial stability with host tissues and biomechanical mismatch of elastic modulus. These problems stem from weak bonding of implant to the adjacent bone and high elastic modulus of bulk metallic implants. Developments in tissue engineering have demonstrated that those problems can be solved using porous implant components based on biocompatible metallic materials, simply by providing better interaction with bone. This is partly due to higher degree of bone growth into porous surfaces and higher degree of body fluid transport through three-dimensional interconnected array of pores (Weiner and Wagner 1998), leading to improved implant fixation. Furthermore, relatively low elastic modulus of porous metals as compared with those of bulk metals is expected to reduce the extent of stress shielding, which causes the well-known implant loosening, and hence to prolong implant life-time (Pillar 1987).

Two methods of processing of Ti-based porous implant structures and/or coatings are currently used. The first process is based on the sintering of Ti and/or Ti6Al4V powder compacts preformed under pressure. Using this method, porous Ti and Ti6Al4V compacts potentially to be used in biomedical applications were previously

prepared successfully with 3-D inner connected open pores (Banhart 2001, Körner and Singer 2002). The method allows a direct near net-shape fabrication of porous implant components having elastic modulus comparable with that of natural bone and with a relatively homogeneous pore structure and low level of porosity (<40%). The pore size ranged between 50 and 200 µm, depending on the powder size and compaction pressure used (Banhart 2001 and Martin et al. 2000). It was further shown that the use of Ti6Al4V powder increased the strength of the compacts significantly as compared with pure Ti powder (Martin et al. 2000). The optimum pore size ranges required for the attachment and proliferation of new bone tissue and the transport of body fluids are however given between 200 and 500 µm (Marieb 1998). To reach the optimum pore size range, a space holder material having the particle size in the optimum pore size range for the bone tissue attachment is used in the powder compacts. It was further noted that for the preparation of highly porous foam parts, the particle size of metal powder should be smaller than the average particle size of space holder (Banhart 2001). A particle size smaller than 150 µm is normally considered to be sufficient for the homogeneous coating of 200-500 µm size space holder particles with Ti powder. Furthermore, the consolidation pressure used for the compaction of metal powder-space holder mixture must be high enough for the preparation of mechanically strong compacts that would retain their geometry throughout the foaming process. The compaction of Ti powder is usually conducted under a uniaxial pressure ranging between 100 and 200 MPa, while higher pressures, or a binder material, may be required for the compaction of the harder Ti6Al4V powder.

This experimental study was conducted to optimization of production parameters (compaction pressure, particle diameter, space holder percentage, sintering temperature and time) to produce stronger Ti6Al4V foams and designing appropriate form that can potentially be used in biomedical applications including human cortical bone replacement and spinal cages for spine surgery.

CHAPTER 2

LITERATURE REVIEW

2.1. Bone Structure and Formation Mechanism

2.1.1. Structure of Bone

Bones are organs composed of hard living tissue providing structural support to the body. It is a hard matrix of calcium salts deposited around protein fibers. Minerals make bone rigid and proteins (collagen) provide strength and elasticity (Marieb 1998 and Netter 1987)

The outer layer of bone is called Cortical bone. Eighty percent of skeletal bone mass is cortical bone. Cancellous bone (also called trabecular bone) is an inner spongy structure that resembles honeycomb, which accounts for 20% of bone mass (Netter 1987 and Tortora 1989). This spongy mesh–like bone is designed for strength similar to steel rods within a concrete structure. The structure of bone can be schematically illustrated as in Figure 2.1..
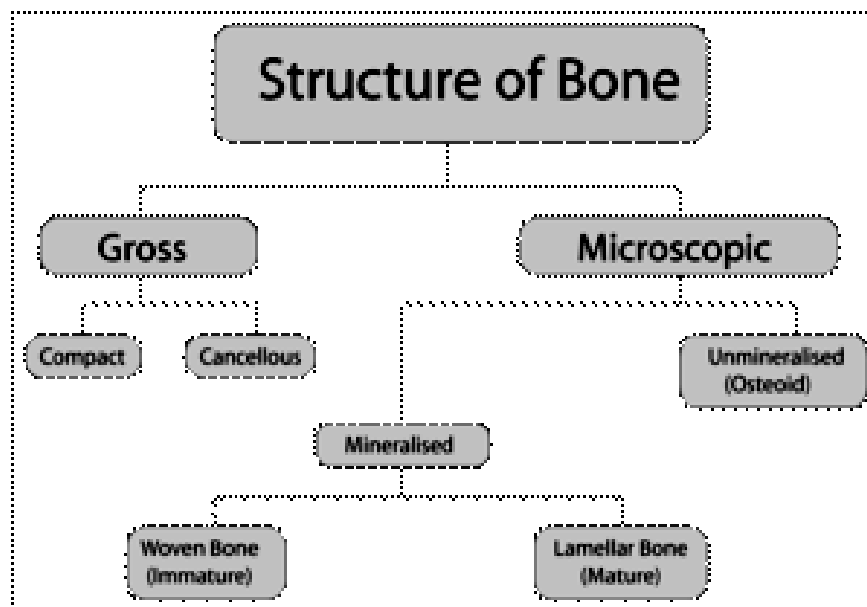
Figure 2.1.Structure of bone.
(Source: Marieb 1998 and Netter 1987)

2.1.2. Classification of Bone

The inner bone cavities contain bone marrow where red blood cells are produced.

The shape of bone is described as long, short, flat, or irregular (Figure 2.2.). They are further classified as Axial or Appendicular. Axial bones are protective. For example, spinal vertebrae act to protect the spinal cord (Whitfield and Willick 2000). Appendicular bones are the limbs. Although there are many shapes and sizes of skeletal bone, the bones that make up the spinal column are unique.
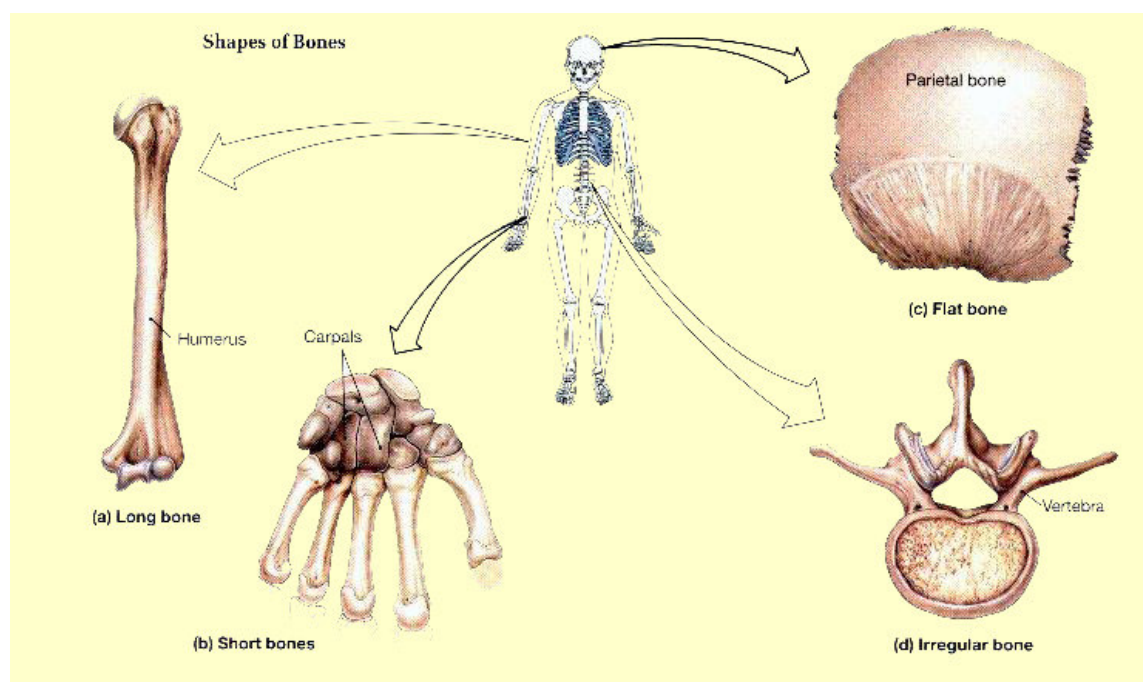
Figure 2.2.   Classification of bones according to its shape: long bones: They have a shaft and two ends; the shaft contains red or yellow bone marrow, this is why it is called "marrow-bone" in Hungarian, the flat bones: Sternum, scapula and different types of skull bones belong to this category and the short bones: wrist carpals belong here and irregular bones: vertebral bones. (Source: Whitfield and Willick 2000).

2.2. Bone Formation Mechanism

In an adult, bone engages in a continuous cycle of breaking down and rebuilding. Bone absorbing cells called Osteoclasts break bone down and discard worn cells. After a few weeks the osteoclasts disappear and Osteoblasts come to repair the

bone (Lemaire et al. 1997 and Enker and Steffee 1997). During the cycle calcium is deposited and withdrawn from the blood. The process of bone regeneration is shown in Figure 2.3..
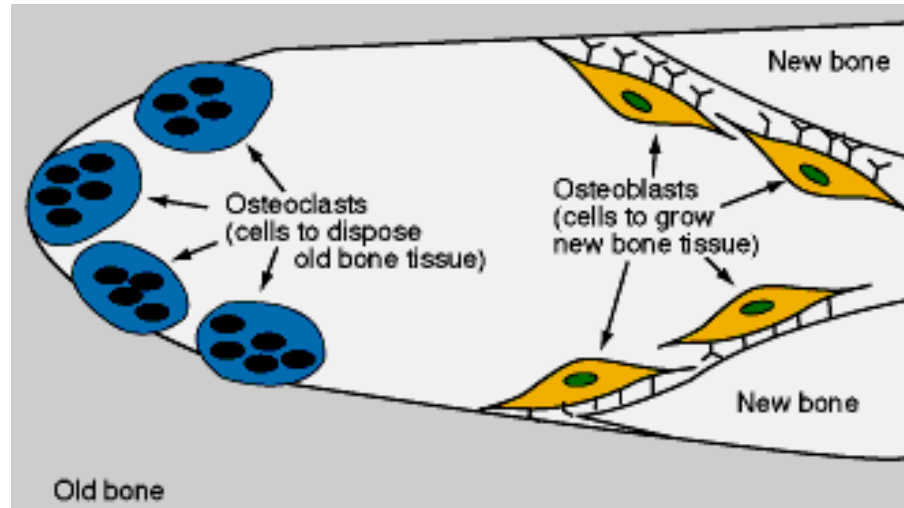
Figure 2.3. Bone regeneration.
(Source: Lemaire et al. 1997)

All the formation mechanism is illustrated in Figure 2.4. The PTH-activated receptors, PTHRI, on the osteoblasts stimulate the expression of FGF-2, which stimulates preosteoblast proliferation. PTHRI also stimulates the expression of IGF-I, which stimulates the expression of the Bcl-2 and Bcl-X_L proteins. These proteins prevent osteoblasts from initiating the suicidal apoptosis mechanism, thereby lengthening their working lives and increasing bone formation.

IGF-1 and FGF-2 stimulate the reversion of the lining cells into osteoblasts. The PTH-stimulated osteoblasts make PTH prohormone, PTHrP, which is processed into components that may also stimulate bone formation.

Parathyroid hormone helps to regulate calcium. Calcium is important because of the wide variety of effects that it has on the body. Whenever the plasma concentration of Ca^{++} begins to fall, the parathyroid glands are stimulated to secrete increase amounts of parathyroid hormone (PTH), which acts to raise the blood Ca^{++} back to normal levels. Parathyroid hormone helps to raise the blood Ca^{++} concentration primarily by stimulating the activity of osteoclasts to resorb bone. It also promotes the formation of 1,25-dihydroxyvitamin D_3 (Lemaire et al. 1997 and Enker and Steffee 1997).
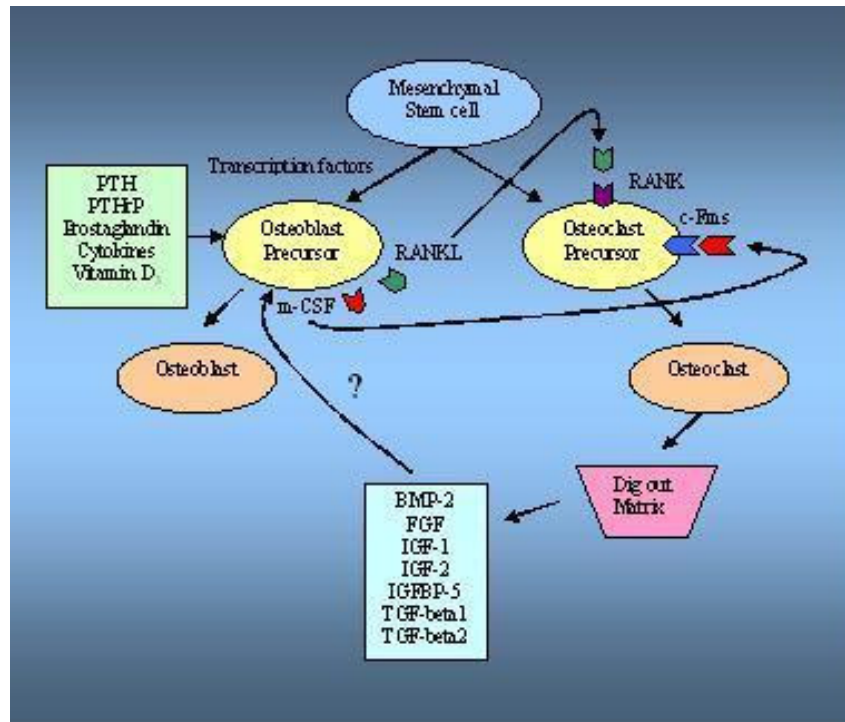
Figure 2.4. Bone formation diagram.
(Source: Enker and Steffee 1997)

2.3. Spinal Anatomy

The three main functions of the spine are to:

• Protect the spinal cord, nerve roots and several of the body's internal organs.

• Provide structural support and balance to maintain an upright posture.

• Enable flexible motion.

Typically, the spine is divided into four main regions: cervical, thoracic, lumbar and sacral. Each region is listed in Figure 2.5..
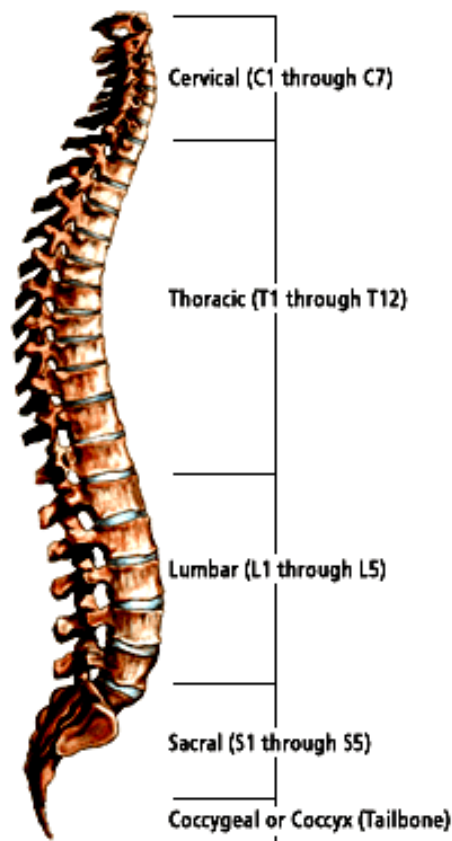
Figure 2.5. Regions of the spine.
(Source: Keller et al. 1989 and Box et al. 2005)

Cervical Spine, the neck region of the spine is known as the cervical spine. This region consists of seven vertebrae, which are abbreviated C1 through C7 (top to bottom). These vertebrae protect the brain stem and the spinal cord, support the skull, and allow for a wide range of head movement.

The first cervical vertebra (C1) is called the Atlas. The Atlas is ring-shaped and it supports the skull. C2 is called the Axis. It is circular in shape with a blunt peg-like structure (called the Odontoid Process or "dens") that projects upward into the ring of the Atlas. Together, the Atlas and Axis enable the head to rotate and turn. The other cervical vertebrae (C3 through C7) are shaped like boxes with small spinous processes (finger-like projections) that extend from the back of the vertebrae.

Thoracic Spine, Beneath the last cervical vertebra are the 12 vertebrae of the Thoracic Spine. These are abbreviated T1 through T12 (top to bottom). T1 is the smallest and T12 is the largest thoracic vertebra. The thoracic vertebra are larger than the cervical bones and have longer spinous processes.

In addition to longer spinous processes, rib attachments add to the thoracic spine's strength. These structures make the thoracic spine more stable than the cervical or lumbar regions. In addition, the rib cage and ligament systems limit the thoracic spine's range of motion and protect many vital organs (Keller et al. 1989 and Box et al. 2005).

Lumbar Spine, the Lumbar Spine has 5 vertebrae abbreviated L1 through L5 (largest). The size and shape of each lumbar vertebra is designed to carry most of the body's weight. Each structural element of a lumbar vertebra is bigger, wider and broader than similar components in the cervical and thoracic regions.

The lumbar spine has more range of motion than the thoracic spine, but less than the cervical spine. The lumbar facet joints allow for significant flexion and extension movement but limit rotation (Keller et al. 1989 and Box et al. 2005).

Sacral Spine, the Sacrum is located behind the pelvis. Five bones (abbreviated S1 through S5) fused into a triangular shape, form the sacrum. The sacrum fits between the two hipbones connecting the spine to the pelvis. The last lumbar vertebra (L5) articulates (moves) with the sacrum. Immediately below the sacrum are five additional bones, fused together to form the Coccyx (tailbone).

The Pelvis and the Skull, although not typically viewed as part of the spine, the pelvis and the skull are anatomic structures that closely inter-relate with the spine, and have a significant impact on the patient's balance.

Spinal Planes, to help further understand and describe the anatomy, spine specialists often refer to specific body planes. A body plane is an imaginary flat, two-dimensional surface that is used to define a particular area of anatomy.

2.3.1. Vertebral Structure

All vertebrae consist of the same basic elements, with the exception of the first two cervical vertebrae.
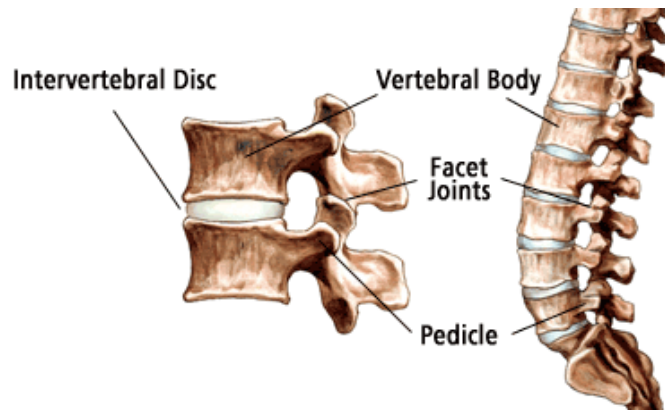
Figure 2.6. Vertebral structure.
(Source: Keller et al. 1989 and Box et al. 2005)

The outer shell of a vertebra is made of cortical bone. This type of bone is dense, solid and strong. Inside each vertebra is cancellous bone, which is weaker than cortical bone and consists of loosely knit structures that look somewhat like a honeycomb. Bone marrow, which forms red blood cells and some types of white blood cells, is found within the cavities of cancellous bone (Frank and Kennet 1963).

Vertebrae consist of the following common elements (Figure 2.6.):

• Verterbral Body: The largest part of a vertebra. If looked at from above it generally has a somewhat oval shape. When looked at from the side, the vertebral body is shaped like an hourglass, being thicker at the ends and thinner in the middle. The body is covered with strong cortical bone, with cancellous bone within.

• Pedicles: These are two short processes, made of strong cortical bone, that protrude from the back of the vertebral body.

• Laminae: Two relatively flat plates of bone that extend from the pedicles on either side and join in the midline.

• Processes: There are three types of processes: articular, transverse and spinous. The processes serve as connection points for ligaments and tendons.

2.4. Design of Experiment Methods

Design of Experiment (DoE) is a structured, organized method that is used to determine the relationship between the different factors (X) affecting a process and the output of that process (Y). DoE involves designing a set of ten to twenty experiments, in which all relevant factors are varied systematically. When the results of these

experiments are analyzed, they help to identify optimal conditions, the factors that most influence the results, and those that do not (Ronald 1926) DoE methods require well-structured data matrices. When applied to a well-structured matrix, analysis of variance delivers accurate results, even when the matrix that is analyzed is quite small.

Experimental design is a strategy to gather empirical knowledge, i.e. knowledge based on the analysis of experimental data and not on theoretical models. It can be applied whenever you intend to investigate a phenomenon in order to gain understanding or improve performance. Building a design means, carefully choosing a small number of experiments that are to be performed under controlled conditions (Ronald 1926). There are four interrelated steps in building a design:

1. Define an objective to the investigation, e.g. better understand or sort out important variables or find optimum.

2. Define the variables that will be controlled during the experiment (design variables), and their levels or ranges of variation.

3. Define the variables that will be measured to describe the outcome of the experimental runs (response variables), and examine their precision.

4. Among the available standard designs, choose the one that is compatible with the objective, number of design variables and precision of measurements, and has a reasonable cost.

Standard designs are well-known classes of experimental designs. They can be generated automatically as soon as you have decided on the objective, the number and nature of design variables, the nature of the responses and the number of experimental runs you can afford. Generating such a design will provide you with a list of all experiments you must perform, to gather enough information for your purposes.

DoE is widely used in research and development, where a large proportion of the resources go towards solving optimization problems. The key to minimizing optimization costs is to conduct as few experiments as possible. DoE requires only a small set of experiments and thus helps to reduce costs (Ronald 1926 and Desrosières 2004).

2.4.1. $^{(k-p)}$ Fractional Factorial Designs at 2 Levels

In many cases, it is sufficient to consider the factors affecting the production process at three levels. For example, the temperature for a sintering process may either

be set a little higher or a little lower, the amount of compaction pressure in a manufacturing process can either be slightly increased or decreased, etc. The experimenter would like to determine whether any of these changes affect the results of the production process. The most intuitive approach to study those factors would be to vary the factors of interest in a full factorial design, that is, to try all possible combinations of settings (Desrosières 2004 and Hacking 1990). This would work fine, except that the number of necessary runs in the experiment (observations) will increase geometrically. if you want to study 7 factors, the necessary number of runs in the experiment would be $2^7 = 128$. To study 10 factors you would need $2^{10} = 1,024$ runs in the experiment. Because each run may require time-consuming and costly setting and resetting of machinery, it is often not feasible to require that many different production runs for the experiment. In these conditions, *fractional factorials* are used that "sacrifice" interaction effects so that main effects may still be computed correctly.

In our experiments, compaction pressure, sintering temperature, used Ti6Al4V particle size, sintering time, volumetric ratio between Ti6Al4V particles versus Ammonium which was used as a space holder are design factors.

2.5. Design Methodology

To be able to manufacture a spinal cage by means of optimum strength, biocompatibility, and suitable form for target market, six design steps were used. Each design step is detailed with various considerations that are important in creating high quality products.

The design of complete product includes the following 6 steps:
1. Creation of product specification
2. Gathering data
3. Recognizing design constrains
4. Design prototypes and test
5. Monitoring the performance
6. Manufacturing the product

2.5.1. Creation of Product Specification

A detailed specification for the product serves as the guide for production method which should have to be used.

It is extremely important to create a complete product specification to avoid potential delays that can occur later on in product development.

A detailed product specification should contain the following information:

• An outline of the product concept

• An exact description of what the product does

• An exact description of what the product interacts with

The outline of the product is the most important part of the development of new material and describe as basically what the problem is. In our case the main problem is that patient has disabilities by means of restriction in body movement, apoplexy and in a very good chance drug addiction to prevent heavy aches which are occurred because of the vertebral diseases. Vertebral diseases will be considered under another chapter later.

The product eliminates the bone graft usage which is still using in the surgical operations because of porous structure. Furthermore structural characteristic of this foam material allows bone in growth inside through the material so the product never moves in its cavity which is known as implant loosing. Because the product interacts with the bone, elastic modulus of this material is comparable with the human cortical bone.

2.5.2. Gathering Data

After describing the full product specification in detail, the second step to design a new material is gathering data. There are some common methods for gathering data. Common methods are as follows:

• Interviewing

• Observation

• Concept Mapping

Interviewing is the most widely used technique in requirements engineering (Stigler 1990 and Lindley 1985)

Analysts interview future users of the system individually to find out

- what the present system does and
- what changes are needed.

The information gathered during the interviews enables the analysts to design a new system that will eliminate the problems of the current one. An interview is a systematic attempt to collect information from a person (Siddall 1982 and Avriel 1973).

Interviewing is an important skill for systems analysts because success depends on an ability to identify:

- Factors that influence the operations of systems, and
- The elements (documents, procedures, policies, etc.) that make up systems. Without accurate and complete information:
- The new system would probably not contain the necessary features to meet the needs of the organization
- Poorly performed interviews can affect the attitudes of the users and have a negative effect on the entire project effort.

2.5.3. Design Constraints

The following sections detail the design constraints that have been discussed in product specification part. The following requests need to be taken into account when considering the overall design of spinal cage manufacturing:

- Functional Constraints
- The product should be modular, with the possibility to accept some kind of dimensional changes in vertebra between different sex and age group
- The product should be capable of providing easy in use during the surgical operation
- Forces involved- loading direction, magnitude, load, impact
- Material- biomaterial which is suitable to use in human body
- Safety Requirements

- Operational- direct, indirect, hazard elimination
- Environmental-there is no observed environmental effect like air, sea etc on spinal cages.
- Quality Constraints
- Standards- Ti6Al4V spherical powders are purchased with the standard of ASTM F-1580

Reliability-design life, failure, statistics

2.5.4. Design Prototypes and Test

After the product is properly defined, a prototype can be built. A functioning prototype is important for ensuring that the product will work as envisioned. There is often some fine-tuning required after a prototype is built and tested (Rothman 1982 and Weinstein 1992). The amount of time needed to revise a product depends on the type of change required. Small changes to the product's application flow can usually be made relatively quickly.

2.5.5. Monitoring the Performance

Actually this step is in interaction with prototype design. After collecting the test data of the first prototype, results are used for some fine-tuning which is called as feedback process. Monitoring the performance is the step applied after data collection from prototype testing.

2.6. Vertebral Diseases and Spinal Surgery

In this chapter common types of vertebral diseases and surgical techniques used for the spinal surgery will be explained in detail.

2.6.1. Vertebral Diseases

There are 5 main disc problems the orthopedists are faced with. The reason of designing Ti6Al4V spinal cages is treatment of a fractured (broken) vertebra, correction of deformity (spinal curves or slippages), elimination of pain from painful motion, treatment of instability, and treatment of some cervical disc herniations. In the Figure 2.7., these 5 main types of problem are illustrated clearly

There are 5 main disc problems the orthopedists are faced with. The reason of designing Ti6Al4V spinal cages is treatment of a fractured (broken) vertebra, correction of deformity (spinal curves or slippages), elimination
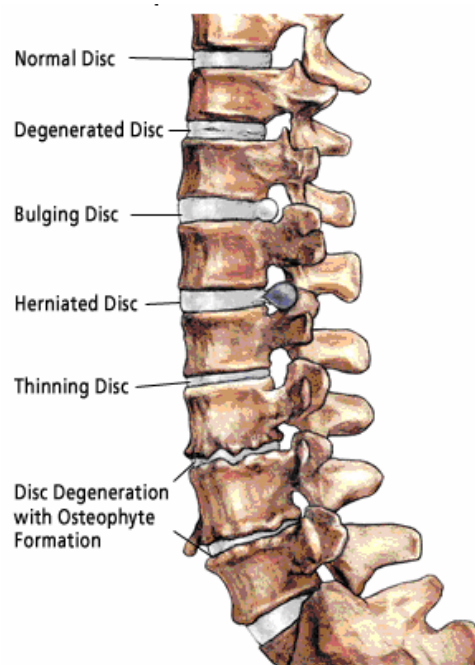
Figure 2.7. Examples of Disc problems.
(Source: Rothman 1982 and Weinstein 1992)

2.6.1.1. Disc Degeneration

Degenerative disc disease refers to a syndrome in which a compromised disc causes low back pain. Lumbar degenerative disc disease usually starts with a torsional (twisting) injury to the lower back, such as when a person rotates to put something on a shelf or swing a golf club. However, the pain is also frequently caused by simple wear and tear on the spine (Crock H.V. 1986 and Kääpä et al. 1994).

Unfortunately, as we age, our intervertebral discs lose their flexibility, elasticity, and shock absorbing characteristics. The ligaments that surround the disc called the annulus fibrosis, become brittle and they are more easily torn. In Figure 2.8. the soft gel-like center of the disc, called the nucleus pulposus, starts to dry out and shrink. The combination of damage to the intervertebral discs, the development of bone spurs, and a gradual thickening of the ligaments that support the spine can all contribute to degenerative arthritis of the lumbar spine (Crock 1986 and Kääpä et al. 1994).
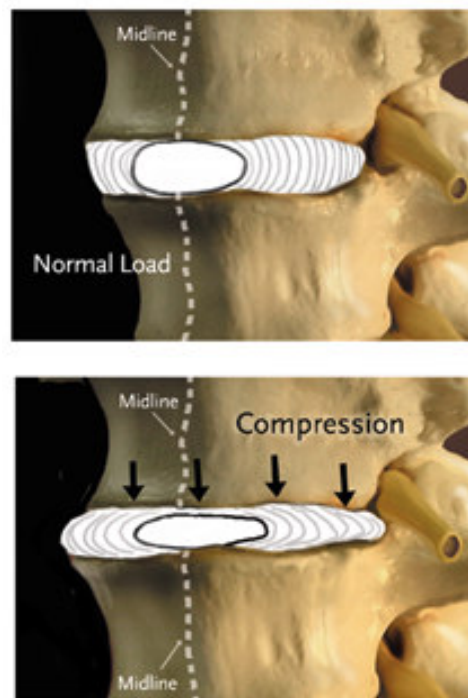
Figure 2.8. Normal and compressive loads.
(Source: Rothman 1982 and Weinstein 1992).

Despite its rather dramatic label, degenerative disc disease is fairly common, and it is estimated that at least 30% of people aged 30-50 years old will have some degree of disc space degeneration (Kääpä et al. 1994).

2.6.1.2. Disc Bulging

A bulging disk is an intervertebral disk that is extending beyond its normal boundary. A bulging disk causes pain if it bulges onto a nerve. This will depend upon how far it is bulging and in which direction. Bulging and herniated disks cause pain

because the soft material flows out, usually onto nerves. The nerves respond by sending pain signals (Pearce R.H et al. 1987 and Crock 1986).

2.6.1.3. Herniated Disc

A herniated disc is a disc that extrudes into the spinal canal. It is also referred to as a bulging disc, ruptured disc or slipped disc. As a disc degenerates, it can herniated (the inner core extrudes) back into the spinal canal, as shown in the Figure 2.9.. The light blue oval area is the disc and it is bulging into the spinal canal on the lower right side of the disc. In the lumbar area, this can cause pain to radiate all the way down the patient's leg to the foot. In the area of the cervical spine, the pain would radiate from the neck down the arm to the fingers.

Figure 2.9. Herniated Disc.
(Source: Pearce, R.H et al. 1987 and Crock 1986)

Approximately 90% of disc herniations will occur at L4- L5 (lumbar segments 4 and 5) or L5- S1 (lumbar segment 5 and sacral segment1), which causes pain in the L5 nerve or S1 nerve, respectively (Vernon–Roberts and Pirie 1977).

As you grow older, your discs become flatter -- less cushiony. If a disc becomes too weak, the outer part (annulus) may tear. The inside part of the disc pushes through the tear and presses on the nerves beside it. Herniated discs are most common in people in their 30's and 40's. The treatment is generally open surgery.

2.6.2. Spinal Surgery

Current prosthetic devices have been constructed based on the utilization of one of the following primary properties: hydraulic, elastic, mechanical, and composite. There are several types of prosthetic devices used in the surgery. In the following 6 section, spinal prosthetic devices will be introduced by means of advantages and disadvantages they have got.

2.6.2.1. Prosthetic Disc Nucleus (PDN)

Hydrogel disc replacements primarily have hydraulic properties. Hydrogel prostheses are used to replace the nucleus while retaining the annulus fibrosis. One potential advantage is that such a prosthesis may have the capability of percutaneous placement (Vernon–Roberts and Pirie 1977 and Ray et al. 1999) . The PDN implant is a nucleus replacement which consists of a hydrogel core constrained in a woven polyethylene jacket (Figure 2.10.).
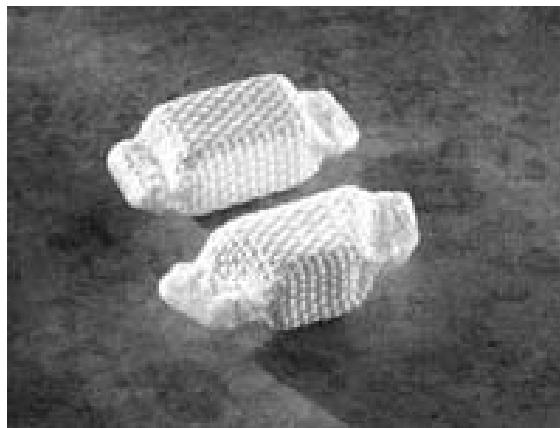

Figure 2.10. Prosthetic Disc Nucleus.
(Source: Raymedica, Inc., Bloomington, MN)

The pellet–shaped hydrogel core is compressed and dehydrated to minimize its size prior to placement. Upon implantation, the hydrogel immediately begins to absorb fluid and expand. The tightly woven ultrahigh molecular weight polyethylene (UHMWPE) allows fluid to pass through to the hydrogel. This flexible but inelastic jacket permits the hydrogel core to deform and reform in response to changes in

compressive forces yet constrains horizontal and vertical expansion upon hydration. Although most hydration takes place in the first 24 hours after implant, it takes approximately 4–5 days for the hydrogel to reach maximum expansion. Placement of two PDN implants within the disc space provides the lift that is necessary to restore and maintain disc space height. This device has been extensively assessed with mechanical and in vitro testing, and the results have been good (Schönmayr et al. 1993 and Enker et al. 1999)

Schönmayr et al. reported on 10 patients treated with the PDN with a minimum of 2 years follow–up (Enker et al. 1999). Significant improvement was seen in both the Prolo and Oswestry scores, and segmental motion was preserved. Overall, 8 patients were considered to have an excellent result. Migration of the implant was noted in 3 patients, but only 1 required reoperation. One patient, a professional golfer, responded favorably for 4 months until his pain returned. He had marked degeneration of his facets, and his pain was relieved by facet injections. He underwent a fusion procedure and since has done well.

2.6.2.2. Acroflex Disc

Two elastic type disc prostheses are the Acroflex prosthesis proposed by Steffee and the thermoplastic composite of Lee (Enker and Steffee 1997 and Deiter M.P. 1988). The first Acroflex disc consisted of a hexane based polyolefin rubber core vulcanized to two titanium endplates. The endplates had 7 mm posts for immediate fixation and were coated with sintered 250 micron titanium beads on each surface to provide an increased surface area for bony ingrowth and adhesion of the rubber. The disc was manufactured in several sizes and underwent extensive fatigue testing prior to implantation. Only 6 patients were implanted before the clinical trial was stopped due to a report that 2–mercaptobenzothiazole, a chemical used in the vulcanization process of the rubber core, was possibly carcinogenic in rats (Kostuik 1997). The 6 patients were evaluated after a minimum of 3 years, at which time the results were graded as follows: 2 excellent, 1 good, 1 fair, and 2 poor (Lee et al. 1991). One of the protheses in a patient with a poor result developed a tear in the rubber at the junction of vulcanization. The second generation Acroflex–100 consists of an HP–100 silicone elastomer core bonded to two titanium endplates (Figure 2.11.).

Figure 2.11. Acroflex Disc.
(Source: DePuy Acromed, Raynham, MA)

In 1993 the FDA approved 13 additional patients for implantation (Hedman et al. 1992). The results of this study have not yet been published. Lee et al. have published a report on the development of two different disc prostheses created in a manner to simulate the anisotropic properties of the normal intervertebral disc (Enker and Steffee 1997).

2.6.2.3. Articulating Disc

Several articulating pivot or ball type disc prostheses have been developed for the lumbar spine. Hedman and Kostuik developed a set of cobalt–chromium–molybdenum alloy hinged plates with an interposed spring (Marnay 1991). These devices have been tested in sheep. At 3 and 6 months post–implantation there was no inflammatory reaction noted and none of the prostheses migrated. Two of the three 6–month implants had significant bony ingrowth. It is not clear whether motion was preserved across the operated segments (Link and Link 1999). Dr. Thierry Marnay of France developed an articulating disc prosthesis with a polyethylene core (Aesculap AG & Co. KG., Tuttlingen, Germany). The metal endplates have two vertical wings and the surfaces which contact the endplates are plasma–sprayed with titanium. Good to excellent results were reported in the majority of patients receiving this implant (Griffith et al. 1994).

.

2.6.2.4. Charité Disc

The most widely implanted disc to date is the Link SB Charité disc (Waldemar Link GmbH & Co, Hamburg, Germany). Currently more than 2000 of these lumbar intervertebral prostheses have been implanted worldwide (Lemaire 1997). The Charité III consists of a biconvex ultra high molecular weight polyethylene (UHMWPE) spacer. There is a radiopaque ring around the spacer for x–ray localization. The spacers are available in different sizes. This core spacer interfaces with two separate endplates. The endplates are made of casted cobalt–chromium–molybdenum alloy, each with three ventral and dorsal teeth. The endplates are coated with titanium and hydroxyapatite to promote bone bonding (Figure 2.12.).

Figure 2.12. CHARITÉ™ Artificial Disc
(Source: DePuy Spine, Inc.).

The Food and Drug Administration (FDA) has approved the CHARITÉ™ Artificial Disc (DePuy Spine, Inc. of Raynham, MA) for use in treating pain associated with degenerative disc disease. The device was approved for use at one level in the lumbar spine (from L4-S1) for patients who have had no relief from low back pain after at least six months of non-surgical treatment.

Although there is great concern regarding wear debris in hip prostheses in which UHMWPE articulates with metal, this does not appear to occur in the Charité III. This prosthesis has been implanted in over a thousand European patients with relatively good results. In 1994 Griffith et al. reported the results in 93 patients with 1–year follow–up (Lemaire et al. 1997). Significant improvements in pain, walking distance, and mobility were noted. 6.5% of patients experienced a device failure, dislocation, or migration. There

were 3 ring deformations, and 3 patients required reoperation. Lemaire et al. described the results of implantation of the SB Charité III disc in 105 patients with a mean of 51 months of follow–up (David 1999). There was no displacement of any of the implants, but 3 settled. The failures were felt to be secondary to facet pain. It was described that a cohort of 85 patients reviewed after a minimum of at least 5 years post–implantation of the Charité prosthesis (Cummins et al. 1998). 97% of the patients were available for follow–up. 68% had good or better results. 14 patients reported the result as poor. Eleven of these patients underwent secondary arthrodesis at the prosthesis level.

2.6.2.5. Bristol Disc

There have been several reports on results from a cervical disc prosthesis which was originally developed in Bristol, England. This device was designed by Cummins (Gibson and Ashby 1997). The original design has been modified. The second generation of the Cummins disc is a ball and socket type device constructed of stainless steel. It is secured to the vertebral bodies with screws. Cummins et al. described 20 patients who were followed for an average of 2.4 years. Patients with radiculopathy improved, and those with myelopathy either improved or were stabilized. Of this group, only 3 experienced continued axial pain. Two screws broke, and there were two partial screw back–outs. These did not require removal of the implant. One joint was removed because it was "loose." The failure was due to a manufacturing error. At the time of removal, the joint was firmly imbedded in the bone and was covered by a smooth scar anteriorly. Detailed examination revealed that the ball and socket fit was asymmetric. It is important to note that the surrounding tissues did not contain any significant wear debris. Joint motion was preserved in all but 2 patients (Figure 2.13.).
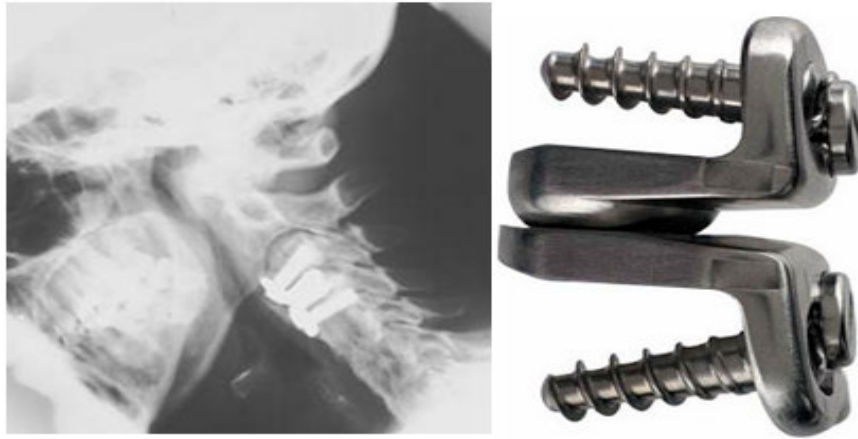
Figure 2.13. Bristol Disc.
(Source: Gibson and Ashby 1997)

Both of these patients had implants at the C6–7 level which were so large that the facets were completely separated. This size mismatch was felt to be the reason motion was not maintained. Subsidence did not occur. This disc prosthesis is currently being evaluated in additional clinical studies in Europe and Australia.

2.6.2.6. Brayn Cervical Disc

The Bryan Cervical Disc System (Spinal Dynamics Corporation, Seattle) is designed based on a proprietary, low friction, wear resistant, elastic nucleus. This nucleus is located between and articulates with anatomically shaped titanium plates (shells) that are fitted to the vertebral body endplates (Figure 2.14.).

Figure 2.14. Bryan cervical disc.
(Source: Spinal Dynamics Corporation)

The shells are covered with a rough porous coating. A flexible membrane that surrounds the articulation forms a sealed space containing a lubricant to reduce friction and prevent migration of any wear debris that may be generated. It also serves to prevent the intrusion of connective tissue. The implant allows for normal range of motion in flexion/extension, lateral bending, axial rotation, and translation. The implant is manufactured in five sizes ranging from 14 mm to 18 mm in diameter. 52 devices were implanted in 51 patients by 8 surgeons in 6 centers in Belgium, France, Sweden, Germany, and Italy. There were no serious operative or postoperative complications. Twenty–six of the patients have been followed for 6 months, and complete clinical and radiographic data is available on 23 patients. 92% of the patients were classified as excellent or good outcomes at last follow–up. Flexion/extension motion was preserved in all patients, and there was no significant subsidence or migration of the devices.

2.6.3. Spinal Fusion

Ti6Al4V foam cages were designed to use in spinal fusion operations. Because the implant materials used for spinal fusion have many advantages than their competitive, the main design criteria was chosen as the material should has to be developed for spinal fusion.

2.6.3.1. What is Spinal Fusion?

The spine is made up of a series of bones called "vertebrae"; between each vertebra are strong connective tissues which hold one vertebra to the next, and acts as a cushion between the vertebrae. The disc allows for movements of the vertebrae and lets people bend and rotate their neck and back. The type and degree of motion varies between the different levels of the spine: cervical (neck), thoracic (chest) or lumbar (low back). The cervical spine is a highly mobile region that permits movement in all directions. The thoracic spine is much more rigid due to the presence of ribs and is designed to protect the heart and lungs. The lumbar spine allows mostly forward and backward bending movements (flexion and extension).

Fusion is a surgical technique in which one or more of the vertebrae of the spine are united together (fused) so that motion no longer occurs between them. The concept

of fusion is similar to that of welding in industry. Spinal fusion surgery, however, does not weld the vertebrae during surgery. Rather, bone grafts are placed around the spine during surgery. The body then heals the grafts over several months - similar to healing a fracture - which joins, or "welds," the vertebra together (Cummins et al. 1998, David 1999 and Elbir et al. 2003). On the other hand, Ti6Al4V foamy spinal cages do not need bone graft because of its structural characteristic. Foam structure allows bone ingrowths inside through the material; so bone graft usage need during the surgery no more design disadvantages for our design.

2.6.3.2. When is Spinal Fusion Needed?

Cervical disc herniations that require surgery usually need not only removal of the herniated disc (discectomy), but also fusion. With this procedure, the disc is removed through an incision in the front of the neck (anteriorly) and a small piece of bone is inserted in place of the disc. Although disc removal is commonly combined with fusion in the neck, this is not generally true in the low back (lumbar spine) (Cummins et al. 1998, David 1999 and Elbir et al. 2003).

Spinal fusion is sometimes considered in the treatment of a painful spinal condition without clear instability. A major obstacle to the successful treatment of spine pain by fusion is the difficulty in accurately identifying the source of a patient's pain. The theory is that pain can originate from painful spinal motion, and fusing the vertebrae together to eliminate the motion will get rid of the pain.

2.6.3.3. How is Fusion Done?

There are many surgical approaches and methods to fuse the spine, and they all involve placement of a bone graft between the vertebrae. The spine may be approached and the graft placed either from the back (posterior approach), from the front (anterior approach) or by a combination of both. In the neck, the anterior approach is more common; lumbar and thoracic fusion is usually performed posteriorly.

The ultimate goal of fusion is to obtain a solid union between two or more vertebrae. Fusion may or may not involve use of supplemental hardware (instrumentation) such as plates, screws and cages. Instrumentation is sometimes used

to correct a deformity, but usually is just used as an internal splint to hold the vertebrae together to while the bone grafts heal.

Whether or not hardware is used, it is important that bone or bone substitutes be used to get the vertebrae to fuse together. The bone may be taken either from another bone in the patient (autograft) or from a bone bank (allograft). Fusion using bone taken from the patient has a long history of use and results in predictable healing. Autograft is currently the "gold standard" source of bone for a fusion. Allograft (bone bank) bone may be used as an alternative to the patient's own bone. Although healing and fusion is not as predictable as with the patient's own bone, allograft does not require a separate incision to take the patient's own bone for grafting, and therefore is associated with less pain. Smoking, medications you are taking for other conditions, and your overall health can affect the rate of healing and fusion, too.

Currently, there is promising research being done involving the use of synthetic bone as a substitute for either autograft or allograft. It is likely that synthetic bone substitutes will eventually replace the routine use of autograft or allograft bone.

With some of the newer "minimally invasive" surgical techniques currently available, fusion may sometimes be done through smaller incisions. The indications for minimally invasive surgery (MIS) are identical to those for traditional large incision surgery; however, it is important to realize that a smaller incision does not necessarily mean less risk involved in the surgery (Lemaire et al. 1997 and David 1999)

2.6.3.4. How Long Will It Take To Recover?

The immediate discomfort following spinal fusion is generally greater than with other types of spinal surgeries. Fortunately, there are excellent methods of postoperative pain control available, including oral pain medications and intravenous injections. Another option is a patient-controlled postoperative pain control pump. With this technique, the patient presses a button that delivers a predetermined amount of narcotic pain medication through an intravenous line. This device is frequently used for the first few days following surgery.

Recovery following fusion surgery is generally longer than for other types of spinal surgery. Patients generally stay in the hospital for three or four days, but a longer stay after more extensive surgery is not uncommon (Deiter 1988). A short stay in a

rehabilitation unit after release from the hospital is often recommended for patients who had extensive surgery, or for elderly or debilitated patients.

It also takes longer to return to a normal active lifestyle after spinal fusion than many other types of surgery. This is because you must wait until your surgeon sees evidence of bone healing. The fusion process varies in each patient as the body heals and incorporates the bone graft to solidly fuse the vertebrae together. The healing process after fusion surgery is very similar to that after a bone fracture. In general, the earliest evidence of bone healing is not apparent on X-ray until at least six weeks following surgery. During this time, the patient's activity is generally restricted. Substantial bone healing does not usually take place until three or four months after surgery (Lemaire et al. 1997). At that time activities may be increased, although continued evidence of bone healing and remodeling may continue for up to a year after surgery.

The length of time required you must be off of work will depend upon both the type of surgery and the kind of job you have. It can vary anywhere from approximately 4-6 weeks for a single level fusion in a young, healthy patient with a sedentary job to as much as 4-6 months for more extensive surgery in an older patient with a more physically demanding occupation.

In addition to some restrictions in activity, a brace is sometimes used for the early post-operative period. There are many types of braces that might be used. Some are very restrictive and are designed to severely limit motion, while others are intended mainly for comfort and to provide some support (Lemaire et al. 1997 and Watkins 1987). The decision to use a brace or not, and the optimal type of brace, depends upon your surgeon's preference and other factors related to the type of surgery.

Following spinal fusion surgery, a postoperative rehabilitation program may be recommended by your surgeon. The rehabilitation program may include back strengthening exercises and possibly a cardiovascular (aerobic) conditioning program, and a comprehensive program custom-designed for the patient's work environment in order to safely get the patient back to work. The decision to proceed with a postoperative rehabilitation program depends upon many factors. These include factors related to the surgery (such as the type and extent of the surgery) as well as factors related to the patient (age, health and anticipated activity level.) Active rehabilitation may begin as early as 4 weeks postoperatively for a young patient with a single level fusion.

2.7. Productions Methods of Cellular Metallic Materials

Foams and other highly porous materials with a cellular structure are known to have many interesting combinations of physical and mechanical properties, such as high stiffness in conjunction with very low specific weight or high gas permeability combined with high thermal conductivity. For this reason, nature frequently uses cellular materials for constructional or functional purposes (e.g. wood or bones). Among man-made cellular materials, polymeric foams are currently the most important ones with widespread applications in nearly every sector of technology. Less known is that even metals and alloys can be produced as cellular materials or foams and that these materials have such interesting properties that exciting new applications are expected in the near future. Cellular solids and their properties have been described in much detail by Gibson and Ashby. A frequently cited review of cellular metallic materials was published in 1973 (Kulkarni and Ramakrishnan 1973). Since then, many new developments concerning the production, characterisation and application of metal foams have occurred.

According to Figure 2.15. which lists the designations for all possible dispersions of one phase in a second one (where each phase can be in one of the three states of matter), foams are uniform dispersions of a gaseous phase in either a liquid or a solid (Wen et al. 2001). The single gas inclusions are separated from each other by portions of the liquid or solid, respectively. Thus the cells are entirely enclosed by the liquid or solid and are not interconnected. The term foam in its original sense is reserved for a dispersion of gas bubbles in a liquid. The morphologyof such foams, however, can be preserved by letting the liquid solidify, thus obtaining what is called a solid foam.
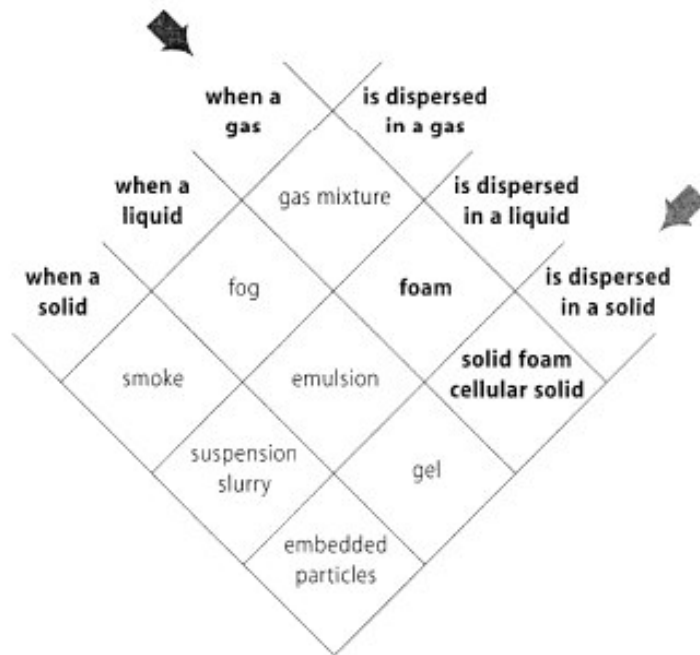
Figure 2.15. Dispersions of one phase into a second one. Each phase can be in one of
the three states of matter (Source: Wen et al. 2001).

Metallic foams means a solid foam. The liquid metallic foam is merely a stage that occurs during the fabrication of the material. Solid foams are a special case of what is more commonly called a cellular solid. As in a liquid the minimisation of surface energy only allows for certain foam morphologies, the solid foam, which is just an image of its liquid counterpart, is restricted in the same way. In contrast, cellular solids are not necessarily made from the liquid state and can therefore have nearly any morphology, e.g. the typical open structure of sintered powders. Often such porous structures are also named foams.

There are many ways to manufacture cellular metallic materials. Some methods are similar to techniques used for foaming aqueous or polymer liquids, whereas others are specially designed by taking advantage of characteristic properties of metals such as their sintering activity or the fact that they can be electrically deposited. The various methods can be classified according to the state the metal is processed in. The processes are summarised in Figure 2.16. each one corresponding to one of the states of matter: one can start

(i) from solid metal in powdered form

(ii) from liquid metal

(iii) from metal vapour or gaseous metallic compounds

(iv) from a metal ion solution
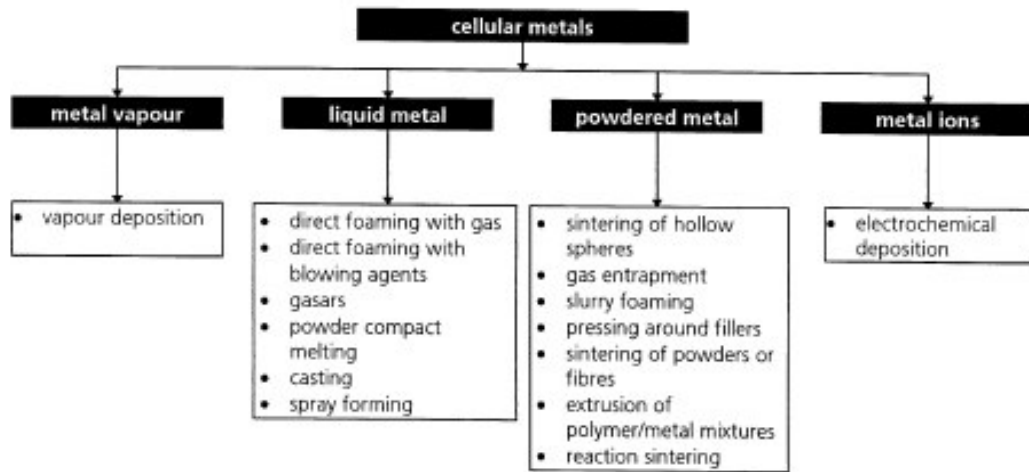
Figure 2.16. Overview of the various ''families'' of production methods for cellular metallic materials (Source: Lemaire et al. 1997).

2.8. Solid State Processing of Cellular Ti for Biomedical Applications

Although, melting methods have been successfully applied to the manufacture of Al, Zn and Mg foams, they are not suitable for the manufacture of Ti foams due to the high melting temperature and reactivity of Ti. In the PM approach, designed structures are manufactured either by sintering of hollow spheres or by melting or partial melting of powder compacts that contain a gas evolving element (e.g.TiH$_2$) (Banhart, 2001). Since these methods unavoidably result in enclosed pores (closed cell foam), they are also not suitable for the manufacture of foamed metal implants because of the requirement of body fluid transport. Open cell implant foam metals can be however successfully manufactured by a versatile PM based process known as space holder method (Martin et al. 2000, Kulkarni and Ramakrishnan 1973)

The method can be used to manufacture fully and/or partially (as coatings on solid implants for bone fixation) foamed biomedical metals. The size, level and geometry of pores can be easily altered by varying the size, amount and shape of space holder. Therefore, it is one of the appropriate methods for manufacturing designed foam metal implants.

The processing steps of space holder method are schematically presented in Figure 2.17.. The process starts with mixing of metal powders with a suitable space holder material, followed by a compaction step (e.g. uniaxial and isostatic pressing) that produces metal powder-space holder mixture compact. The green compact is then heat

treated at a relatively low temperature to release the space holder, resulting in an unfired open cell foam metal structure. Finally, the compact is sintered at relatively high temperatures to provide structural integrity. This method allows a direct near net-shape fabrication of foamed implant components with a relatively homogeneous pore structure and a high level of porosity (60-80%).

Ti or Ti-6Al-4V powder   Space holder

Mixing with solvent

Compaction

Space holder removal

Sintering
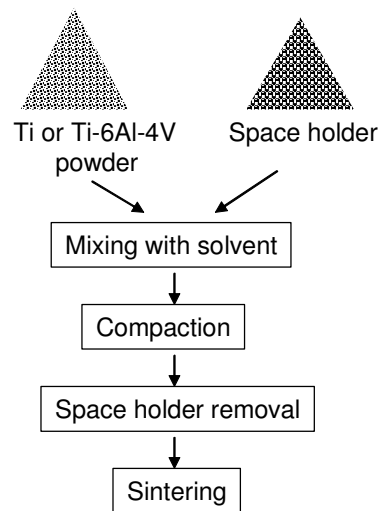
Figure 2.17. Processing steps of space holder method
(Source: Martin et al. 2000).

Ti and its alloys are known to be very reactive and can easily form interstitial solid solutions with other elements including carbon, oxygen and nitrogen. Since the presence of these elements is detrimental for the ductility, the reaction between Ti powder and the cracking products of the space holder in a temperature range of 300-600 ^{o}C must be avoided (Martin et al., 2000). It is therefore proposed that space holder should be removed at temperatures below about 200 ^{o}C (Martin et al. 2000). Ammonium hydrogen carbonate and carbamide (urea) are the materials identified to satisfy this criterion and currently used for the processing of Ti foams

2.8.1. Characterization

Cellular metals and alloys can be characterized in many ways. The objective is either to obtain mechanical or physical data characteristic of the cellular material investigated or to carry out a technological characterization of a component containing cellular metal. Cellular material is a construction consisting of a multitude of struts,

membranes or other elements which themselves have the mechanical properties of some bulk metal. Testing a cellular material is therefore equivalent to testing any engineering component. Hence, a cellular structure can be considered as a homogeneous medium which is represented by averaged material parameters.

The overall density of a porous material can be determined by weighing it and by measuring its volume using Archimedes' principle. According to this principle liquid should not be penetrated into pores of metal. If the sample to be characterized does not have a closed outer skin, penetration of liquid into the pores has to be prevented by coating its surface with a polymer or paraffin film.

The liquid processing methods yield cellular materials with closed cells or even a closed outer skin. However, in practice imperfections occur while making the foams such as in the cooling stage after processing.

The liquid processing methods yield cellular materials with closed cells or even a closed outer skin. However, in practice imperfections occur while making the foams such as in the cooling stage after processing. Such imperfections can include little holes or cracks in the cell walls or in their outer skin. Penetration techniques are ideal for detecting such surface defects. In this technique, a liquid chemical is firstly applied to the cellular metal to be investigated. The chemical is eventually absorbed by the holes and cracks. After drying the surface, a coloring developer is applied which creates color where the penetrant chemical has been retained. In this way, maps of the imperfections can be obtained in a simple visual manner

CHAPTER 3

OBJECTIVES

The aim of this experiment was to process and design the porous Ti6Al4V spinal cages for spinal surgery. In accordance with this aim, optimization of production parameters (compaction pressure, particle diameter, space holder percentage, sintering temperature and time) to produce stronger Ti6Al4V foams and designing appropriate form that can potentially be used in biomedical applications including human cortical bone disc replacement and spinal cages for spine surgery were investigated in this thesis.

The goals of this study can be summarized as follows:

• To study the effect of production parameters - compaction pressure, particle diameter, space holder percentage, sintering temperature and time-on yield strength of the porous Ti6Al4V material.

• To understand the percentage porosity and spherical particle size interaction

• To investigate the alternative production parameters for manufacturing

• To study the design methodology applied in the industry

• To get insight into the design specifications and modelling of Ti6Al4V spinal cages

• To investigate the suitable form of spinal cage which is ideal for disc replacement

• To study the commercial spinal surgery methods by means of their advantages and disadvantages on patients.

• To understand the spinal fusion method used in the spinal surgery and to problems of this surgical method

• To minimize the disadvantages of the Ti6Al4V spinal cages and spinal fusion method.

• To produce prototype models for first step animal testings.

CHAPTER 4

EXPERIMENTAL STUDY

4.1. Materials

Spherical Ti6Al4V alloy powders which were used in sintering of the powder foams were manufactured by Phelly Materials with atomization process. Table 4.1. gives the chemical composition of the used powder and ASTM 1580-1 standard of Ti6Al4V alloy powder (Wen et al. 2001).

Table 4.1. ASTM standard for Ti6Al4V powder and chemical composition of used powder. (Wen et al. 2001)

Element	Al	V	O	Fe	C	H	N	Cu	Sn	Ti
ASTM F1580-01	5.5~6.75	3.5~4.5	0.2	0.3	0.08	0.015	0.05	0.1	0.1	Balance
Testing Results	6.13	3.89	0.17	0.11	0.02	0.013	0.024	<0.05	<0.05	Balance

The particle size of the powder ranged between 23 and 90 µm with a mean particle size of 70.5µm. Amonium bicarbonate was used as space holder and its size ranged between 350 and 500 µm with a mean particle size of 170 µm. The particle size of the powder ranged between 23 and 90 µm with a mean particle size of 70.5µm. Amonium bi carbonate was used as space holder and its size ranged between 350 and 500 µm with a mean particle size

The particle sizes of the sieved powders and space holders were arranged as <90µm and 350-500µm, respectively. The SEM micrographs of Ti6Al4V powder and space holder are given in Figure 4.1. and 4.2. Ti6Al4V powder particles are spherical and nearly uniform in particle size.
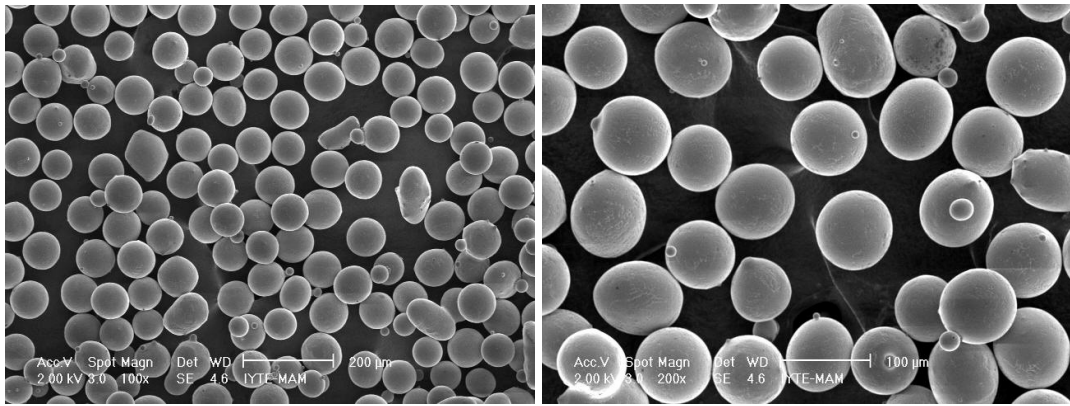
Figure 4.1. SEM micrographs of Ti6Al4V powder (<90μm)
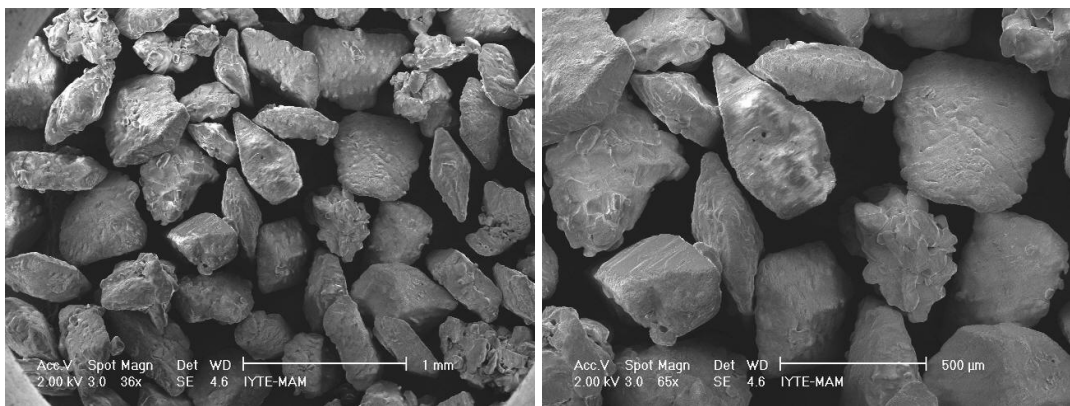
Figure 4.2. SEM micrographs of Space Holder 315-500 μm.

4.2. Methods

The methods included in this study can be summarized in three parts. These parts are foam compaction and sintering, compression testing, porosity measurements. Overall process can be summarized as in the Figure 4.3.
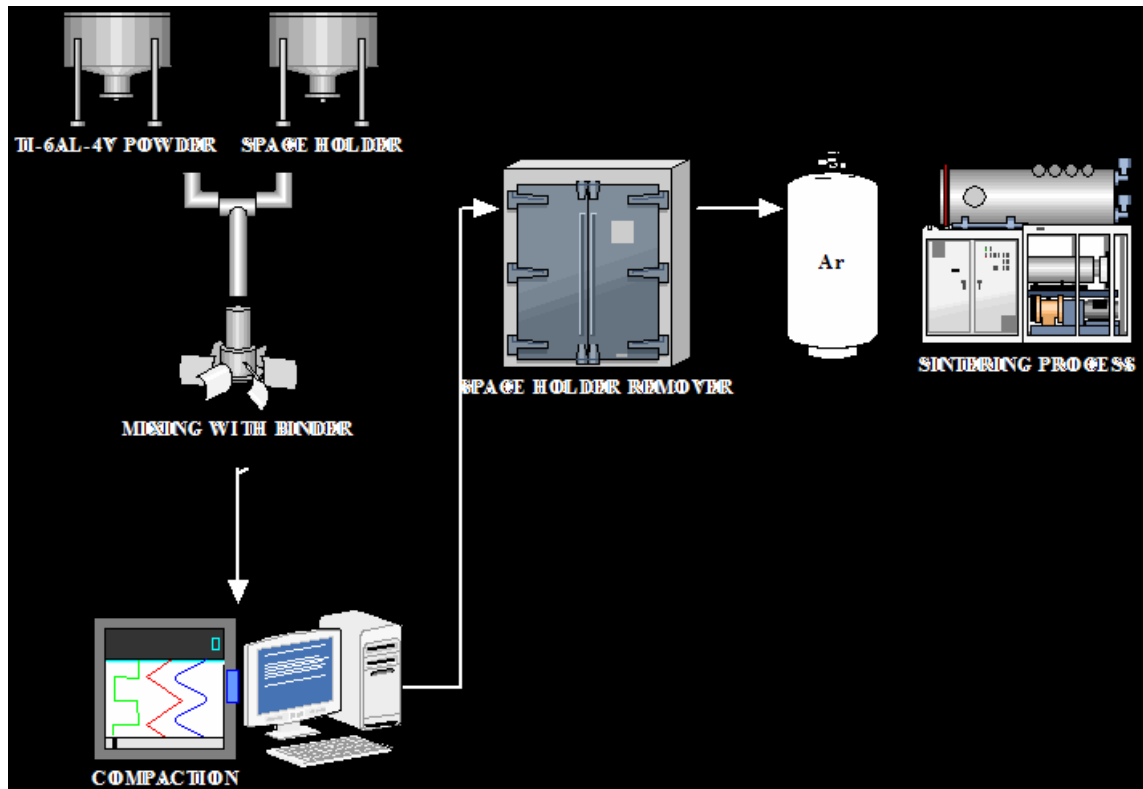
Figure 4.3. Foam compaction procedure

4.2.1. Foam Compaction and Sintering

Before compaction, Ti6Al4V alloy powder was stirred with amonium bi carbonate in the three different volume ratios as 52 %, 62 % and 72 %. PVA solution 10 % by volume was used as binding material and it was added as 10 % of the weight. Then the foams were formed 10 mm in length and 15 mm in diameter by compaction at room temperature in a steel die. Compaction pressures were chosen as 200, 300, 400 and 500 MPa. The ammonium bi carbonate was removed at 200 ^{o}C for 5 hours. After the removal of space holder, sintering was done in a tightly enclosed horizontal tube furnace under the 99.998% pure argon. Different sintering temperatures ranging from 1200 to 1300 ^{o}C and different time slices ranging from 2 to 6 hours were chosen based on the previous sintering studies of Ti foam and powder compacts (Martin et al. 2000 and Wen et al. 2001).

The Ti6Al4V foams were placed inside an enclosed Ti6Al4V box on a graphite plate at room temperature before inserting the oven which is shown in Figure 4.4.. The graphite plate prevented the bonding between Ti6Al4V box and foams. Heating and

cooling programs were applied. In the heating cycle, the foams were kept at 450 ^{o}C for ½ hour in order to allow the burning of the binder and the foams were heated and cooled with a rate of 5 ^{o}C per min.
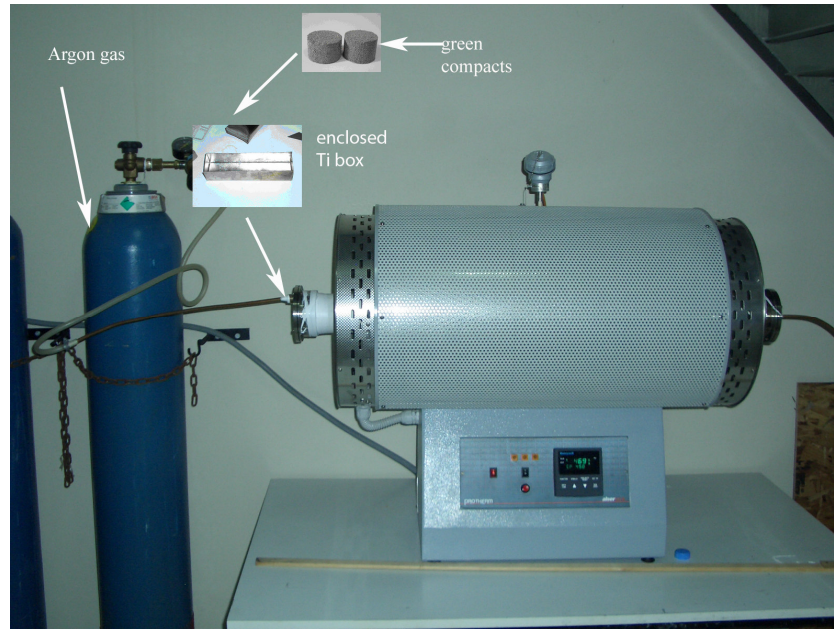
Figure 4.4. The Argon oven used in the sintering of powder compacts and foams.

4.2.2. Compression Testing

In this study, universal tension-compression test machine, SHIMADZU AG-I was used for the quasi-static compression tests of 15 mm in diameter and 10 mm in length cylindrical foam samples. In order to prevent shear forces formed by uneven surfaces of the test specimens, eccentric compression test plate was used in all tests, shown in Figure 4.5. Tests were performed at a cross-head speed of 2 mm/min corresponding to a strain rate of $2x10^{-3}$ s^{-1} to obtain the stress-strain curves. The friction between sample and the test plates was reduced by lubrication during the compression test. The experiments were performed triplicates. Elastic modulus, yield stress, ultimate compressive stress and failure strain values were found from the determined stress-strain curves. The measured strain values were corrected with the compliance of the compression test machine.
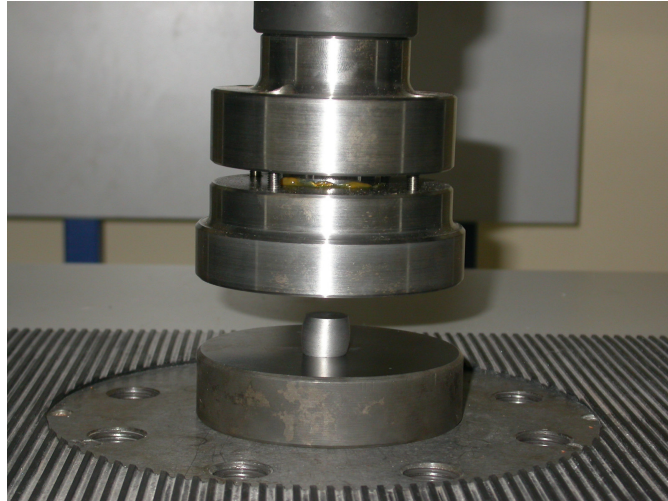
Figure 4.5. Eccentric compression testing apparatus.

4.2.3. Porosity and Pore Size Calculations

Archimedes' method was used to calculate the percent porosity of sintered foam. The open and closed porosities of foams were calculated by the differences between dry and wet weights. First of all, the volumes of the foams were measured in water. Then the foams were covered with paraffin and their weights in air and in boiling water were measured. Paraffin blocked the entrance of the water to the foam samples.

Once the density of the foams was calculated, porosities (P) were calculated using density values by the following equations;

$$P = 1 - \rho_{rel} \tag{4.1}$$

$$\rho_{rel} = \frac{\rho_{foam}}{\rho_{solid}} \tag{4.2}$$

where,

ρ_{rel} : the relative density of the foam

ρ_{foam} : the density of foam

ρ_{solid} : the density of Ti6Al4V.

In order to determine the mean pore size of sintered Ti6Al4V, porous foams were transversely cut and epoxy-mounted. The mean pore sizes of the Ti6Al4V foams were calculated applying the linear intercept method on the images of the polished surface of the foams by a Nikon Eclipse L150 optical microscope. At least 5 random lines were drawn onto the image of the powder foam and then pore sizes intercepting with the random lines were measured.

4.2.4. Designing of Spinal Cages

4.2.4.1. Dimensioning

For the prototype model, cervical (C1-C7) and lumbar (L1-L5) region of the spine was used for negative model. All the dimensions were measured by the help of Photoshop version 6.0 and Microsoft commercial package.

Vertebras' images were taken with a regular scale by the orthopedist OMER AKCALI and labeled according to position in the spine and orientation in the body (upward or downward). For example, in the vertebra image number 8a-1; '8' means vertebra in the 8th order; 'a' means back side of the vertebra or the face looking downward; '1' means sample number.

The scale was used as a reference material to convert number of pixels between two points to the actual dimension (AD) in mm. The dimension between two points (1cm long) was measured with the help of dimensioning tool in software package as a number of pixels (Figure 4.6.).
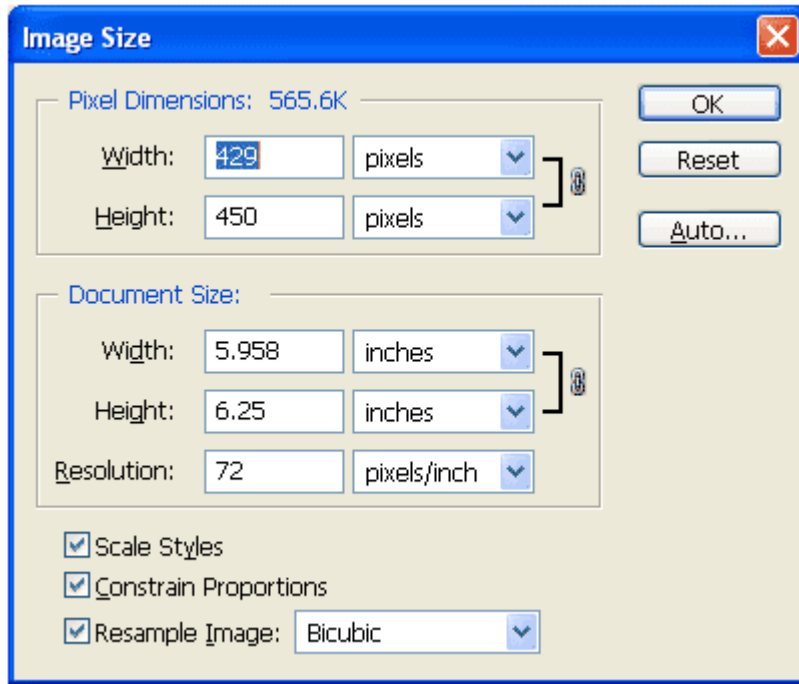
Figure 4.6. Width, height and pixel measurement in photoshop

This procedure was repeated for 10 times from the different regions of the scale to calculate the percentage error and standard deviation in measuring. In Figure 4.7. (b), W and H represent respectively width and height of the selected region as a relative dimension (RD). To convert the relative dimension to actual dimension, relative dimension was multiplied with multiplication factor determined from the scale.

(a)
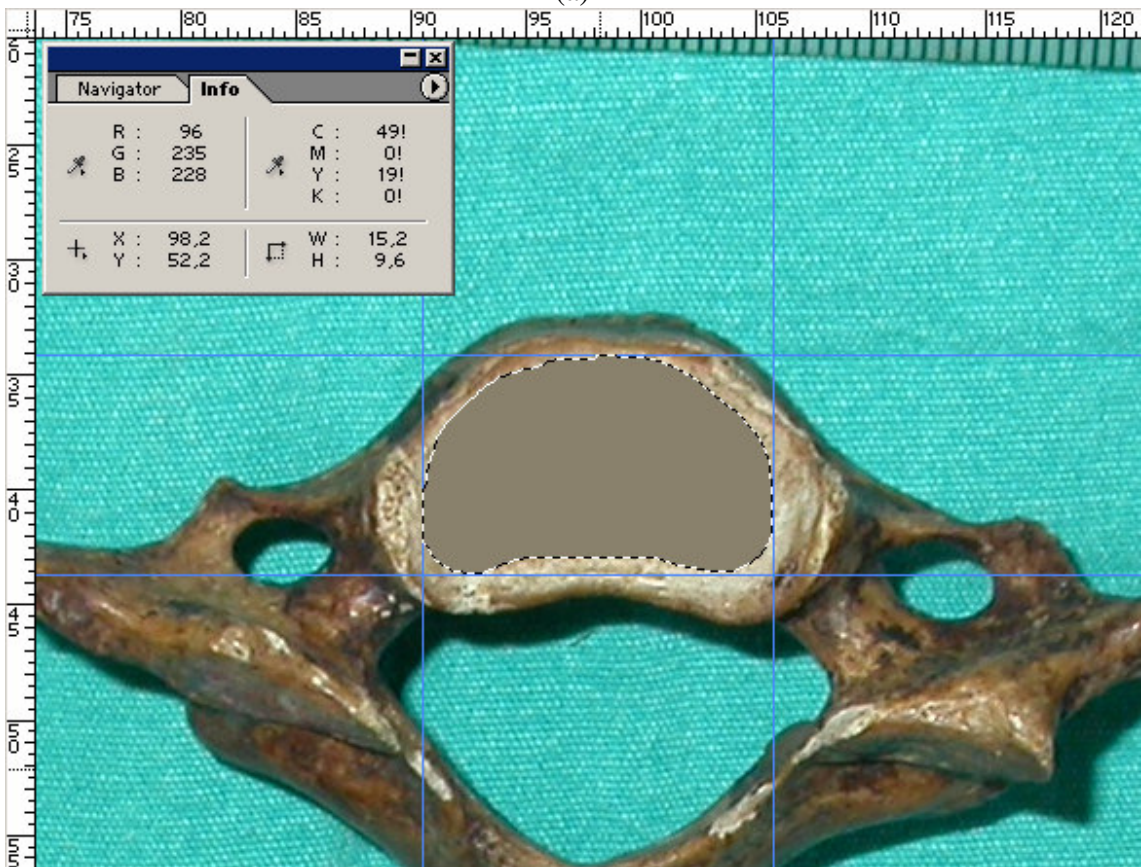
(b)

Figure 4.7. Dimensioning method (a) C2-C4 vertebras with the scale (b) calculating the number of pixel

Multiplication factor = $\dfrac{RD_{sc}}{RD_{sf}}$ (4.3)

RD_{sc}: relative dimension read from the ruler

RD_{sf} : relative dimension read from the software

AD = RD$_{sf}$ * multiplication factor (4.4)

AD: actual dimension in mm

4.2.4.2. Modelling

Based on the consultations with orthopedists'- Dr.Omer Akcali and Hipokrat R&D Department-recommendations the servical model was constructed. Entire model was designed according to the vertebral body (Figure 6.6.-b). After taking the dimensions of the vertebral body, the restriction by means of location of the implant material was decided.

Those restrictions can be summarized as follows:

• Nerves at the foramen have to be keep save during and after the surgical operation

• Implant material has to be fixed between two vertebra to prevent implant moving

• Implant has to be located on vertebral body which is enclosed with thin wall. In addition, it was decided that thin wall could be used as an implant border.

In Figure 4.8 (a), the thin wall which covers the vertebral body (Figure b) is the model size restriction for the prototype.

(a)   (b)
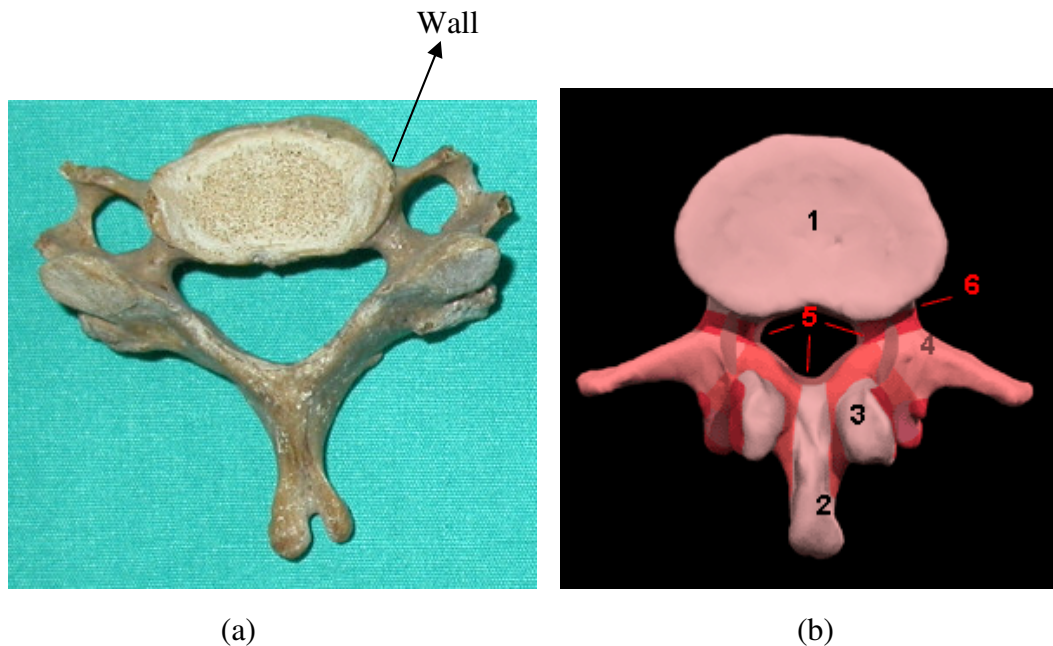
Figure 4.8.   (a) Thin wall (b) 1. Vertebral Body, 2. Spinous, 3. Articular, 4. Transverse, 5. Foramen, 6. Pedicle.

The implant material location should be located 2 mm back from the posterior to prevent the nerves from any operational mistaken during the surgery. As seen in Figure 4.9, the borders of the implant material drawn as a rectangle. After that, course form of the location was highlighted by the help of the photoshop drawing tool in view of the fact that the implant should not be larger than the drawn rectangle.
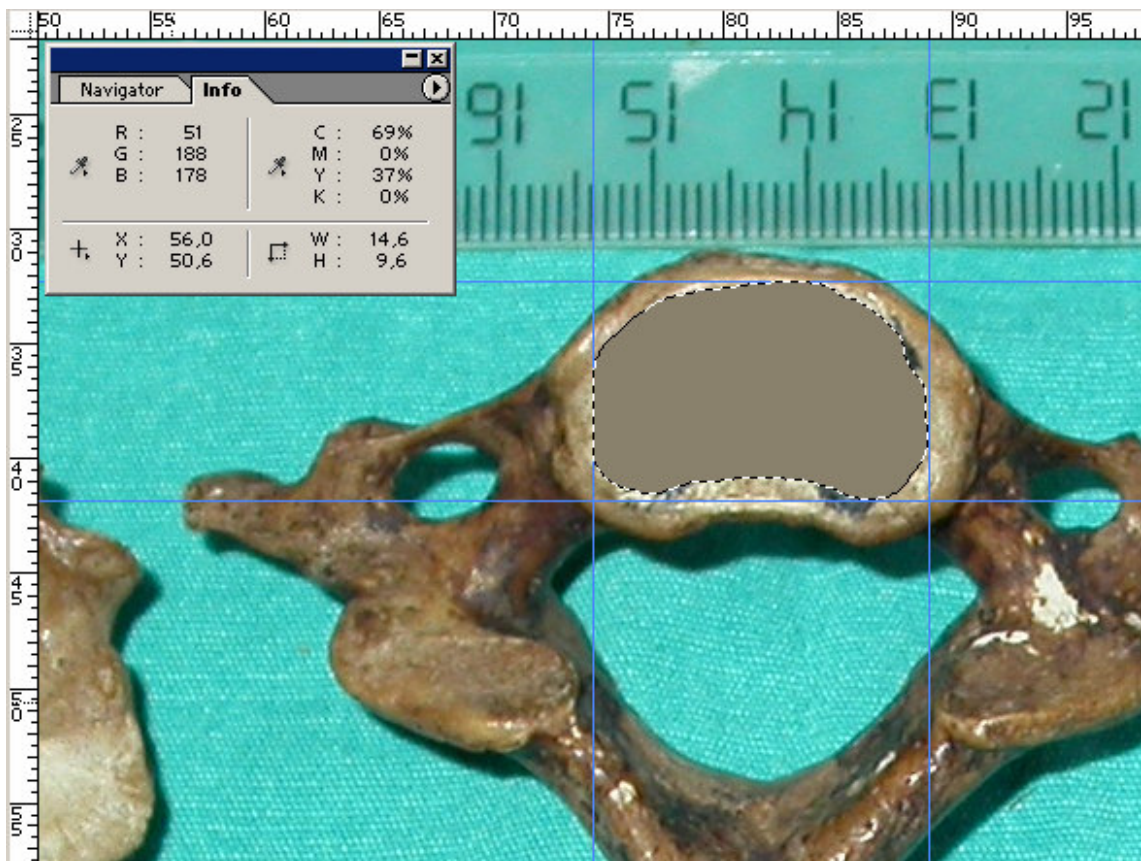
Figure 4.9. The servical model.

4.2.4.3. Prototype

After getting all the dimensions required for manufacturing, first prototype model was produced. In Figure 4.10., two different types of servical cages were produced for different regions of the spine.

Figure 4.10. (a) Vertebra from cervical region (b) Vertebra from lumbar region.

After producing the prototype models, there were some problem like material loosing from the sharp edges and supporting pins need, the protection case was designed (Figure 4.11.).

Figure 4.11. Protection case for foam material.

Because foam material could not be compacted with its own case, foam material should have to be placed inside the protection case after sintering procedure. Furthermore, since the material lost its volume during the sintering, there was shrinkage problem we were facing with. So, all the dimensions required for protection case manufacturing were measured after sintering foam material. Sand blasting method was applied inside of the protection case to get a rough surface. Rough surface between the material and the case provided extra friction and grabbing surface for particles at the outer surface of the material to the protection case. After placing the material inside its own case, the case and material was heated below the $900^{o}C$ under argon together. Second sintering procedure was only for sintering the Ti6Al4V particles to the protection case.

CHAPTER 5

RESULTS AND DISCUSSION

5.1. Compression Mechanical Properties at Quasi-static Strain

The compressive stress-strain curves of foams of particle size <90 µm are shown at various compaction pressures in Figures 5.1., 5.2., 5.3. and 5.4., respectively. The elastic modulus of the foams is determined in the initial region of stress-strain graph and the yield strength is taken as the proportional limit as shown in Figures 5.5. and 5.6.

Figure 5.1. shows all sample test measurements. In the first test shown in Figure 5.1., 200 MPa compaction pressure applied on Ti 6Al4V foams. In the following tests (shown in Figure 5.2., 5.3. and 5.4.) only compaction pressure change in the order to 300, 400 and 500 MPa.. According to the compaction pressure, mechanical property of samples changing was observed. Furthermore high compression (43 MPa) was observed under compaction pressure of 500 MPa. All of these tests results are shown in Figure 5.5., 5.6.
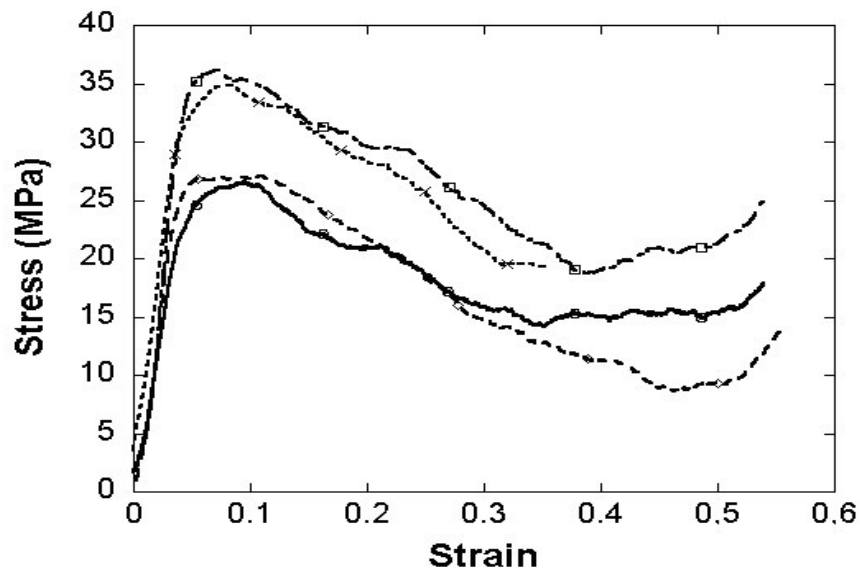
Figure 5.1.   Compression stress-strain curve of foams cold compaction pressure at 200 MPa, T=1200 ºC, 2 h <90 µm Ti6Al4V powder.
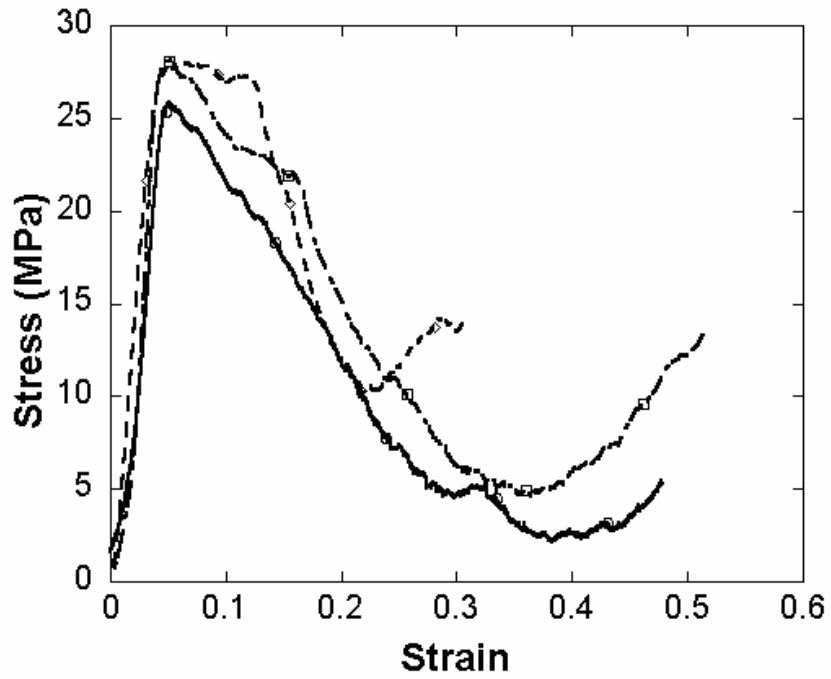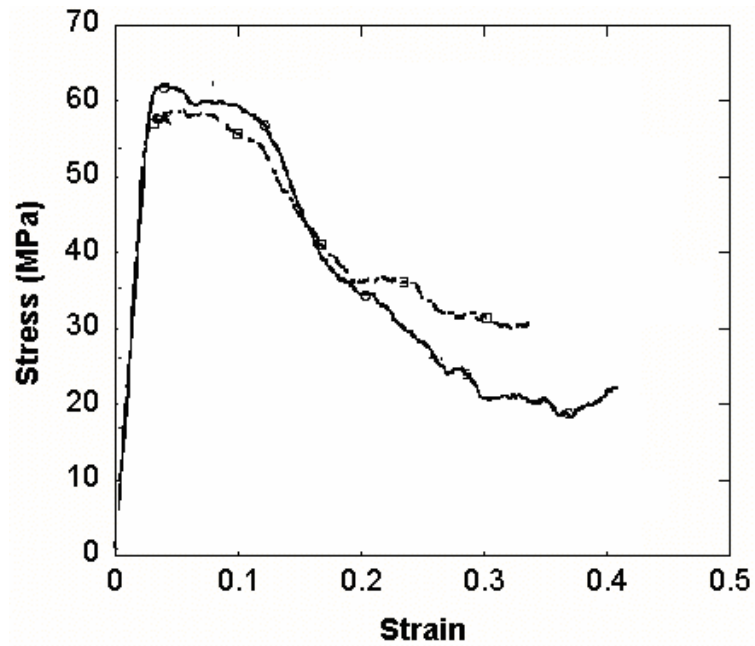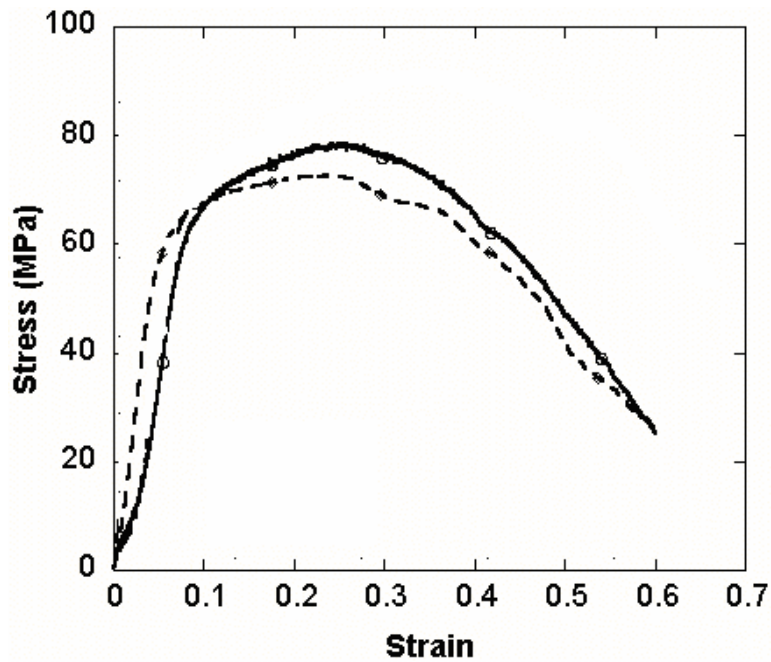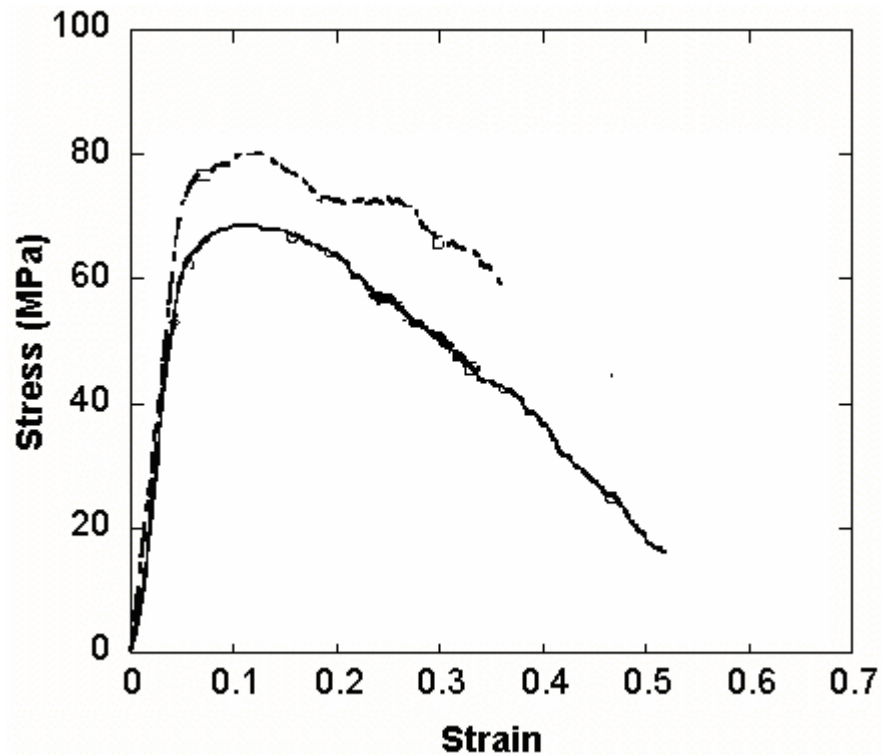
Figure 5.2. Compression stress-strain curve of foams cold compaction pressure at 300 MPa, T=1200 ºC, 2 h <90 μm Ti6Al4V powder.
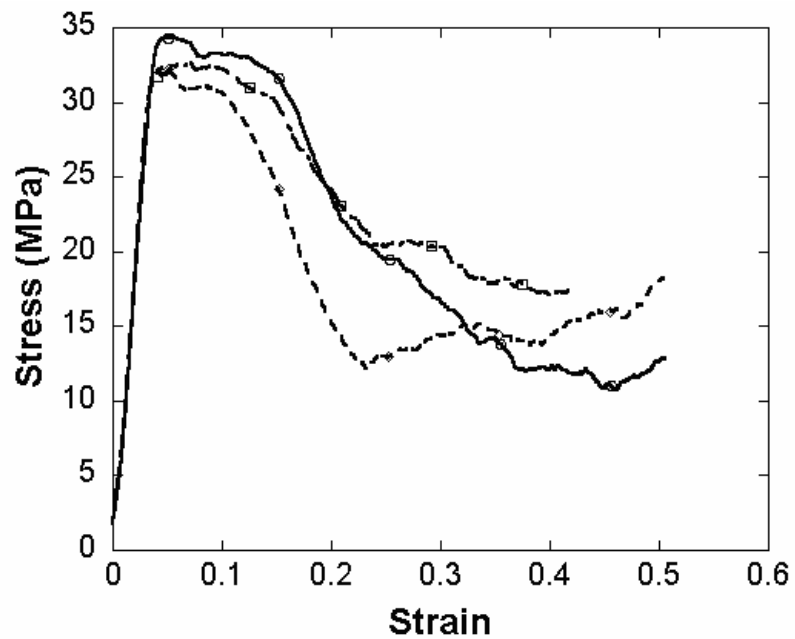
Figure 5.3. Compression stress-strain curve of foams cold compaction pressure at 400 MPa, T=1200 ºC, 2 h <90 μm Ti6Al4V powder.
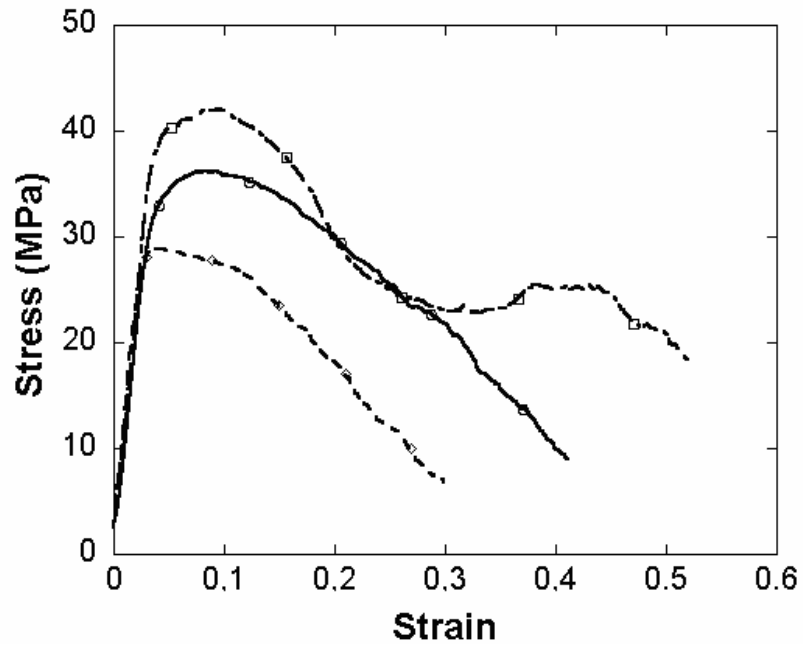
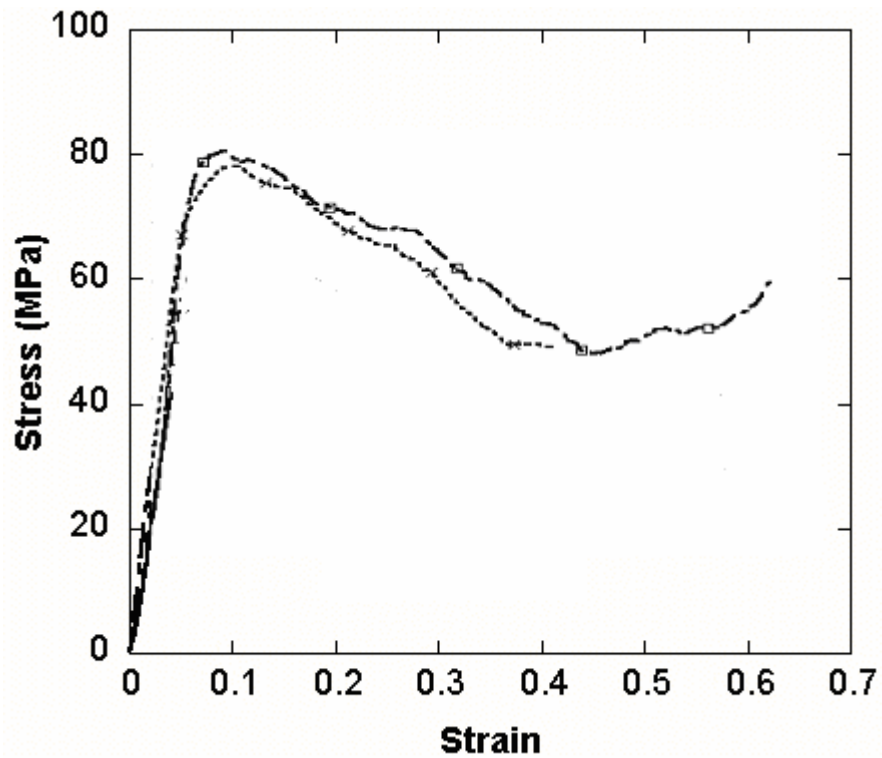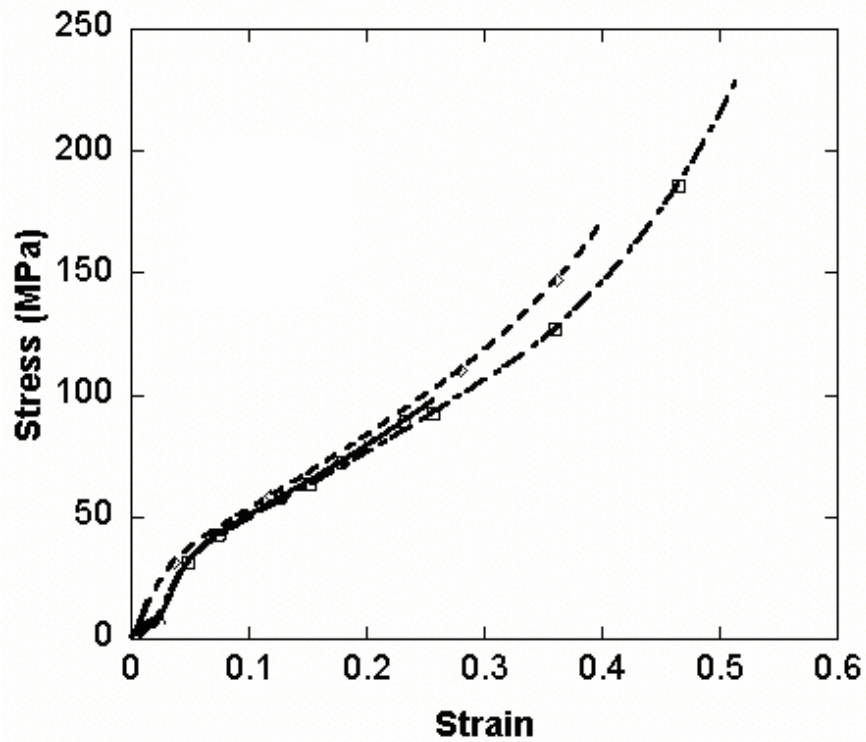Figure 5.4.   Compression stress-strain curve of foams cold compaction pressure at 500 MPa, T=1200 ºC, 2 h <90 µm Ti6Al4V powder.
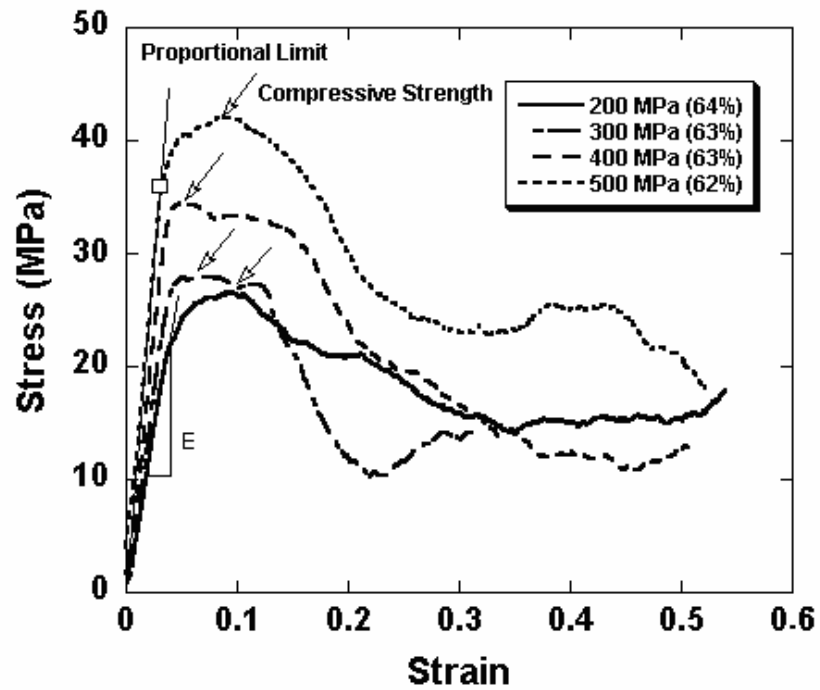
Figure 5.5.   Compression stress-strain curves of foams (cold compaction pressure 200, 300, 400, 500 MPa, T=1200 ºC, 2 h <90 µm) at various compaction pressures.
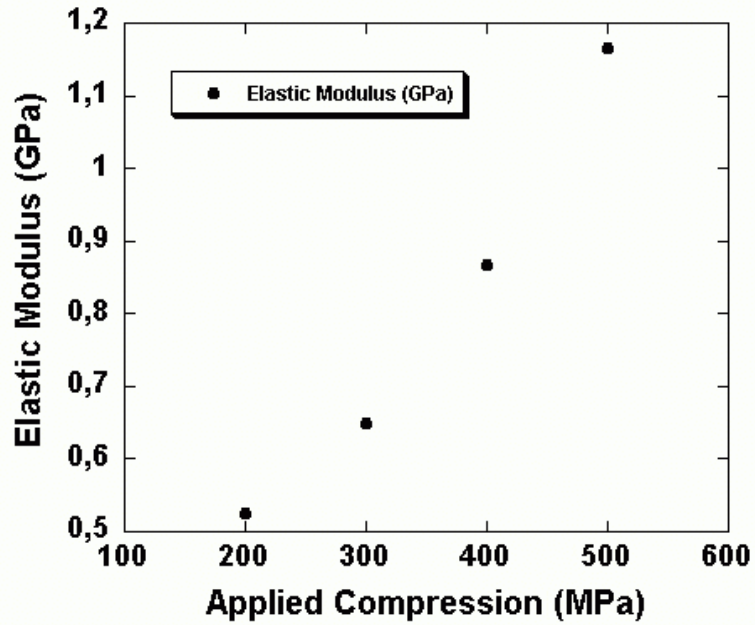
Figure 5.6. Variation of elastic modulus with applied various compaction pressures.

Elastic modulus of Ti6Al4V foam samples were compared by using compression test machine results. Test results shown in Figure 5.6. are between (0.52 - 1,18 GPa).

The compressive stress-strain curves of foams of particle size <90 µm are shown at various compaction pressures in Figures 5.7., 5.8. and 5.9., respectively.
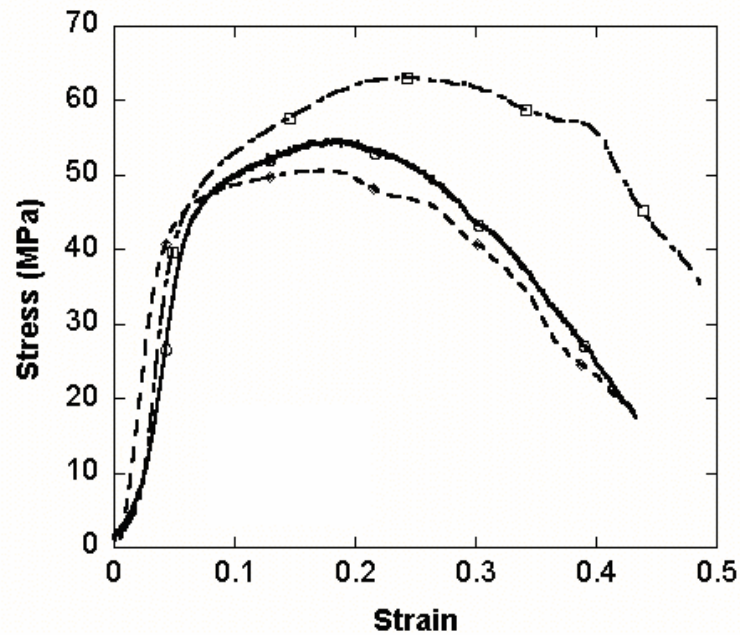
Figure 5.7.   Compression stress-strain curve of foams cold compaction pressure at 300 MPa, T=1300 ℃, 2 h <90 µm Ti6Al4V powder.
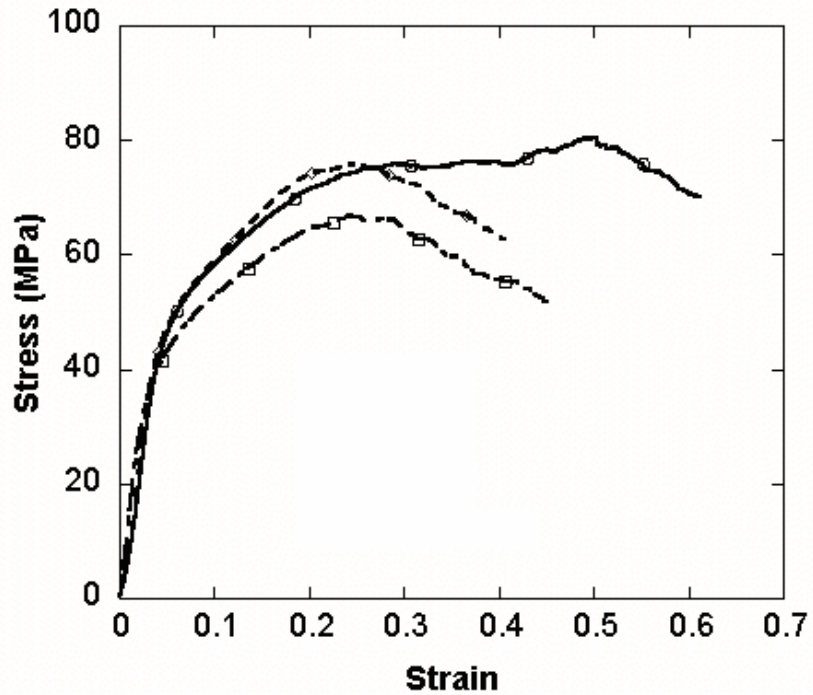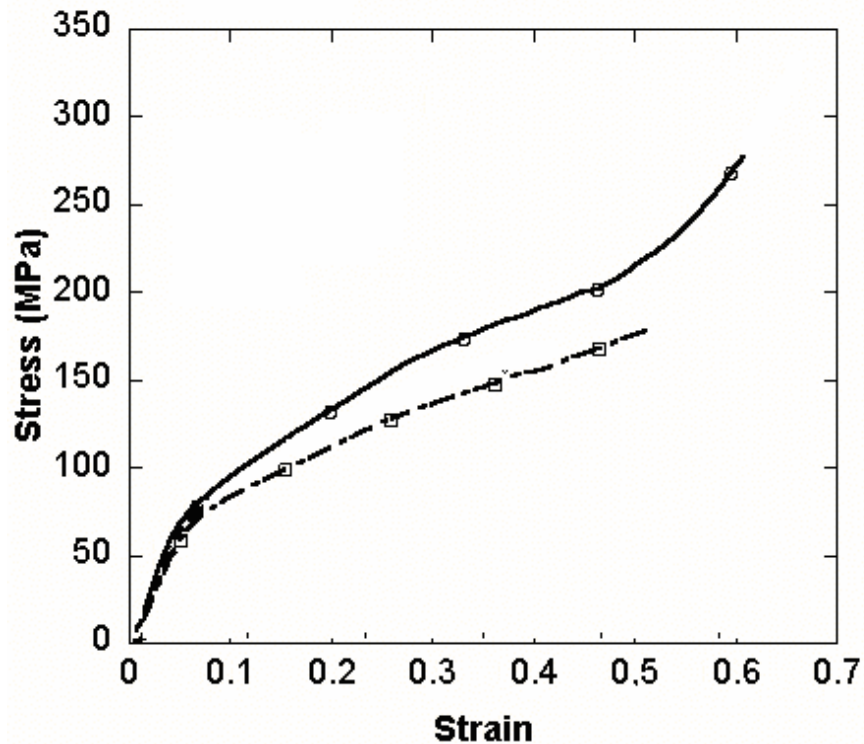
Figure 5.8.   Compression stress-strain curve of foams cold compaction pressure at 500 MPa, T=1300 ℃, 2 h <90 µm Ti6Al4V powder.
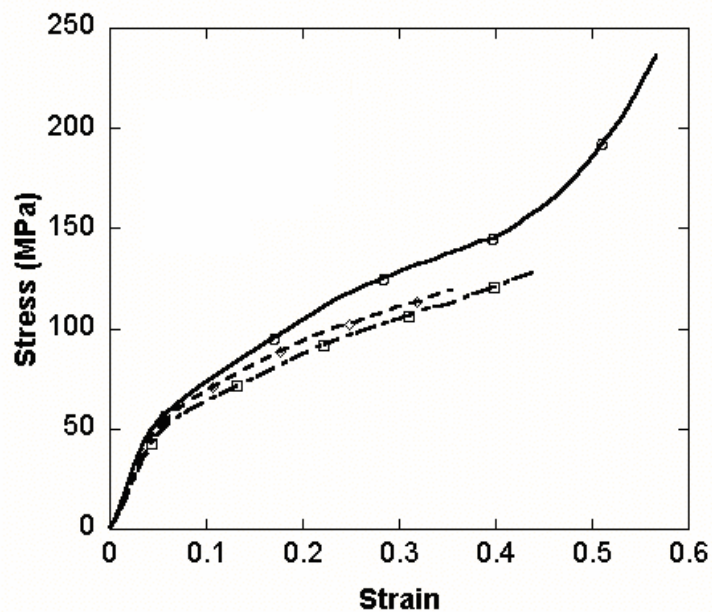
Figure 5.9.   Compression stress-strain curve of foams cold compaction pressure at 700 MPa, T=1300 ℃, 2 h <90 µm Ti6Al4V powder.

In the Figure (5.7.,5.8. and 5.9.), samples compacted under 300, 500 and 700 MPa compaction pressures were sintered in increasing temperature of 1300 ℃ and 2 hours sintering time. Furthermore yield strengths were observed between 40 and 50

MPa. On the other hand, all the samples indicated brittle type fracture characteristic and separated completely under compression load.

Samples only prepared under 500 MPa compaction pressure shows more ductile characteristic than the others. And also, increasing compression strengths were observed by increasing compaction pressure. Furthermore, samples prepared under 700 MPa compaction pressure shows densification characteristic.
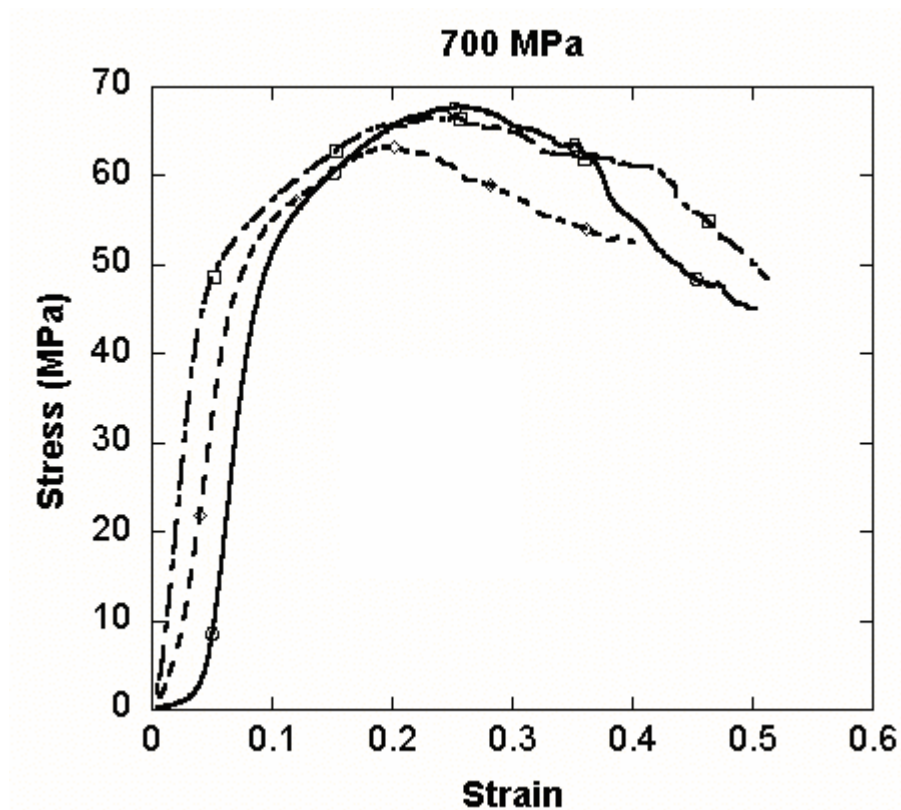
Figure 5.10. Compression stress-strain curve of foams cold compaction pressure at 700 MPa, T=1300 ºC, 4 h <90 µm Ti6Al4V powder.
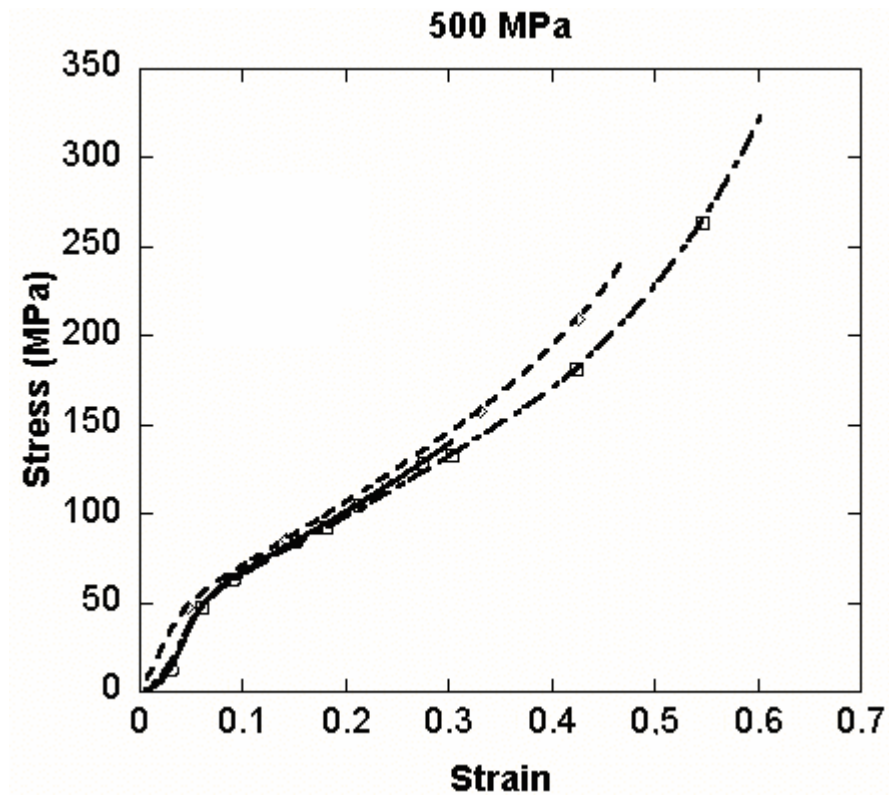
Figure 5.11. Compression stress-strain curve of foams cold compaction pressure at 500
MPa, T=1300 ℃, 4 h <90 µm Ti6Al4V powder.

In the Figure (5.10.,5.11.), samples compacted under 500 and 700 MPa
compaction pressures were sintered in 1300 ℃ and increasing temperature of 4 hours
sintering time. After this procedure, samples compacted under 500 MPa indicated foam
characteristic and also it was observed that compressive strengths of samples were
between 40 and 50 MPa. On the other hand, samples compacted under 700 MPa
separated after compression test again.
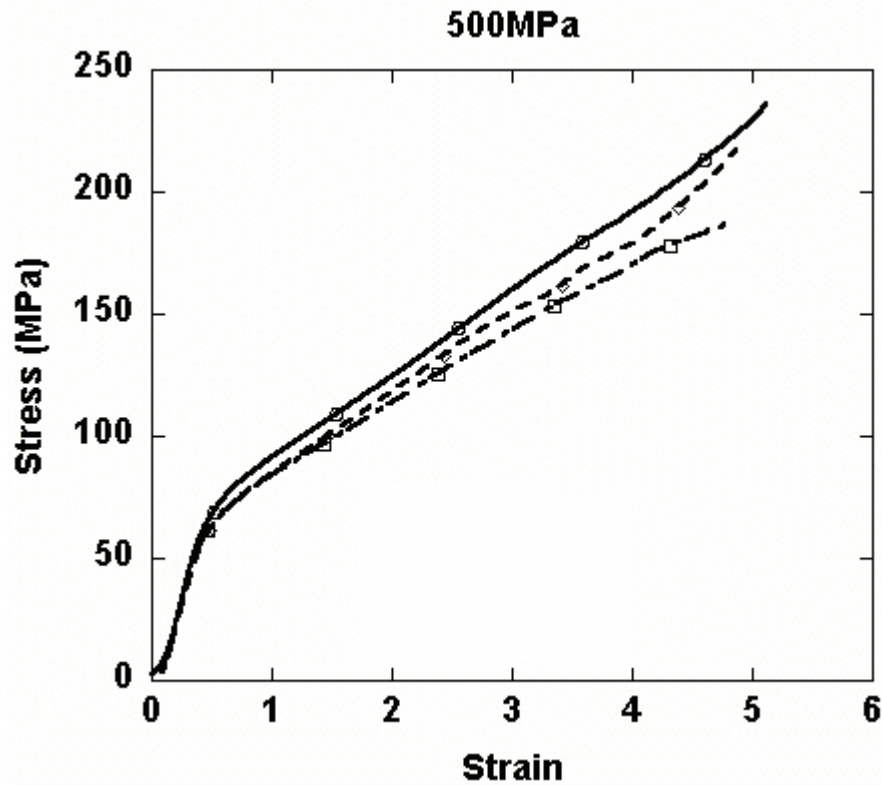
Figure 5.12. Compression stress-strain curve of foams cold compaction pressure at 500 MPa, T=1300 ℃, 6 h <90 µm Ti6Al4V powder.

In order to increase the strength of Ti6Al4V samples compacted under 500 MPa, sintered in 1300℃ and 4 hours (Figure 5.12.), sintering time was increased from 4 hours to 6 hours. And it was observed that compression strength was increased to 60 – 65 MPa. Moreover, Ti6Al4V samples compacted under 500 MPa, sintered in 1300℃ and 6 hours showed foam characteristics.

Ti6Al4V samples which have 52% and 72% porosity range showed undesired results as brittle characteristics and particle separation in 1300 ℃ of sintering temperature and 6 hours of sintering time.

5.1.1. Effect of Compaction Pressure, Sintering Temperature and Time on the Percentage of Porosity

In Figure 5.13., it was observed that percentage of porosity decreases by increasing compaction pressure. Furthermore, variety of sintering temperature and time does not affect Ti6Al4V samples percentage of porosity level.
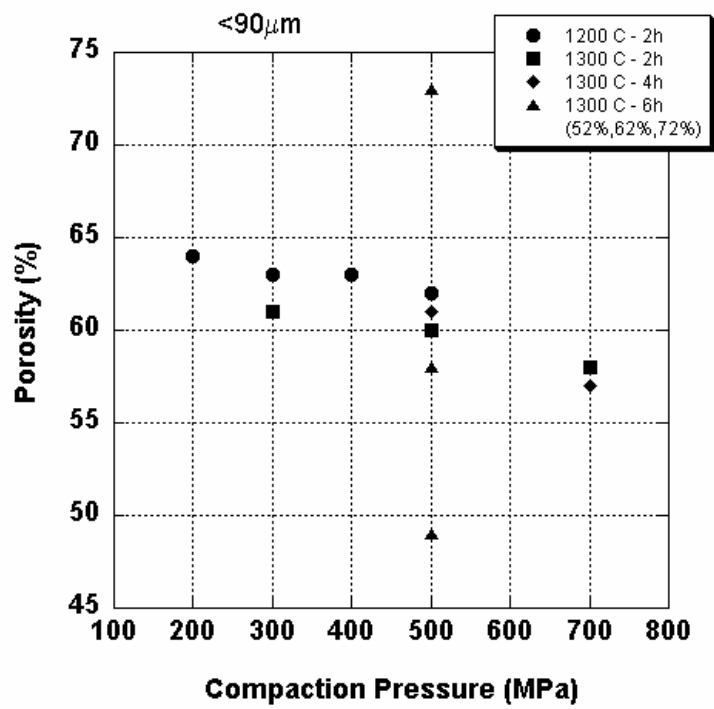
Figure 5.13. Variation of porosity with compaction pressure in each sintering temperature and sintering time.
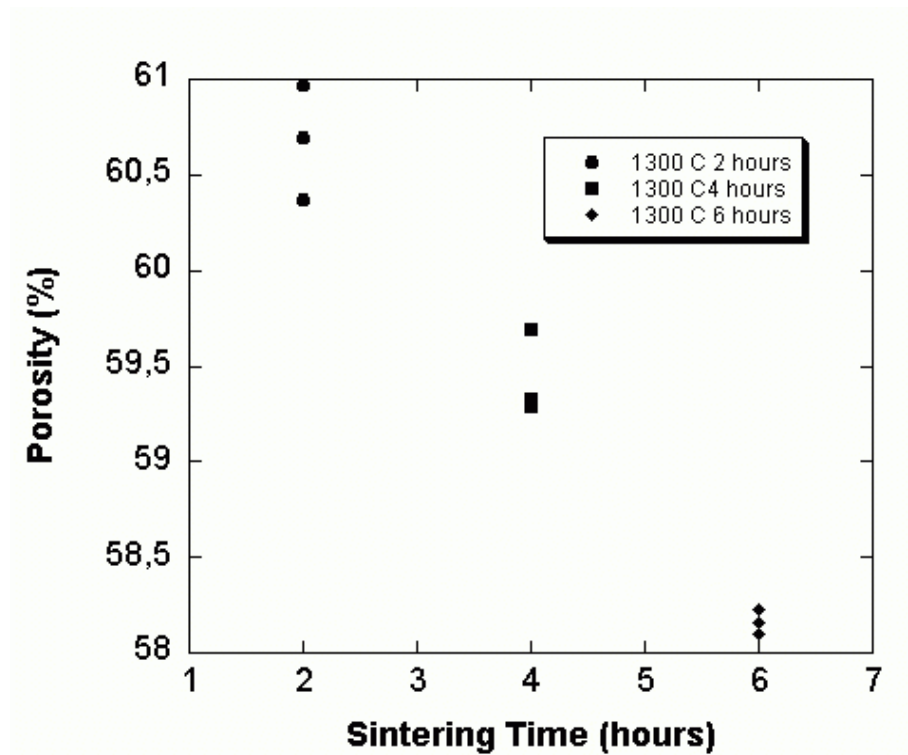
Figure 5.14. Variation of porosity with various sintering time at same sintering temperature.

In Figure 5.14., it was observed that percentage of porosity decreases a little bit by increasing sintering time. It means that sintering time does not affect on percentage porosity level.

5.1.2. Effect of Porosity on the Yield Strength

In Figure 5.15., it was observed that yield strength of Ti6Al4V samples compacted under 500 MPa compaction pressure and 62% of theoretical porosity level decreases by increasing determined percentage of porosity level.
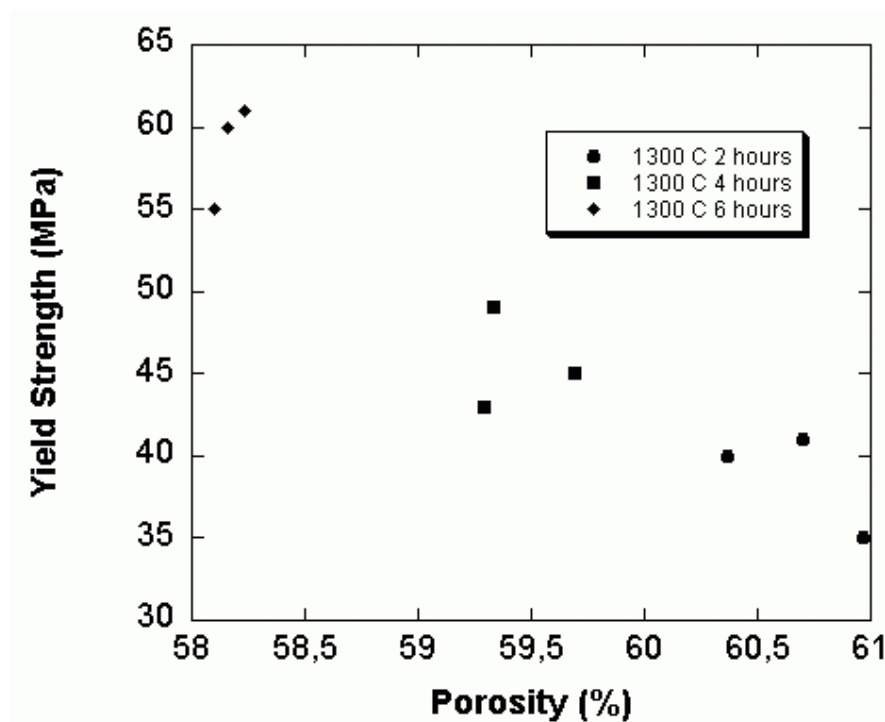
Figure 5.15. Variation of porosity with yield strength at same sintering temperature in each sintering time.

5.1.3. Effect of Sintering Time on the Yield Strength

In Figure 5.16., it was observed that yield strength of Ti6Al4V samples compacted under 500 MPa compaction pressure and 62% of theoretical porosity level increases by increasing sintering time.
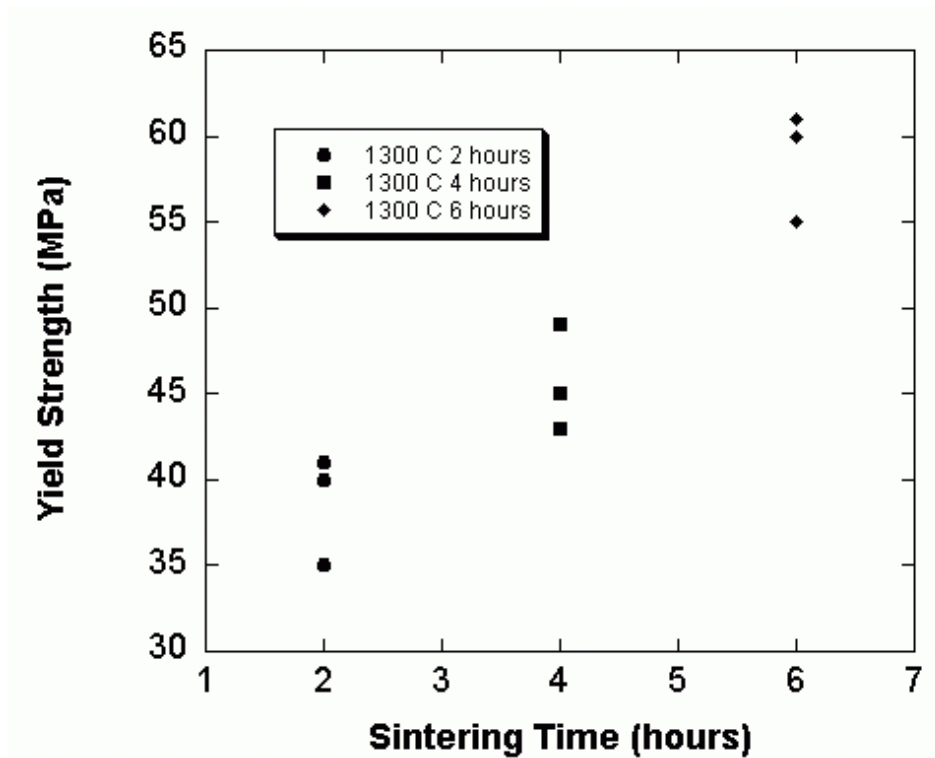
Figure 5.16. Variation of yield strength with various sintering time at same sintering temperature.

5.1.4. Effect of Particle Size on Yield Strength

The compressive stress-strain curves of foams of particle size <90 µm are shown at various compaction pressures in the previous chapters. On the other hand, compressive stress-strain curves of foams of particle size 100-150 µm under 400, 500, 600, 700 MPa at various sintering temperature (1200, 1300, 1350°C), porosity of 50% and 60%.
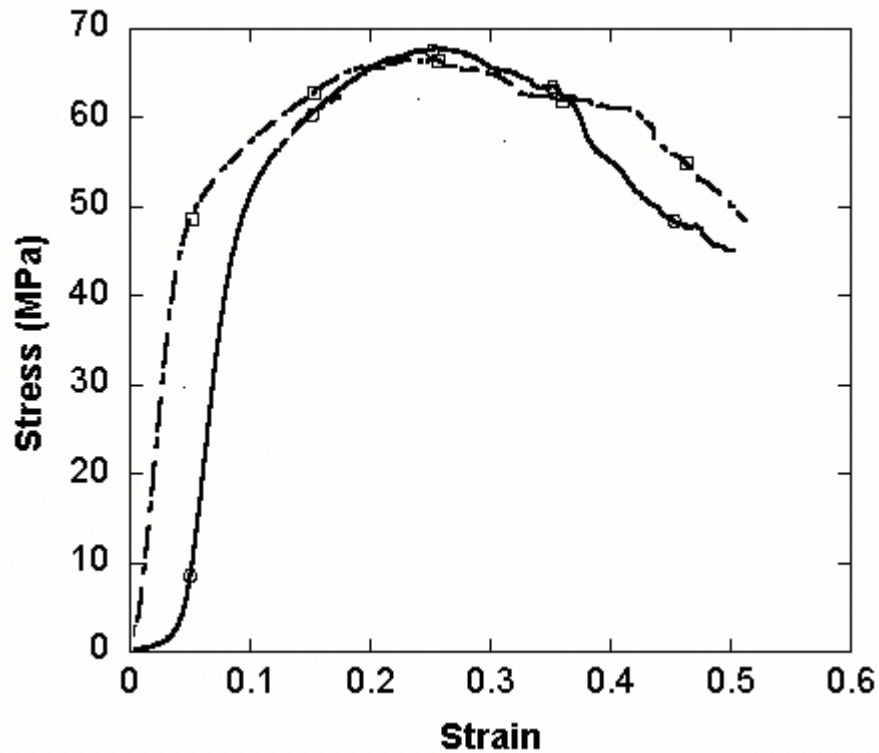
Figure 5.17. Compression stress-strain curve of foams cold compaction pressure at 400 MPa, T=1300 ℃, 4 h, 100-150μm Ti6Al4V powder.

In Figure 5.17., it was observed that yield strength of Ti6Al4V samples compacted under 400 MPa compaction pressure and 50% of theoretical porosity level increases by increasing sintering time. The foam material was sintered under $1300^{o}C$ for 4 hours. The material shows brittle type fracture characteristic and separated completely under compression load.

Figure 5.18. Compression stress-strain curve of foams cold compaction pressure at 500 MPa, T=1300 ℃, 4 h, 100-150µm Ti6Al4V powder.

In Figure 5.18., it was observed that Ti6Al4V samples compacted under 500 MPa compaction pressure and 60% of theoretical porosity level shows more brittle type fracture characteristic than the other materials.

Figure 5.19. Compression stress-strain curve of foams cold compaction pressure at 600 MPa, T=1300 ℃, 4 h, 100-150µm Ti6Al4V powder.

In Figure 5.19., it was observed that Ti6Al4V samples compacted under 600 MPa compaction pressure and 50% of theoretical porosity level shows ductile type fracture characteristic. It shows that increasing compaction pressure makes the material denser and gives strength to material.

Figure 5.20. Compression stress-strain curve of foams cold compaction pressure at 600 MPa, T=1300 °C, 6 h, 100-150μm Ti6Al4V powder.

In Figure 5.20., it was observed that Ti6Al4V samples compacted under 600 MPa compaction pressure and 60% of theoretical porosity level shows brittle type fracture characteristic. The material mostly crushed after a time of compaction procedure.

Figure 5.21. Compression stress-strain curve of foams cold compaction pressure at 700 MPa, T=1300 °C, 4 h, 100-150μm Ti6Al4V powder.

In Figure 5.21., it was observed that Ti6Al4V samples compacted under 700 MPa compaction pressure and 60% of theoretical porosity level shows more ductile than the others. Increasing compaction pressure makes material more resistible to high loading.

Figure 5.22. Compression stress-strain curve of foams cold compaction pressure at 500
MPa, T=1350 ℃, 4 h, 100-150µm Ti6Al4V powder.

In Figure 5.22. and 5.23., it was observed that Ti6Al4V samples compacted
under 500 MPa compaction pressure and 50% of theoretical porosity level shows foam
characteristic stress-strain curve.

Figure 5.23. Compression stress-strain curve of foams cold compaction pressure at 500
MPa, T=1350 ℃, 6 h, 100-150µm Ti6Al4V powder.

5.2. Experimental Design

To optimize Ti6Al4V spinal cage processing parameters, 2^2 factorial method was used. Factorial design were widely used in Ti6Al4V spinal cage design involving several factors where it is necessary to study the joint effect of the factors on a response of yield strength. By using the factorial design we investigate;

- combination of the factors
- main effects on production

In this design, 2 factors (percentage porosity and used Ti6Al4V particle diameter) are investigated in 2 levels with 4 replicates. These levels are quantitative. Thorough this design study, it is assumed that

- the factors are fixed
- the designs are completely randomized
- the usual normality assumption are satisfied

2^2 factorial designs are particularly useful in the early stages of experimental work, when many factors are likely to be investigated. It provides the smallest number of runs with percentages porosity change versus particle powder size.

Because there are only two levels for each factor, it was assumed that the response is approximately linear over the range of the factor level. The experiments were replicated 4 times, so there are 32 runs. The order in which the runs were made was random, so it is a completely randomized design.

According to the this design method, screening is used to variation between the choosen factors (porosity and pore size). Table 5.1. gives over all changing in between the parameters.

Table 5.1. Screening for changing in between porosity and powder size.

Powder size	Porosity (%)					
		40			50	
	200		210	122		129
< 90µm						
	186		196	120		115
	80		130	44		42
100-200µm						
	150		115	53		62

It is understood that by decreasing the percentage porosity and particle diameter during the compaction is concluded as increasing in yield strength. On the other hand, by increasing powder size and percentage porosity in the mixture is concluded as decreasing in yield strength.

In this design experiments, the magnitude and direction of the factor effects to determine which variables are likely to be important was examined. The analysis of variance is used to confirm this interpretation. Actually, Stat Easy statistics software package is useful for setting up and analyzing 2^2 design.

Table 5.2. Combination of levels and factors in the design.

Factor		Combination	Yates	Replicates				Total
A	B							
-	-	A LOW, B LOW	1	200	210	186	196	792
+	-	A HIGH, B LOW	a	80	130	150	115	475
-	+	A LOW, B HIGH	b	122	129	120	115	486
+	+	A HIGH, B HIGH	ab	44	53	42	62	201

By convention, the effect of a factor by a capital letter is denoted. The levels of the factors are arbitrarily called 'low' and 'high' like in Table 5.2.. By convention, the effect of a factor is denoted by a capital letter. Thus 'A' refers to effect of percentage porosity factor, 'B' refers to the effect of particle diameter factor, 'AB' refers to the interaction of both two factors. In 2^2 design the low and high levels of A and B are denoted by '-' and '+'.

In a two-level factorial design, the average effect of a factor is defined as the change in response produced by a change in the level of that factor averaged over the levels of the other factors. Also, the symbols (1), a, b, and ab represents the total of all n replicates which are 4 in our design taken at the treatment combination. Now the effect of A at the low level of B is [a-(1)]/n, and A at the high level of B is [ab-b]/n. Averaging these two quantities yields the main effect of A:

$$A = \frac{1}{2n}\{[ab-b]+[a-(1)]\}$$

The average main effect of B is found from the effect of B at the low level of A and at the high level of A as

$$B = \frac{1}{2n}\{[ab-a]+[b-(1)]\}$$

The interaction effect AB is defined as the average difference between the effect of A at the high level of B and the effect of A at the low level of B. Thus,

$$AB = \frac{1}{2n}\{[ab-b]-[a-(1)]\}$$

So,

$$A = \frac{1}{2(4)}(201+475-486-792) = -75.25$$

$$B = \frac{1}{2(4)}(201+486-475-792) = -72.5$$

$$AB = \frac{1}{2(4)}(201+792-475-486) = 4$$

This means, the effect of A (percentage porosity) is negative; this suggests that increasing A from the low level 40% to the high level 50% will decrease the yield strength. The effect of B (particle diameter) is negative; this suggests that increasing the diameter size of the Ti6Al4V spherical particle will decrease the yield strength. The interaction effect is relatively small to the two main effects.

To complete the anova, SS_A, SS_B, and SS_{AB} has to be figured out.

$$SS_A = \frac{[ab+a-b-(1)]^2}{4n}$$

$$SS_A = \frac{362404}{16} = 22650.25$$

$$SS_B = \frac{\{[ab-a]+[b-(1)]\}^2}{4n}$$

$$SS_B = \frac{336400}{16} = 21025$$

$$SS_{AB} = \frac{\{[ab-b]-[a-(1)]\}^2}{4n}$$

$$SS_{AB} = \frac{1024}{16} = 64$$

The total sum of squares is found in the usual way, that is,

$$SS_T = \sum_{i=1}^{2}\sum_{j=1}^{2}\sum_{k=1}^{n} j_{ijk}^2 - \frac{y_{...}^2}{4n}$$

SS$_T$=285640-238632.25=47007

In general, SS$_T$ has 4n-1 degrees of freedom. The error sum of squares, with 4(n-1) degrees of freedom, is computed by subtraction as

$$SS_E = SS_T - SS_A - SS_B - SS_{AB}$$

SS$_E$=47007-22650.25-21025-64=3268

Table 5.3. Analysis of variance for the experiment.

Source of variation	Sum of Squares	Degrees of Freedom	Mean Square	F_0	P-Value
A	22650.25	1	22650.25	83.17	0.0001
B	21025	1	21025	77.2	0.0001
AB	64	1	64	0.23	>0.25
Error	3268	12	272.33		
Total	47007	15			

The complete anova is summarized in Table 5.3.. Based on the P-values, the main effects are statistically significant. This confirms initial interpretation of the data based on the magnitudes of the factor effects.

In Figure 5.24., Tabled data, processed by the STAT EASY statistical software to see the changining in the data more clear.
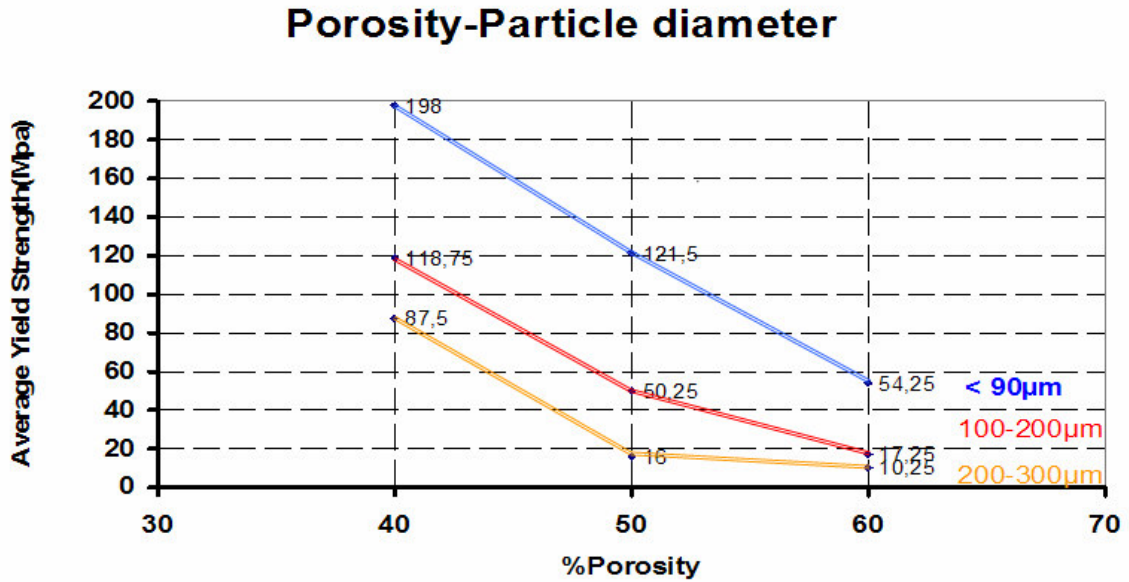
Figure 5.24. Percentage Porosity- Particle Diameter change with respect to yield strength.

According to this commercial program, parameters affect on processing method and suitable variation for the manufacturing method was indicated. The formula for the optimization process is,

$$y = 87.5 - 77.4 - 110.5x(1) + 33.25x(1)x(2)$$

x1: Particle diameter

x2: Percentage Porosity

5.3. Comparative Analysis

The surgical equipments used for the spinal fusion technique and the other techniques are number of advantages and disadvantages. The main differences between the products by means of advantages and disadvantages are as follows;

CHARITE ARTIFICIAL DISK

**(DePuy Spine, Inc. Johnson & Johnson Company)**

Advantages;

• CHARITÉ Artificial Disc design allows your spine to move. Patients were observed to have motion between 0 and 21 degrees while bending forward and backward.

• CHARITÉ Artificial Disc requires no bone graft.

Disadvantages;

• Technology is not appropriate for everyone.

• Allergic reaction to the implant materials

• Implants that bend, break, loosen or move

• Pain or discomfort

• Paralysis

• Spinal cord or nerve damage

• Spinal fluid leakage

• The need for additional surgery

BAK/L: (Zimmer Spine, Inc)

Advantages;

• Postoperative pain may be minimized through a decrease in the amount of surgical intervention.

• Operative procedure time and length of stay in the hospital can be less than other fusion methods.

• Return to daily activities can be much quicker.

Disadvantages;

• Bone graft is required

• Disk looses ability to move

• Implants that break, loosen or move

• Spinal cord or nerve damage

• The need for additional surgery

Prosthetic Disc Nucleus (PDN)

Advantages;

• Percutaneous placement

• Operative procedure time and length of stay in the hospital can be more than other fusion methods.

Disadvantages;

• Disk looses ability to move

• Implants that break, loosen or move

• Need to maintain disc space height

• The need for additional surgery

Articulating Disc

Advantages;

• Operative procedure time and length of stay in the hospitalis moderate

• No migration

Disadvantages;

• Problem with particle loosing form the endplate during the surgery

• Implants that break, loosen or move

• The need for additional surgery

Bristol disc

Advantages;

• Percutaneous placement

• Operative procedure time and length of stay in the hospital is moderate

Disadvantages;

• Pain or discomfort

• Paralysis

- Spinal cord or nerve damage
- Spinal fluid leakage
- The need for additional surgery

Brayn Cervical

Advantages;
- No need for bone graft
- Operative procedure time and length of stay in the hospital is less

Disadvantages;
- Pain or discomfort
- Paralysis
- Spinal cord or nerve damage
- Spinal fluid leakage
- The need for additional surgery
- Pain or discomfort

Ti6Al4V Spinal cages

Advantages
- No bone graft usage.
- Return to daily activities much quickly.
- No needs for additional surgery.
- Surgical operation time and length of stay in the hospital are less than other fusion methods.
- Near final shape fabrication.
- Lowest manufacturing cost value among the competitors in the industry.
- Technology is appropriate for everyone.
- No allergic reaction to the implant materials.

Disadvantages of TASC
- Disk looses its ability to move (Spinal Fusion).

• Possible crumbling under high degree of impact loading.

• Low machinability.

5.4. Model Evaluation

To be able to manufacture a spinal cage by means of optimum strength, biocompatibility, and suitable form for target market, six design steps were used. Each design step is detailed with various considerations that are important in creating high quality products.

The design of complete product includes the following 6 steps:

1. Creation of product specification
2. Gathering data
3. Recognizing design constrains
4. Design prototypes and test
5. Monitoring the performance
6. Manufacturing the product

For the first step, creation of product specifications, the outline of the product is described as

• this material will be used for spine with the spinal fusion technique

• no bone graft usage

Furthermore, 'this material provides bone-in growth inside its porous structure' describes what the most important concept has related to this invention. In our case the main problem is that patient has disabilities by means of restriction in body movement, apoplexy and in a very good chance drug addiction to prevent heavy aches which are occurred because of the vertebral diseases.

The product eliminates the bone graft usage which is still using in the surgical operations because of porous structure need. Furthermore structural characteristic of this foam material allows bone in growth inside through the material so the product never moves in its cavity which is known as implant loosing. Because the product interacts with the bone, elastic modulus of this material is comparable with the human cortical bone.

After describing the full product specification in detail, the second step is gathering data was performed. During the data gathering, interviewing, observation techniques were used.

All issues about what the present system does and what changes are needed are gathering by either observing or interviewing with Dr. Omer Akcali (orthopedist), Sinan Cetiner (R&D department manager), Prof. Dr.Mustafa Guden, Egemen Akar (researcher).

The design constraints were discussed after gathering all datas.

So the functional constrains are:

• The product should be modular, with the possibility to accept some kind of dimensional changes in vertebra between different sex and age group

• The product should be capable of providing easy in use during the surgical operation

• Forces involved- loading direction, magnitude, load, impact

• Material- biomaterial which is suitable to use in human body

After the product was properly defined, a prototype was build. For the prototype model, cervical (C1-C7) and lumbar (L1-L5) region of the spine was used for negative model.

Vertebras' images taken with a regular scale by the orthopedist Dr. Omer Akcali. This scale was used as a reference material to convert number of pixels between two points to the actual dimension (AD) in mm. W and H represent respectively width and height of the selected region as a relative dimension (RD). To convert the relative dimension to actual dimension, relative dimension was multiplied with multiplication factor determined from the scale.

$$\text{Multiplication factor} = \frac{RD_{sc}}{RD_{sf}}$$

$$AD = RD_{sf} * \text{multiplication factor}$$

AD: actual dimension in mm

RD_{sc} is relative dimension read from the ruler and RD_{sf} is relative dimension read from the software.

In Table 5.4. , the measured dimensions for the first 5 vertebra image coded as 8, 8a, 9, 9a, 10, 10a, 11, 11a, 12, 12a can be seen. The rest of the measurements are in the appendix b.

Table 5.4. Measurements of dimensions (W*H) for the first 5 vertebras.

Image Number	$RD_{sc(mm)\ width}$	$RD_{sc(mm)\ height}$
8	20.11	13.11
8a	20.42	13.63
9	19.48	12.36
9a	21.06	13.42
10	22.02	14.73
10a	19.96	12.25
11	19.78	12.13
11a	20.23	12.4
12	20.56	14.58
12a	20.85	15.03

In the Table 5.5., RD_{sc}, RD_{sf}, multiplication factor, actual dimension (AD) are tabulated for the first 5 vertebras.

Table 5.5. Actual dimensions for the vertebras.

Image Number	$RD_{sc(mm)}$	RD_{sf}	Multiplication Factor	AD(mm)
8	20.11	18.12	1.11	20.11
8a	20.42	2.37	8.6	20.42
9	19.48	1.91	10.2	19.48
9a	21.06	2.22	9.5	21.06
10	22.02	2.45	9	22.02
10a	19.96	2.27	8.8	19.96
11	19.78	2.54	7.8	19.78
11a	20.23	2.56	7.9	20.23
12	20.56	2.67	7.7	20.56
12a	20.85	2.61	8	20.85

According to the first functional constrain, the product should be modular, with the possibility to accept some kind of dimensional changes in vertebra between different sex and age group, the smallest dimensions by means of width and height usage for the product was decided. Because the smallest dimensions are suitable for all age group vertebral body inside the adult group (age bigger than 18), the first functional constraint is done.

In Figure, it was observed two different form of cervical for different regions of the spine.
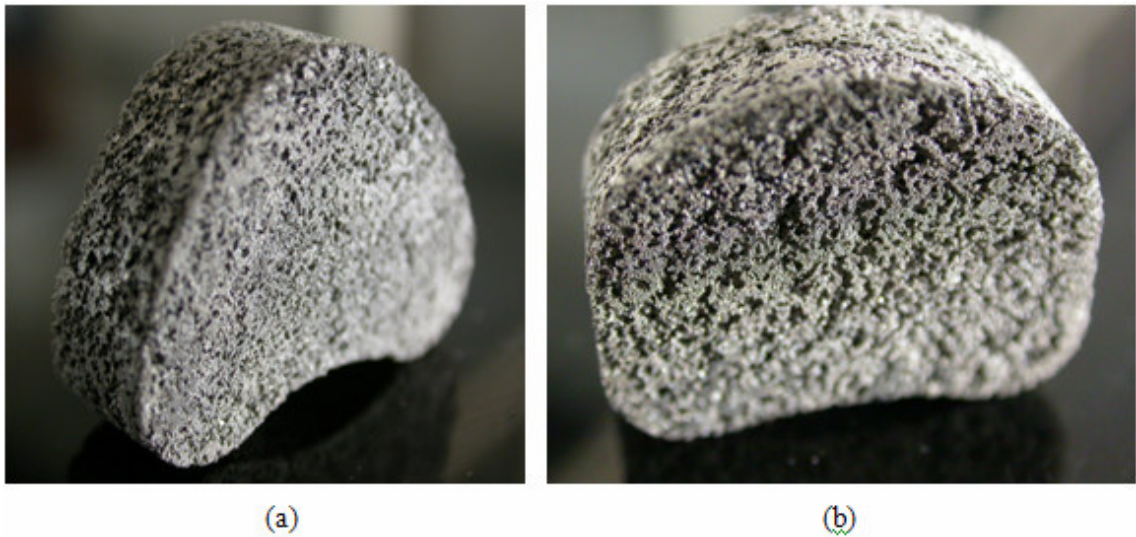
Figure 5.25. (a) Vertebra from cervical region (b) Vertebra from lumbar region.

After first prototype, it was understood that supporting pin is necessary to prevent the motion during and after the surgical operations. The research team (Hipokrat R&D department) gave a decision to put two supporting pins like in Figure 5.26..

Figure 5.26. Second prototype with supporting pins.

According to the feedback data gathered from the second prototype, it was understood that losing of pins from the material inside after the sintering process is to

easy. On the other hand, particle loosing from the sharp edges was observed. To be able to design most reliable model, external type pin usage was decided instead of using internal pin and jacket type protection case produced to prevent sharp edges. Unfortunately, because producing the complex shape as a jacket material was really hard, third prototype had circular cross section. In Figure 5.27., it is obvious that third prototype is more sufficient than the previous 2 prototype model.

Figure 5.27. Third Prototype with supporting pins and jackets.

After getting good responses from the third prototype model, fourth prototype was produced as desired form. The jacket to protect the edges and external pins can be seen in the Figure 5.28..

Figure 5.28. The fourth prototype with external pins.

5.5. Shrinkage Effect

Because foam material could not be compacted with its own protection case, foam material should have to be placed inside the protection case after sintering procedure. Furthermore, since the material lost its volume during the sintering, there was a shrinkage problem. Volumetric shrinkage is calculated as:

$$\%\text{change in volume} = \frac{\Delta V}{V_I}$$

V_i : initial volume of the samples

V_f : final colume of the samples

ΔV : volumetric change

To be able to figure out total idea about all of the sample produced, the averages of ΔV is calculated as 4.43% with the standard deviation of 1.17. In the Figure 5.28., the volumetric change according to change in compaction pressure can be seen. It was observed that increasing the compaction pressure shows increasing behavior on volumetric change.

All the dimensions required for protection case manufacturing were measured after sintering foam material. Because it was seen in the early experiments that the microstructure of the Ti6Al4V does not change, after placing the material inside its own case, the case and material was heated below the 900°C under argon together. Second sintering procedure was only for sintering the Ti6Al4V particles to the protection case.
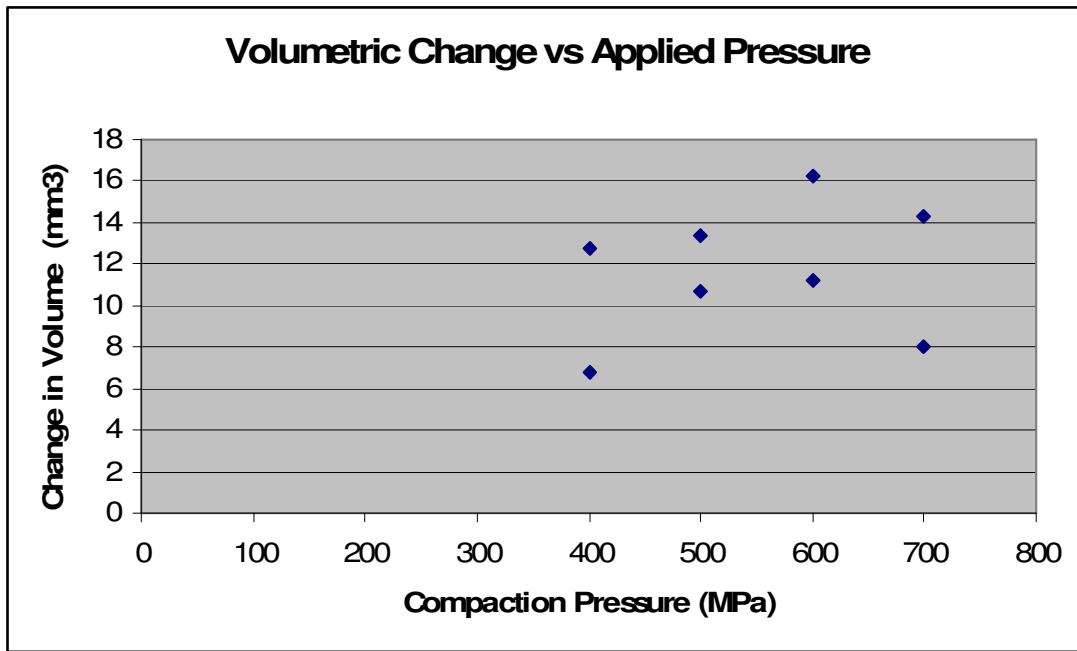
Figure 5.29. Samples compacted under various pressure volume change.

In the Figure 5.29., it is observed that increasing sintering temperature increases the volume change. This means under high temperature sintering, material loses more volume than the lower degrees sintering process.
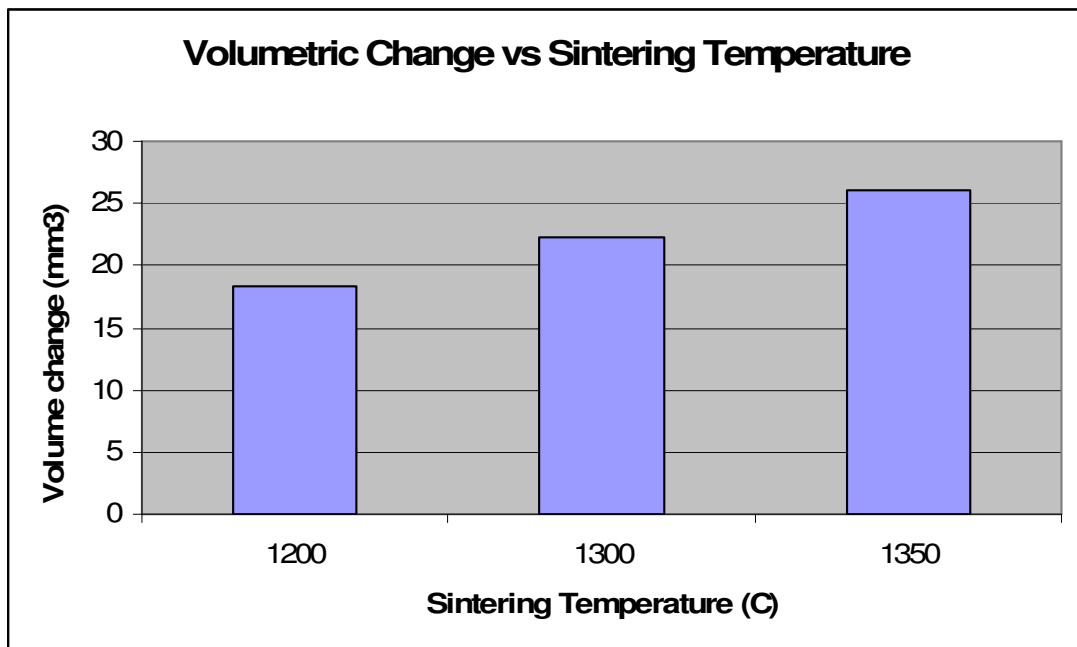
Figure 5.30. Volumetric change according to the change in sintering temprature.

64 samples were sintered under different sintering temperature, sintering time. Samples sintered under the same sintering temperature but different sintering time showed different volumetric changes. In the Figure 5.30. , it is observed that increasing sintering time increases the volumetric change.
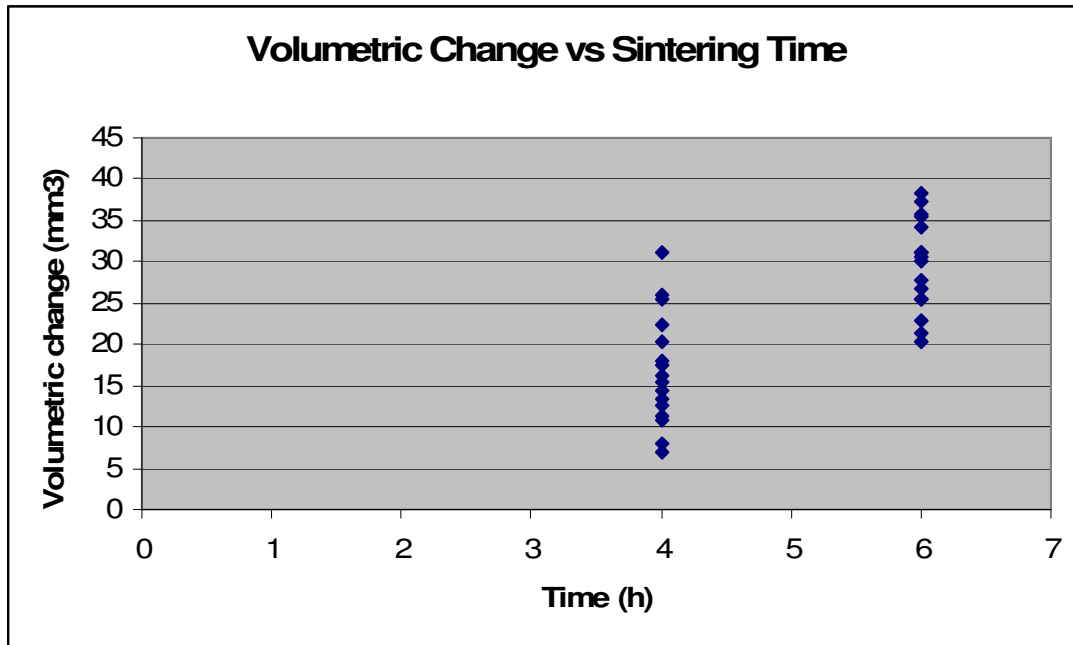
Figure 5.31. Volumetric change under 4h and 6 h sintering time.

The samples were group under two different main categories. They are percentage porosity (50% and 60%) and compaction pressure (400MPa, 500MPa, 600MPa, 700MPa). Different porosity amount in the samples do not show significant amount of changing in volume after sintering process. The Figure 5.31., it can be seen that volumetric change does not change so much by changing porosity level from 50% to 60%.
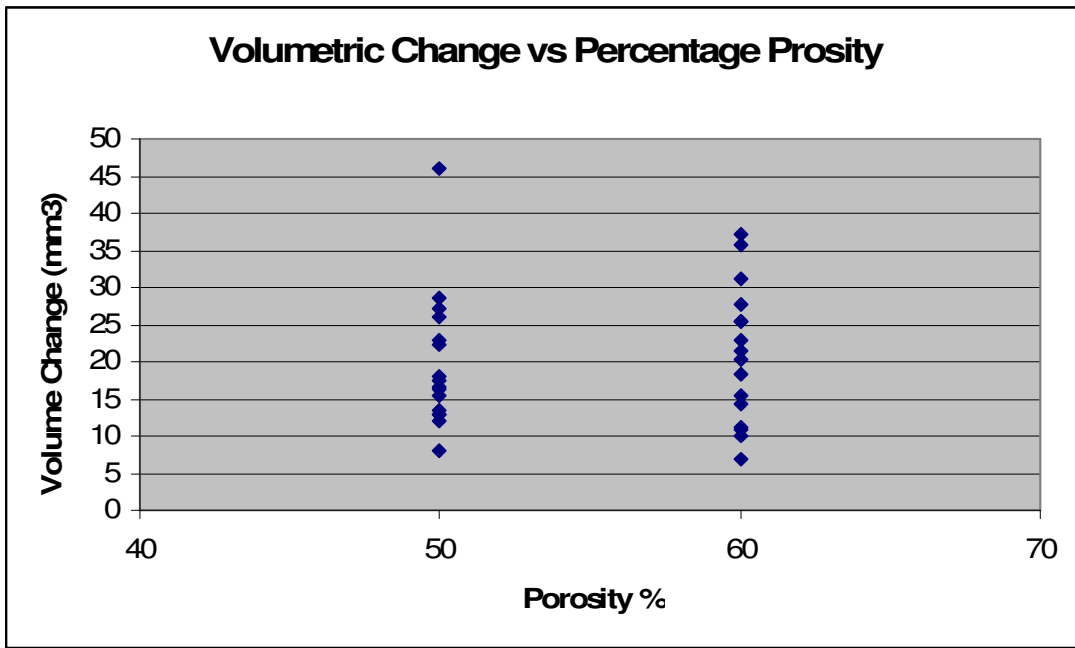
Figure 5.32. Volumetric change after sintering process for samples have different porosity level.

CHAPTER 6

CONCLUSION

This experimental study was conducted to optimization of production parameters (compaction pressure, particle diameter, space holder percentage, sintering temperature and time) to produce stronger Ti6Al4V foams and designing appropriate form that can potentially be used in biomedical applications including human cortical bone replacement and spinal cages for spine surgery. Foams were compacted under 200, 300, 400, 500 and 700 MPa, sintered at 1200 and 1300 °C and 2, 4 and 6 h. The following are concluded :

1. The compression behavior foamed Ti alloy metal varied with cold compaction pressure, sintering temperature and sintering time

2. Foams compacted at 300, 500 and 700 MPa and sintered at 1300 °C for 2 h showed brittle failure. Foams compacted at 500 MPa and sintered at 1300 °C for 6 h showed typical foam metal compression behavior composing localized deformation region and increasing plateau stress.

3. Foams with ductile compression behavior were prepared at cold compaction pressure of 500 MPa at 1300 °C with 6 h sintering time.

4. Foams compacted with 100-150µm particle size Ti6Al4V did not show foam metal compression behavior.

5. 2^2 factorial design methods showed that particle size and percentage porosity of the material are the major parameters should have to be controlled to produce right form cages.

6. PVA (binder) has to be 5% by weight. Less than the experienced amount makes cracks on the surface because during the compaction material loses the binder.

7. Early tests made with the animals in the Hipokrat Surgical Device Manufacturing Company shows that final prototype works. Prototype materials were implanted to 5 different rabbits. After surgical operation, all of them were alive and they were functionally acting like a normal rabbit.

8. Cervical cages with the above parameters were successfully prepared with a porosity of about 60% and pore size of 400 micron.

9. There is a significant interaction between particle size and porosity.

10. Most affective parameters on the processing of Ti6Al4V are compaction pressure, percentage porosity, sintering temperature and particle diameters.

11. The averages of volumetric change because of the sintering process are 4.43% with the standard deviation of 1.17.

12. It is understood that compaction pressure does not have significant effect on shrinkage after sintering process.

13. The form of the final product was determined as material with jacket and supporting pins.

14. Sand blasting was applied to inner surface of the protection case. Sand blasting process is one of the needs to provide better interaction between particles on the Ti6Al4V foam material and case.

15. For the future work, cost analysis should have to be done.

REFERENCES

Avriel, M., Rijckaert, M.J. and Wilde, D.J. 1973. "Optimization and Design", (Prentice-Hall).

Banhart, J. 2001. 'Manufacture, characterization and application of cellular metals and metal foams', *Prog. Mater. Sci*. Vol.46, pp. 559-632.

Box, G. E., Hunter, W.G., Hunter, J.S., Hunter, W.G. 2005. *Statistics for Experimenters: Design, Innovation, and Discovery*, (2nd Edition, Wiley).

Crock, H.V. 1986. "Internal disc disruption: a challenge to disc prolapse 50 years on", *Spine*. Vol.11, pp.650–653.

Cummins, B.H., Robertson, J.T. and Gill, S.G. 1998. "Surgical experience with an implanted artificial cervical joint", *J Neurosurg*. Vol. 88, pp.943–948.

David, T.H. 1999. "Lumbar disc prosthesis: a study of 85 patients reviewed after a minimum follow–up period of five years", *Rachis Revue de Pathologie Vertebrale*. Vol. 11(No. 4–5).

Deiter, M.P. 1988. "Toxicology and carcinogenesis studies of 2–mercaptobenzothiazole in F344/n rats and B6C3F mice", *National Toxicology Program*. Technical Report Series No. 322. (Washington DC: US Department of Health and Human Services).

Desrosières, A. 2004. *The Politics of Large Numbers: A History of Statistical Reasoning, Trans*, (Camille Naish, Harvard University Press).

Elbir, S., Yılmaz, S., Toksoy, K., Guden, M., and Hall, I. W. 2003. "SiC-particulate aluminum composite foams produced by powder compacts: Foaming and compression behavior", *J. Mater. Sci*. Vol.38, pp.4745-4755.

Enker, P. and Steffee, A.D. 1997. "Total disc replacement", in *The textbook of spinal surgery,* edited by K.H. Bridwell and R.L. DeWald. 2nd ed. (Philadelphia: Lippincott–Raven), pp. 2275–2288.

Enker, P. and Steffee, A.D. 1997. "Total disc replacement" in *The textbook of spinal surgery,* edited by K. H. Bridwell and R. L. DeWald, 2nd ed. (Philadelphia: Lippincott–Raven), pp. 2290–2296.

Enker, P., Steffee, A., Mcmillan, C., Keppler, L., Biscup, R. and Miller, S. 1993. "Artificial disc replacement. Preliminary report with a 3–year minimum follow–up", *Spine*. Vol.18, pp.1061–1070.

Frank, Y. and Kenneth M. 1963. "Biographical Memoirs of Fellows of the Royal Society of London", Vol. 9, pp. 91-120.

Gibson, L. J., and Ashby, F. 1997. *Cellular solids: structure and properties*, (Cambridge University Press).

Griffith, S.L., Shelokov, A.P., Büttner–Janz, K., LeMaire, J.P. and Zeegers, W.S. 1994. "A multicenter retrospective study of the clinical results of the LINK® SB Charité intervertebral prosthesis. The initial European experience", *Spine.* Vol.19, pp.1842–1849.

Hacking, I. 1990. "The Taming of Chance", (Cambridge University Press).

Hedman, T.P., Kostuik, J.P., Fernie, G.R. and Hellier, W.G. 1992. "Design of an intervertebral disc prosthesis", *Spine.* Vol.16 (Suppl 6), pp. 256–260.

Kääpä, E., Holm, S., Han, X., Takala, T., Kovanen, V. and Vanharanta, H. 1994. "Collagens in the injured porcine intervertebral disc", *J Orthop Res.* Vol.12, pp. 93–102.

Keller, T.S., Hansson T.H., Abram, A.C., Spengler, D.M. and Panjabi M.M. 1989. "Regional variations in the compressive properties of lumbar vertebral trabeculae", *Spine.* Vol. 14, pp. 1012–1019

Körner, C. and Singer, R. F. 2002. "Processing of metal foams-challenges and opportunities", *Adv. Eng. Mater.* Vol. 2, pp. 159-165.

Keller, T.S., Hansson, T.H., Abram, A.C., Spengler, D.M. and Panjabi, M.M. 1989. "Regional variations in the compressive properties of lumbar vertebral trabeculae. Effects of disc degeneration", *Spine.* Vol.14, pp.1012–1019.

Kirkaldy–Willis, W.H., Wedge, J.H., Yong–Hing, K. and Reilly, J. 1986. "Pathology and pathogenesis of spondylosis and stenosis", *Spine.* Vol.3, pp.319–328.

Kostuik, J.P. 1997. "Intervertebral disc replacement", in *The textbook of spinal surgery,* edited by K.H. Bridwell and R.L. DeWald, (Philadelphia: Lippincott–Raven), pp. 2269–2273.

Kulkarni, S.B. and Ramakrishnan, P. 1973. *Int J Powder Met.* Vol. 9:41.

Lee, C.K., Langrana, N.A., Parsons, J.R. and Zimmerman, M.C. 1991. "Development of a prosthetic intervertebral disc", *Spine.* Vol.16 (Suppl 6), pp. 253–255.

Lemaire, J.P., Skalli, W. and Lavaste, F. 1997. "Intervertebral disc prosthesis. Results and prospects for the year 2000", *Clin Orthop.* Vol. 337, pp. 64–76.

Lindley, D.V. 1985. "Making Decisions", (2nd ed., John Wiley & Sons).

Link, H.D.and Link, S.B. 1999. "Charité III intervertebral dynamic disc spacer", *Rachis Revue de Pathologie Vertebrale.* Vol.11.

Marieb, E.N. 1998. *Human Anatomy & Physiology,* edited by Menlo Park, (California: Benjamin/Cummings Science Publishing).

Marnay, T. 1991. "L'arthroplastie intervertébrale lombaire", *Med Orthop.* Vol. 25, pp.48–55.

Martin, B. Stiller, C. Buchkremer, H. P. Stöver, D. and Baur, H. 2000. "High purity titanium, stainless steel and super alloy parts", *Adv. Eng. Mater.* Vol. 2, pp. 196-199.

Netter, Frank H. 1987. *Musculoskeletal system: anatomy, physiology, and metabolic disorders*, (Summit, New Jersey: Ciba-Geigy Corporation).

Pearce, R.H., Grimmer, B.J., Adams, M.E. 1987. "Degeneration and the chemical composition of the human lumbar intervertebral disc", *J Orthop Res.* Vol. 5, pp.198–205.

Pillar, R. M. 1987. "Porous-surfaced metallic implants for orthopedic applications", *J. Biomed. Mater. Res.* Vol. 21, pp. 1-3.

Ray, C.D., Schönmayr, R., Kavanagh, S.A. and Assell R. 1999. "Prosthetic disc nucleus implants", *Riv Neuroradiol.* Vol. 12 (Suppl 1), pp.157–162.

Ronald, F. 1926. "The Arrangement of Field Experiments", *Journal of the Ministry of Agriculture of Great Britain.* Vol.33, pp. 503-513.

Rothman, R.H., Simeone F.A. and Bernini P.M. 1982. "Lumbar disc disease", in *The spine*, edited by Rothman R.H. and Simeone F.A., 2nd ed. (Philadelphia: WB Saunders), pp. 508–645.

Schönmayr, R., Busch, C., Lotz, C. and Lotz–Metz, G. 1999. "Prosthetic disc nucleus implants: the Wiesbaden feasibility study. 2 years follow–up in ten patients", *Riv Neuroradiol.* Vol.12 (Suppl 1), pp.163–170.

Siddall, J.N. 1982. "Optimal Engineering Design", (CRC).

Stigler, S. M. 1990. "The History of Statistics: The Measurement of Uncertainty before 1900", (Belknap Press/Harvard University Press).

Tortora, G. J. 1989. *Principles of Human Anatomy*, 5th ed. (New York: Harper & Row, Publishers).

Vernon–Roberts, B. and Pirie, C.J. 1977. "Degenerative changes in the intervertebral discs of the lumbar spine and their sequelae", *Rheumatol Rehab.* Vol.16, pp.13–21.

Watkins, R.G. 1987. "Results of anterior interbody fusion" in *Lumbar spine surgery: techniques and complications,* edited by A. H. White, R.H. Rothman, C.D. Ray, (St. Louis: CV Mosby), pp. 408–432.

Weiner, S. and Wagner, H. D. 1998. "The material bone:structure-mechanical function relations", *Annu. Rev. Mater. Sci.* Vol. 28, pp. 271-298.

Weiner, S. and Wagner, H. D. 1998. "The material bone: structure-mechanical function relation", *Annu. Rev. Mater. Sci.* Vol. 28, pp. 271-298.

Weinstein, P.R. 1982. "Anatomy of the lumbar spine" ,in *Lumbar disc disease*, edited by Hardy R.W. (New York: Raven Press), pp. 5–15.

Weinstein, J.N. 1992. "Clinical efficacy and outcome in the diagnosis and treatment of low back pain" (New York: Raven Press).

Wen, C. E., Yamada, Y., Shimojima, K., Chino, Y., Asahina, T., and Mabuchi, M. 2001. "Processing and mechanical properties of autogenous titanium implant materials", *J. Mater. Sci*. Vol.13, pp.397-401.

Wen, C. E., Mabuchi, M., Yamada, Y., Shimojima, K., Chino, Y., and Asahina, T. 2001. "Processing of biocompatible porous Ti and Mg. Script. Mat.", *J. Mater. Sci.* Vol. 45, pp.1147-1153.

Whitfield, J. Morley, P. Willick, G. C.C. 2000. "The Parathyroid Hormones: Bone-Forming Agents for Treatment of Osteoporosis", *Medscape Women's Health eJournal.* Vol. 5, pp. 5.

APPENDIX A

DIMENSIONING METHOD
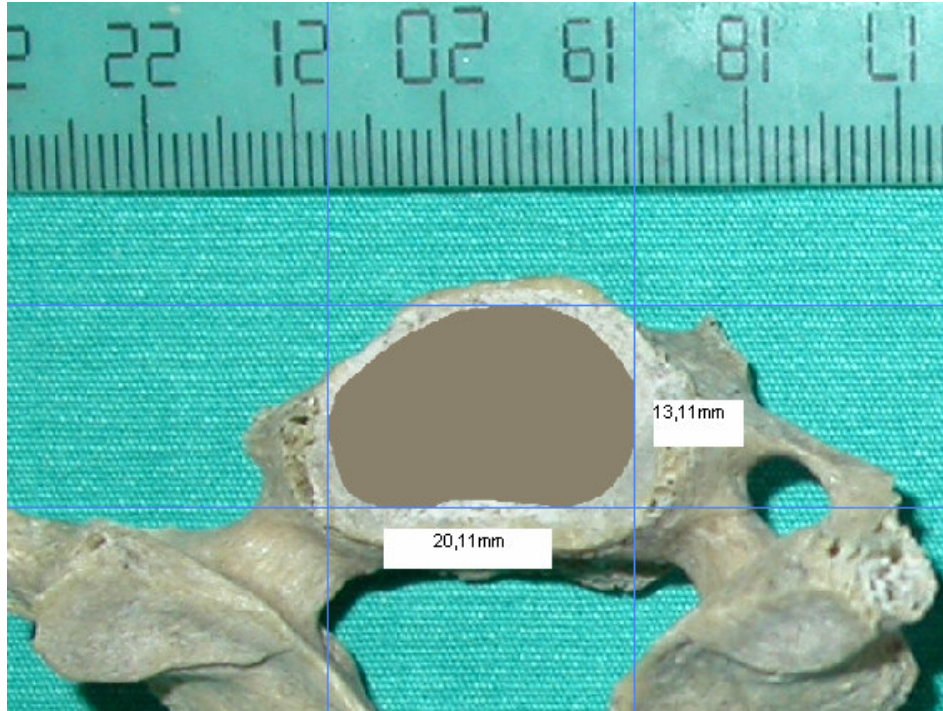
Figure A.1. Vertebra number 8-1.
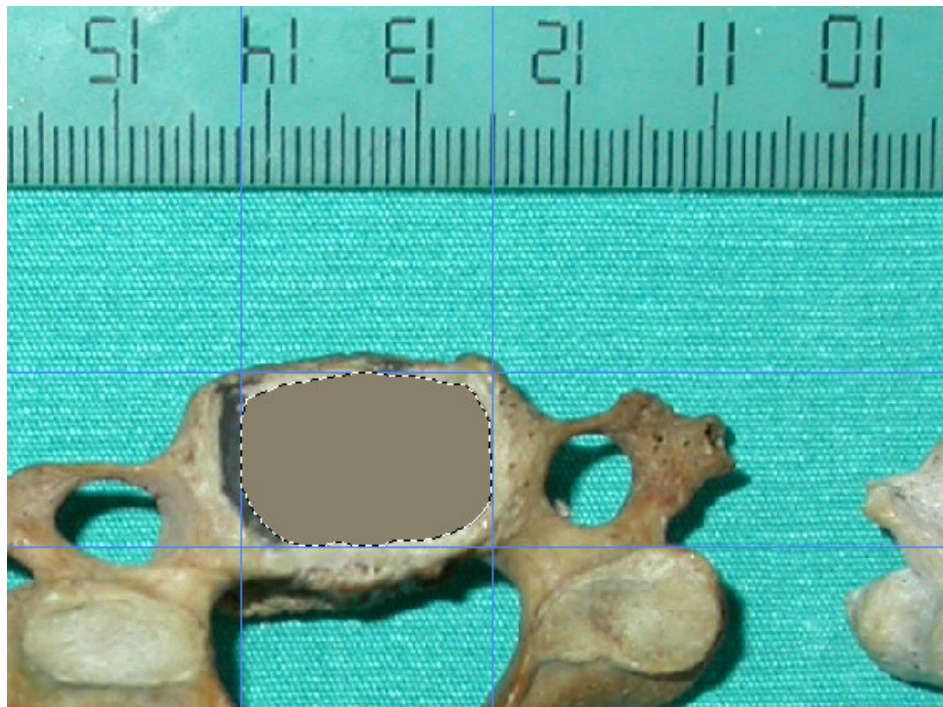
Figure A.2. Vertebra number 8-2.

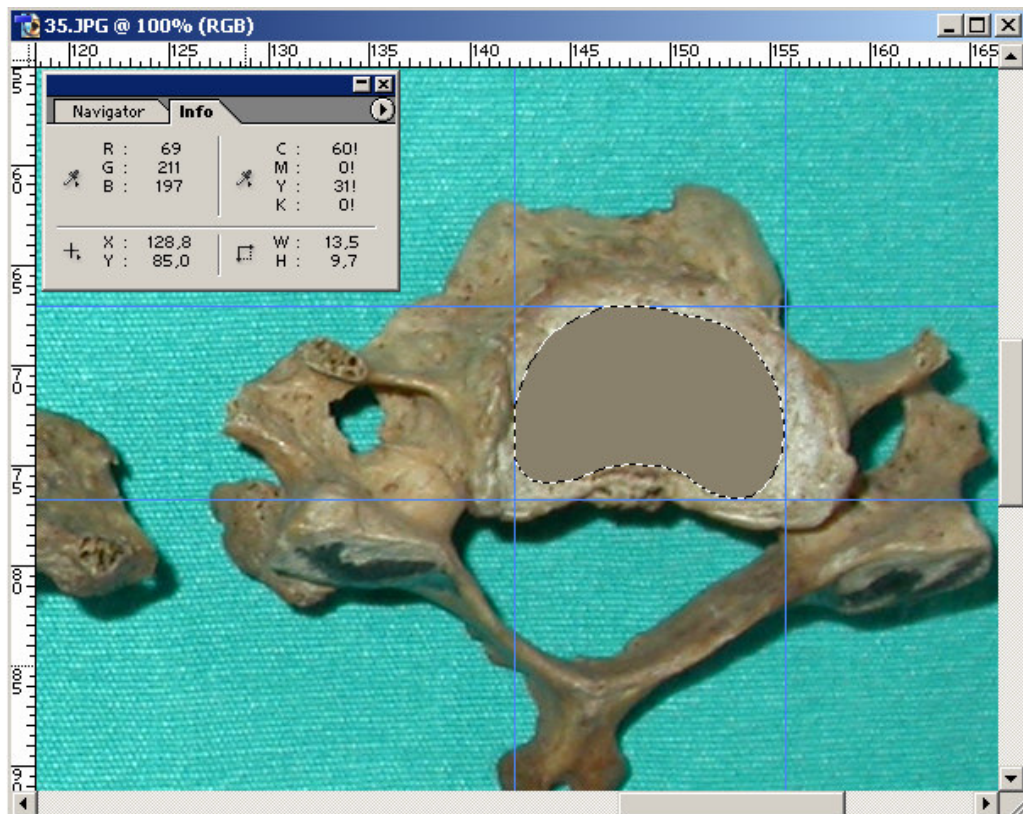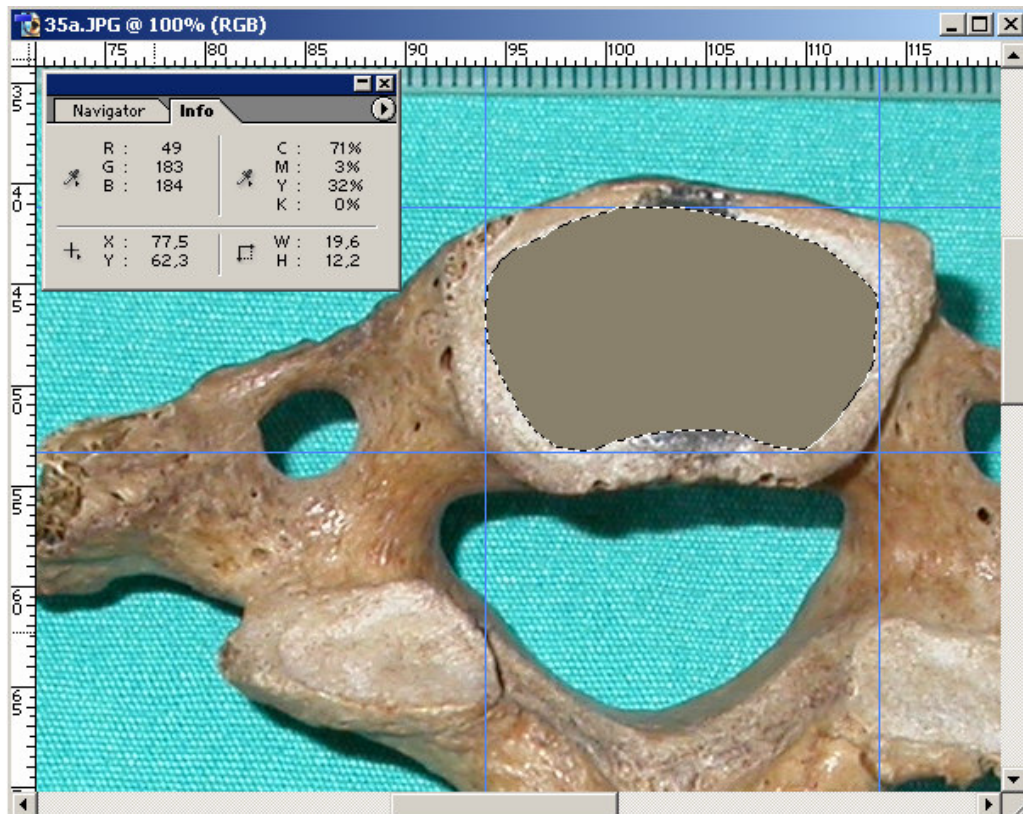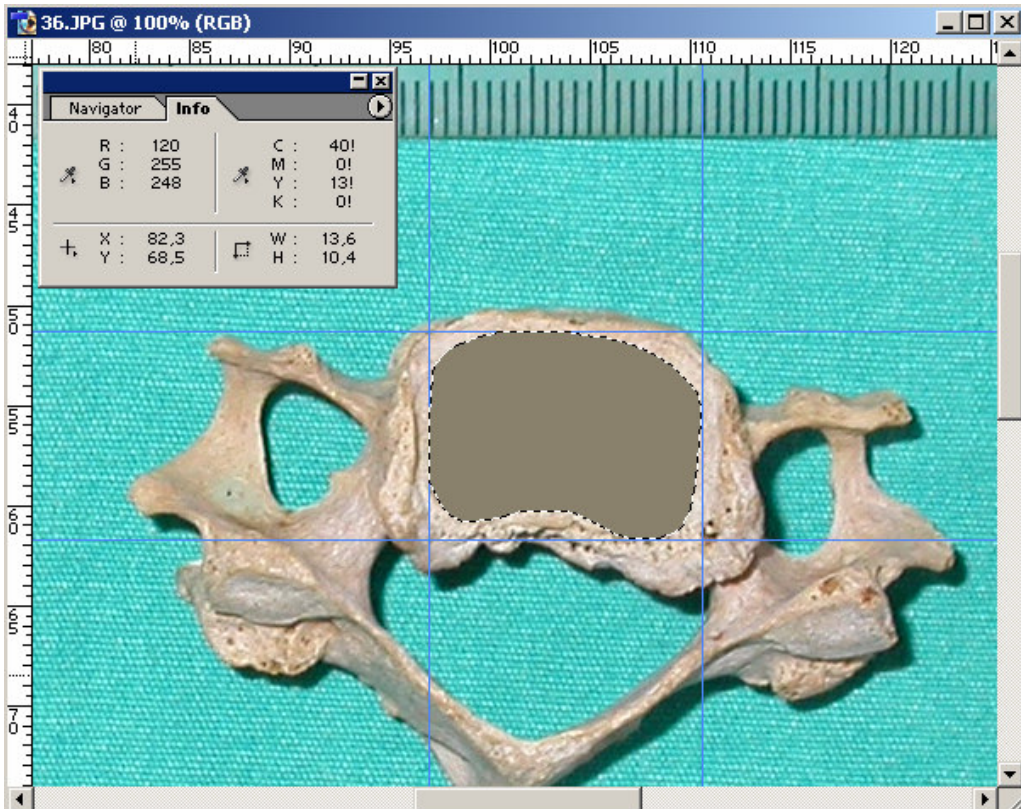Figure A.3. Vertebra number 8-3.

Figure A.4. Vertebra number 8a-1.
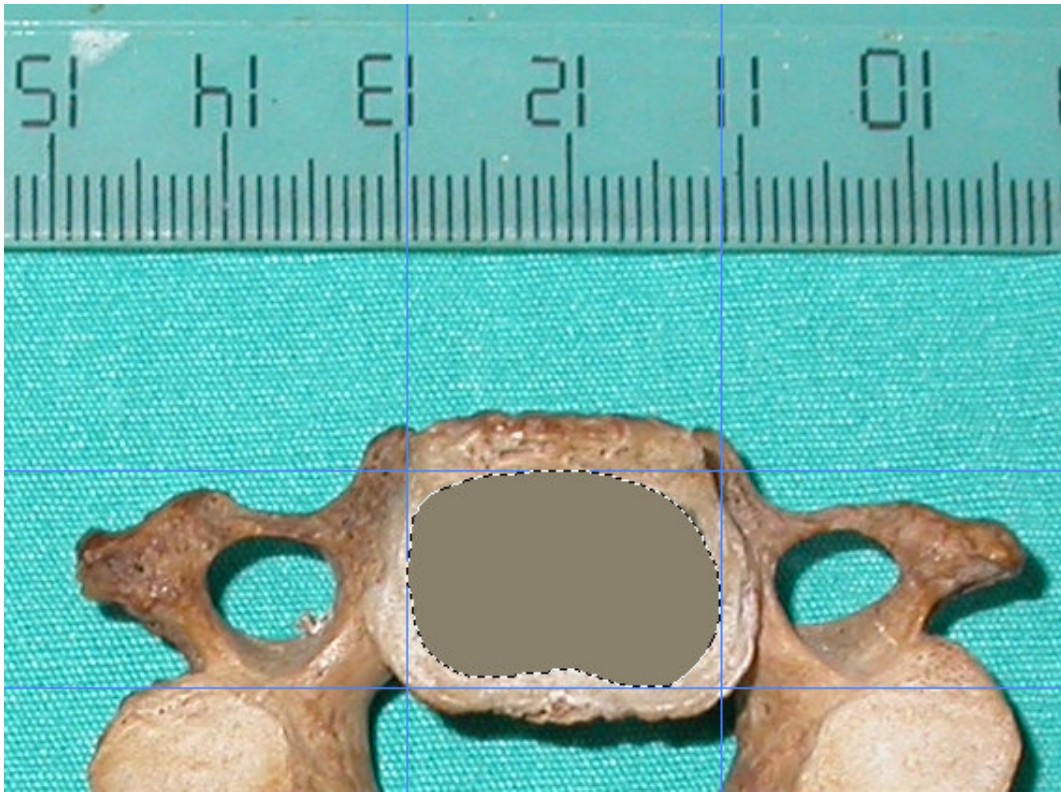
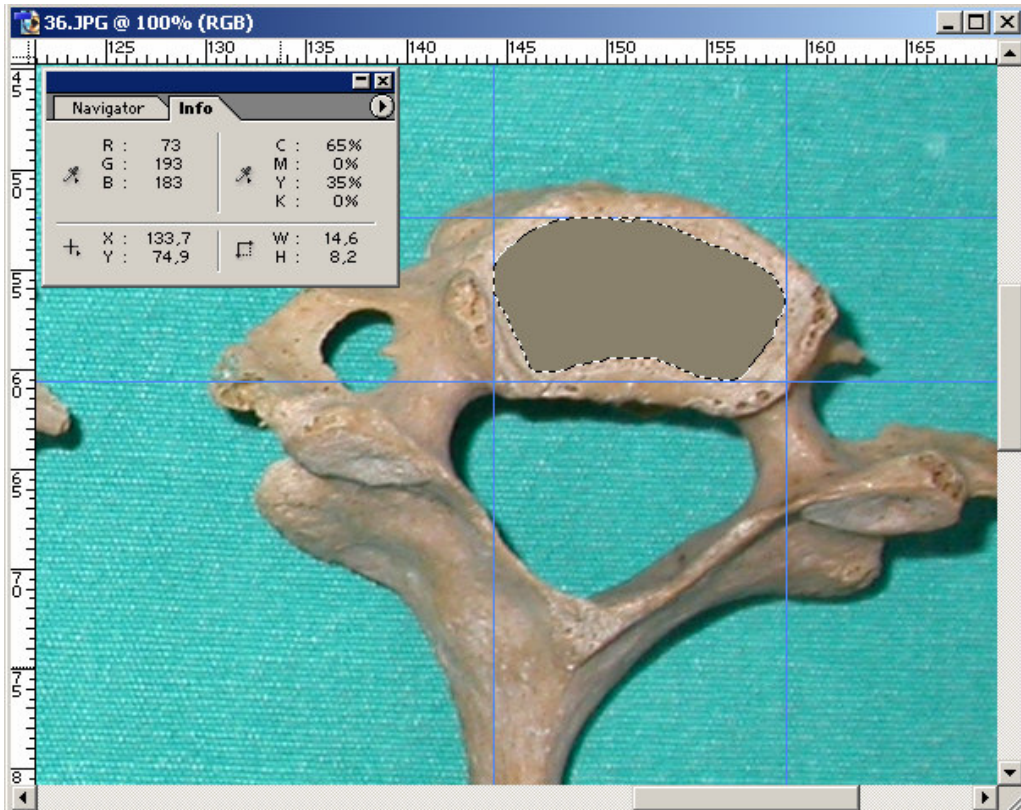Figure A.5. Vertebra number 8a-2.
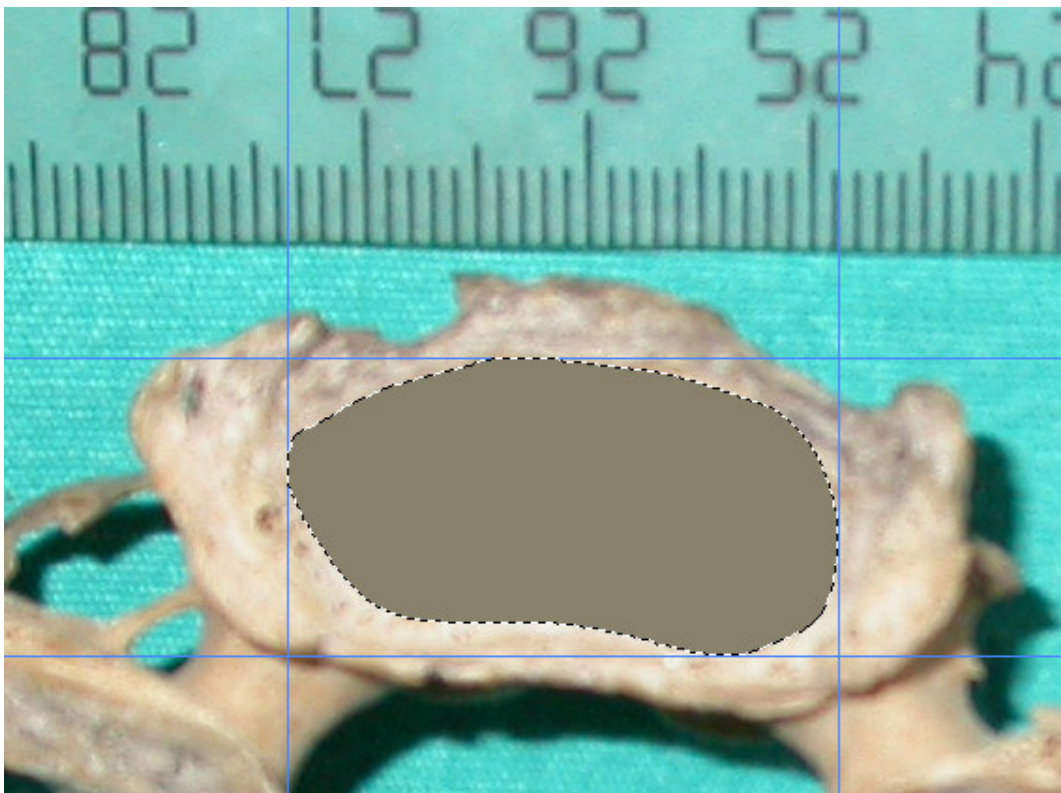
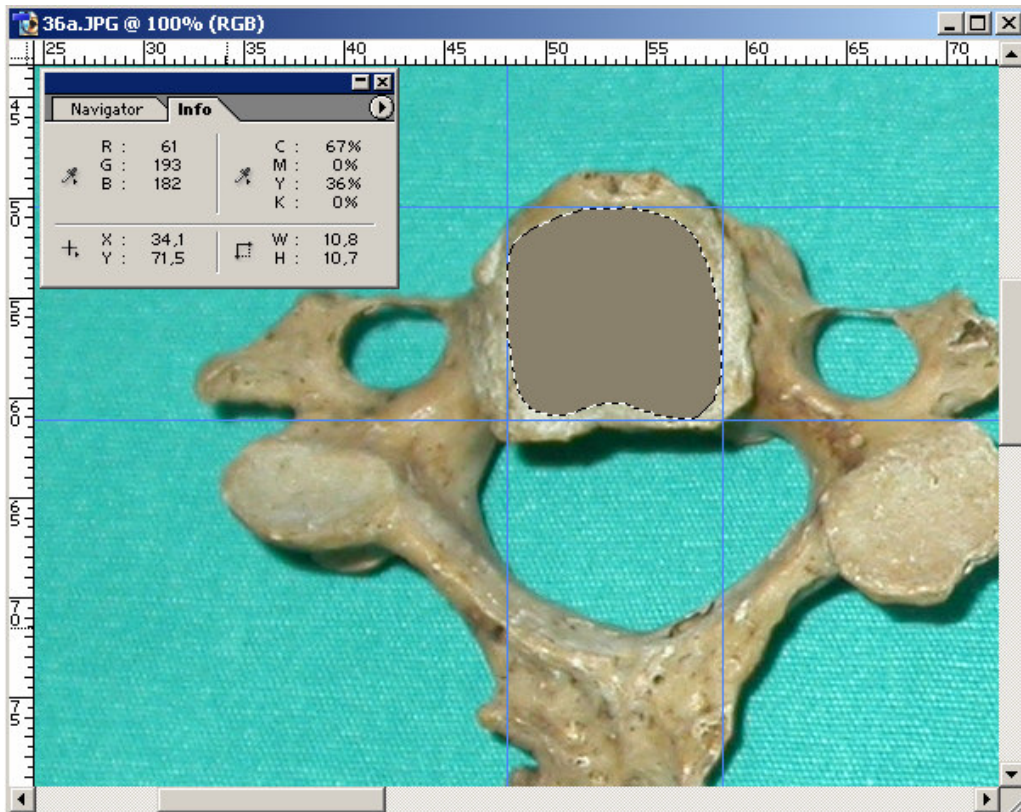Figure A.6. Vertebra number 9-1.
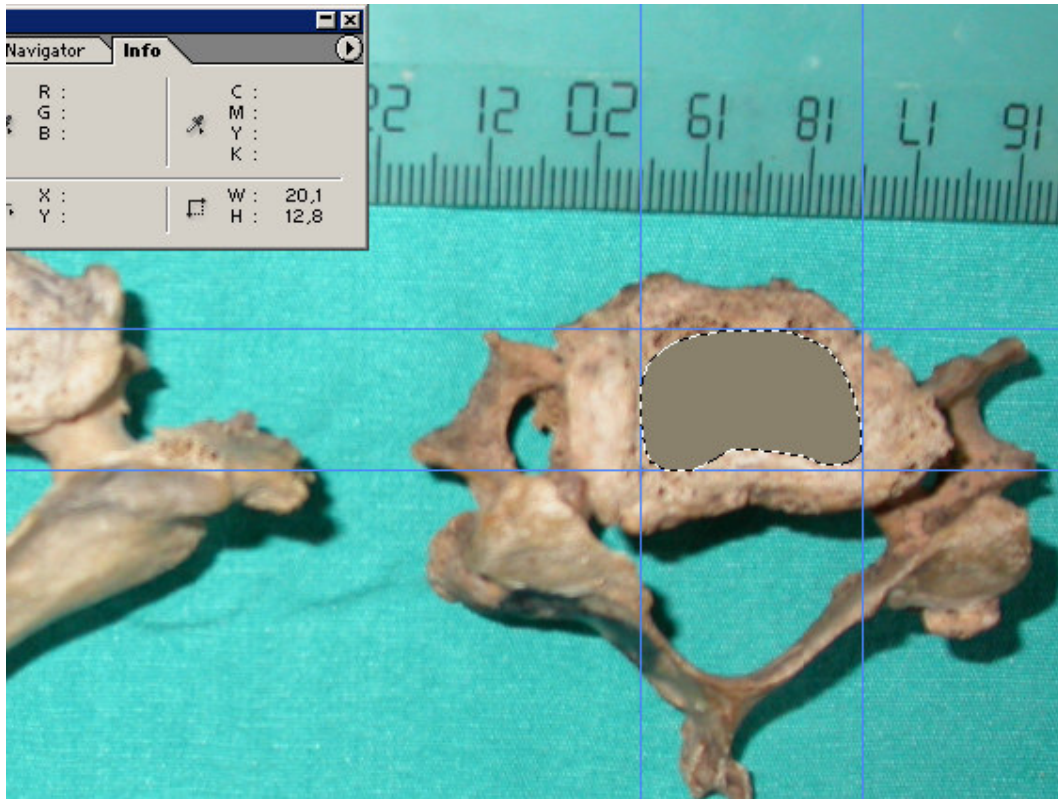
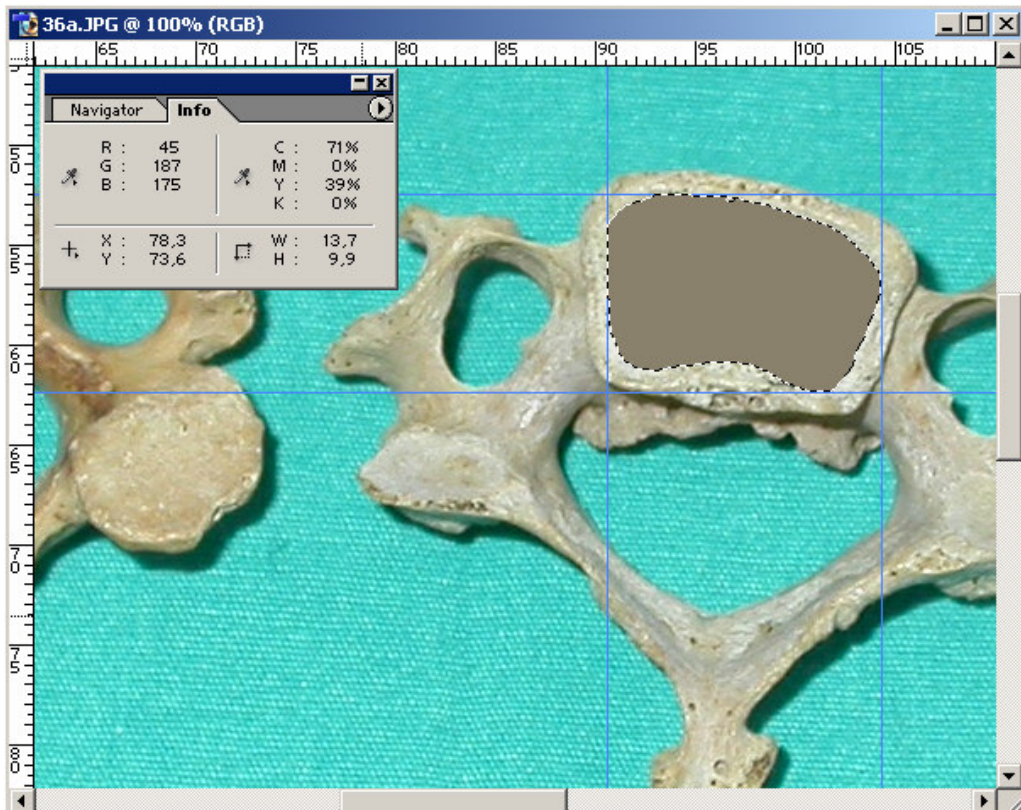Figure A.10. Vertebra number 9-2.
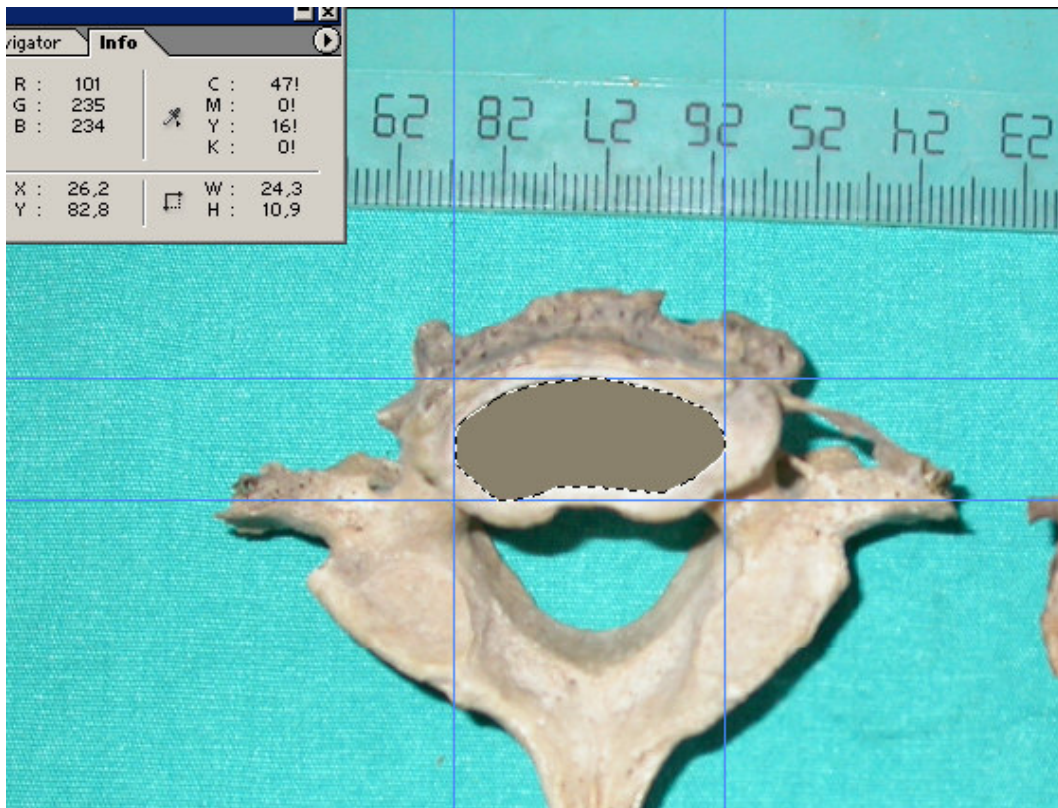
Figure A.11. Vertebra number 9-3.
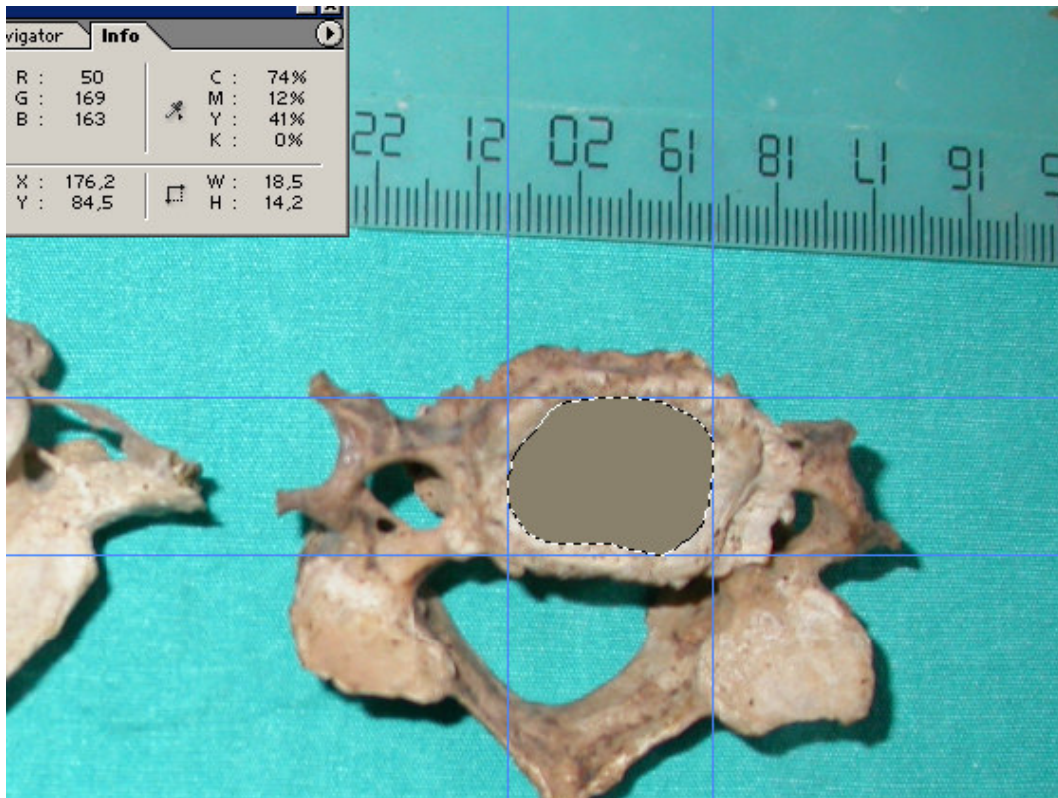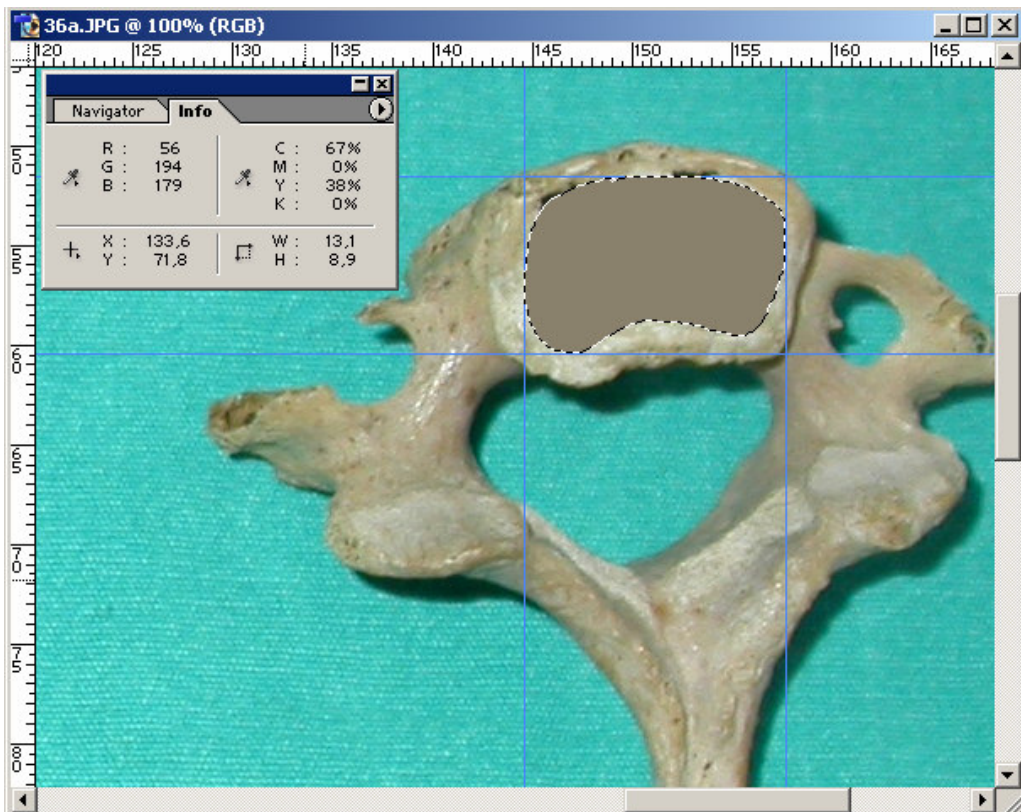
Figure A.12. Vertebra number 9a-1.
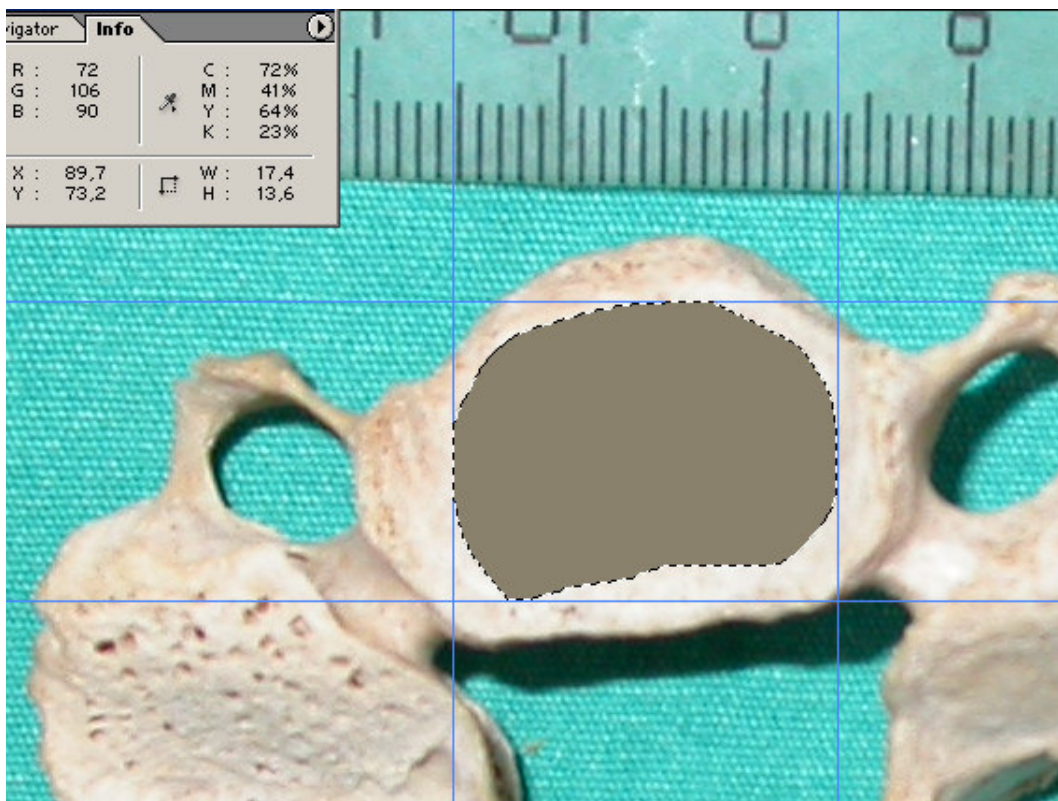
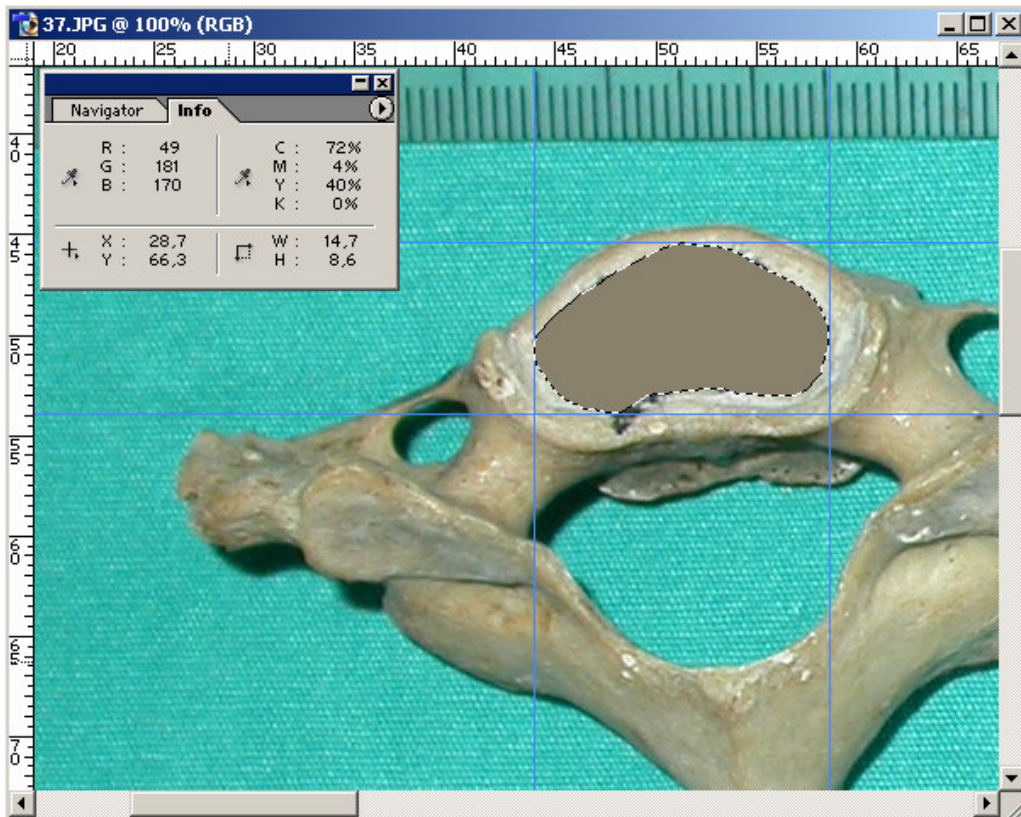Figure A.13. Vertebra number 9a-2.
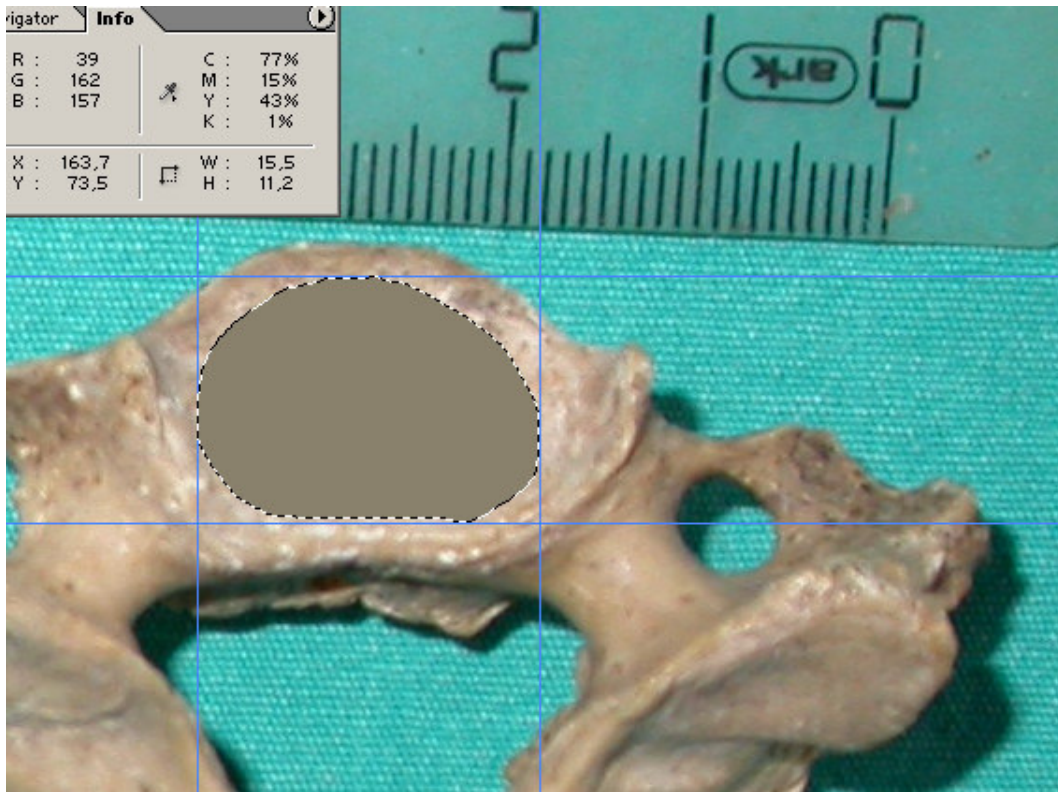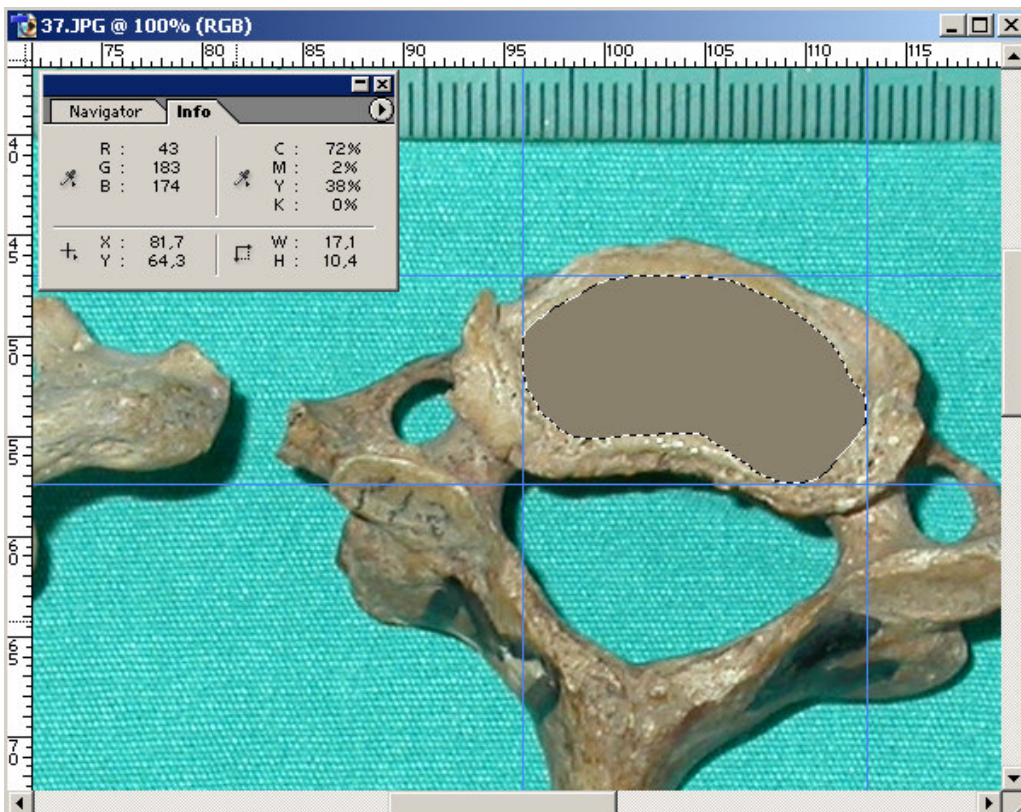
Figure A.14. Vertebra number 10-1.
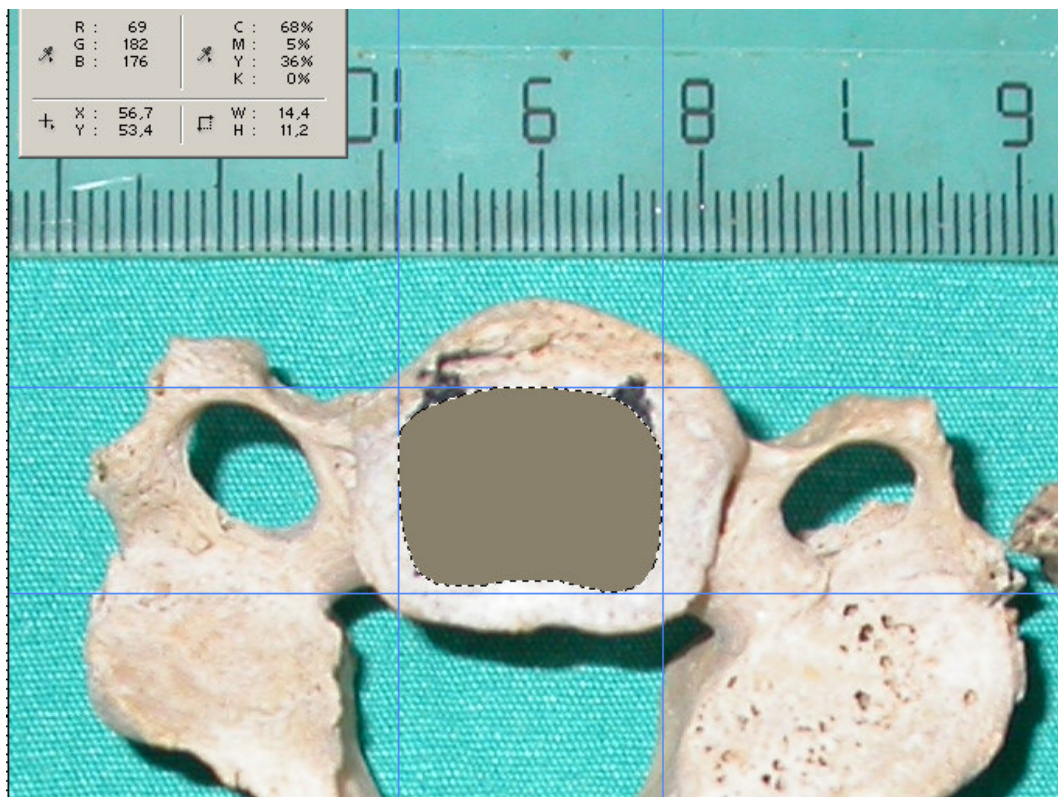
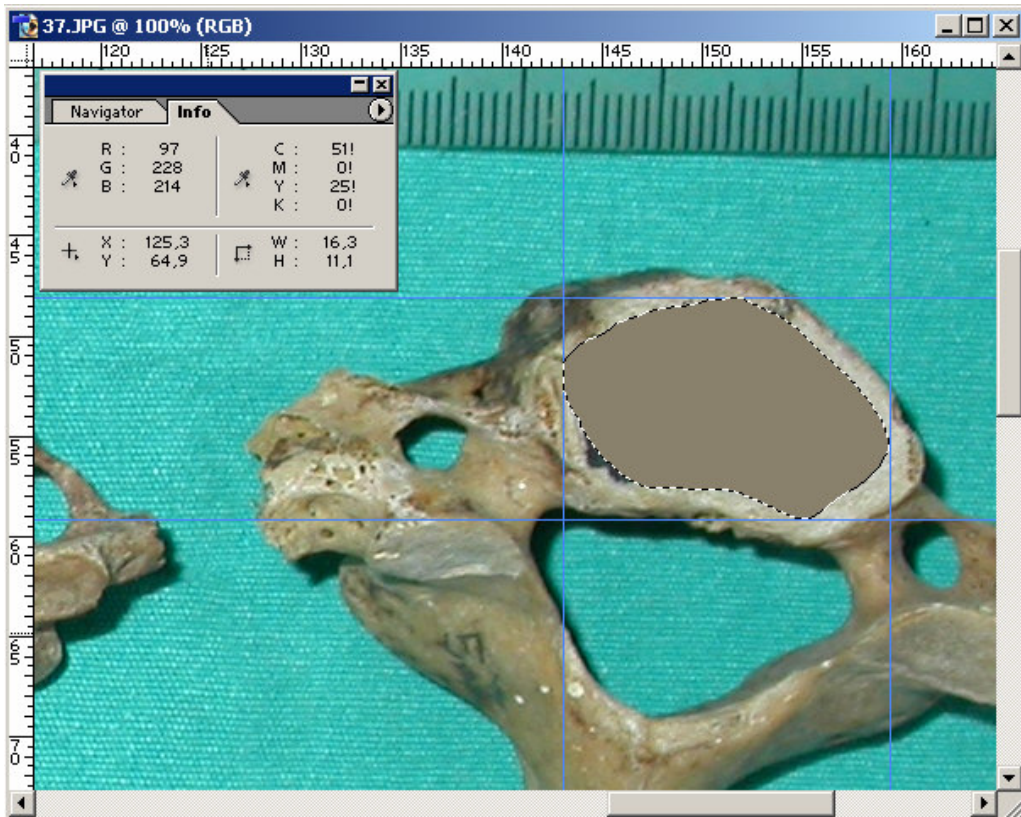Figure A.15. Vertebra number 10-2.
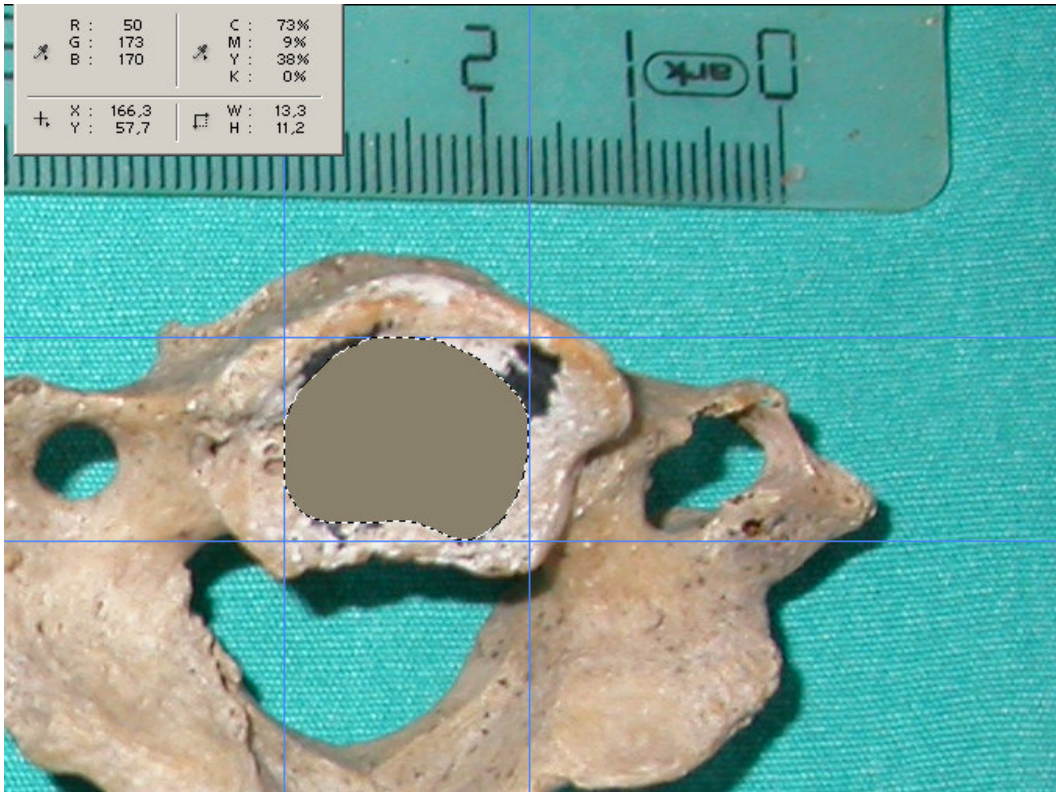
Figure A.16. Vertebra number 10a-1.
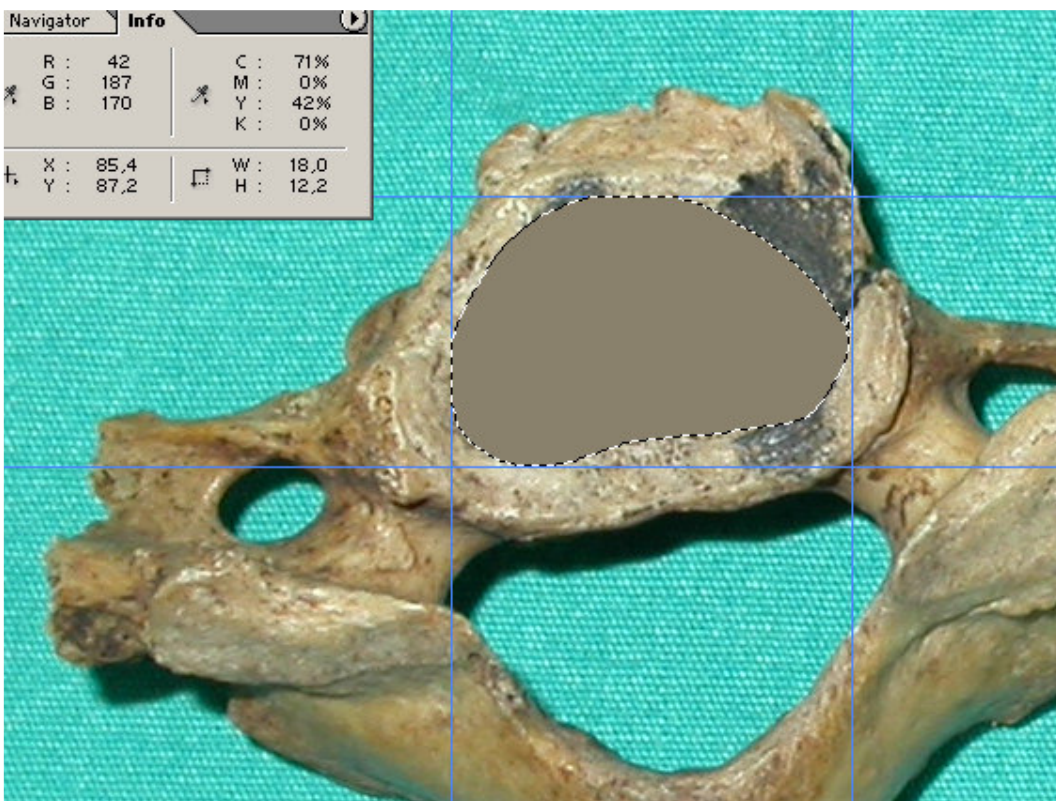
Figure A.17. Vertebra number 10a-2.
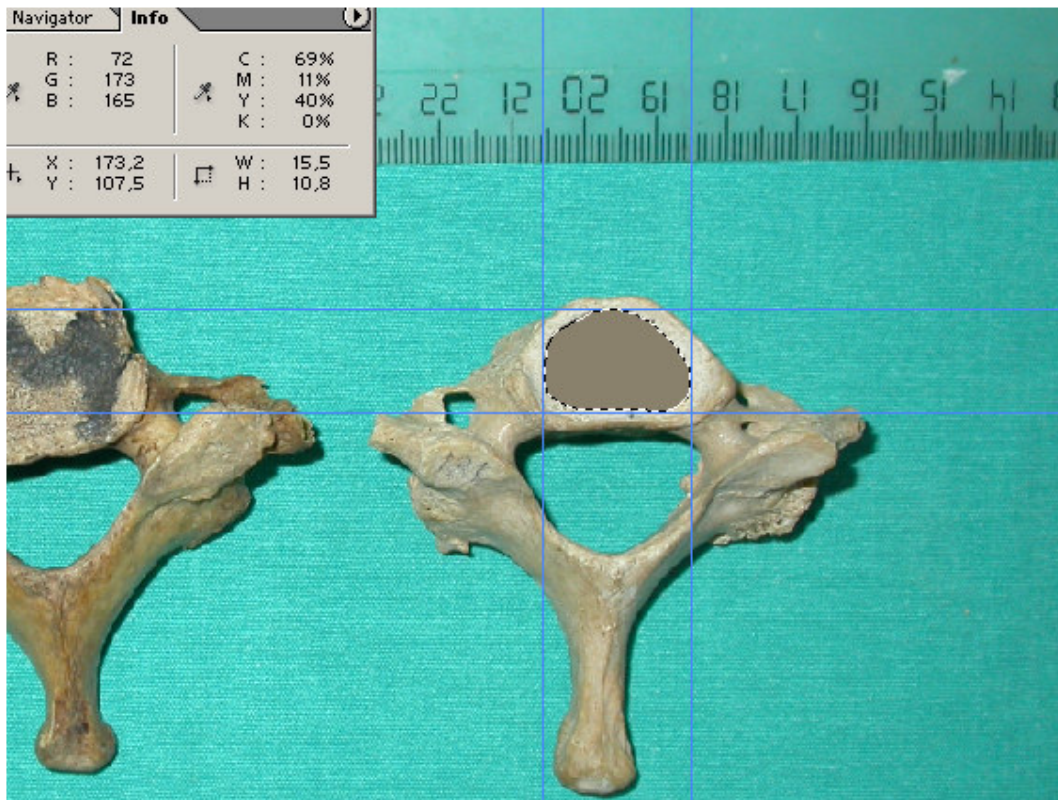
Figure A.18. Vertebra number 11-1.
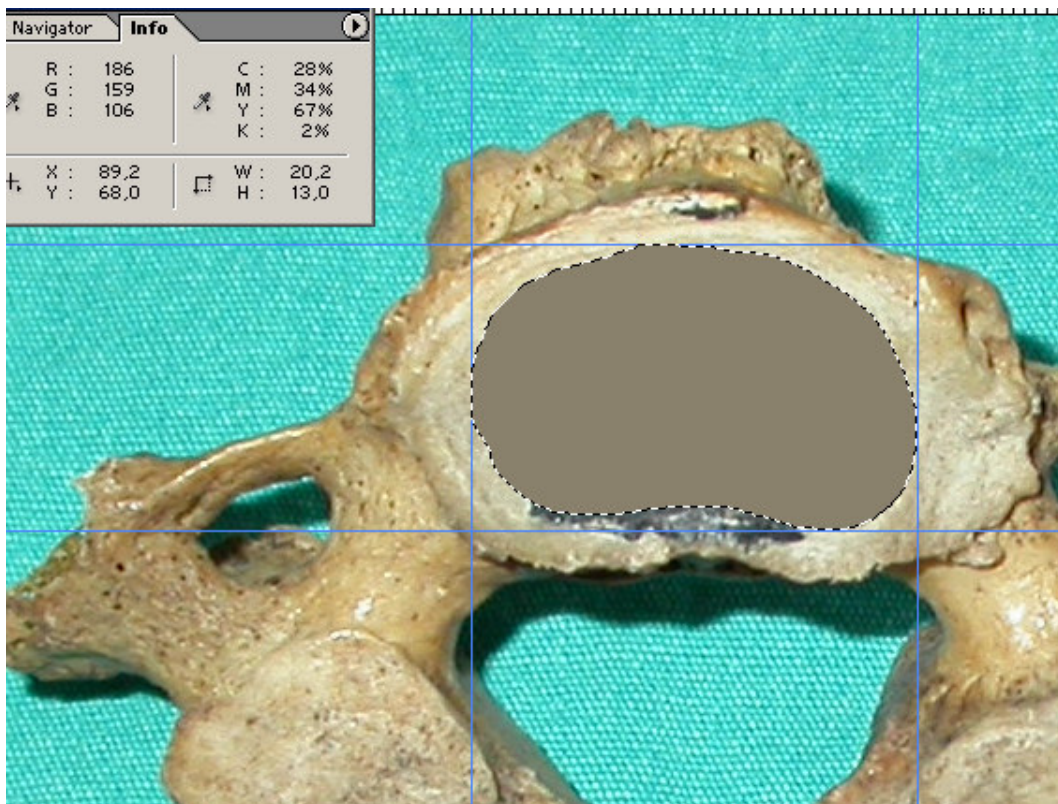
Figure A.19. Vertebra number 11-2.
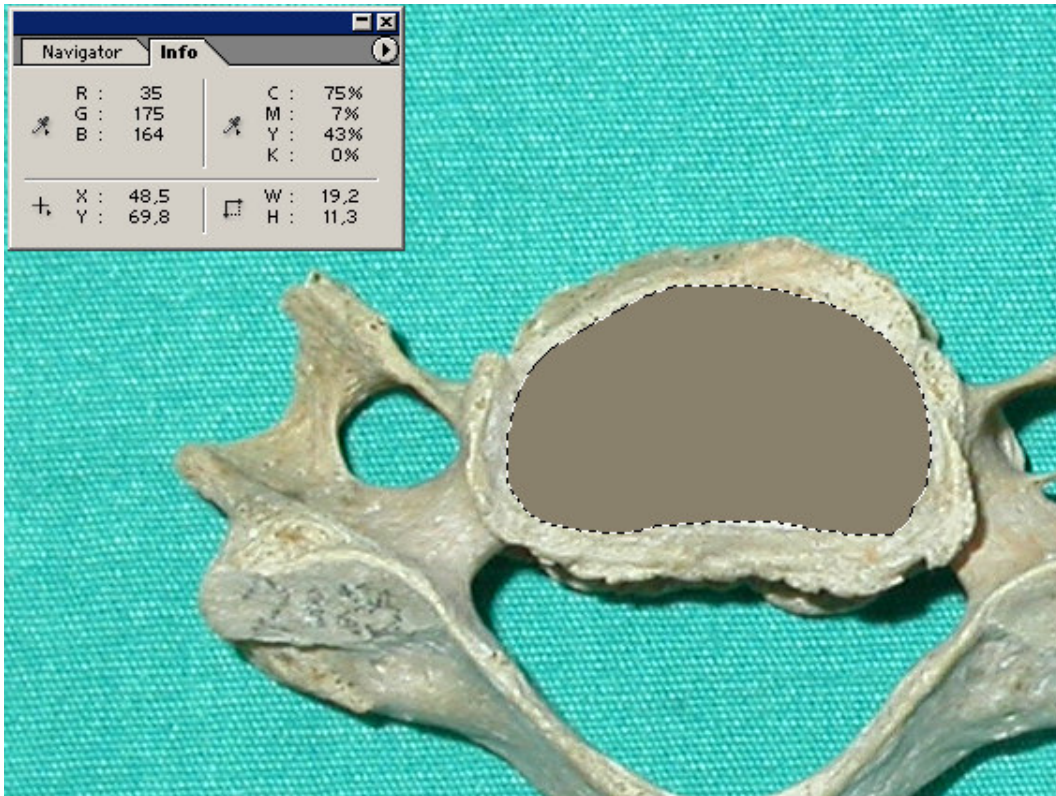
Figure A.20. Vertebra number 11a-1.
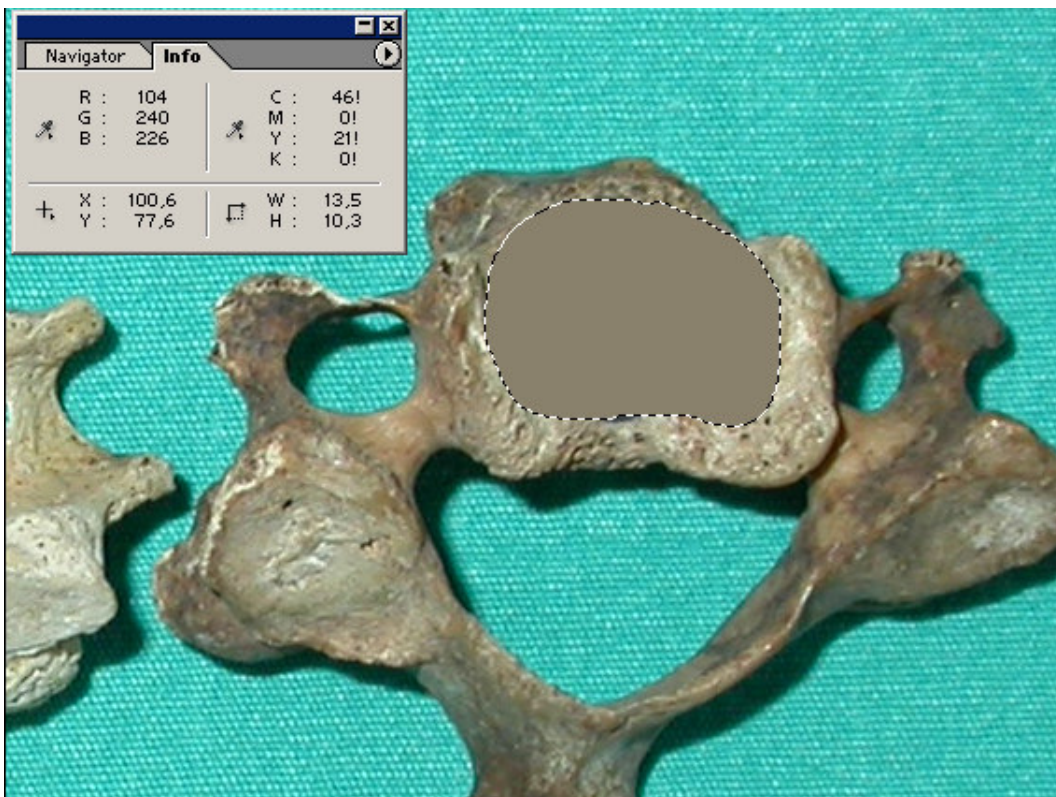
Figure A.21. Vertebra number 11a-2.
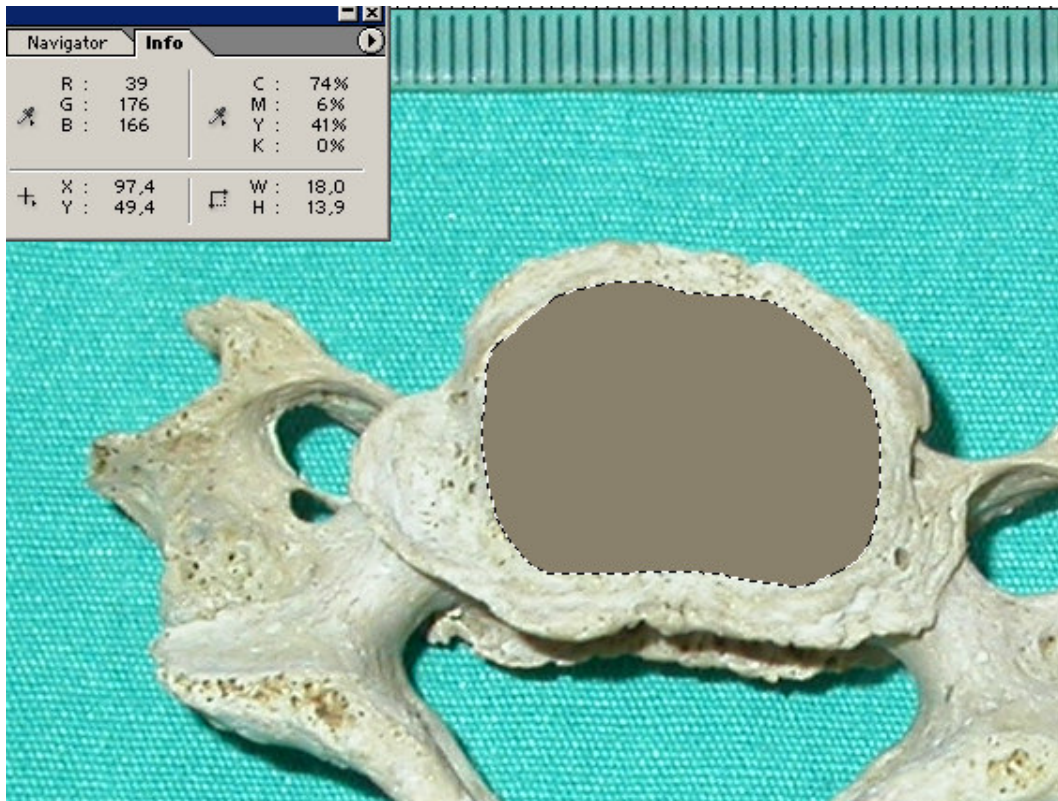
Figure A.22. Vertebra number 12-1.
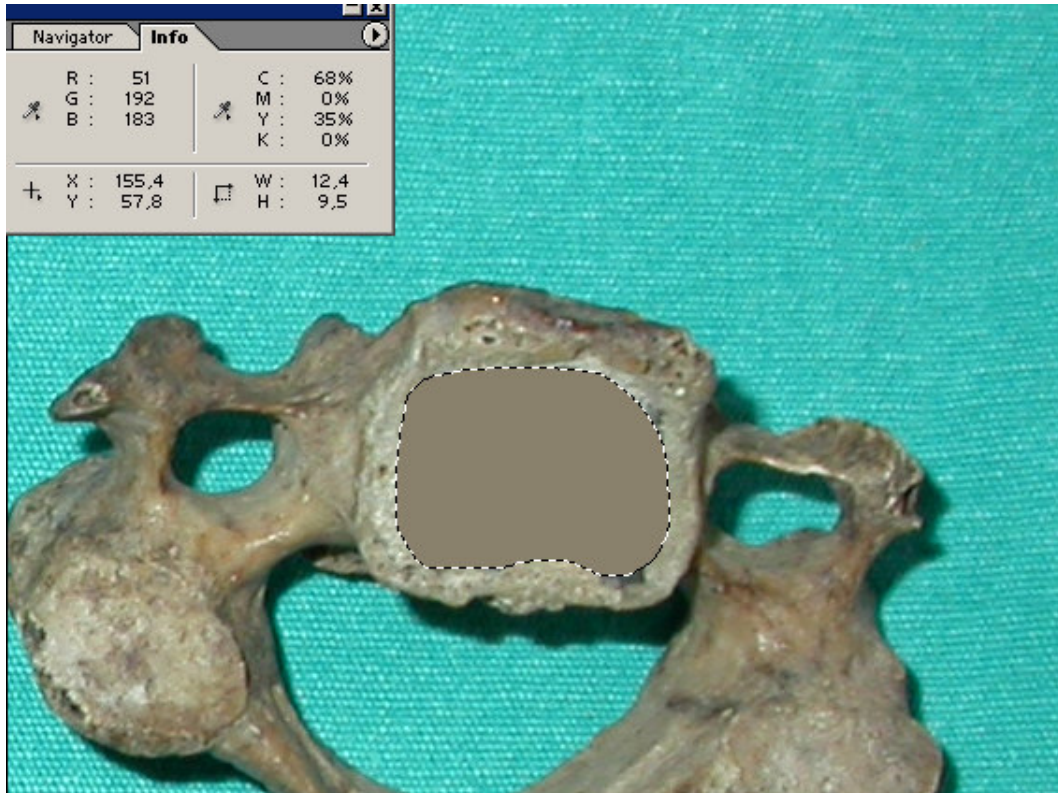
Figure A.23. Vertebra number 12-2.
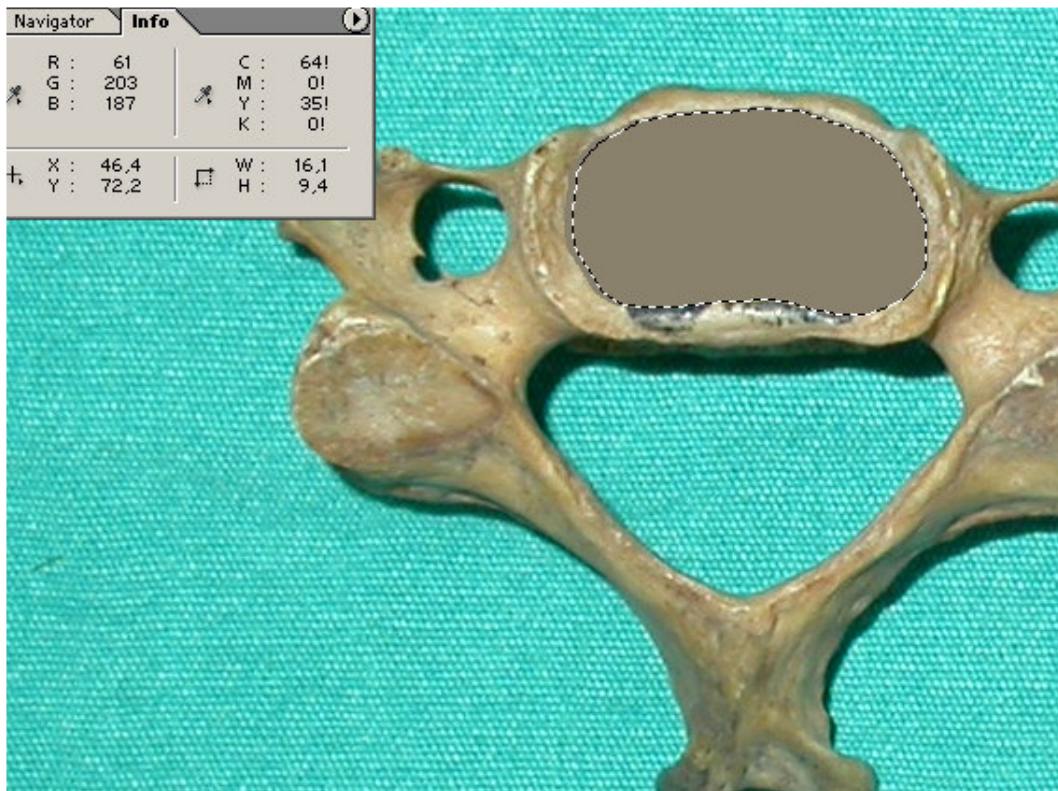
Figure A.24. Vertebra number 12a-1.
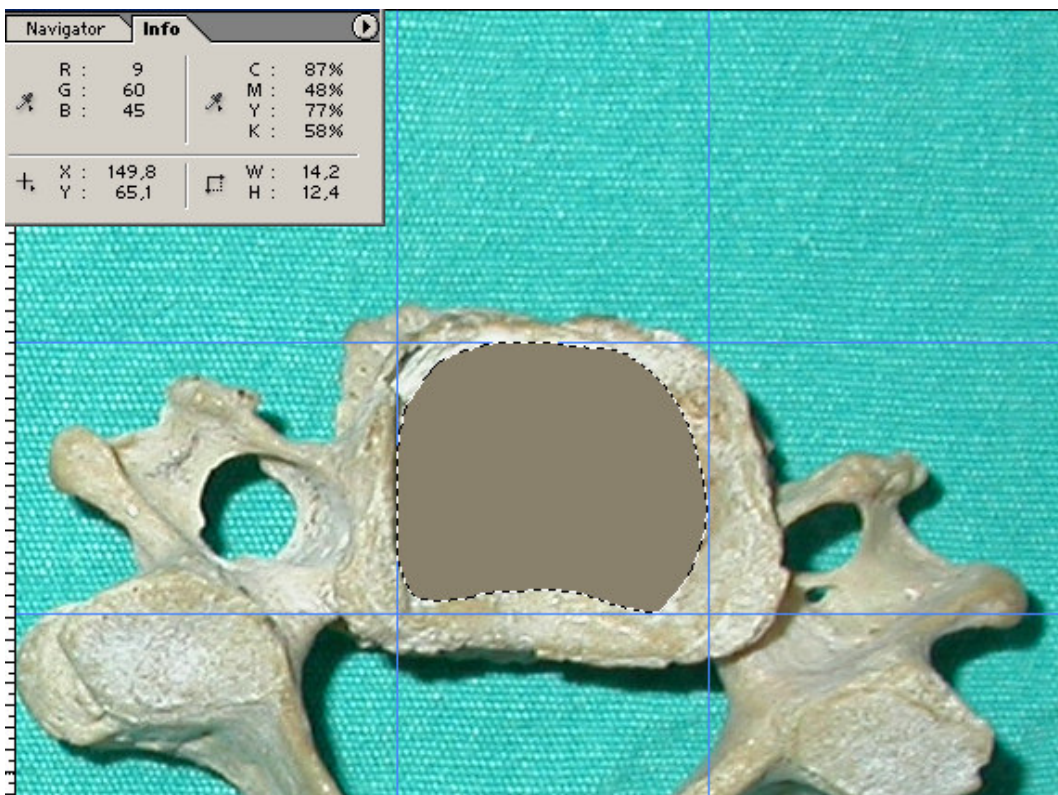
Figure A.25. Vertebra number 12a-2.
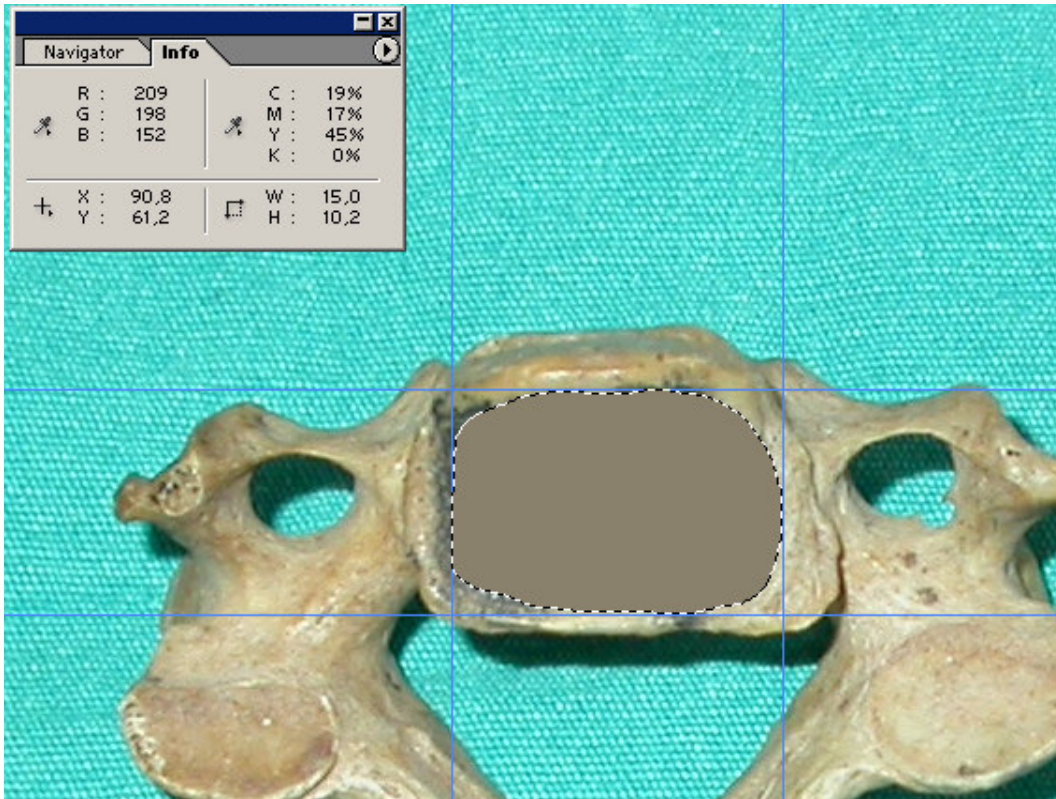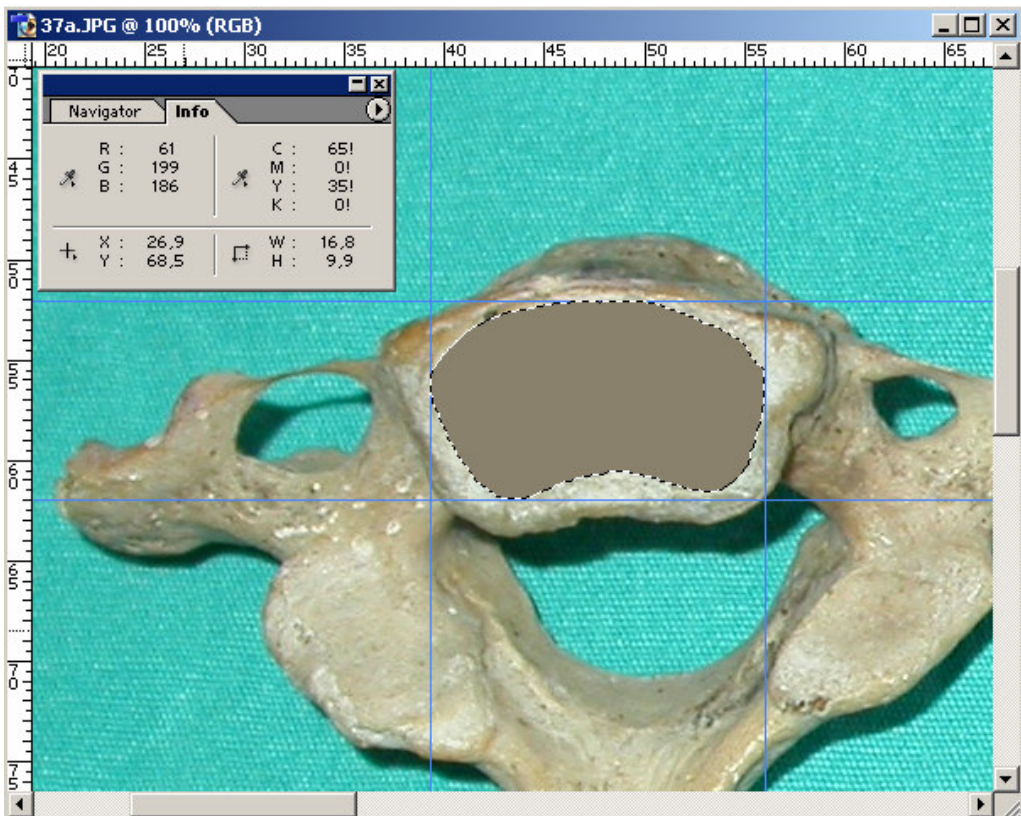
Figure A.26. Vertebra number 13-1.
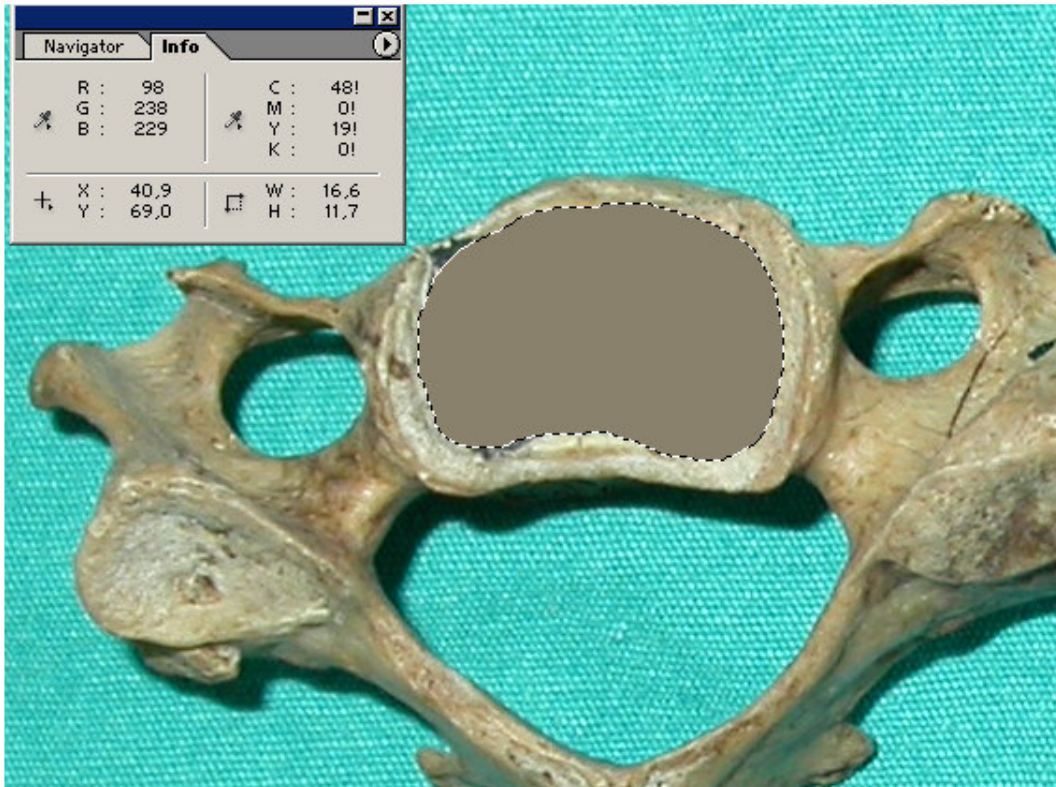
Figure A.27. Vertebra number 13-2.
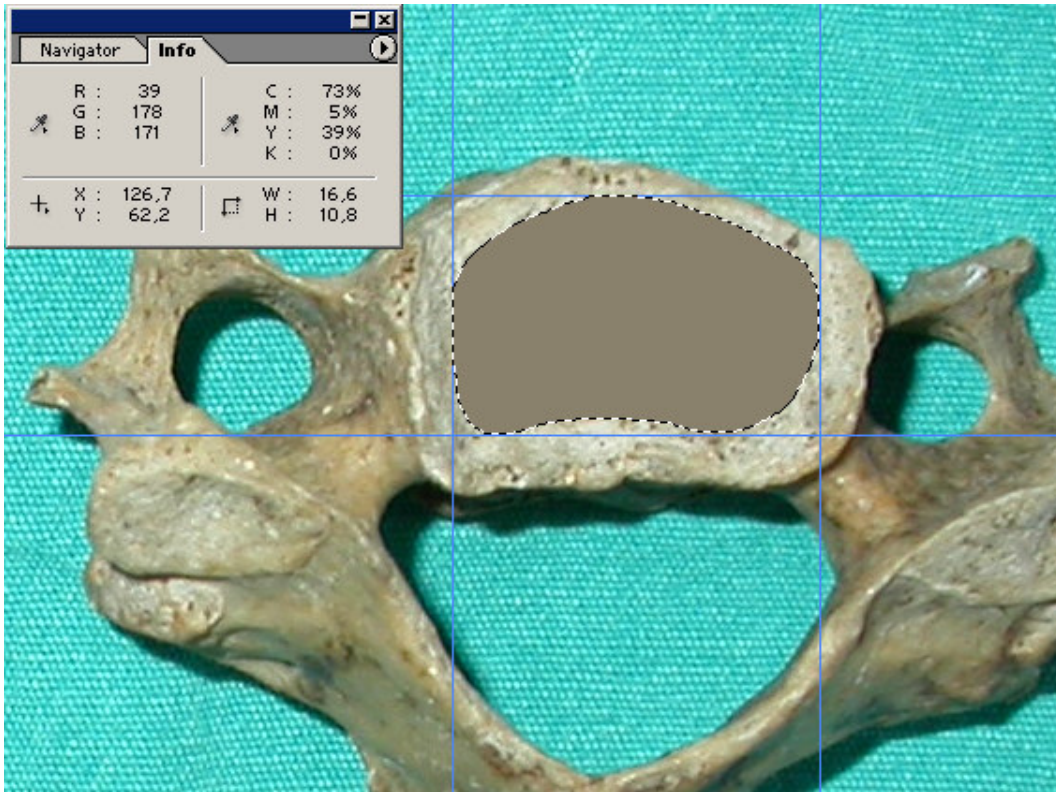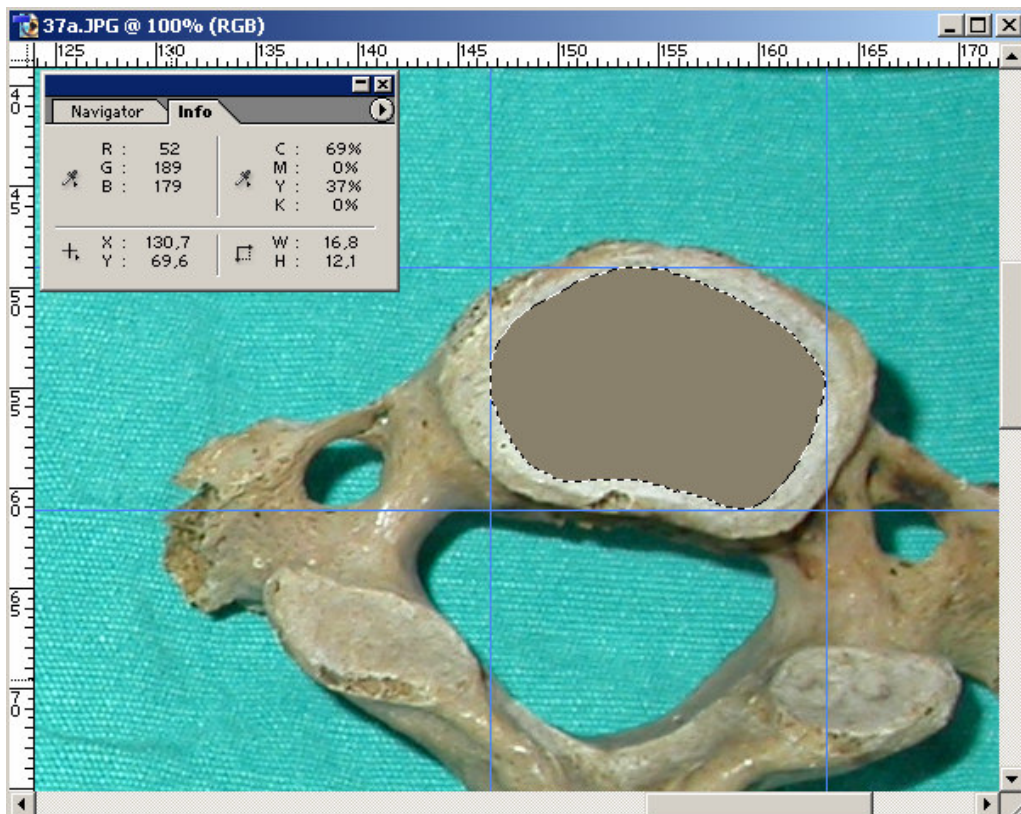
Figure A.28. Vertebra number 13a-1.
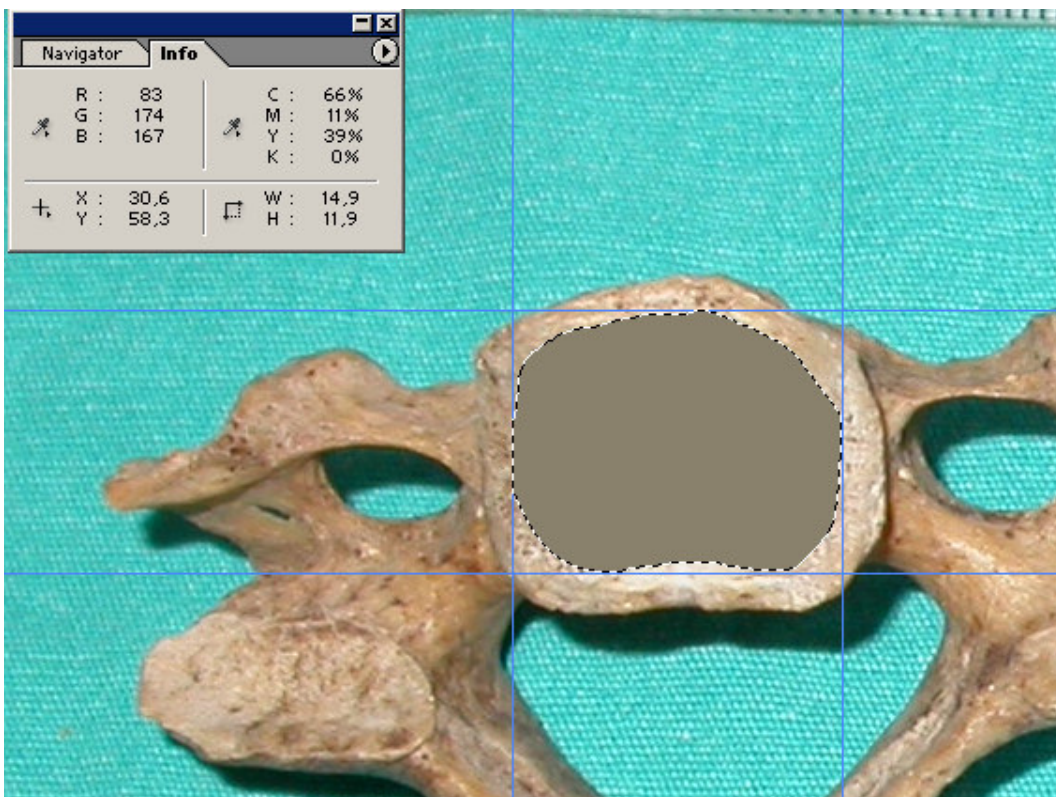
Figure A.29. Vertebra number 13a-2.
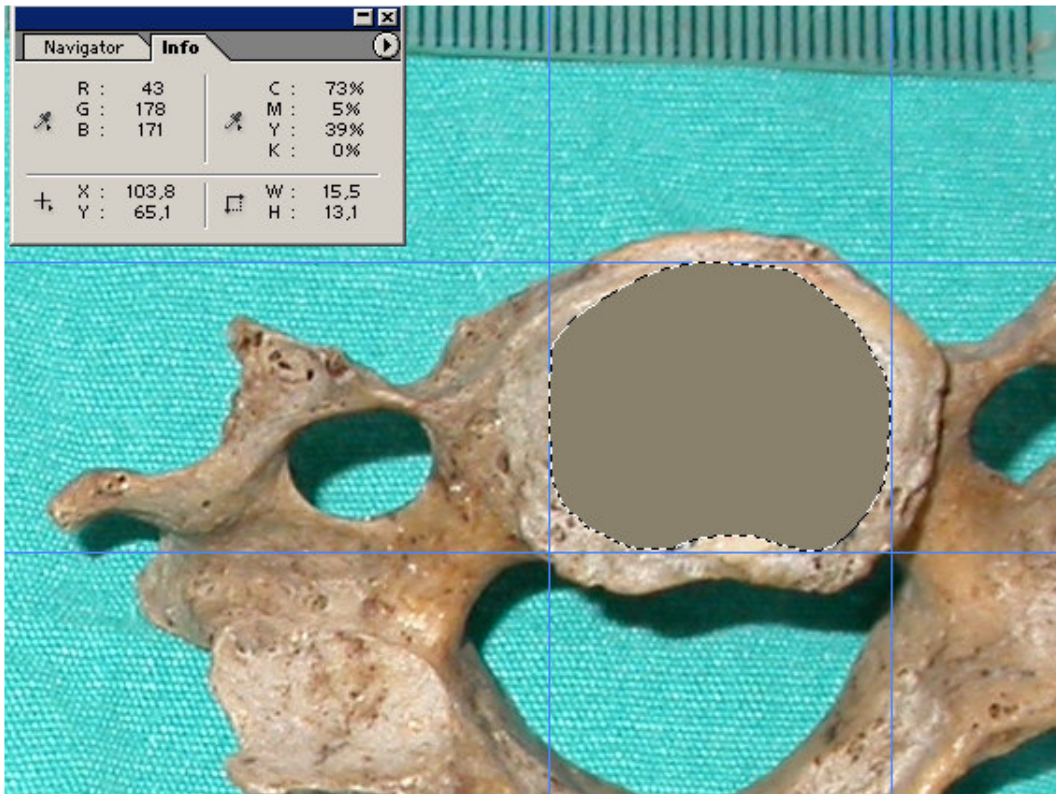
Figure A.30. Vertebra number 14-1.
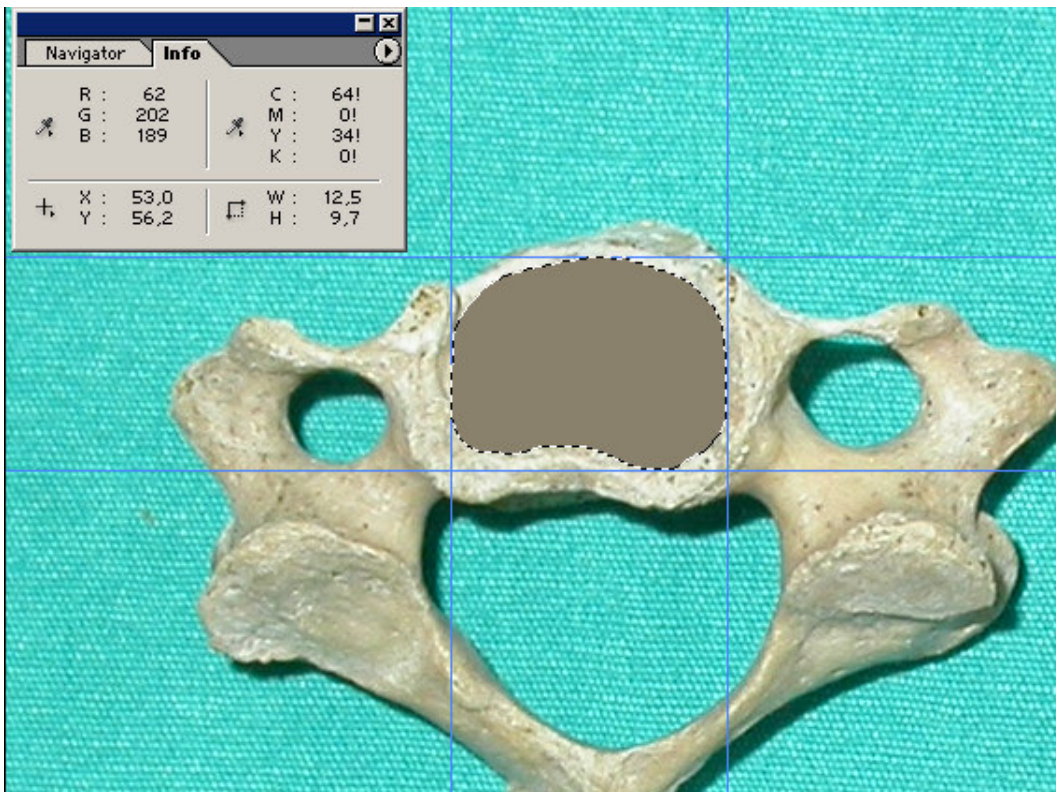
Figure A.31. Vertebra number 14-2.
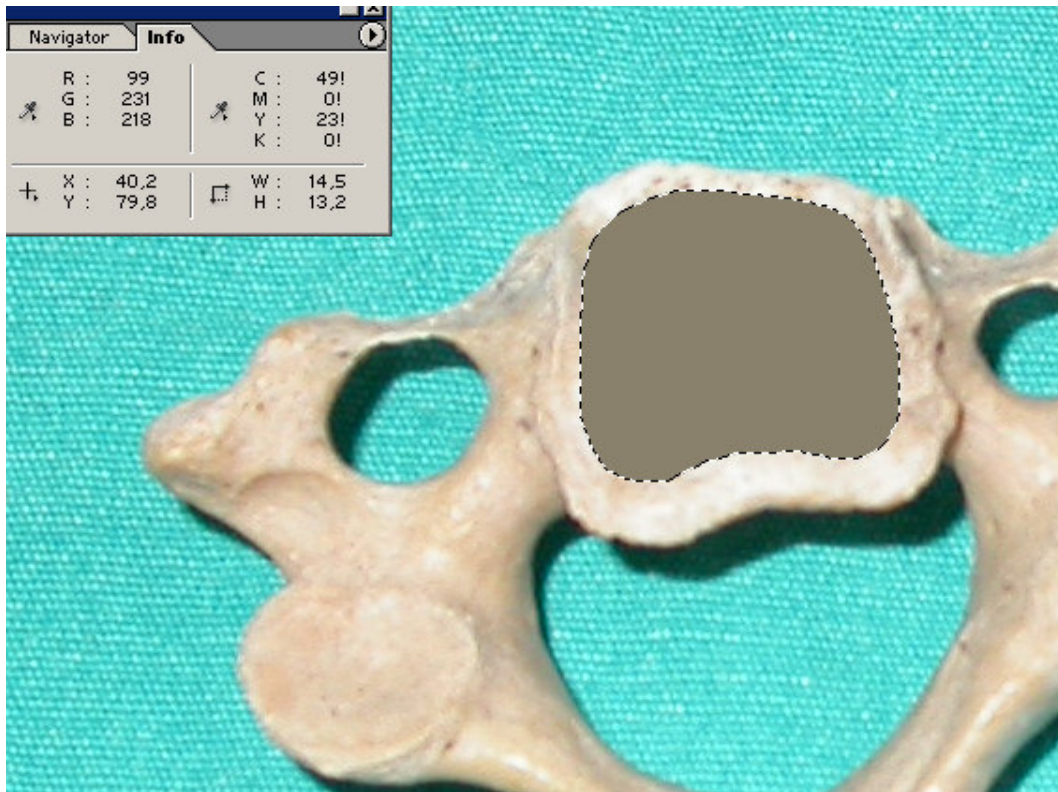
Figure A.32. Vertebra number 14a-1.
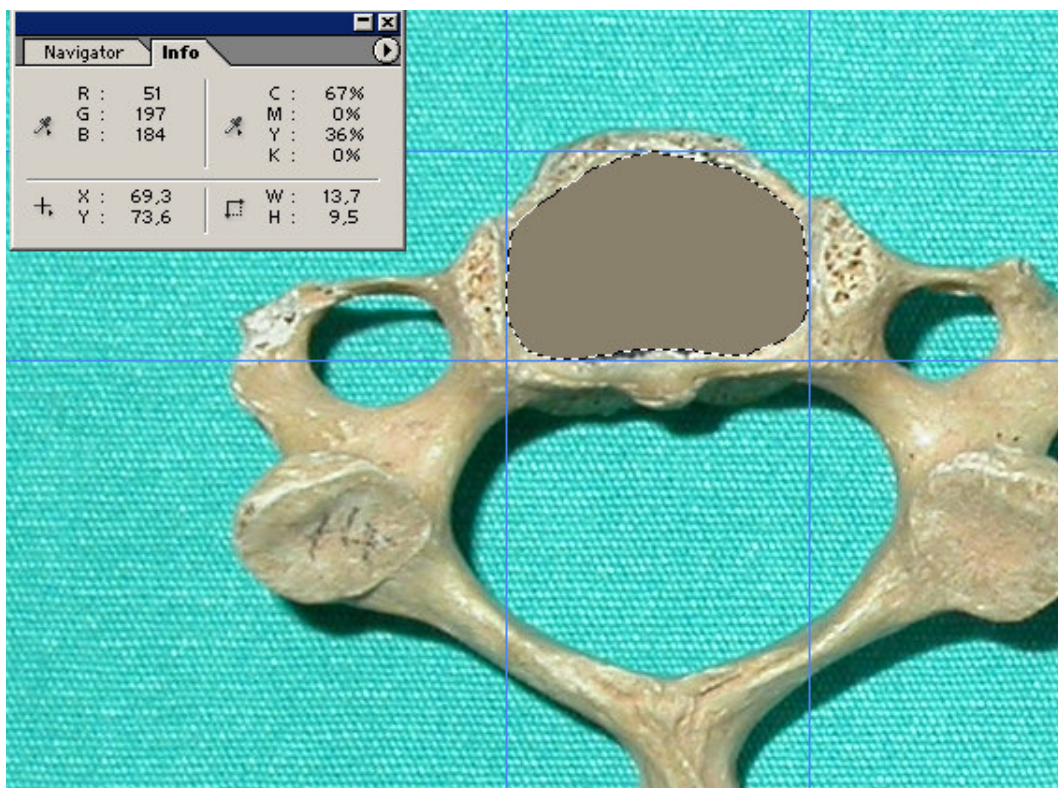
Figure A.33. Vertebra number 14a-2.
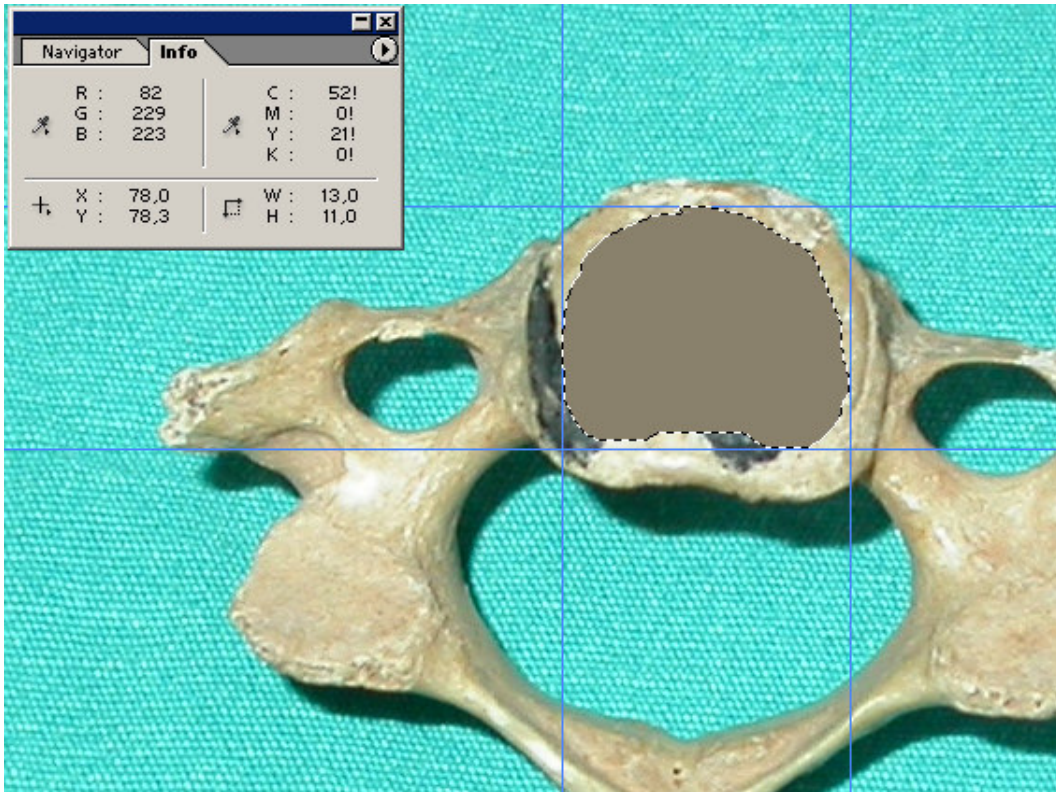
Figure A.34. Vertebra number 15-1.
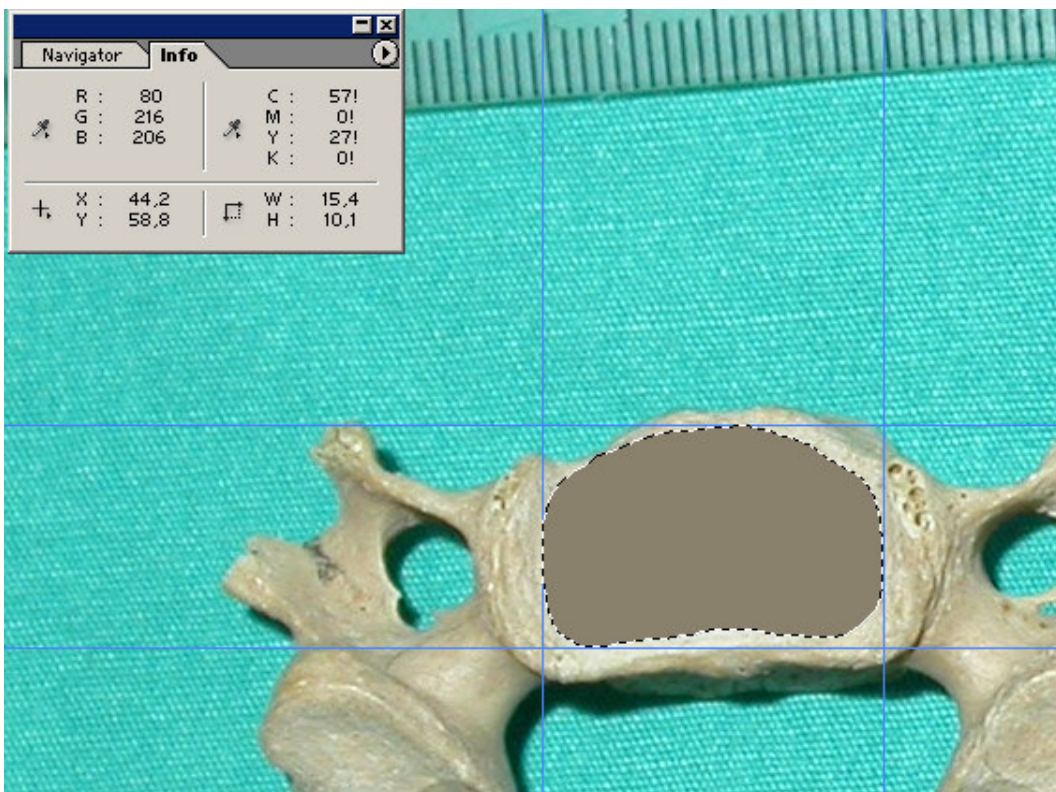
Figure A.35. Vertebra number 15-2.
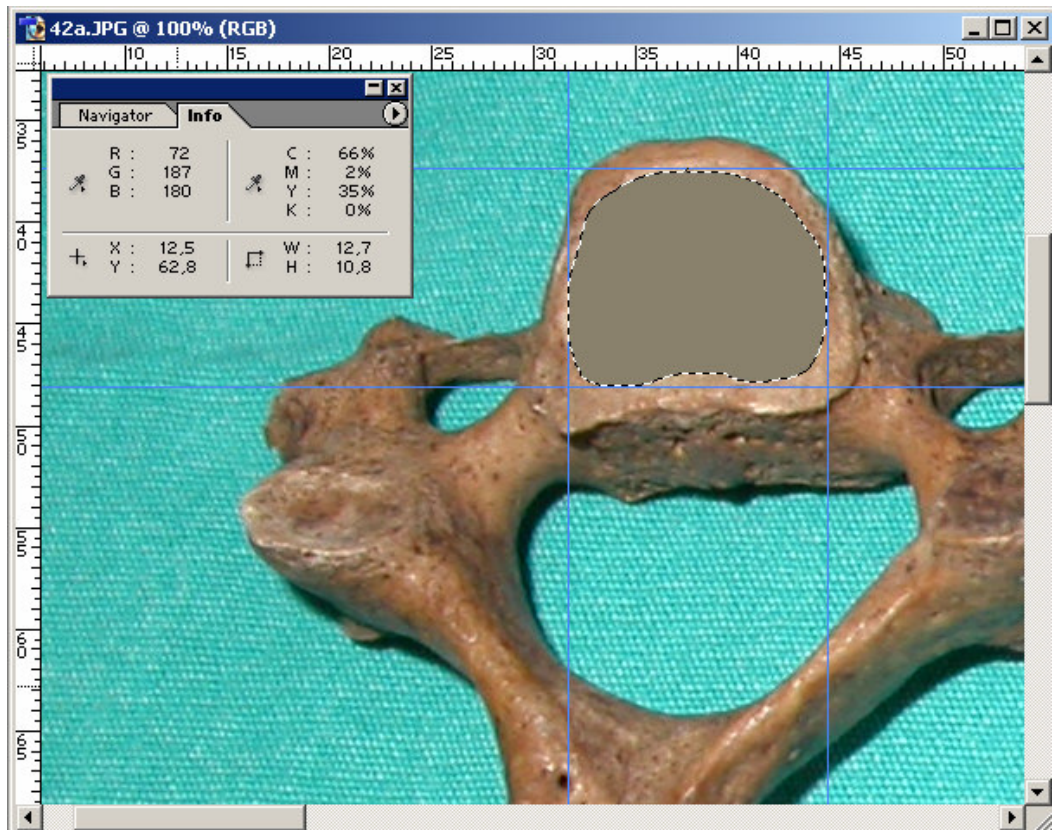
Figure A.36. Vertebra number 15a-1.
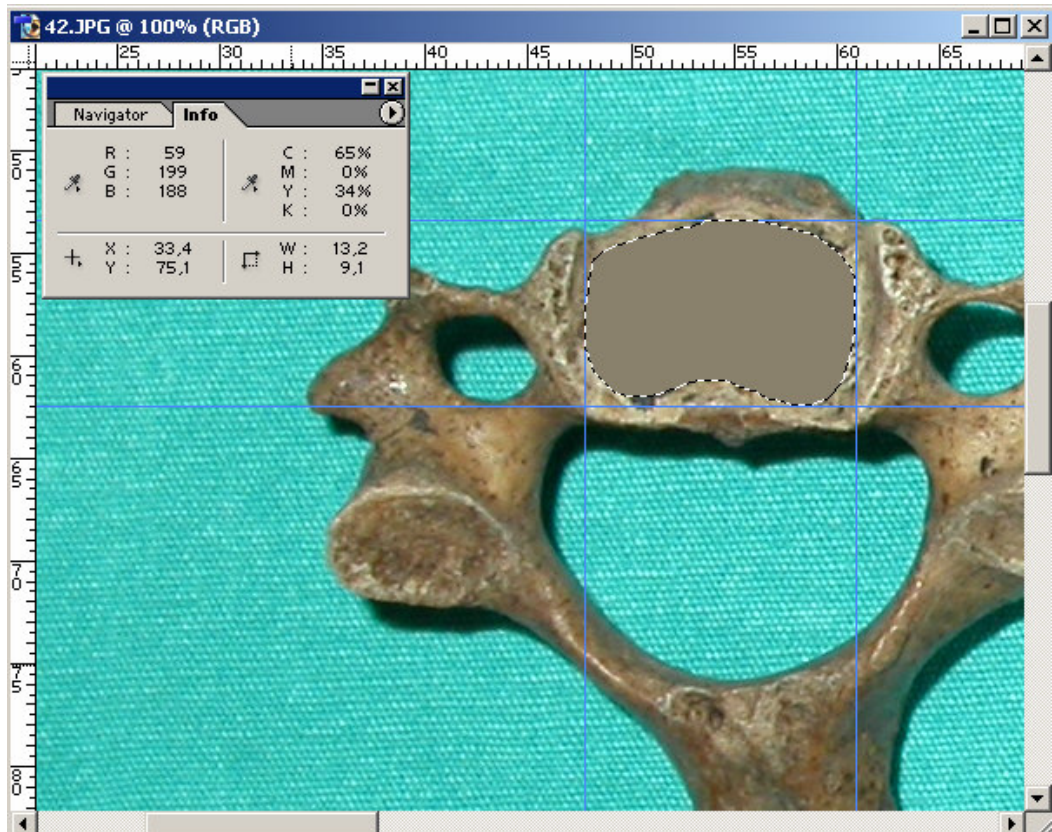
Figure A.37. Vertebra number 15a-2.
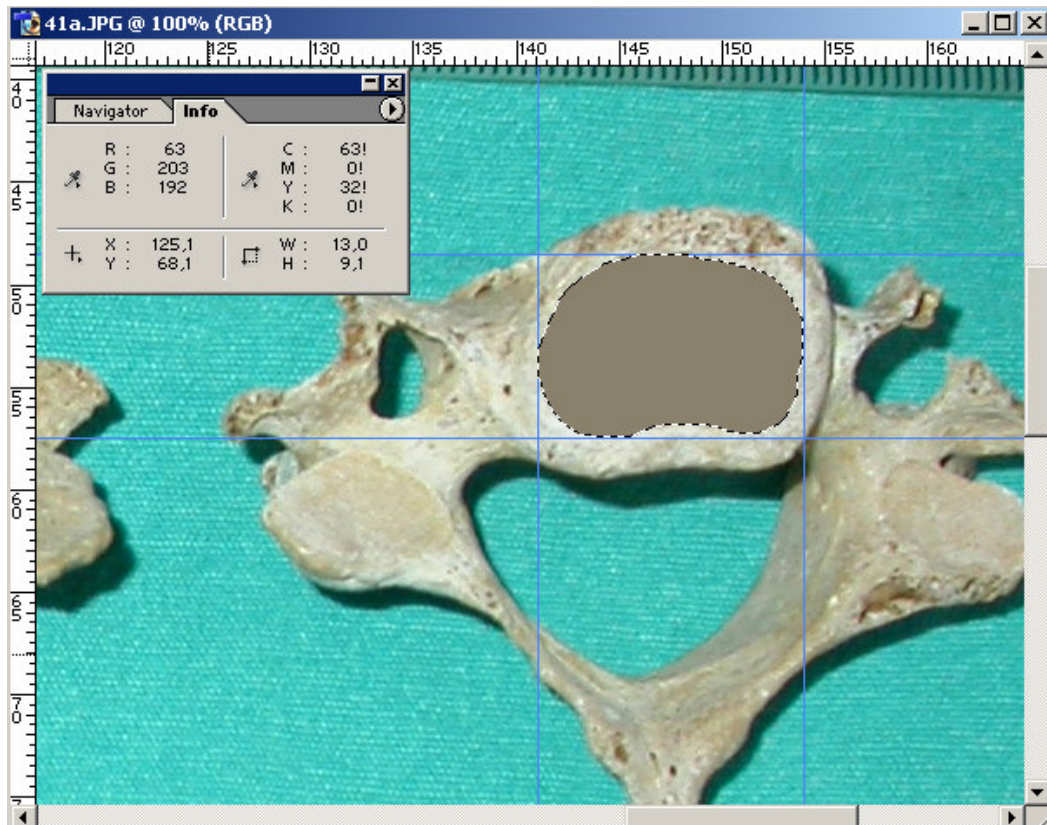
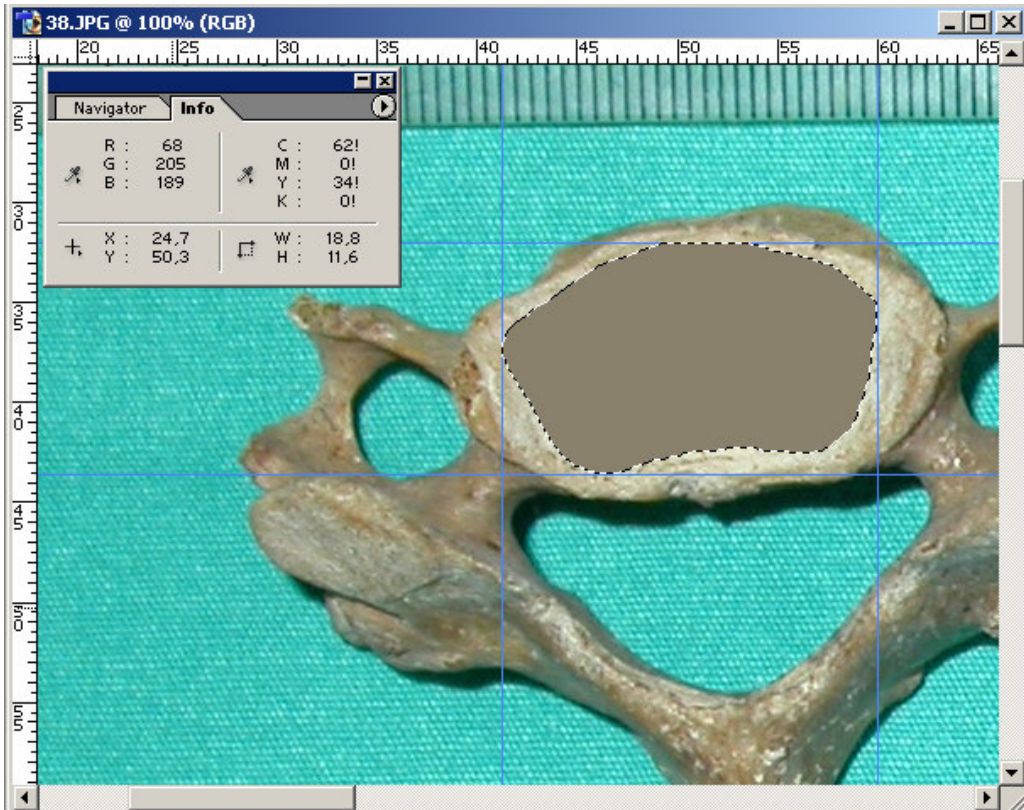Figure A.38. Vertebra number 16-1.
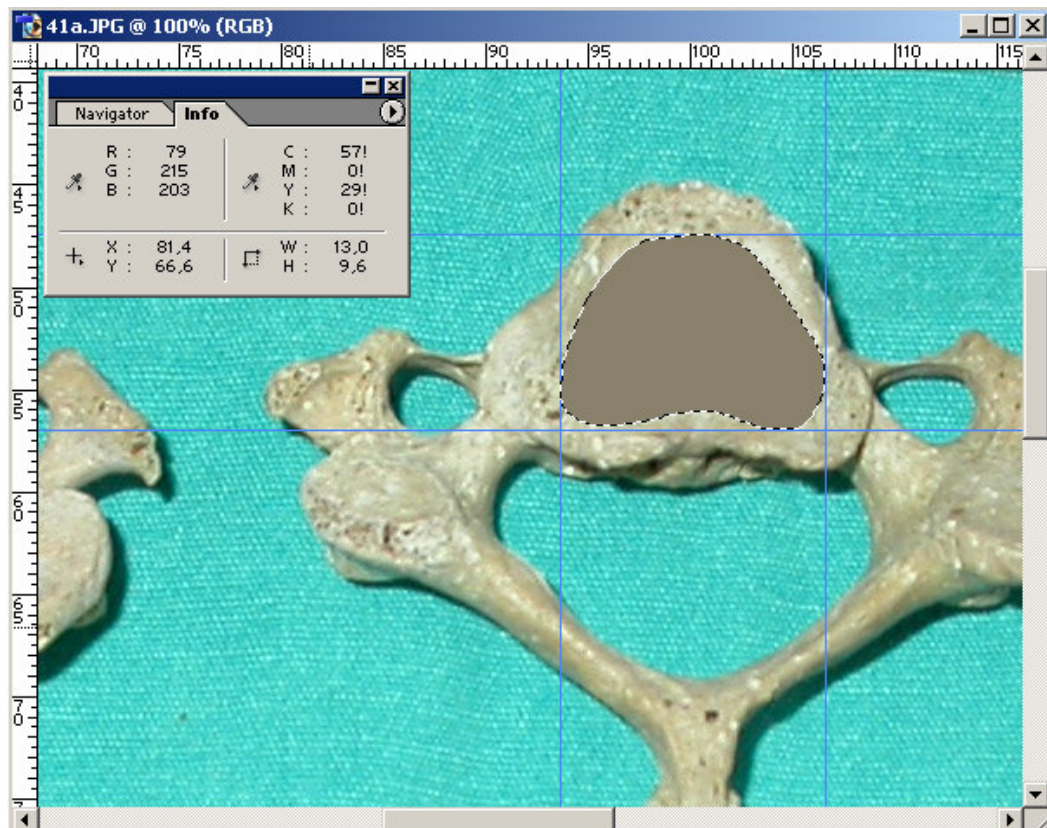
Figure A.39. Vertebra number 16-2.
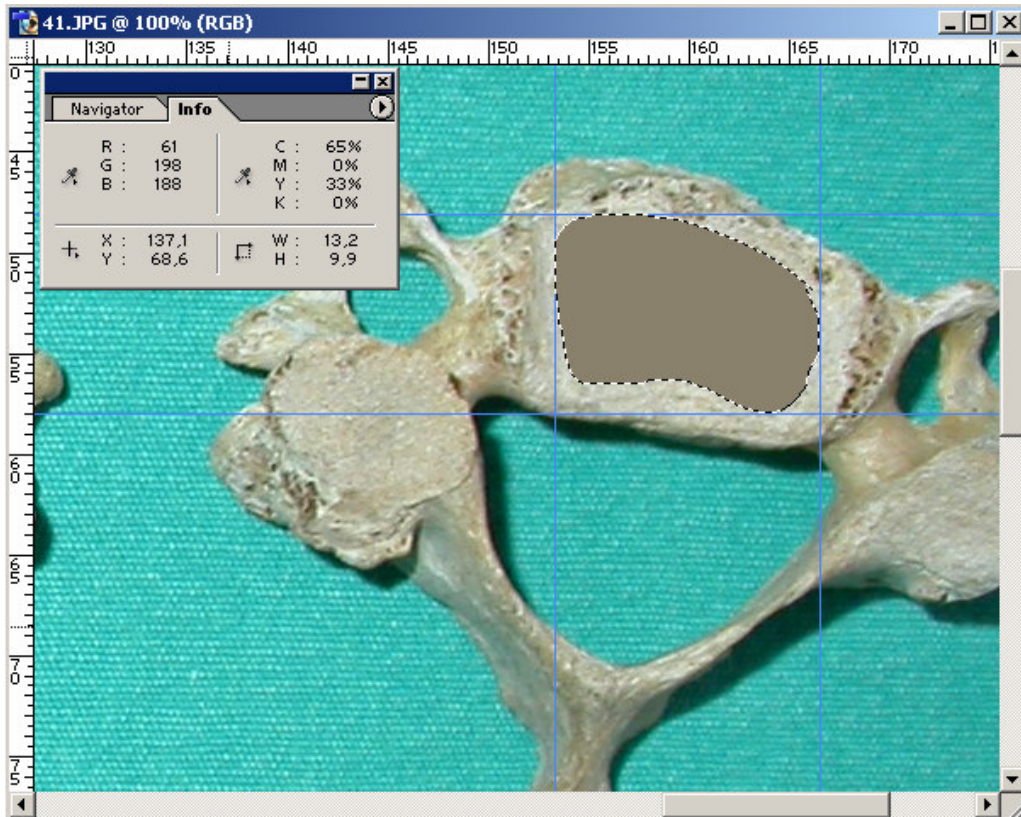
Figure A.40. Vertebra number 16a-1.
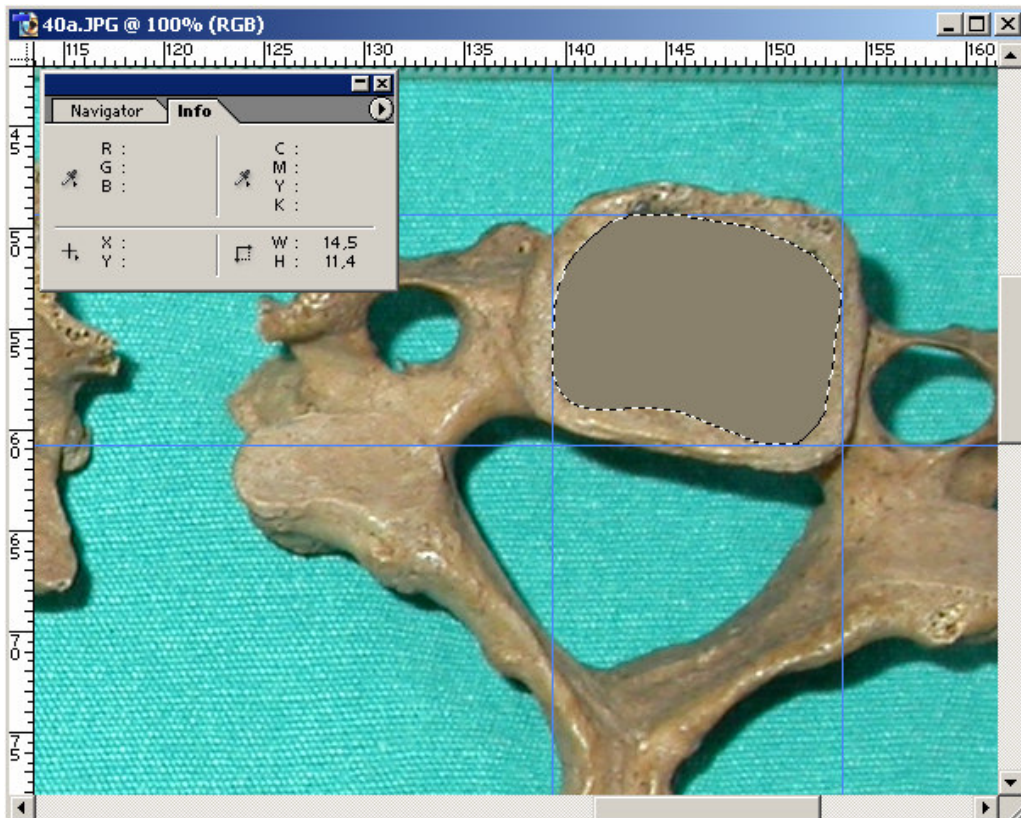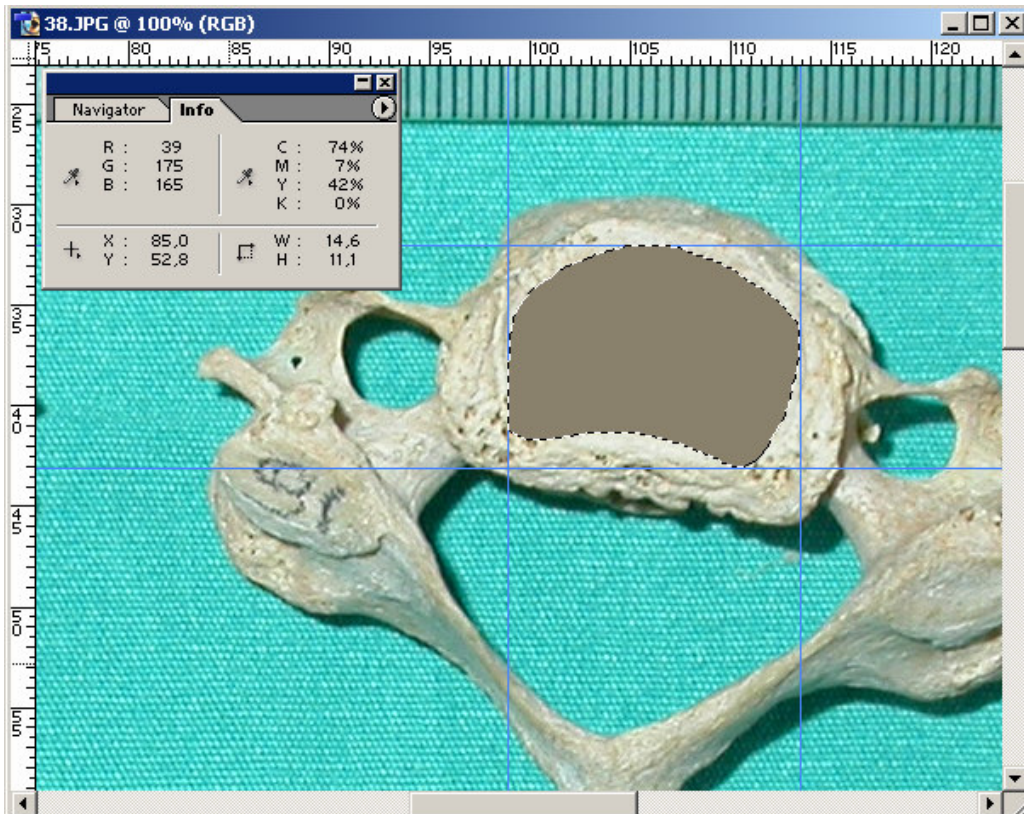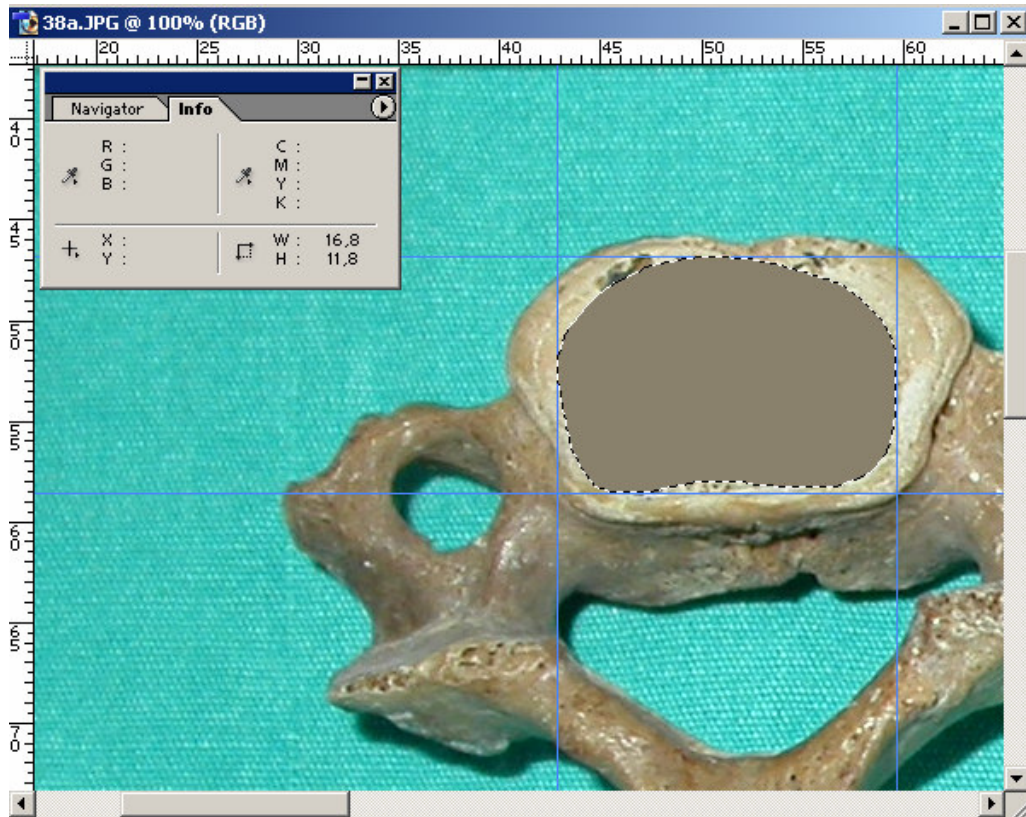

Figure A.41. Vertebra number 16a-2.
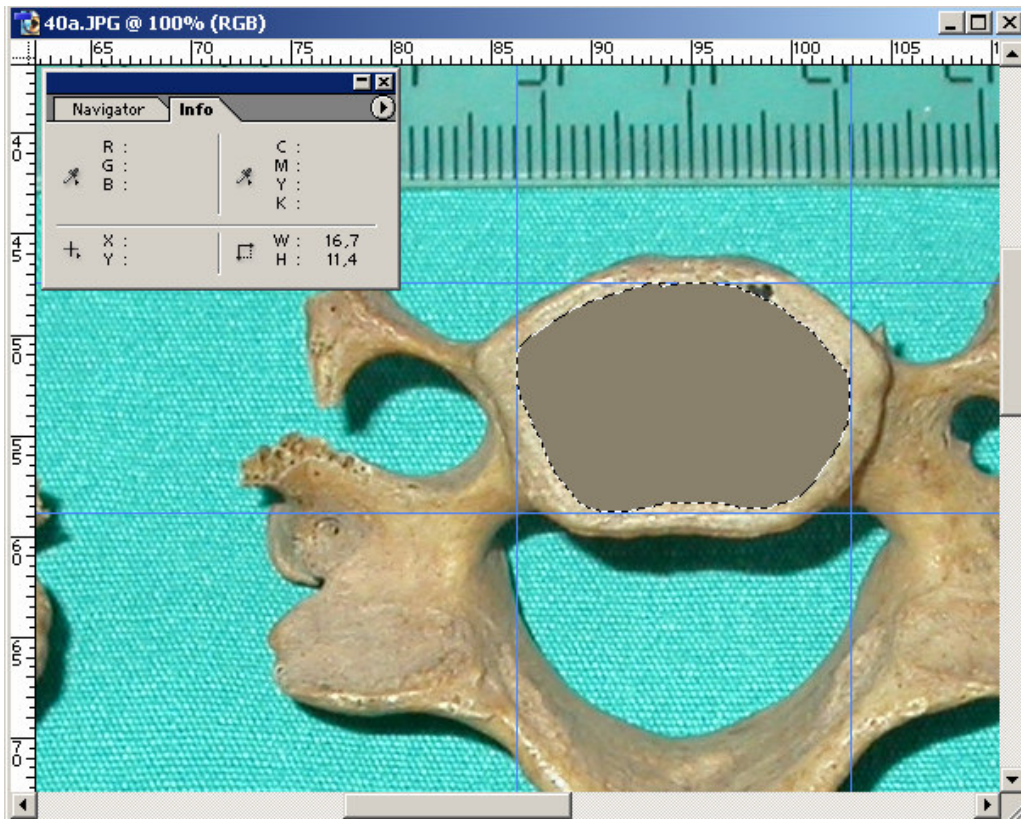
Figure A.42. Vertebra number 17-1.
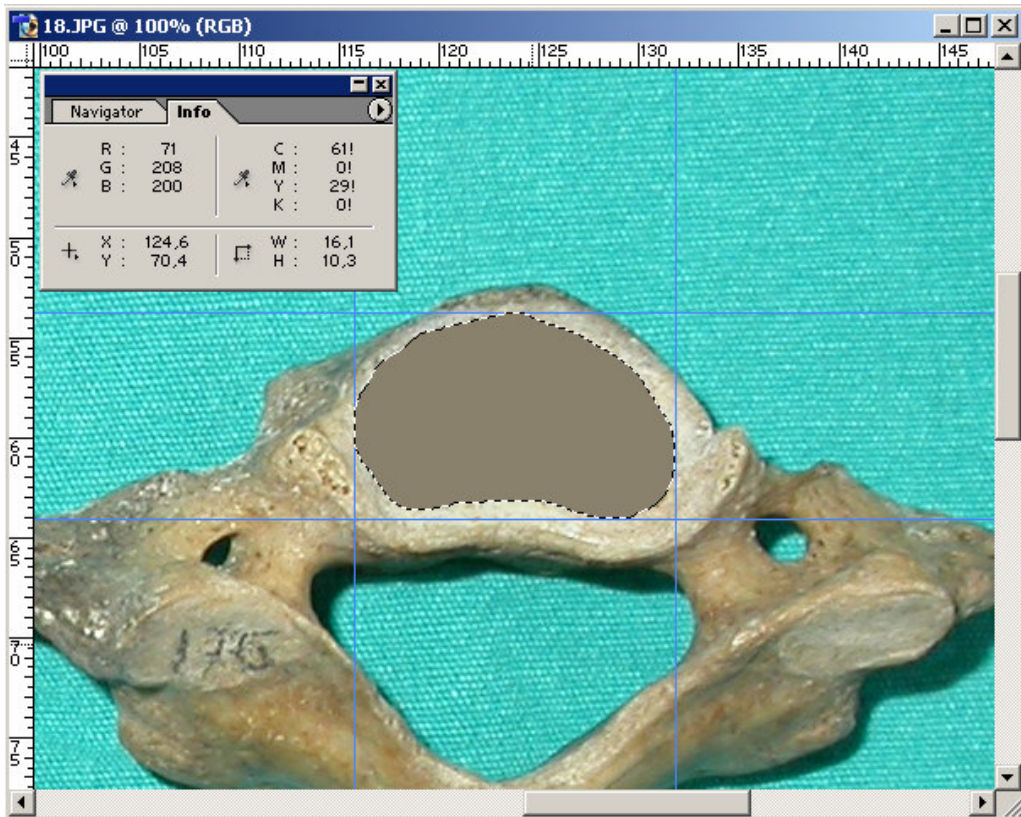
Figure A.43. Vertebra number 17-2.
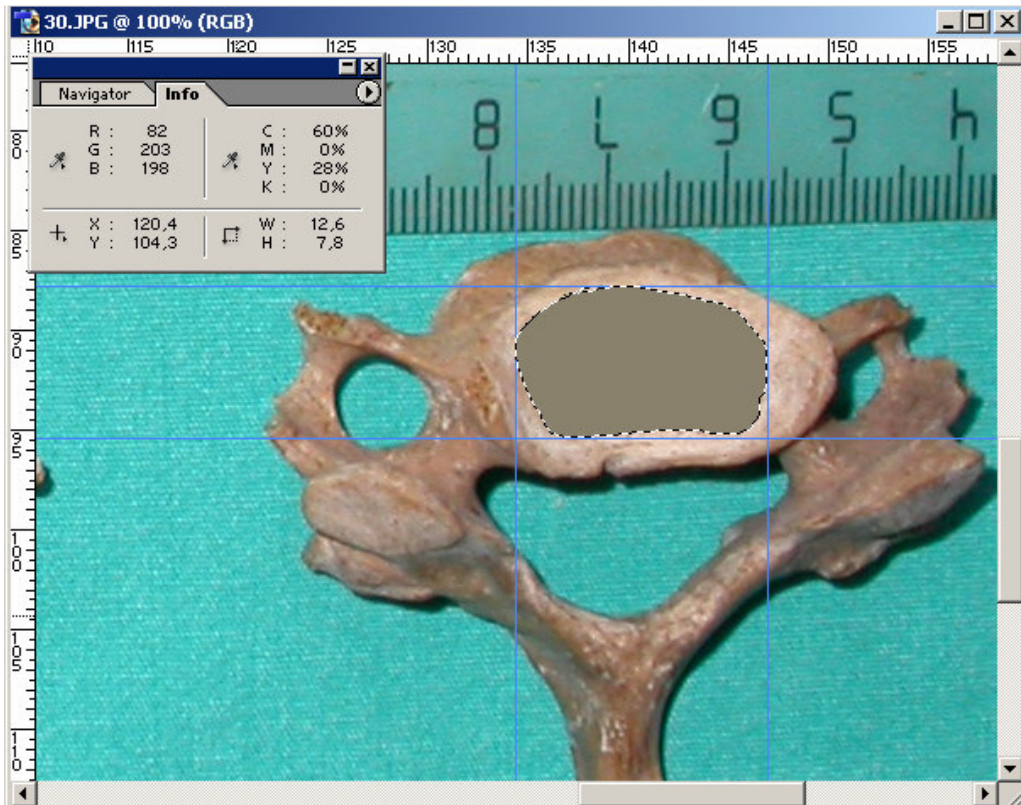
Figure A.44. Vertebra number 17a-1.
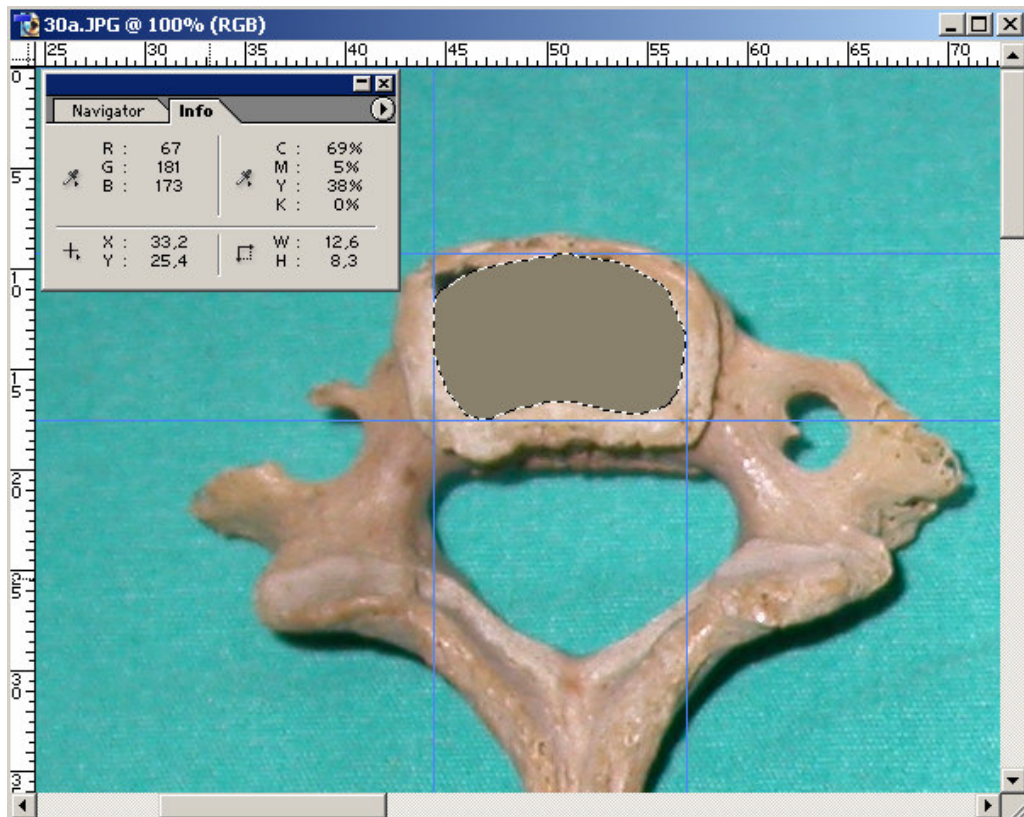
Figure A.45. Vertebra number 17a-2.
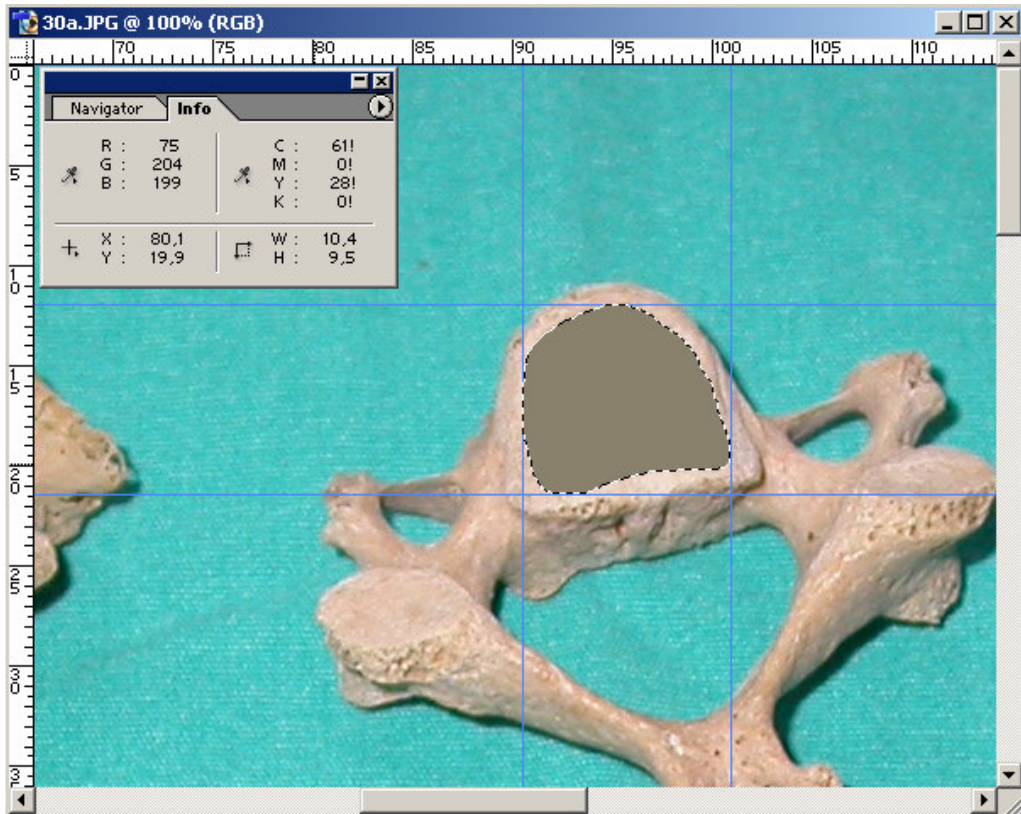
Figure A.46. Vertebra number 18-1.
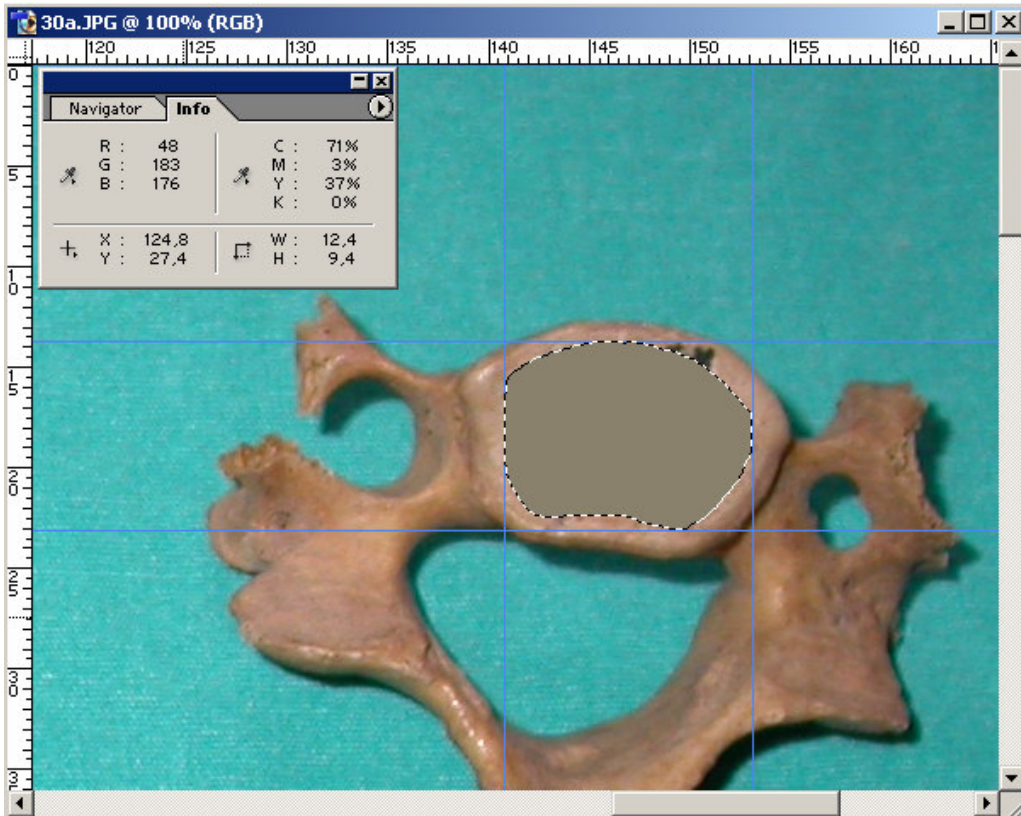
Figure A.47. Vertebra number 18-2.
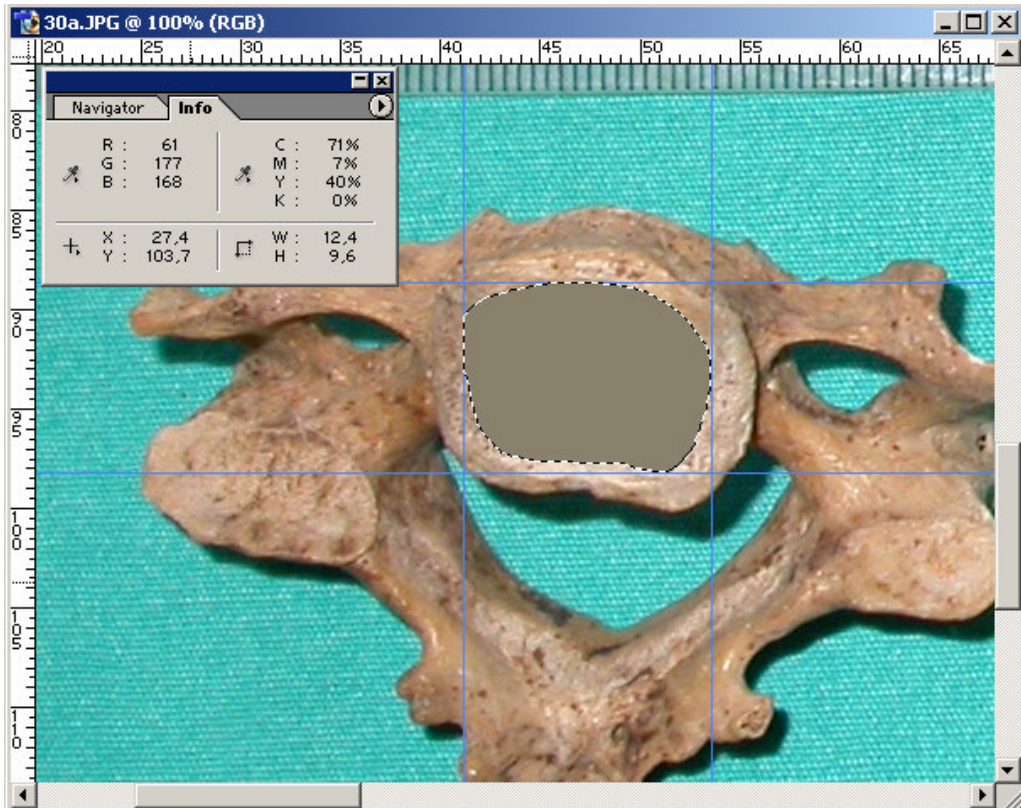
Figure A.48. Vertebra number 18a-1.
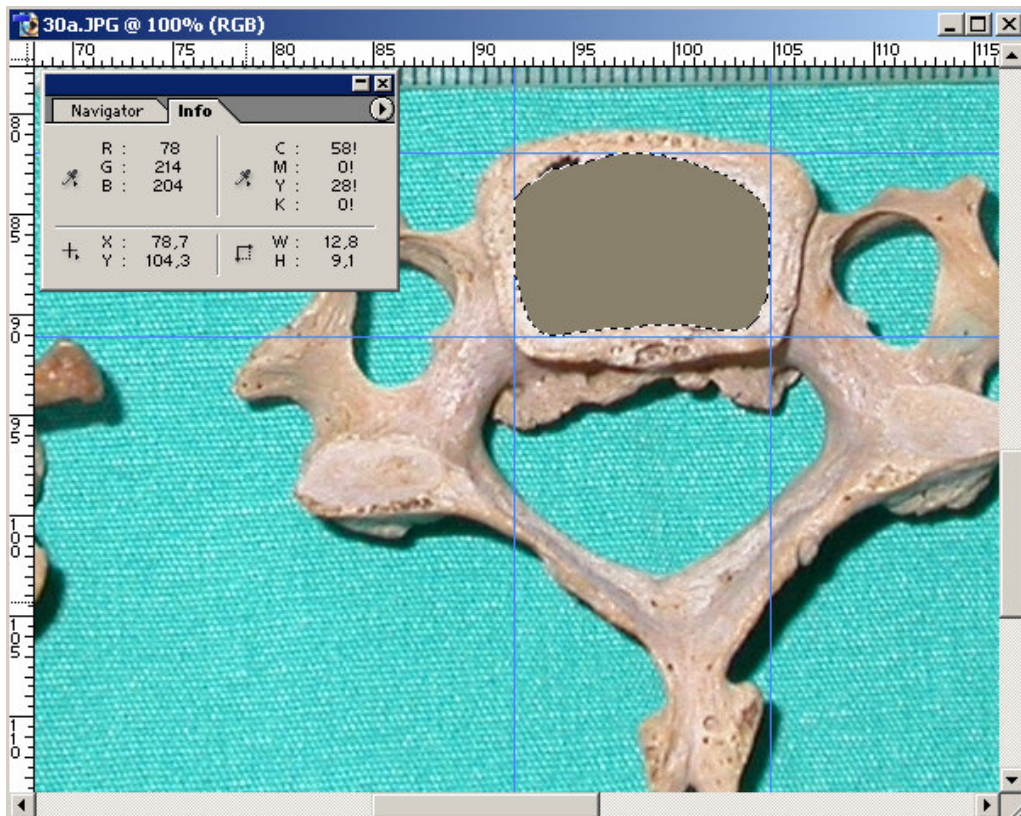
Figure A.49. Vertebra number 18a-2.
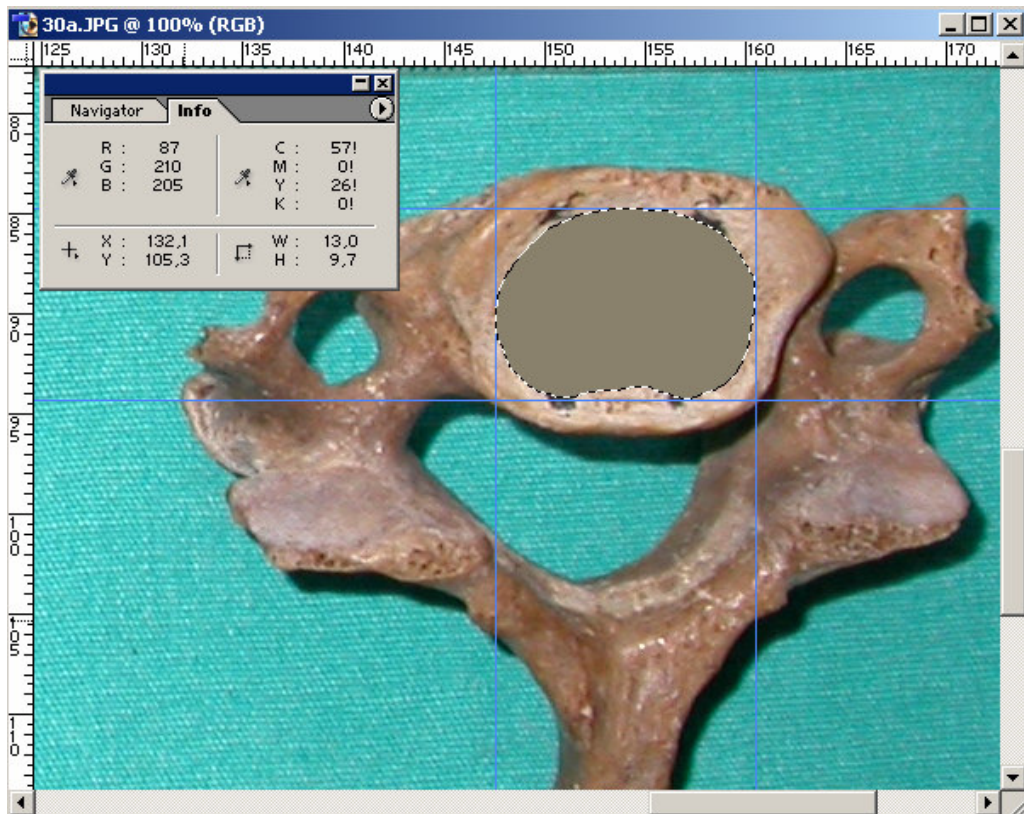
Figure A.50. Vertebra number 19-1.
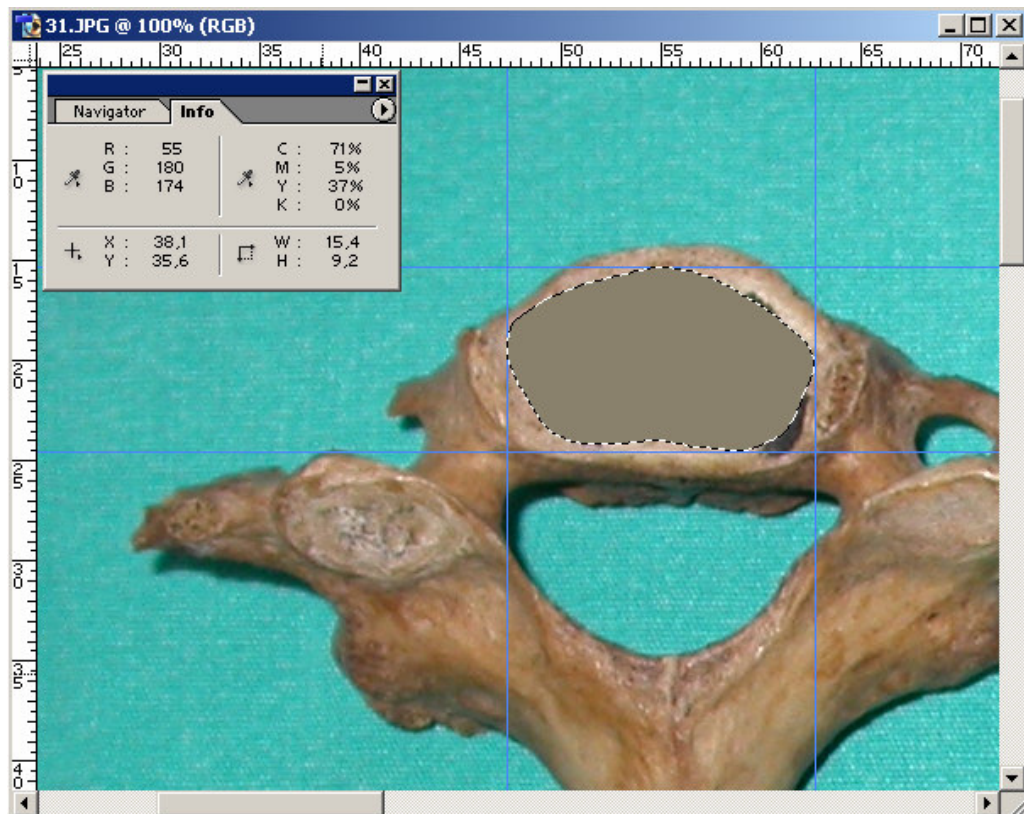
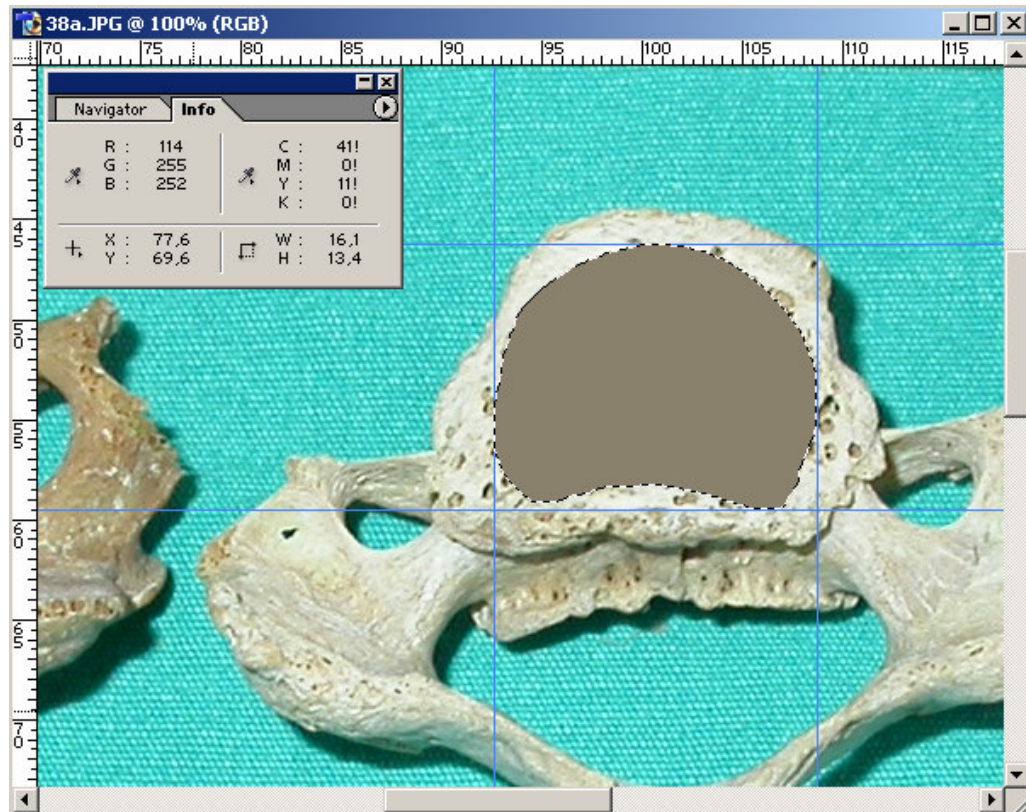Figure A.51. Vertebra number 19-2.
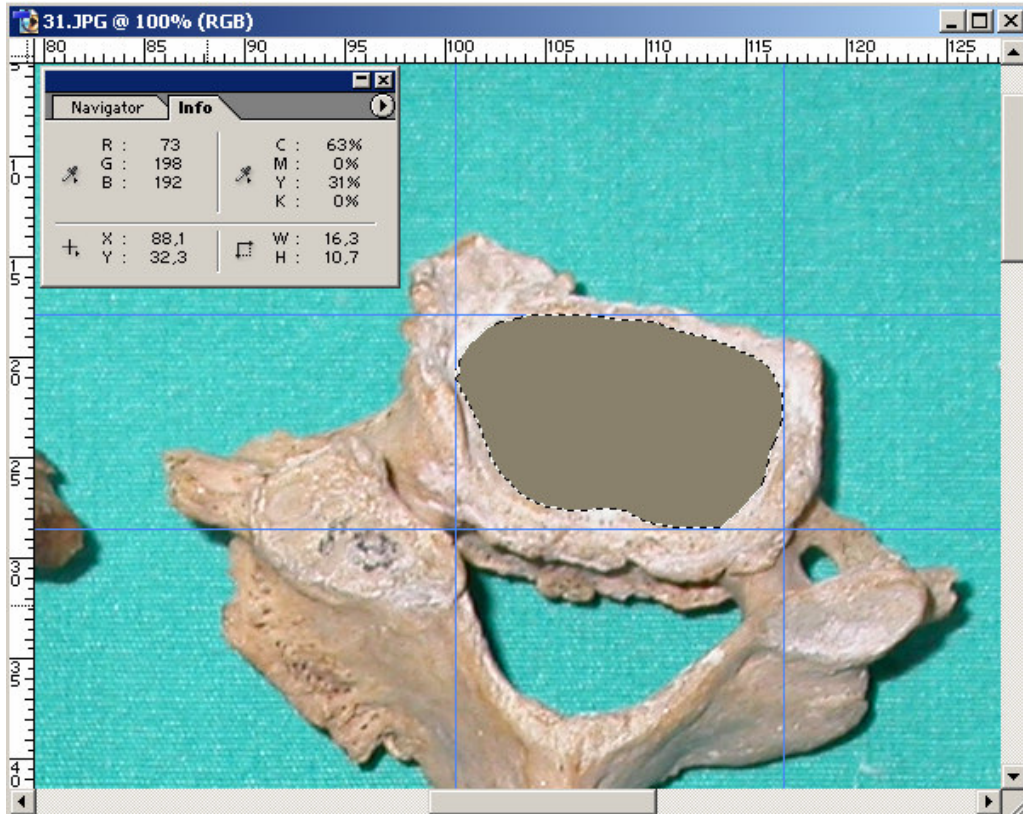
Figure A.52. Vertebra number 19a-1.
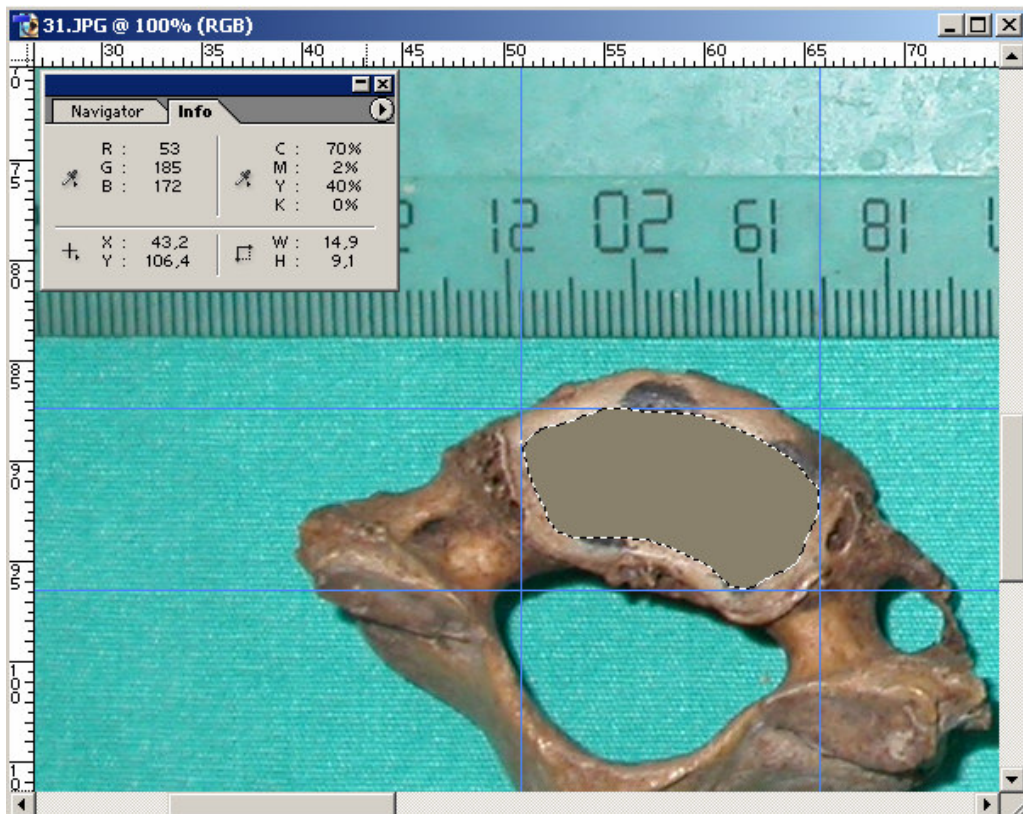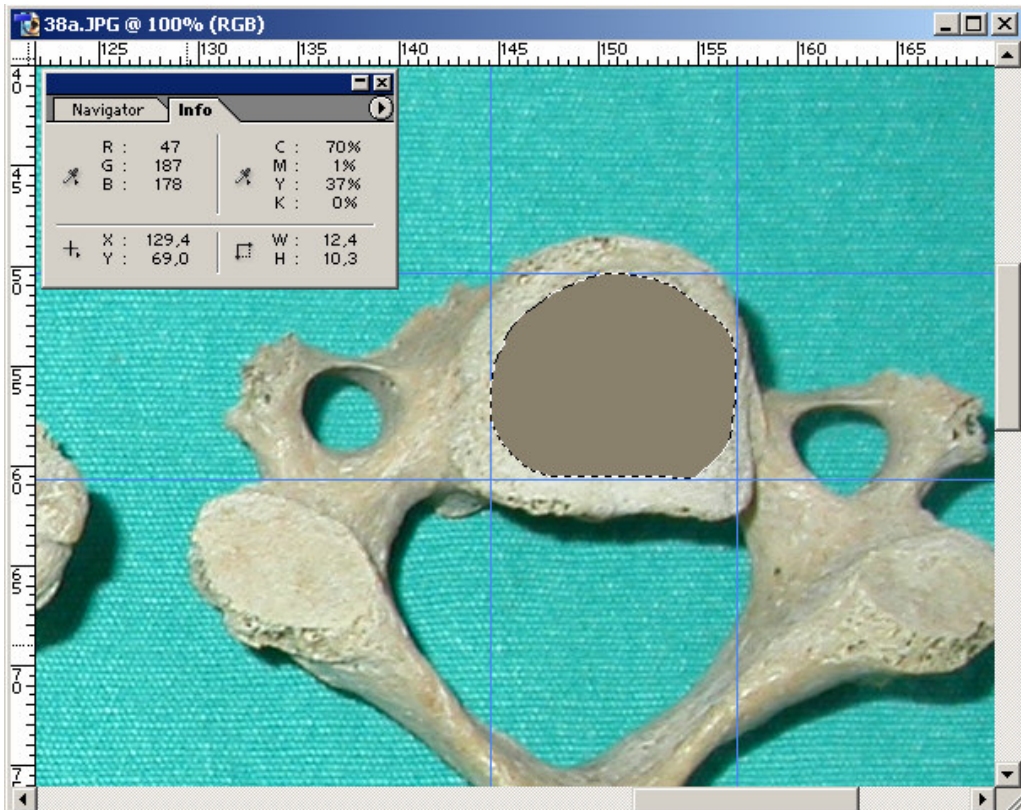

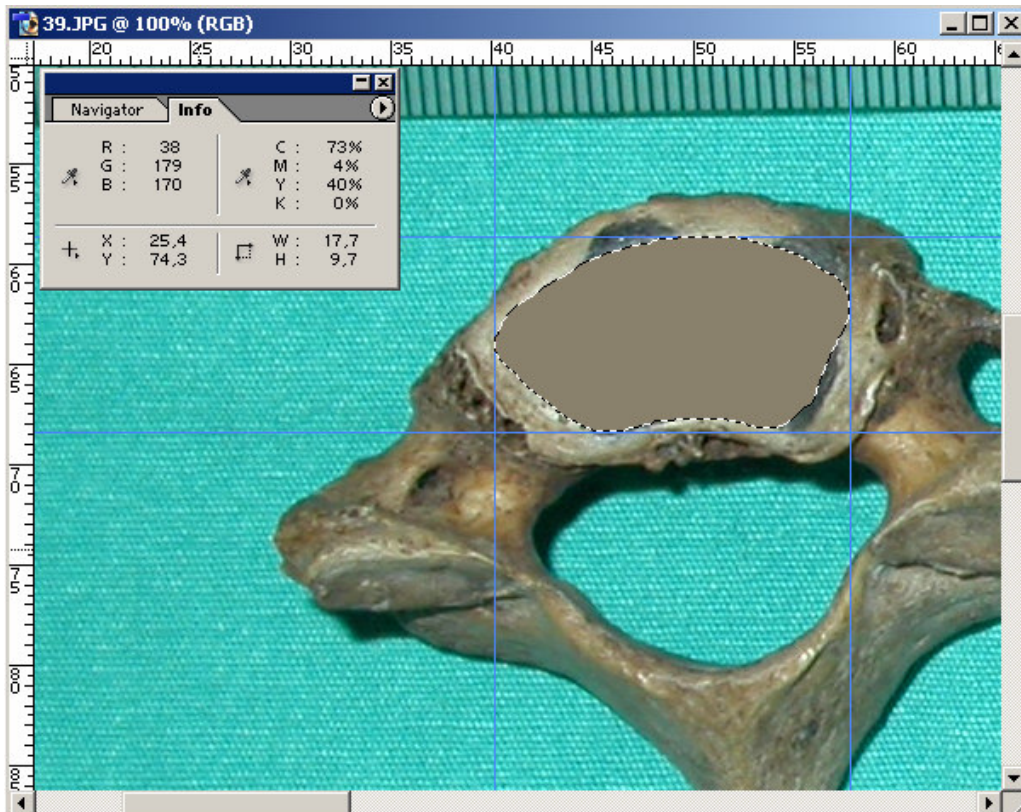Figure A.53. Vertebra number 19a-2.
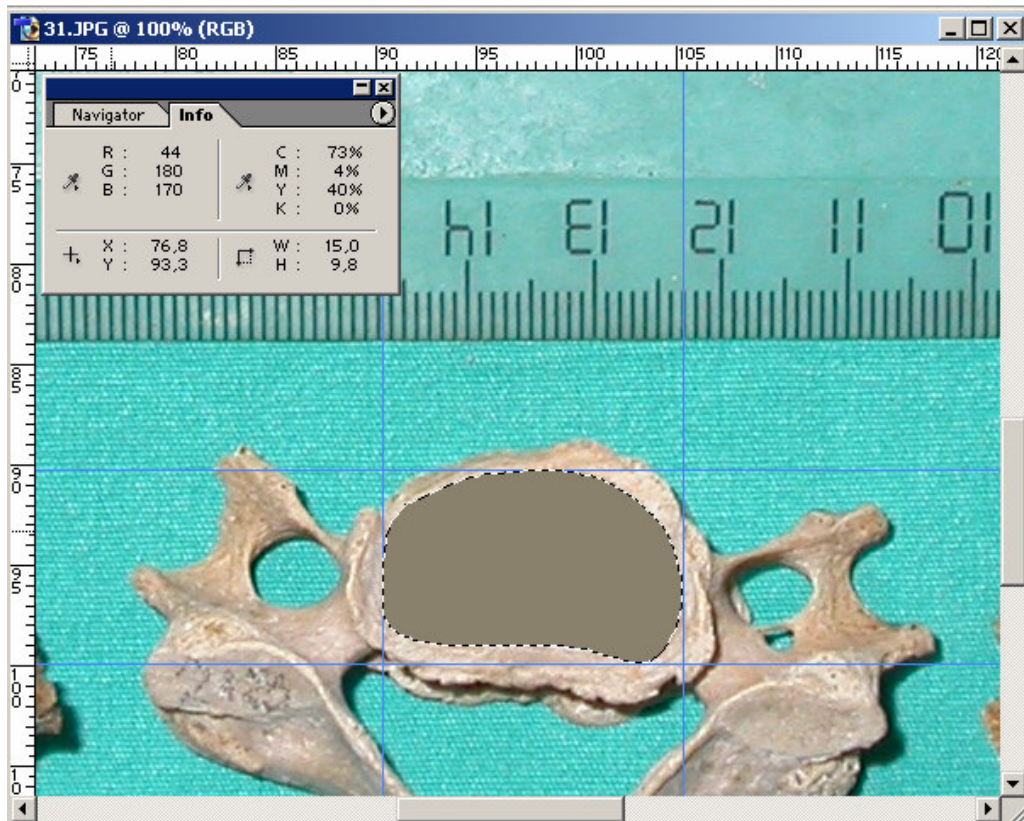
Figure A.54. Vertebra number 20-1.
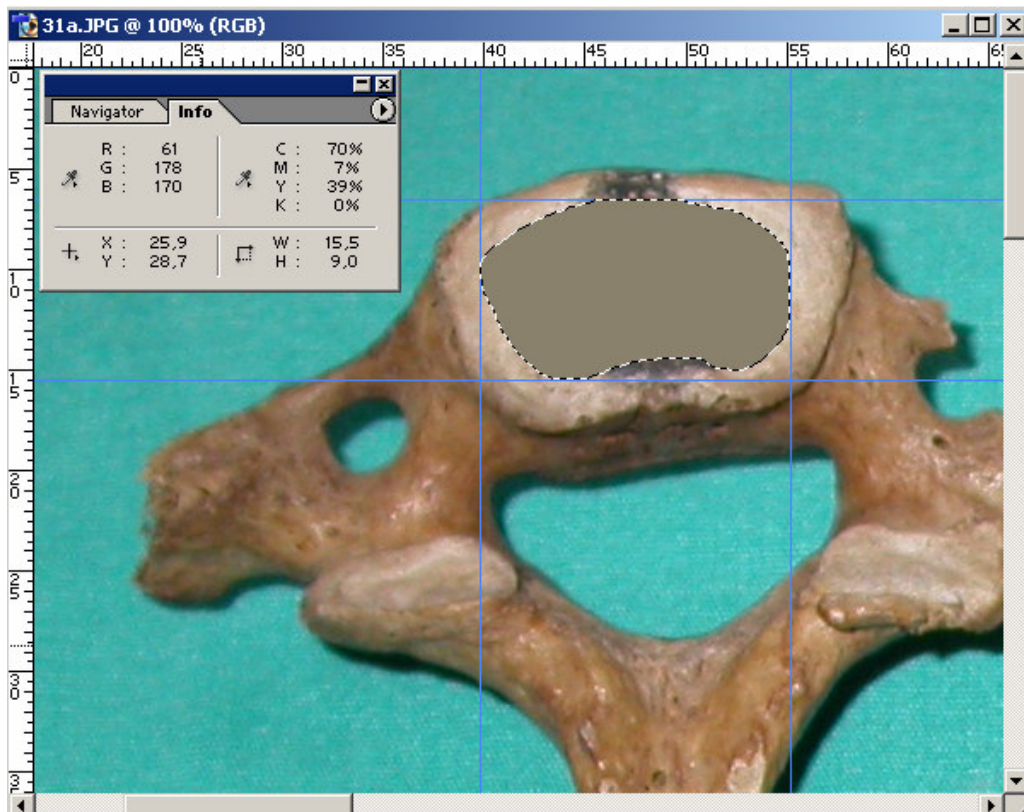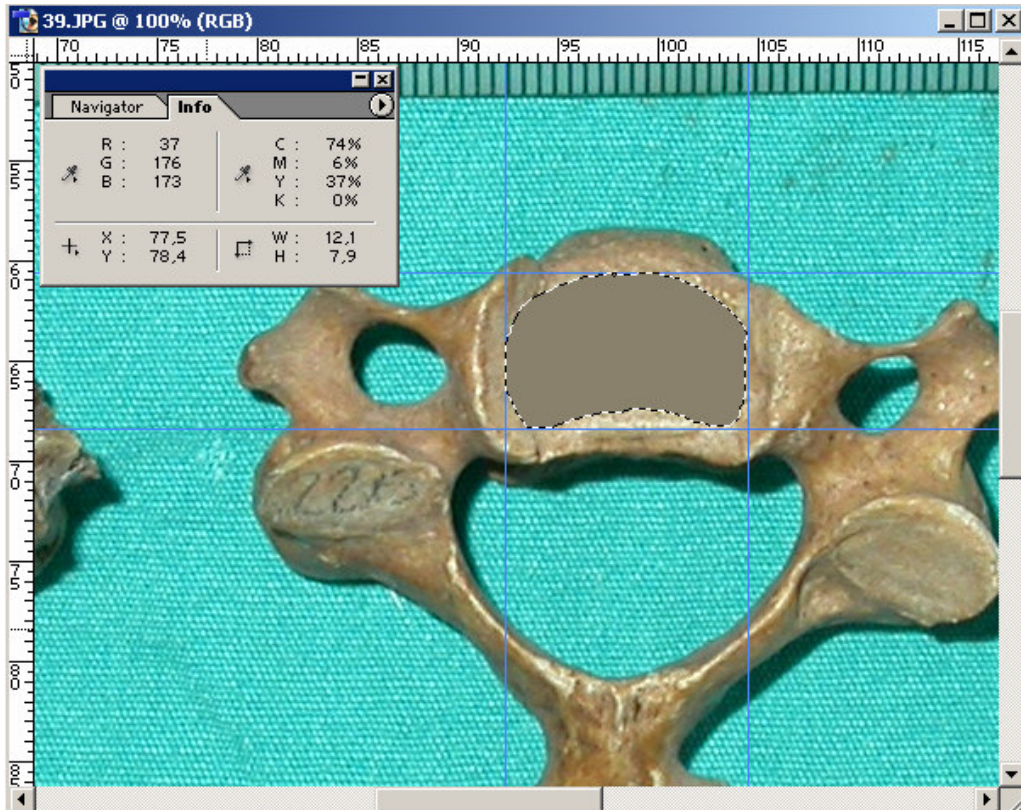

Figure A.55. Vertebra number 20-2.
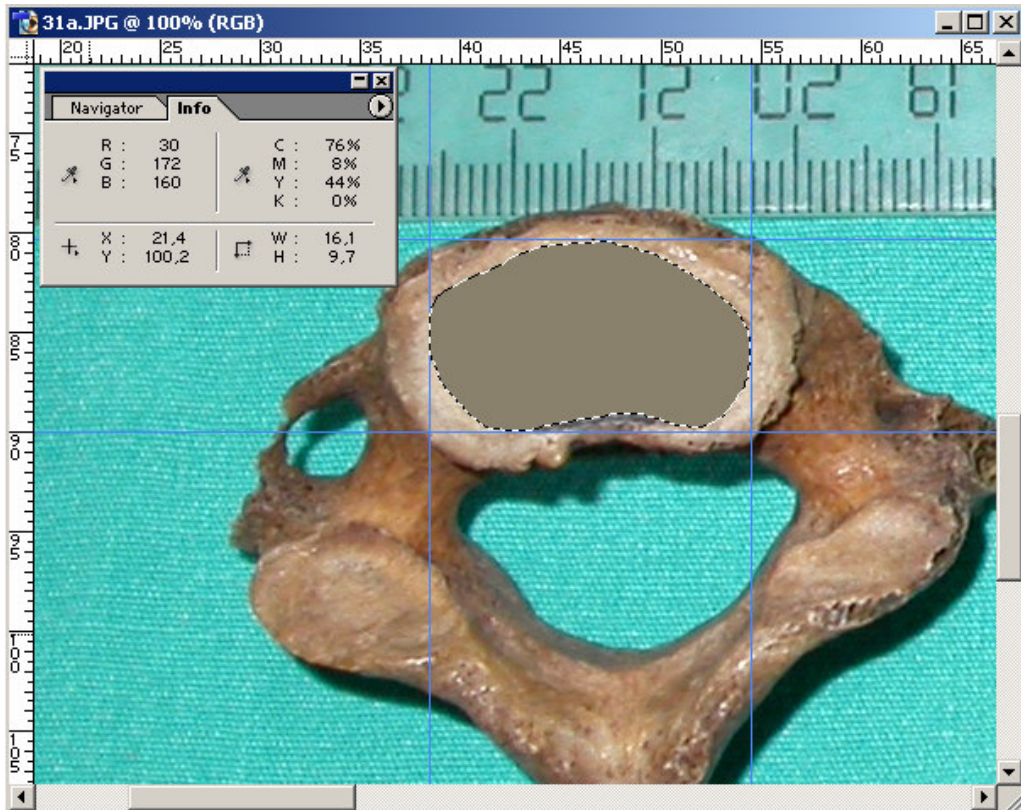
Figure A.56. Vertebra number 20a-1.
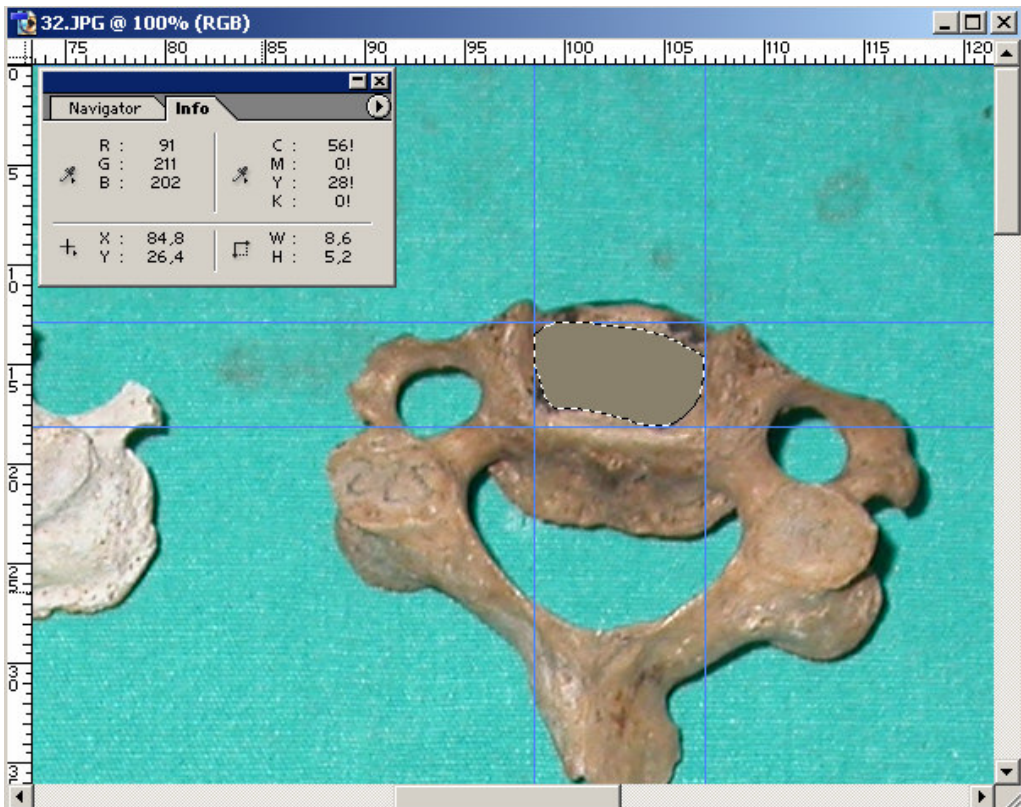
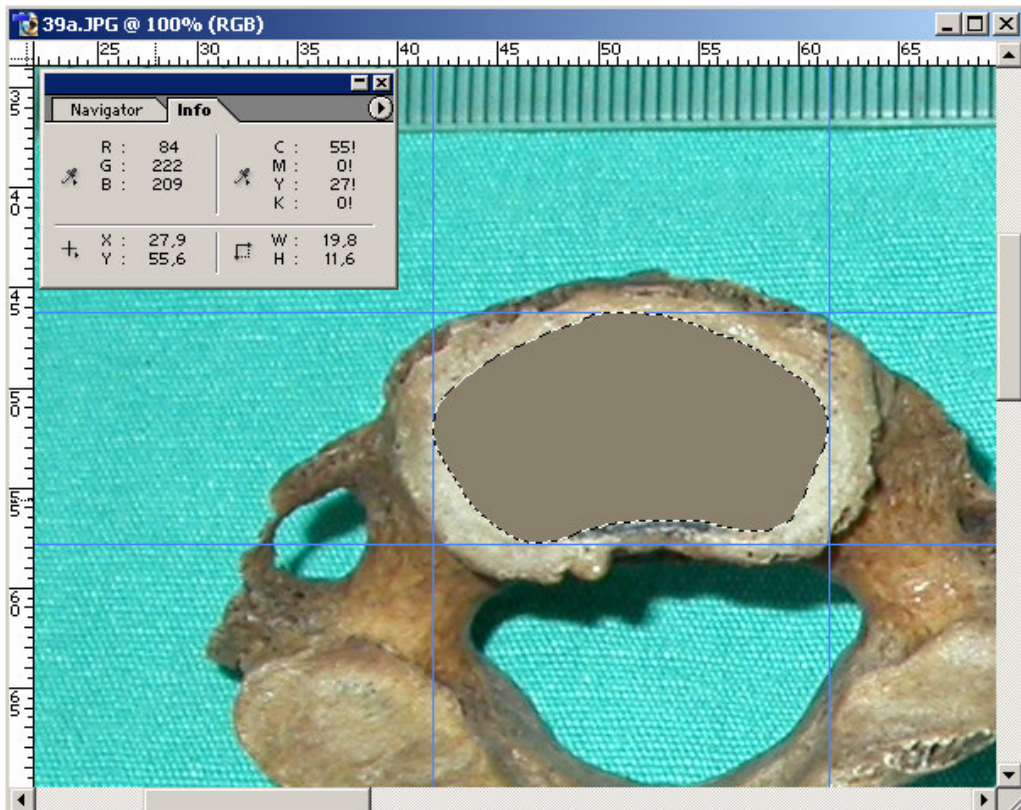

Figure A.57. Vertebra number 20a-2.
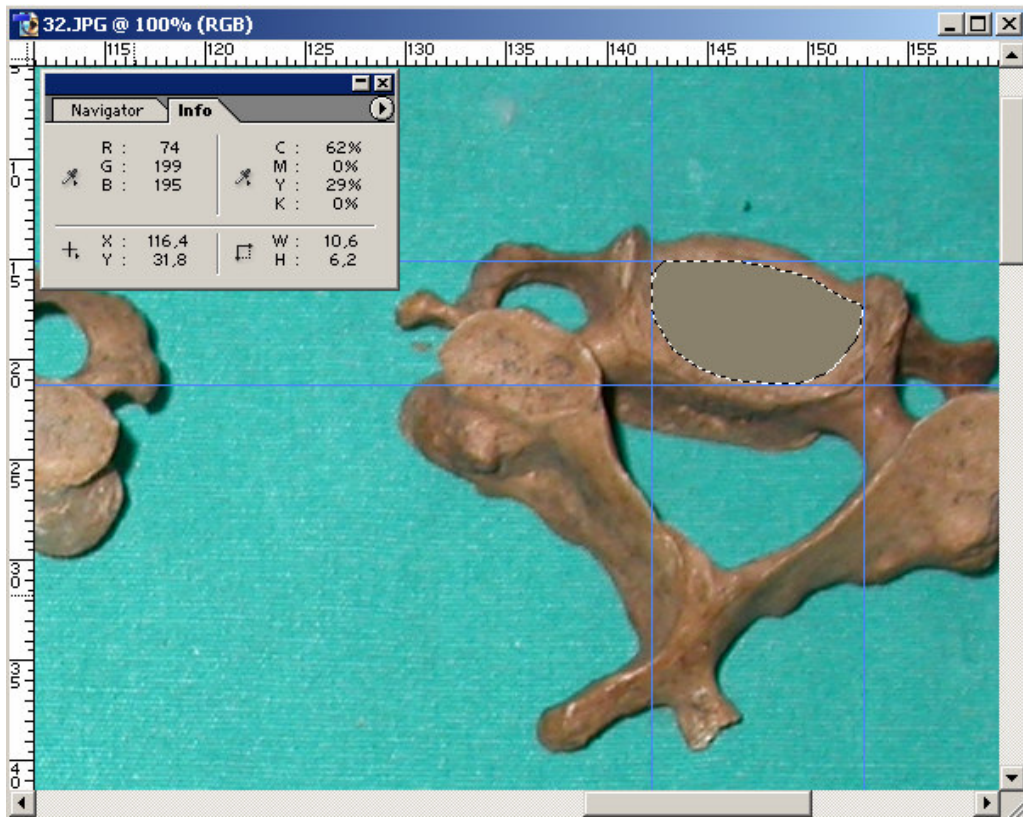
Figure A.58. Vertebra number 21-1.
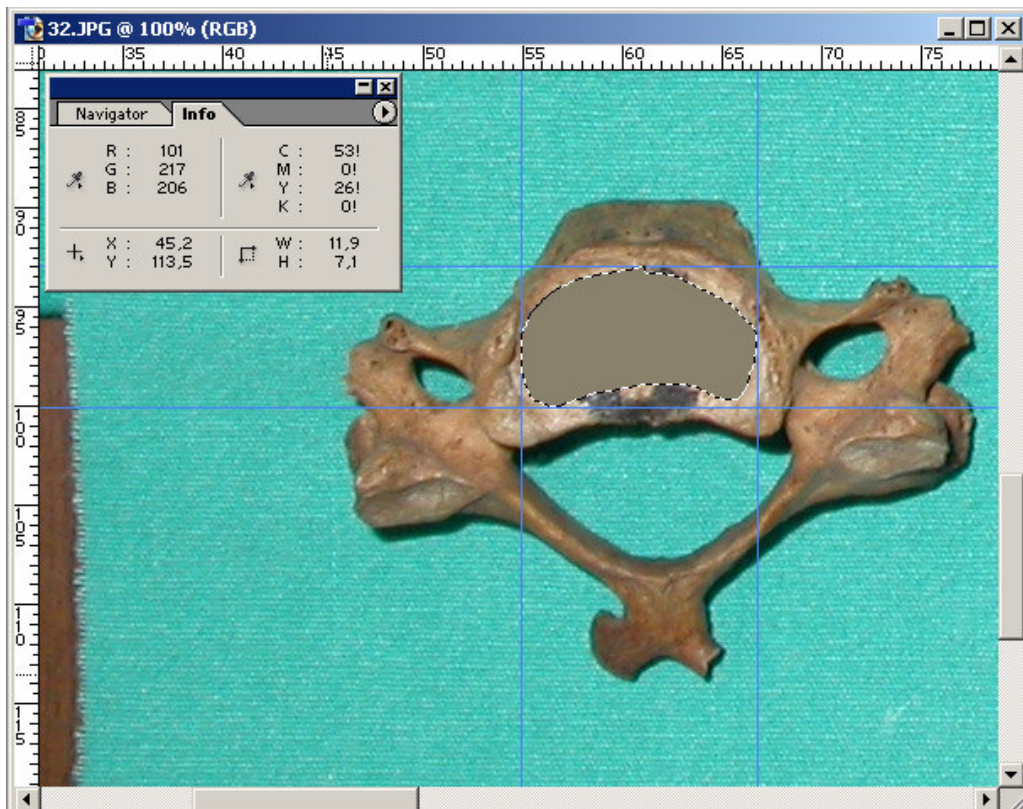
Figure A.59. Vertebra number 21-2.
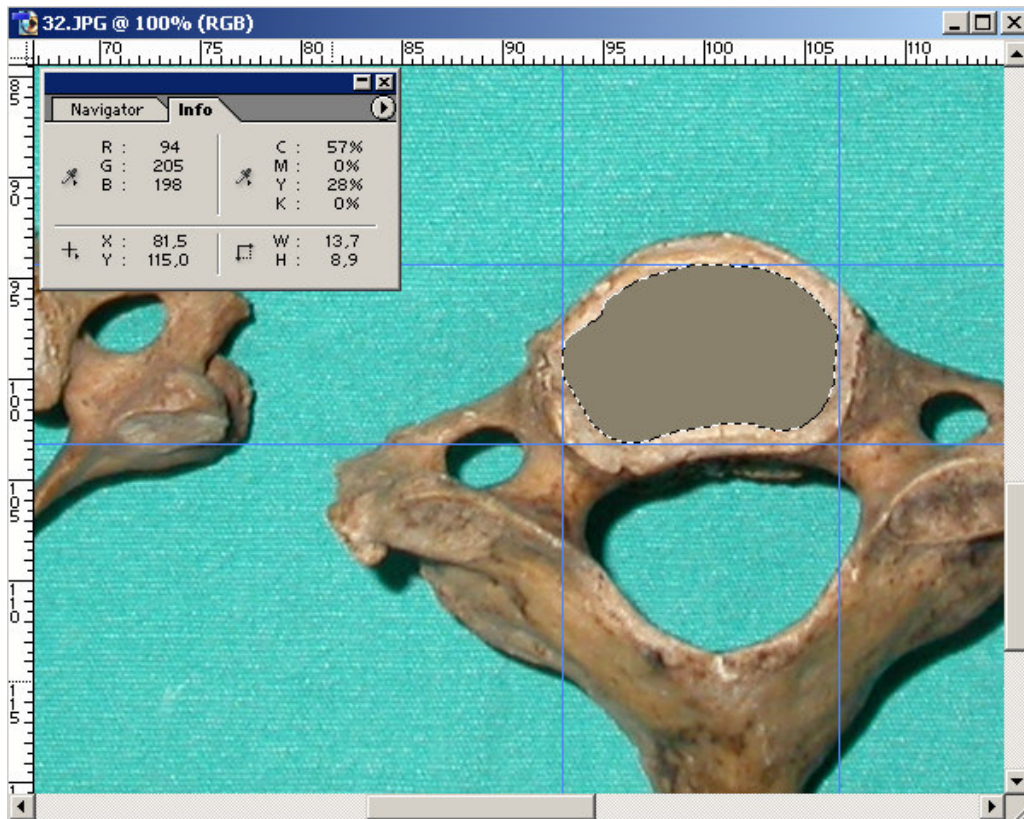
Figure A.60. Vertebra number 21a-1.
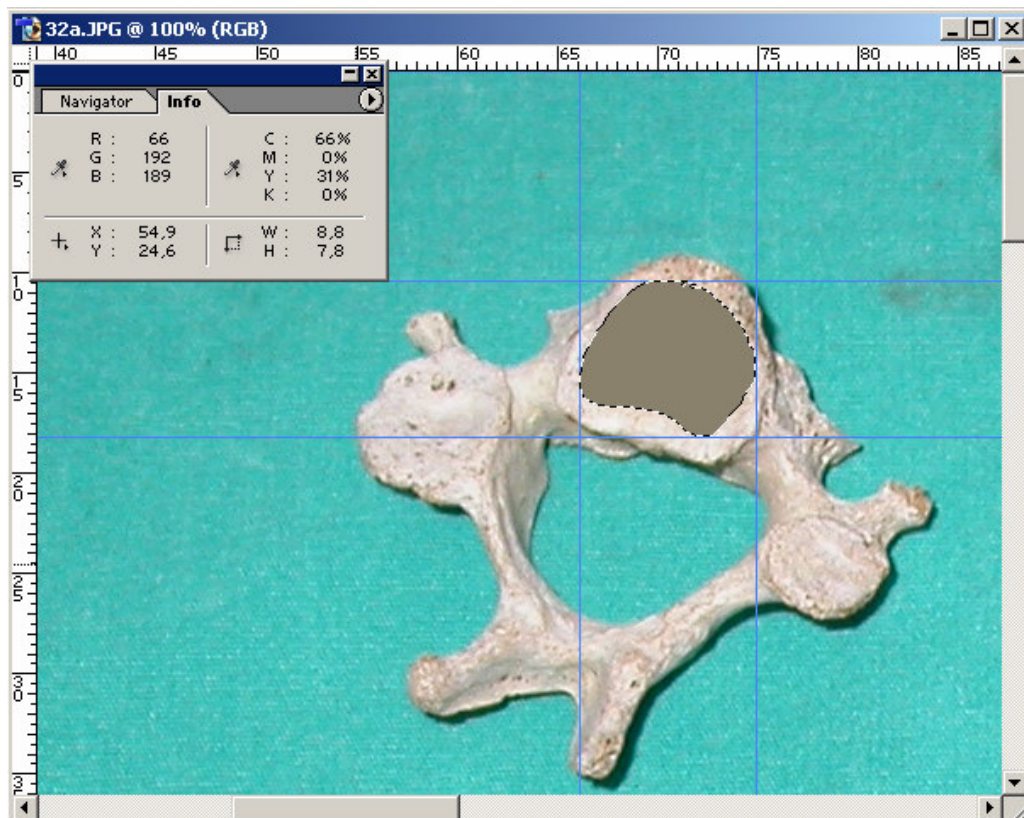
Figure A.61. Vertebra number 21a-2.
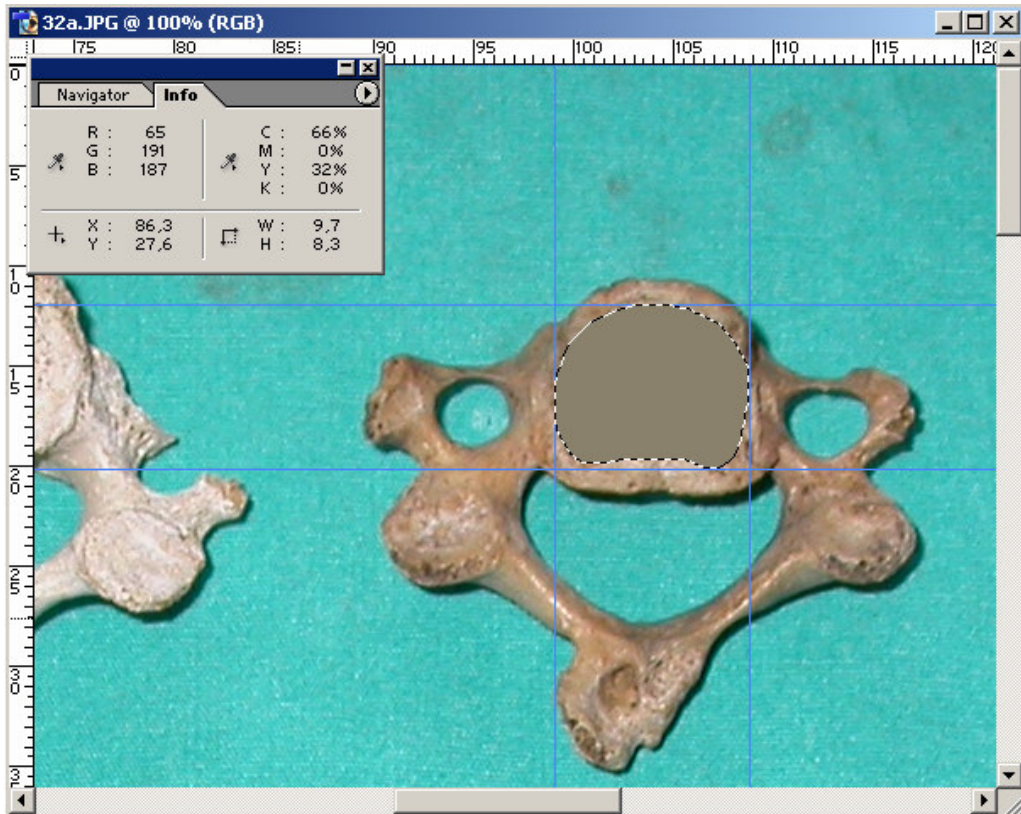
Figure A.62. Vertebra number 22-1.
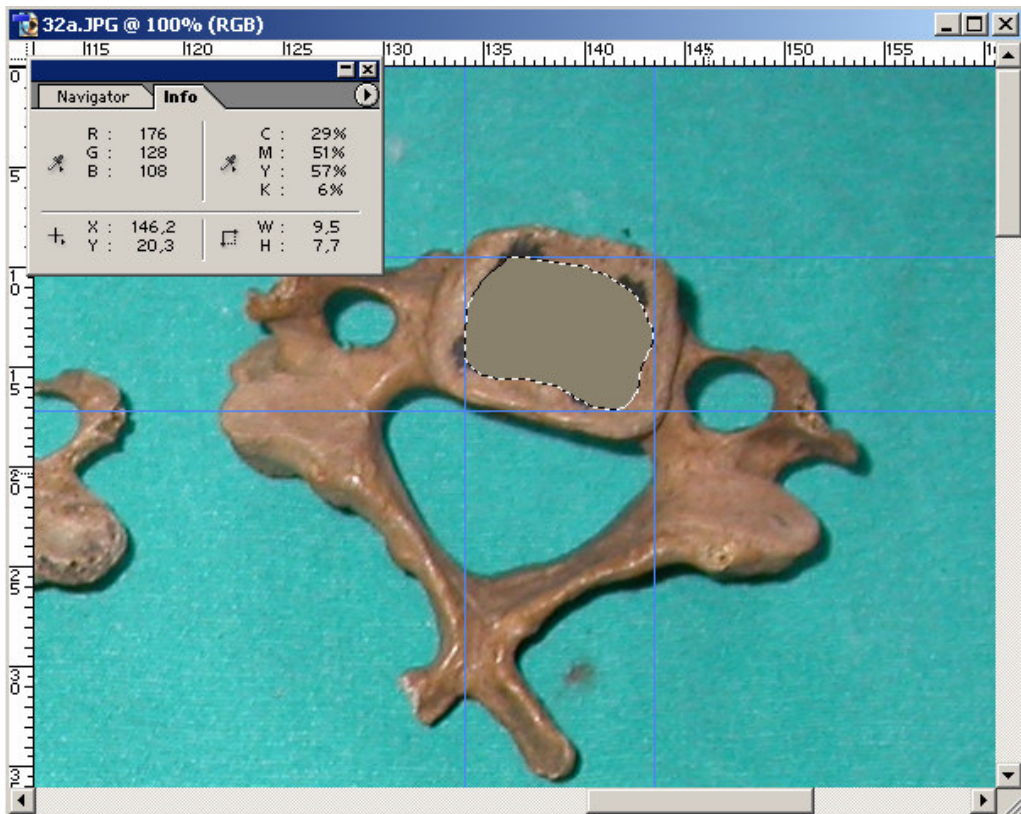
Figure A.62. Vertebra number 22-2.
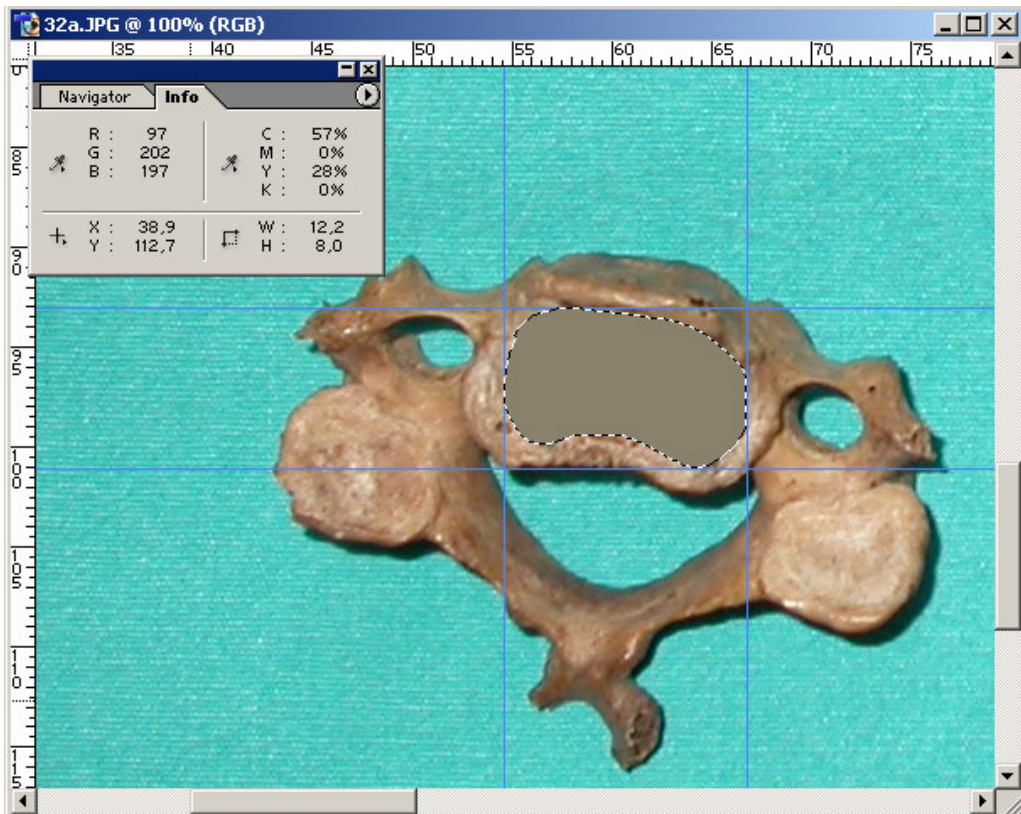
Figure A.63. Vertebra number 22a-1.
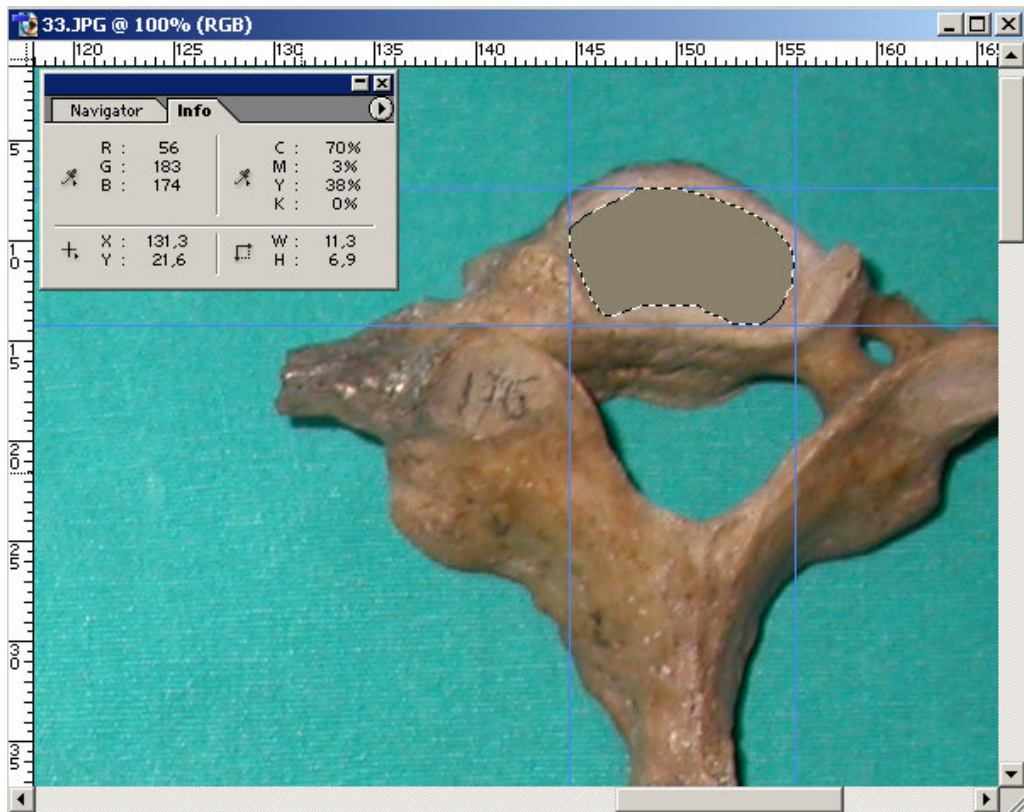
Figure A.64. Vertebra number 22a-2.
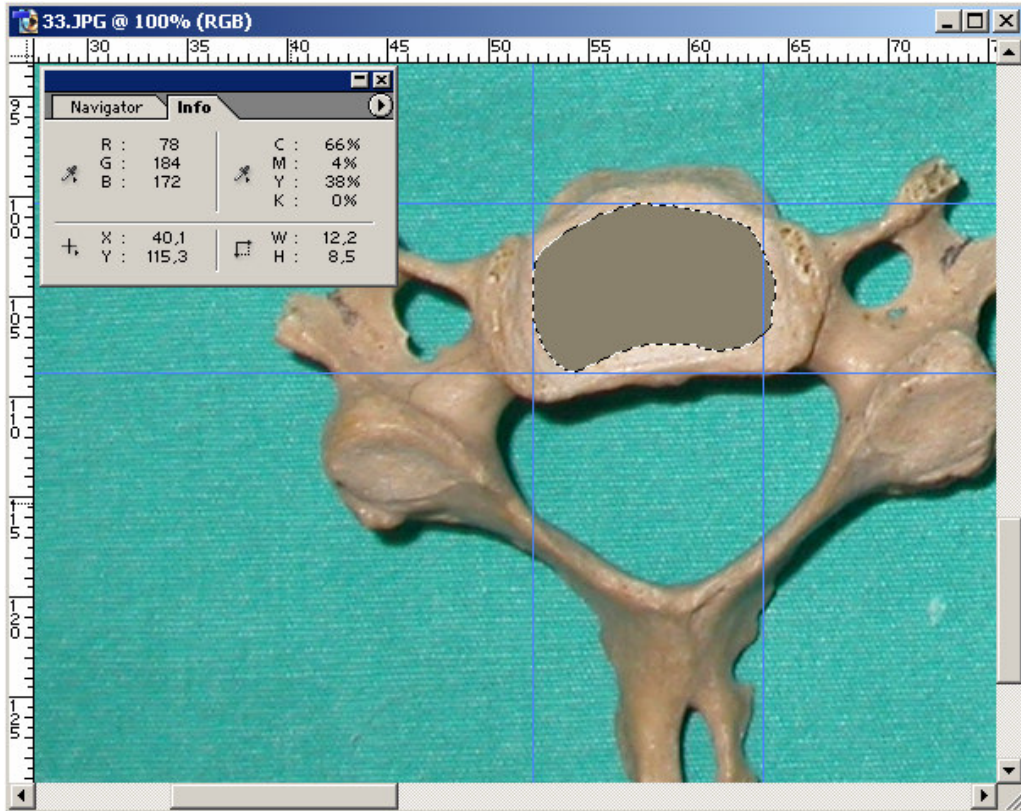
Figure A.65. Vertebra number 23-1.
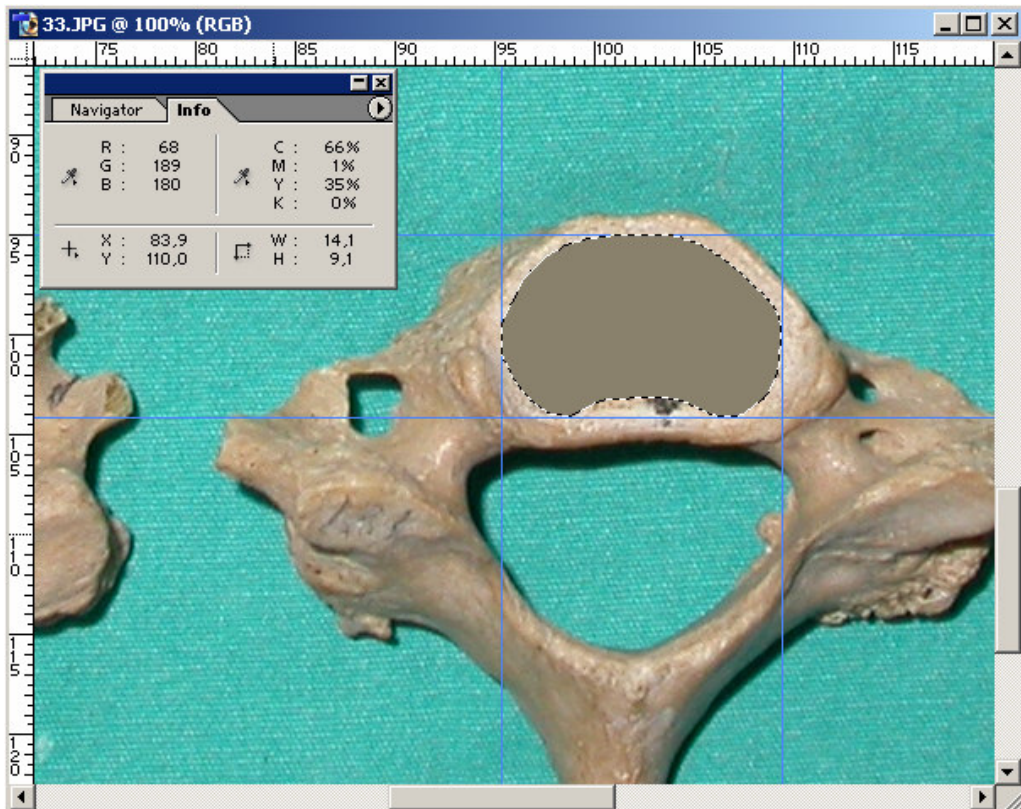
Figure A.66. Vertebra number 23-2.
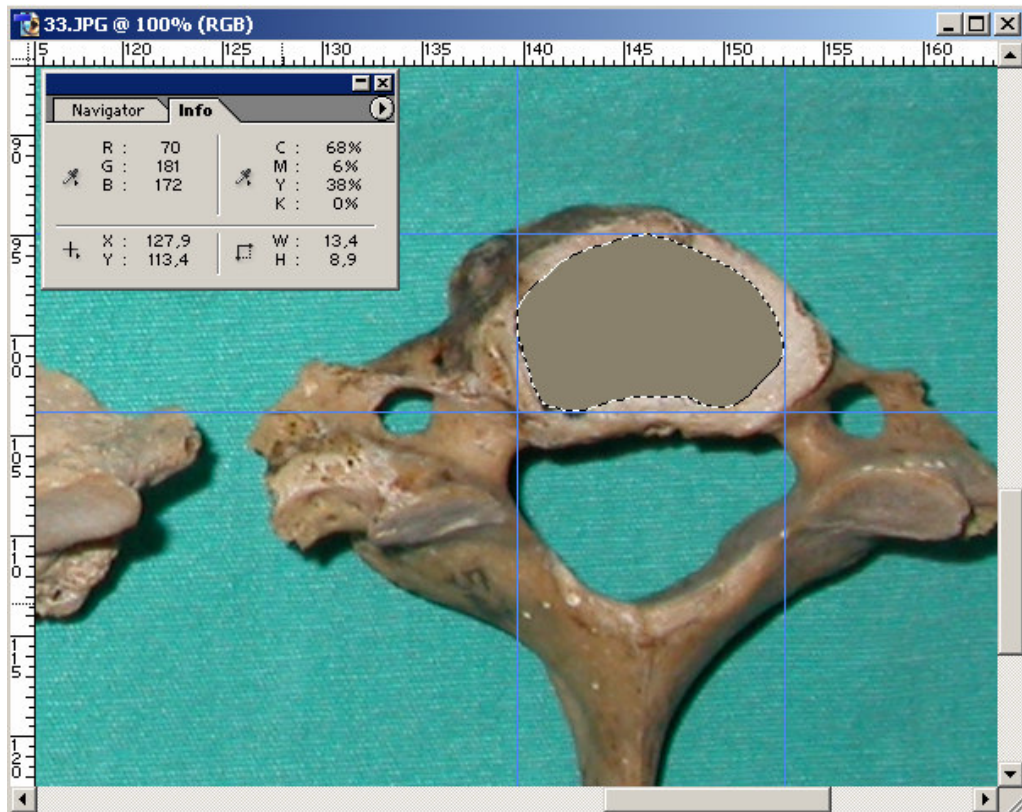
Figure A.67. Vertebra number 23a-1.
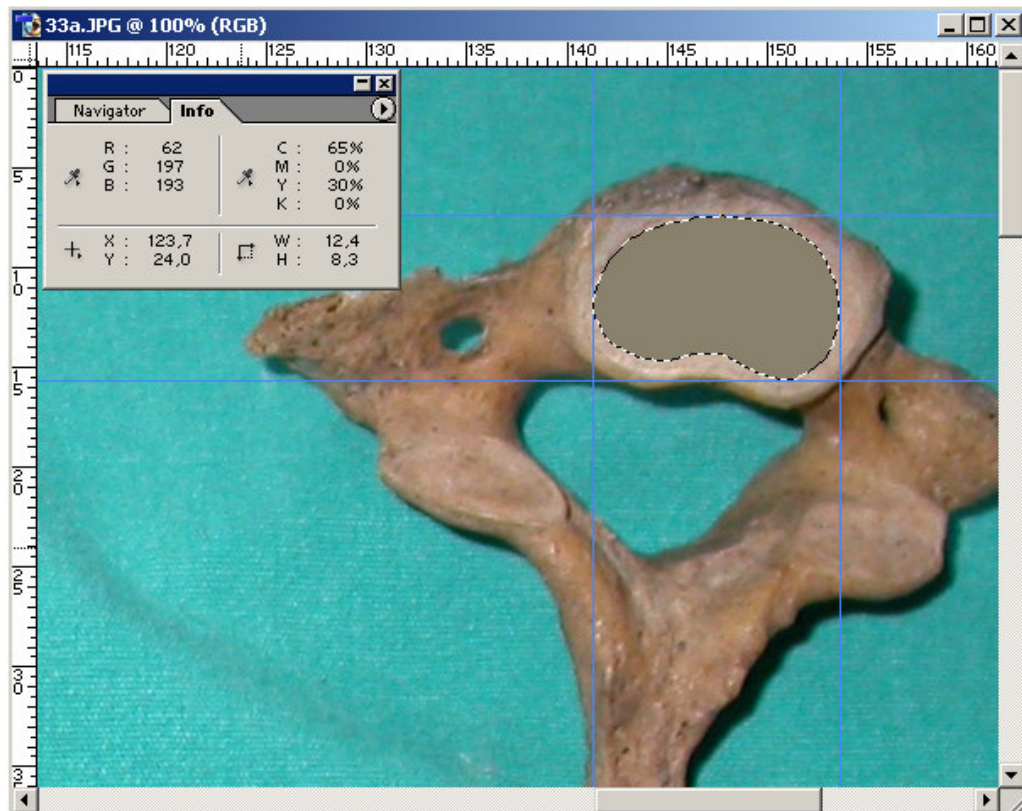
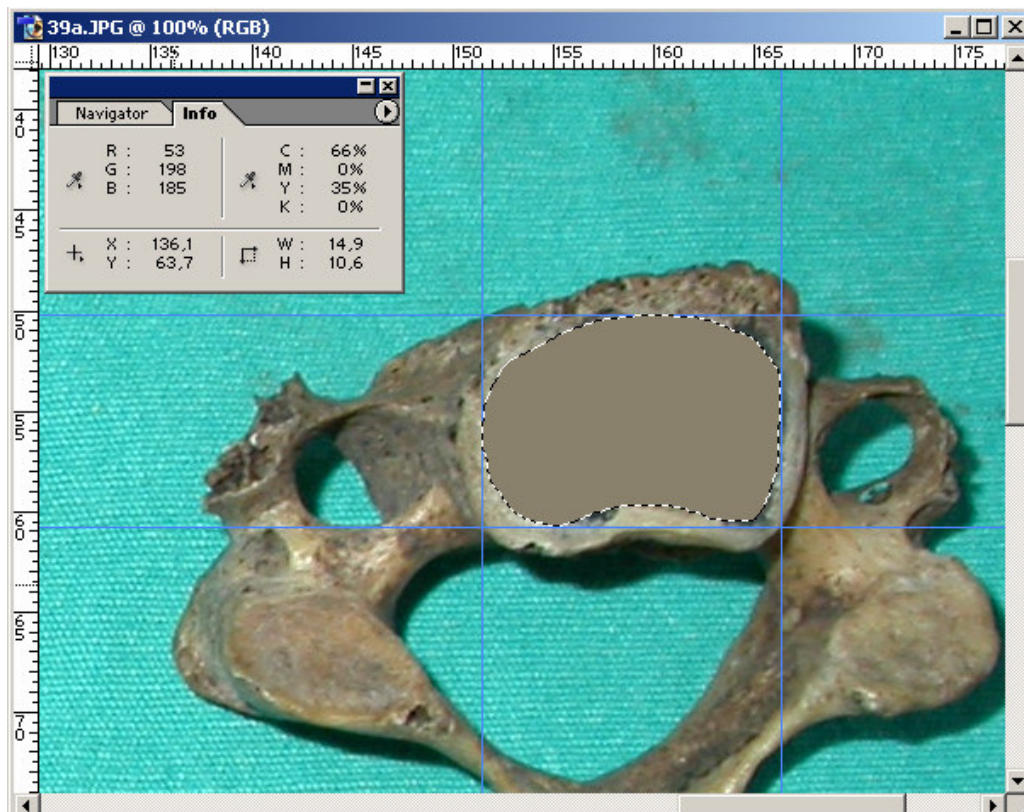Figure A.68. Vertebra number 23a-2.
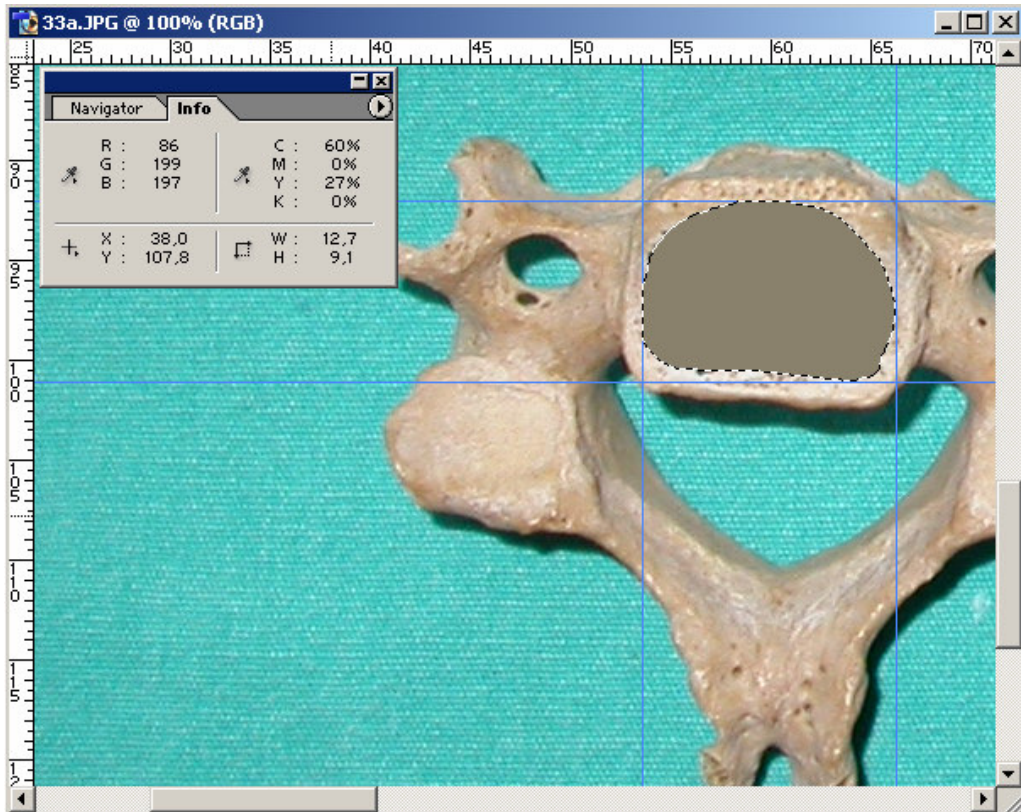
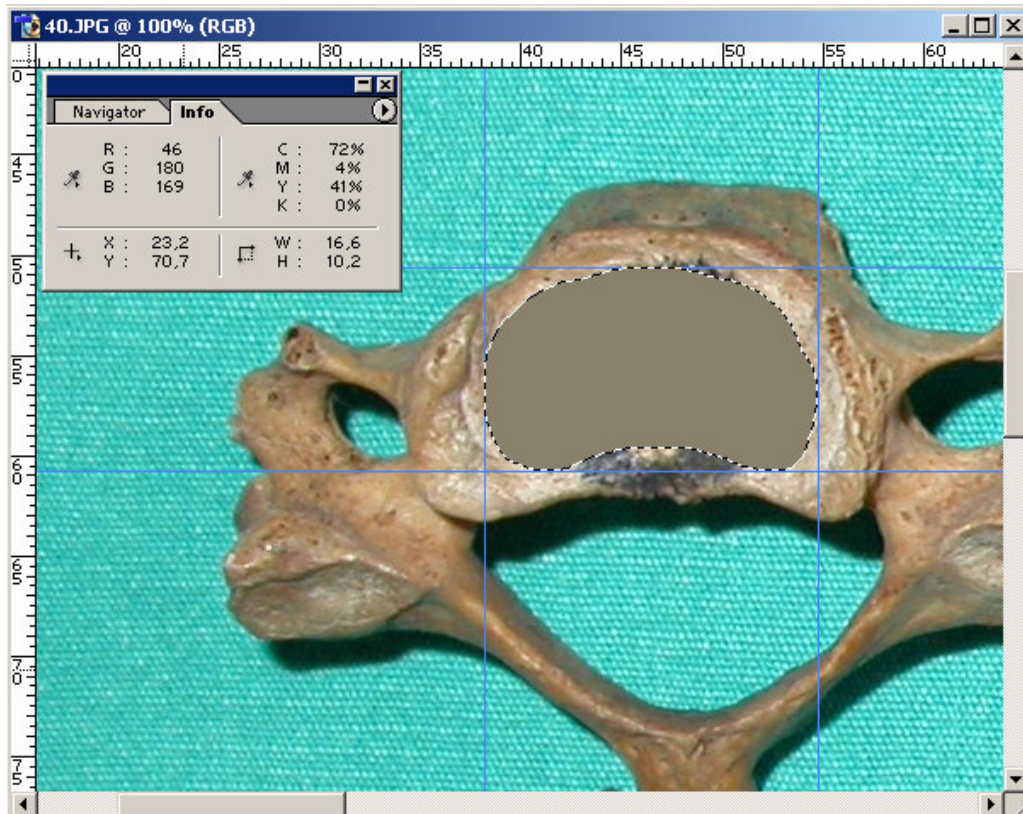Figure A.69. Vertebra number 24-1.
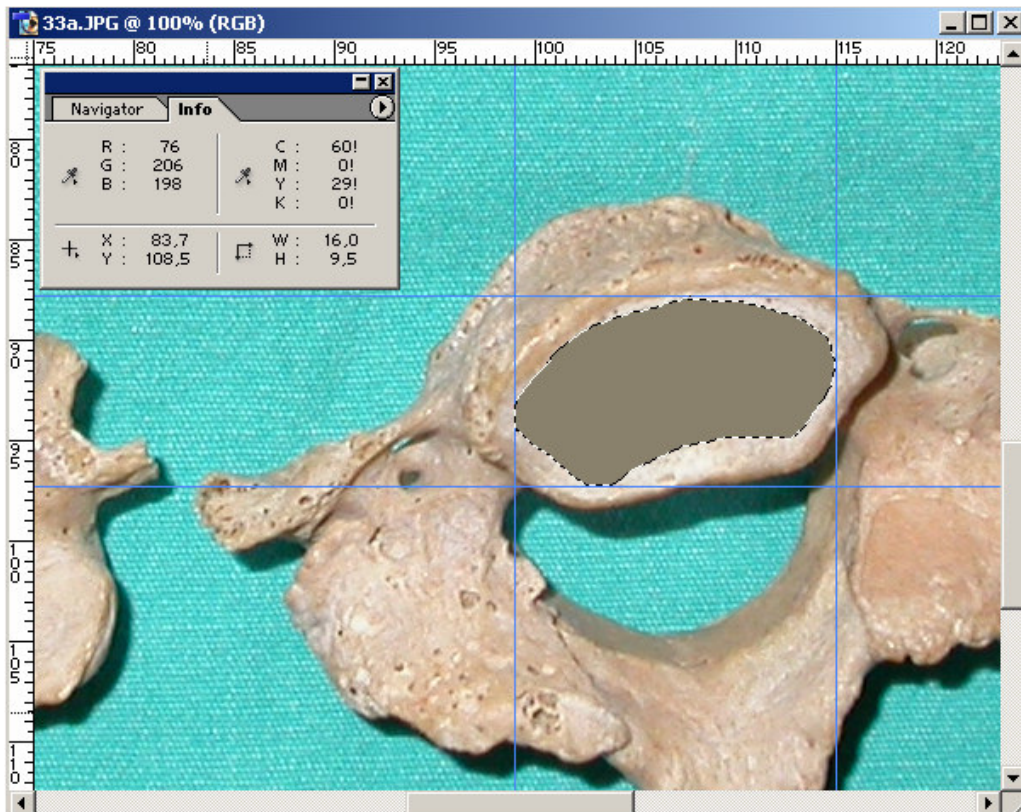
Figure A.70. Vertebra number 24-2.
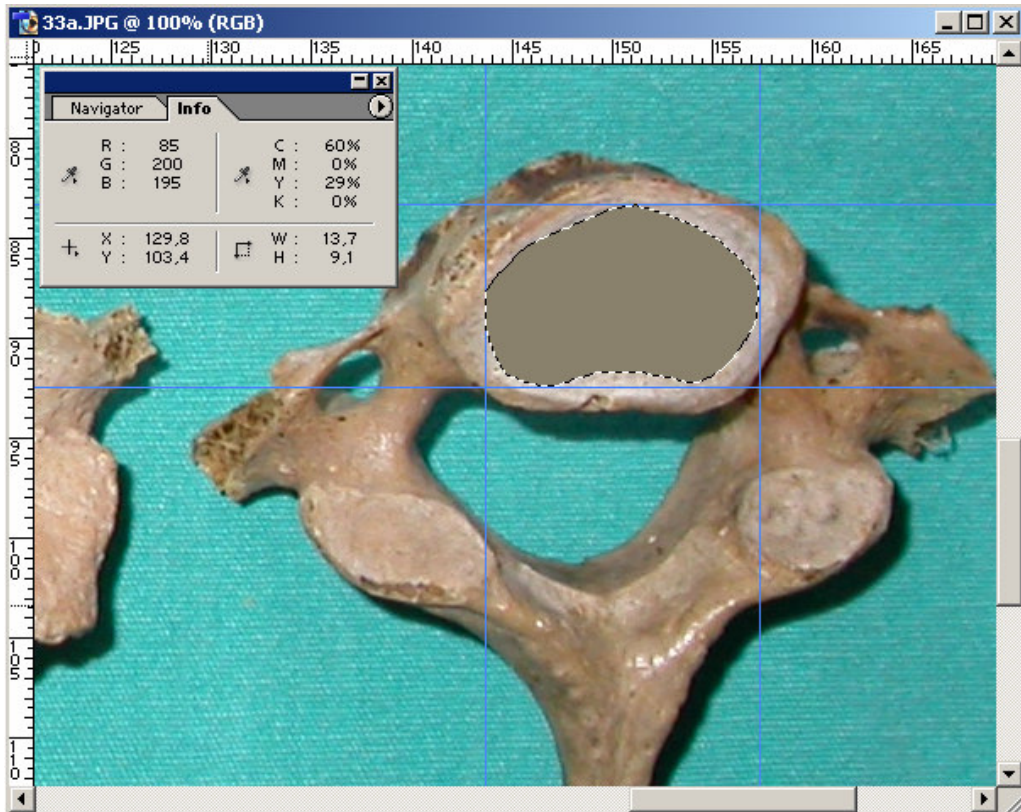
Figure A.71. Vertebra number 24a-1.
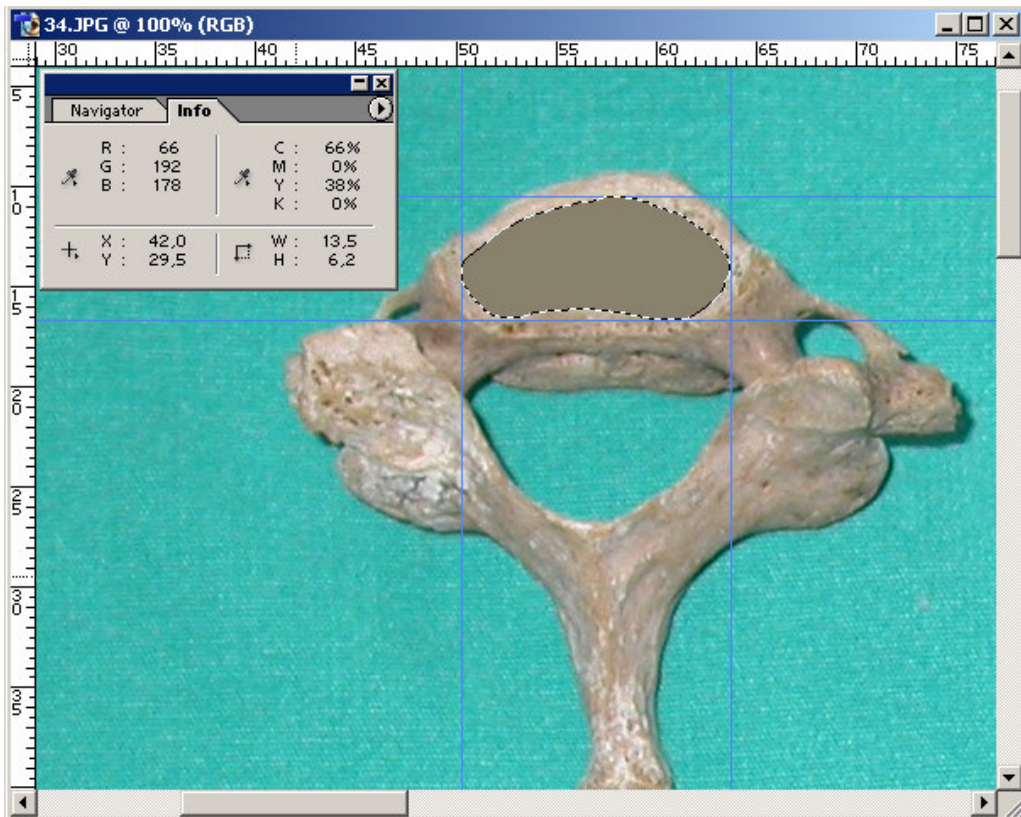
Figure A.72. Vertebra number 24a-2.
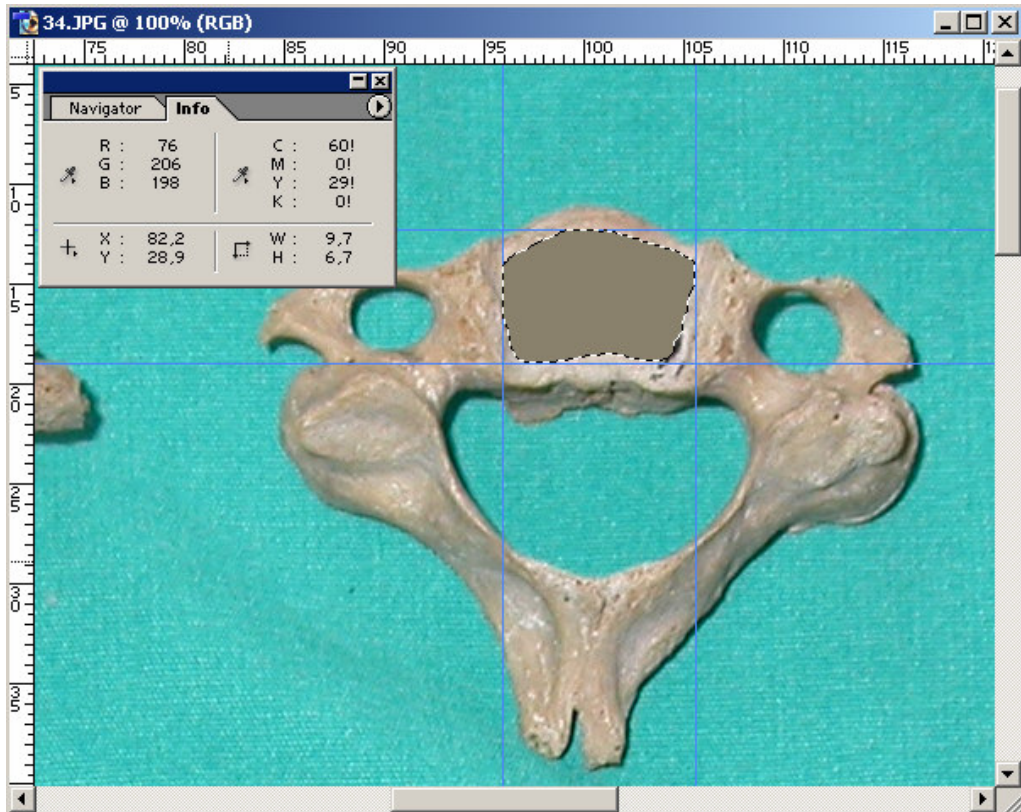
Figure A.73. Vertebra number 25-1.
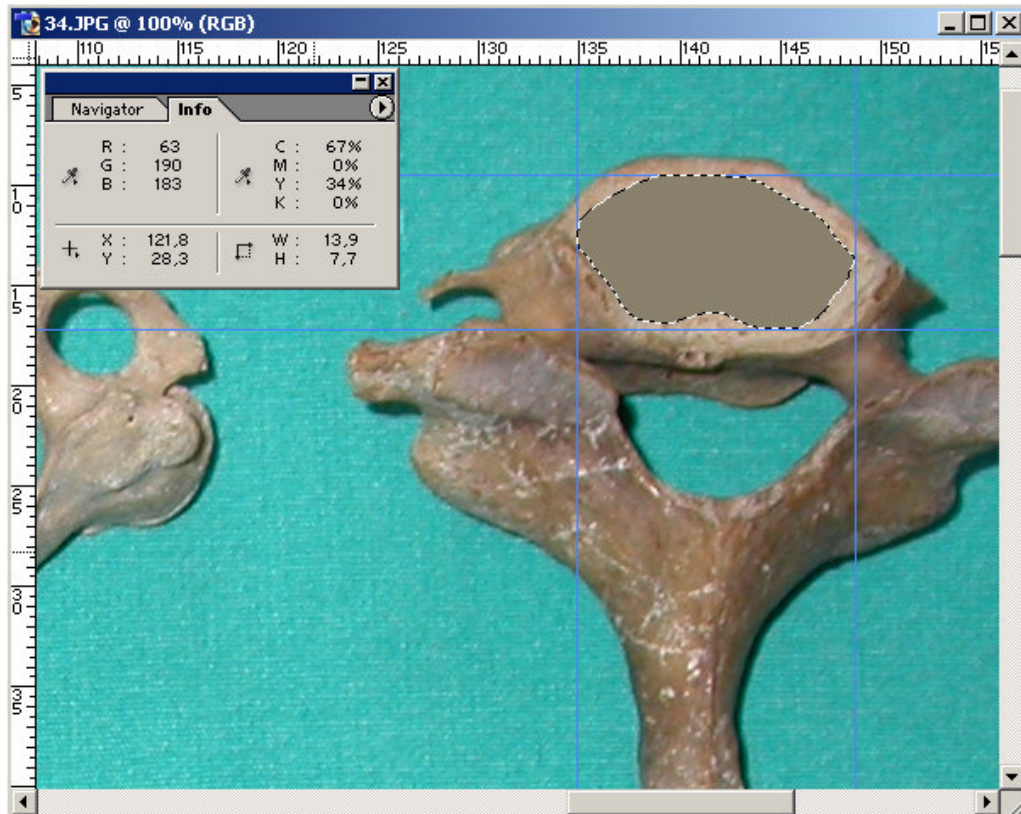
Figure A.74. Vertebra number 25-2.
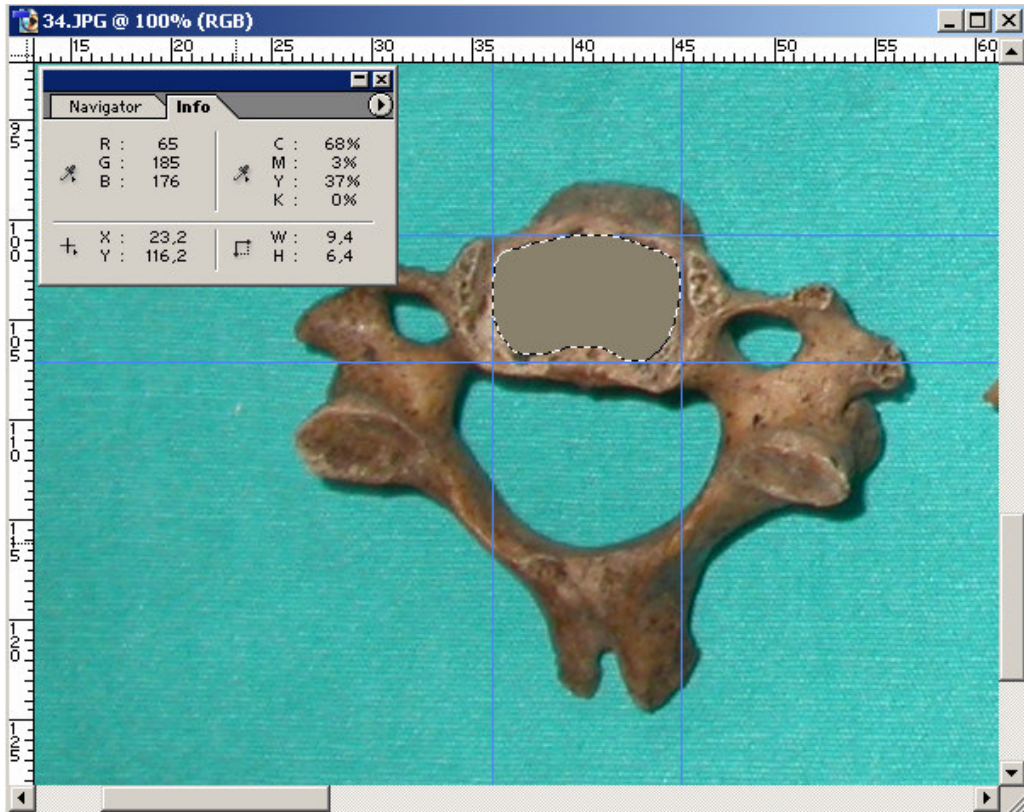
Figure A.75. Vertebra number 25a-1.
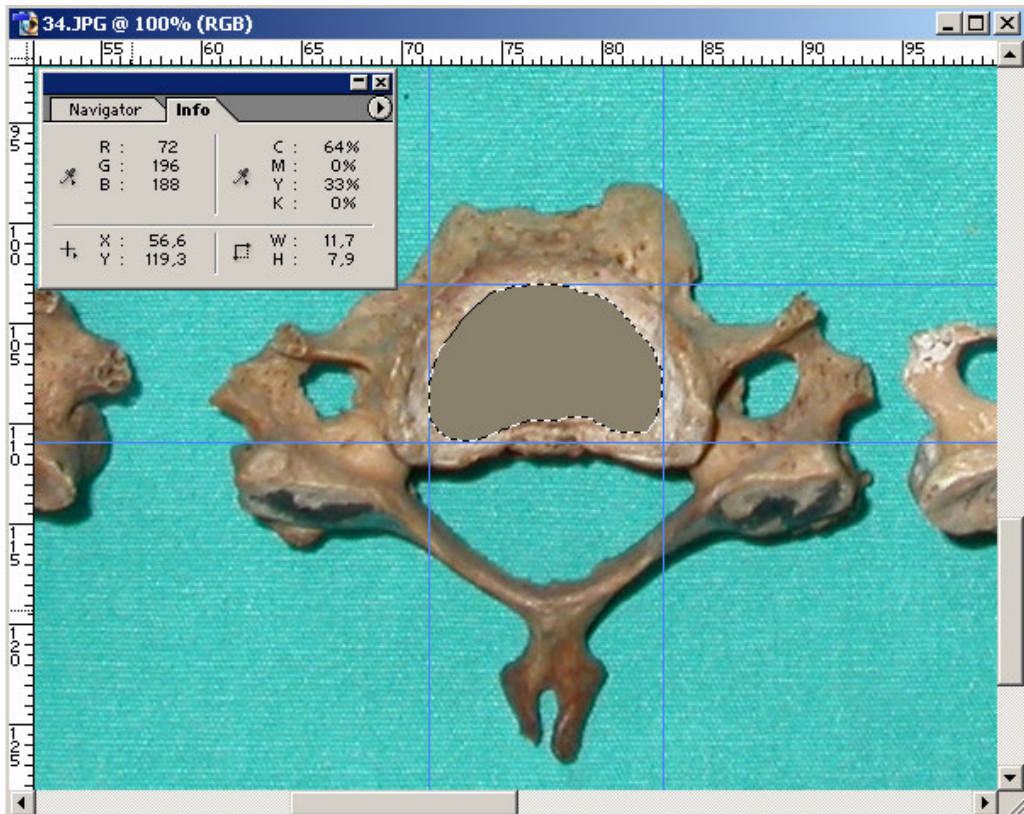
Figure A.76. Vertebra number 25a-2.

Figure A.78. Vertebra number 26-1.

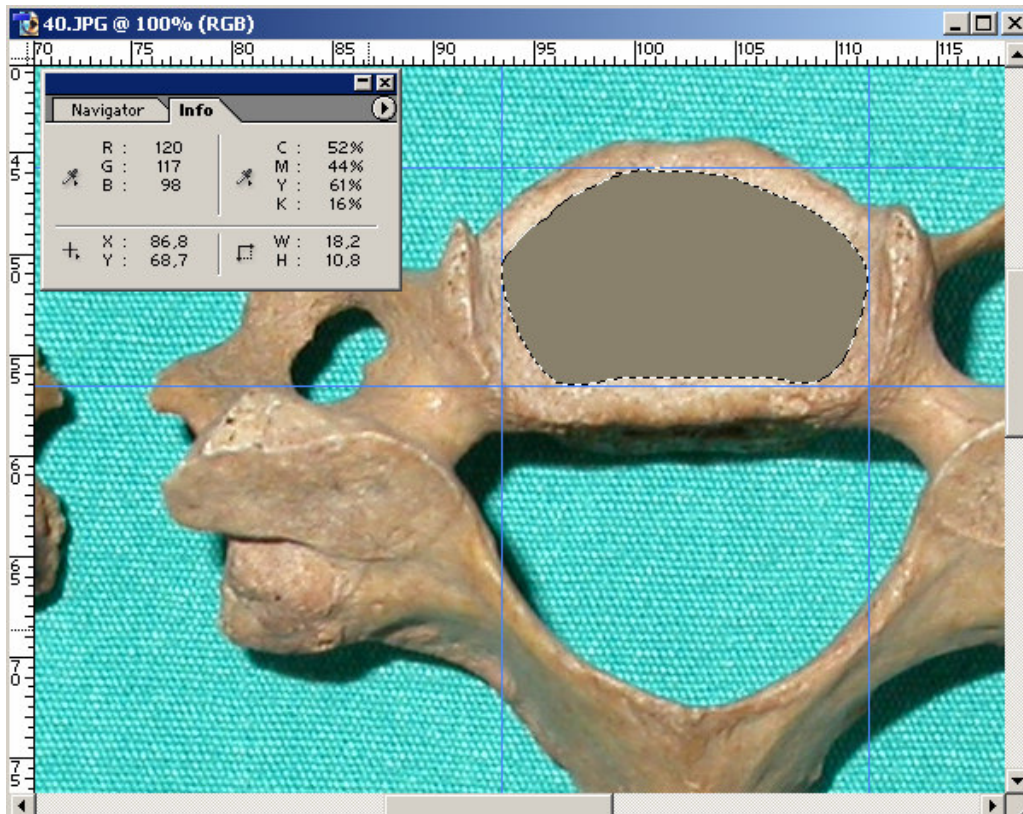Figure A.79. Vertebra number 26-2.
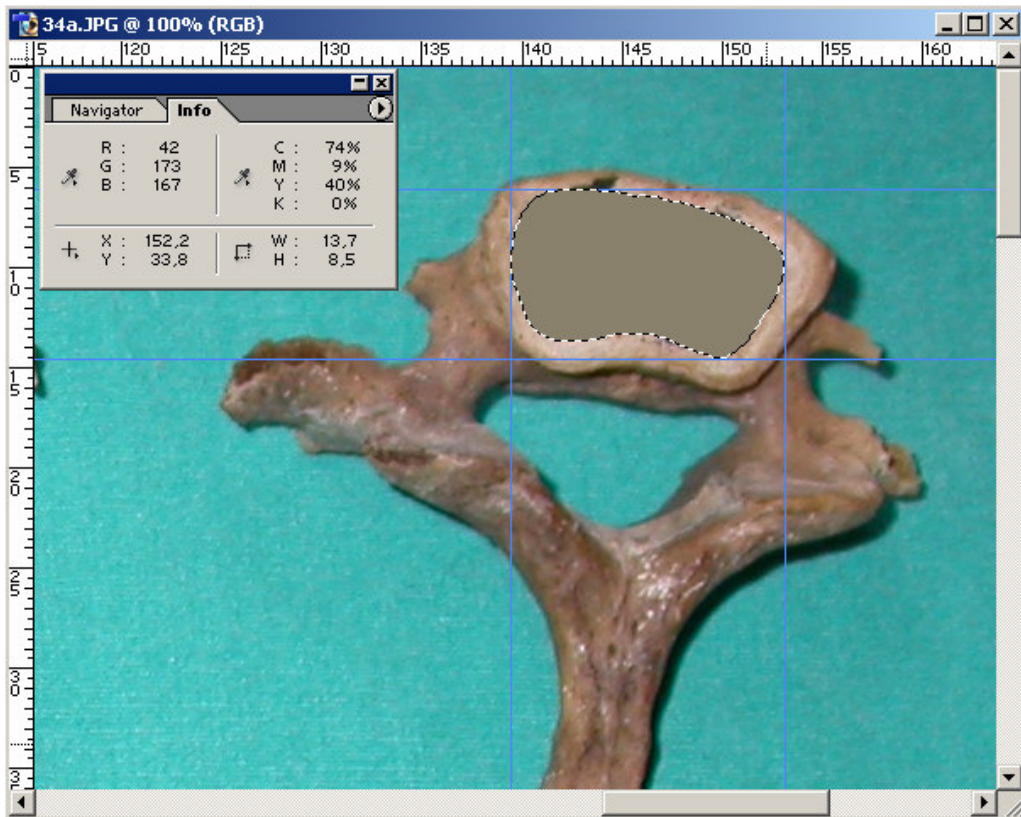
Figure A.80. Vertebra number 26a-1.
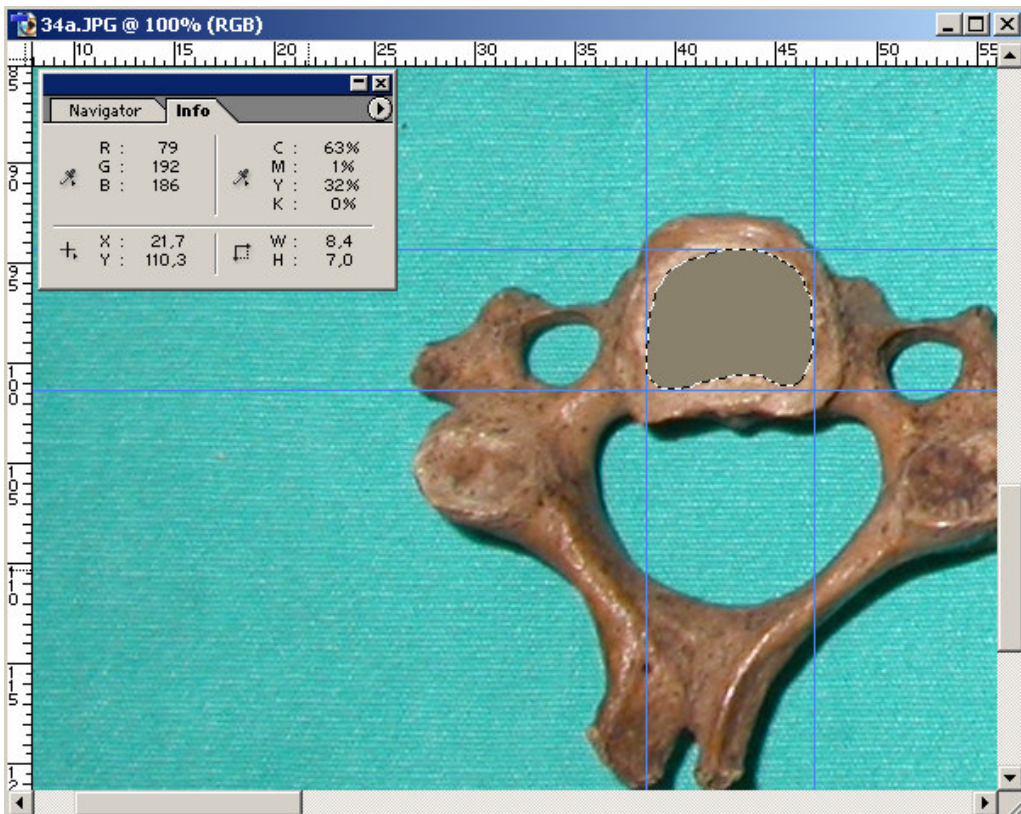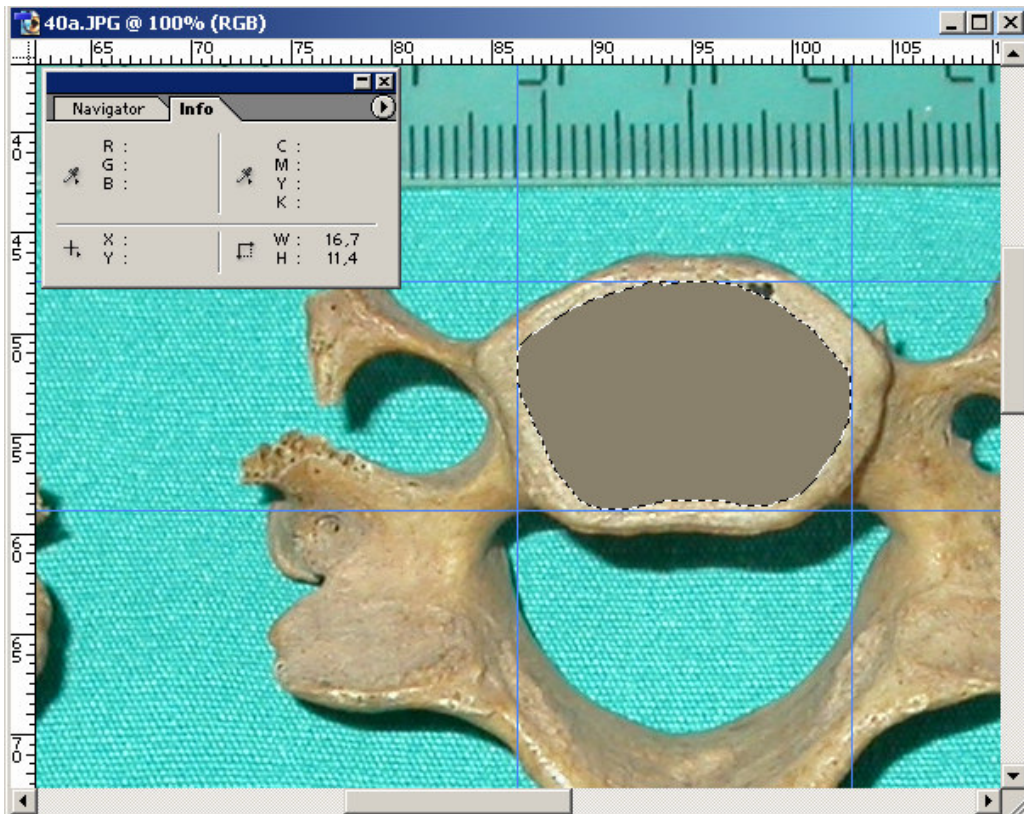

Figure A.81. Vertebra number 26a-2.
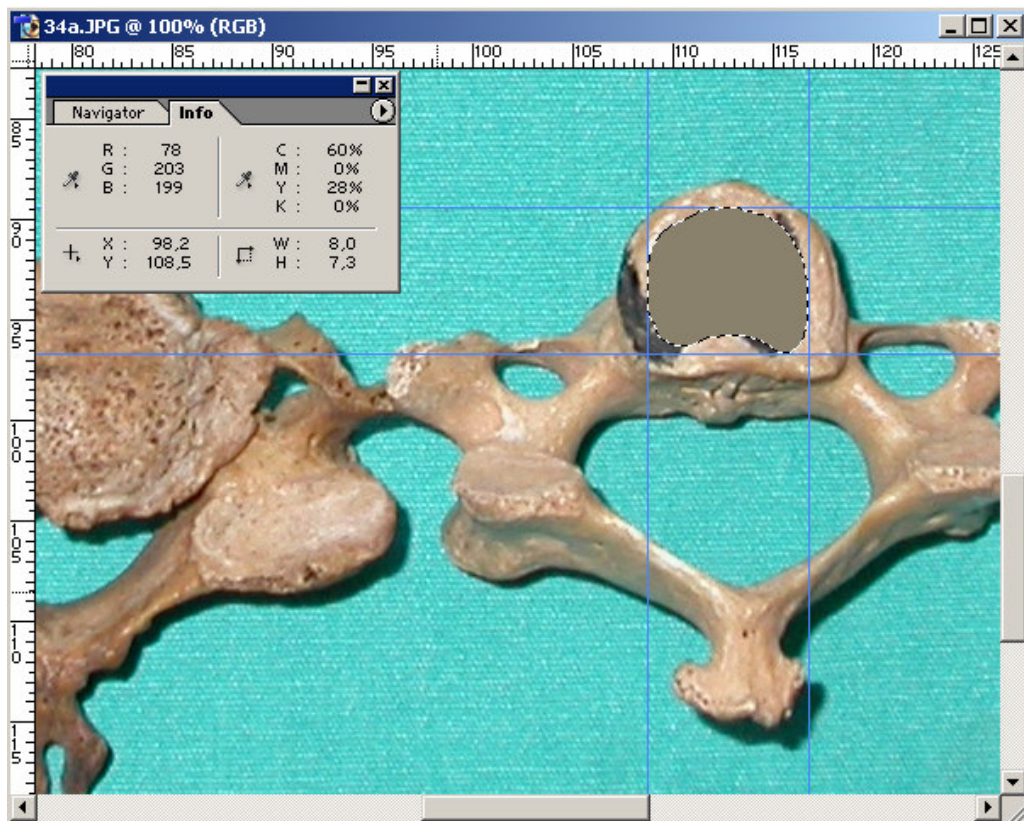
Figure A.82. Vertebra number 27-1.
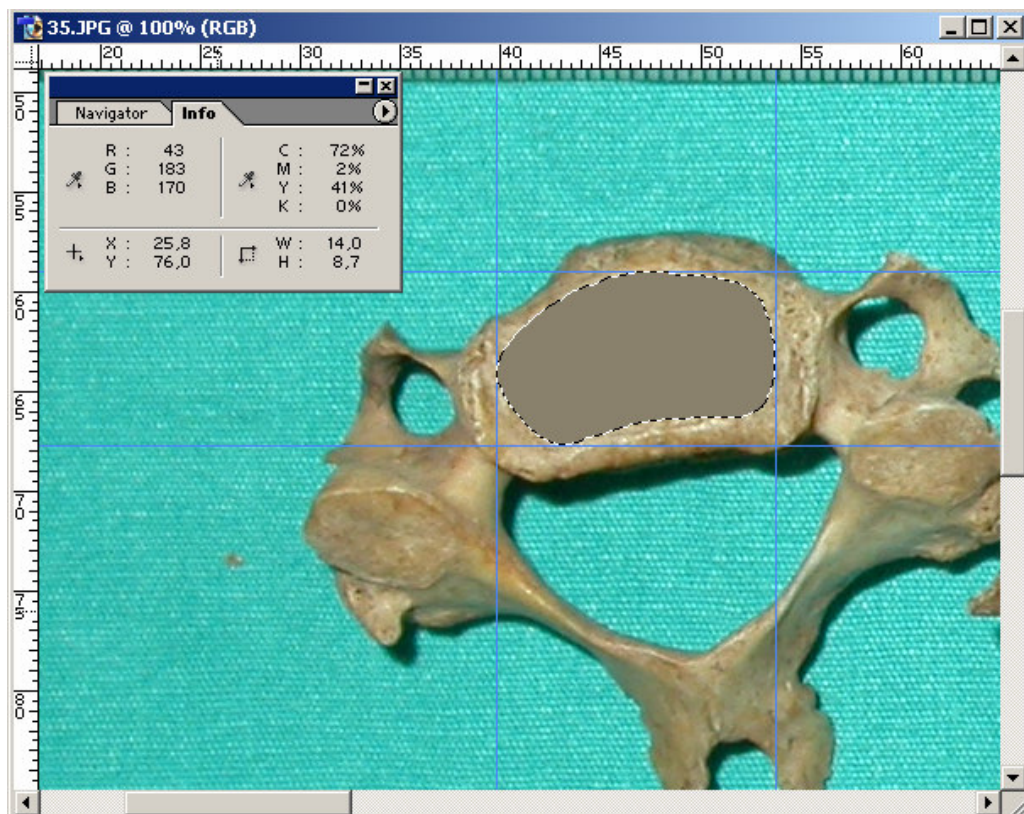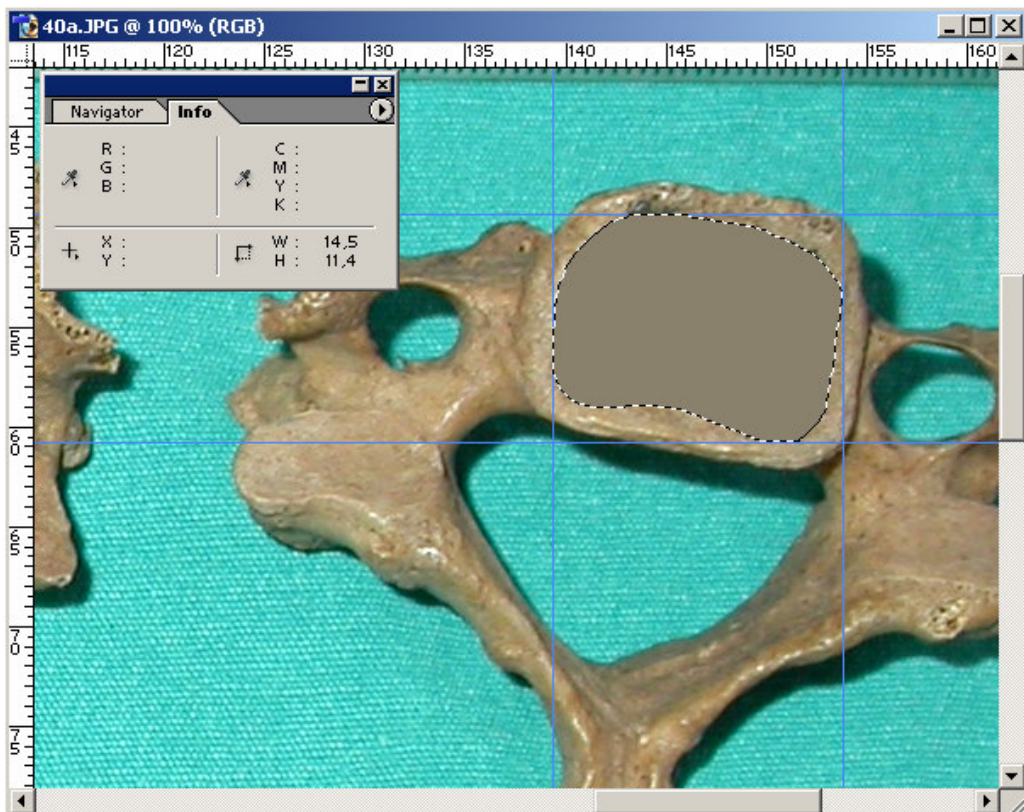

Figure A.83. Vertebra number 27-2.
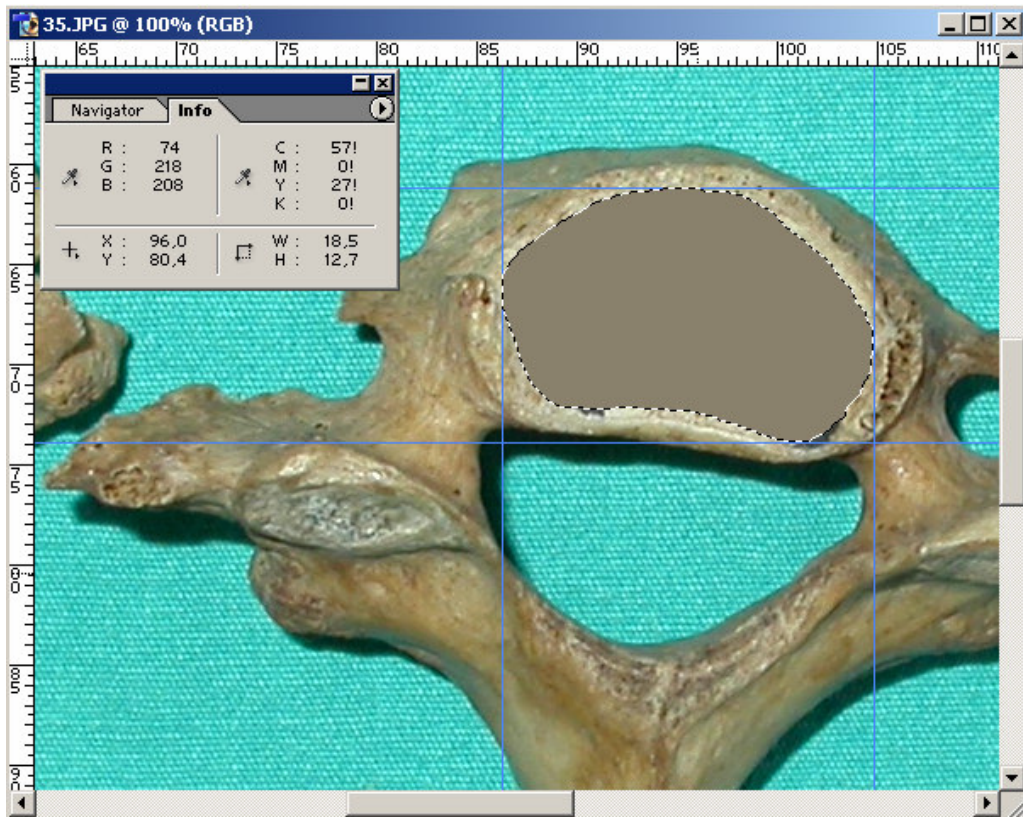
Figure A.84. Vertebra number 27a-1.

Figure A.85. Vertebra number 27a-2.

Figure A.86. Vertebra number 28-1.

Figure A.87. Vertebra number 28-2.

Figure A.88. Vertebra number 28a-1.

Figure A.89. Vertebra number 28a-2.

Figure A.90. Vertebra number 29-1.

Figure A.91. Vertebra number 29-2.

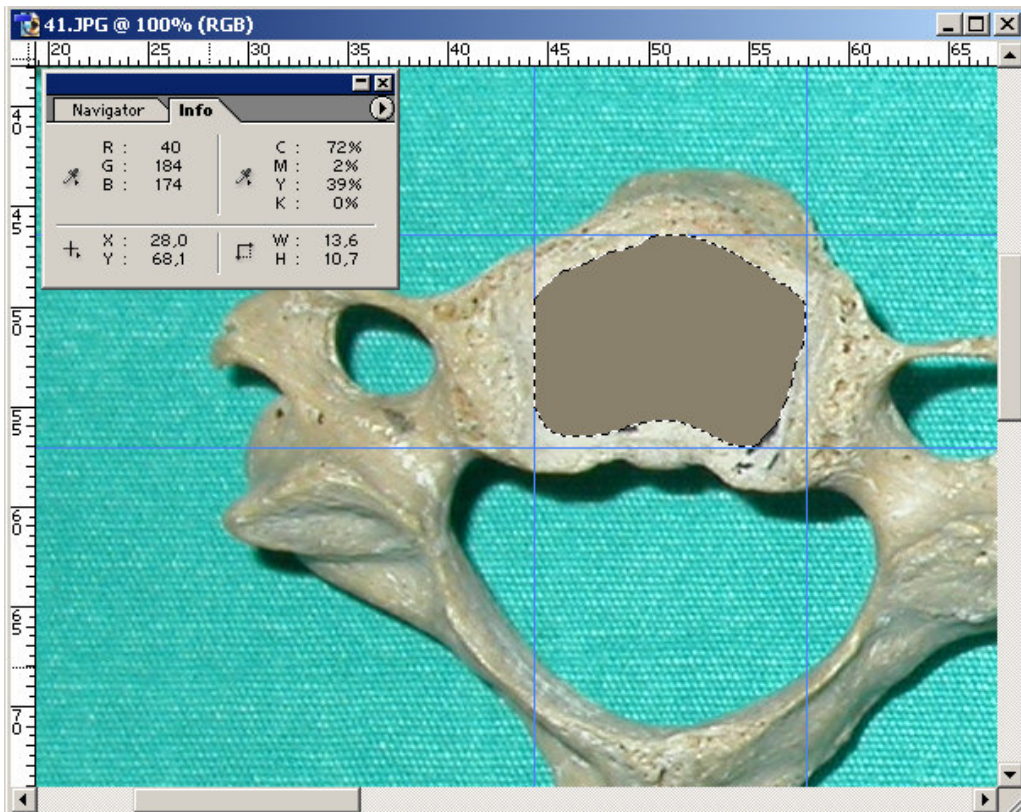Figure A.92. Vertebra number 29a-1.

Figure A.93. Vertebra number 29a-2.

Figure A.94. Vertebra number 30-1.
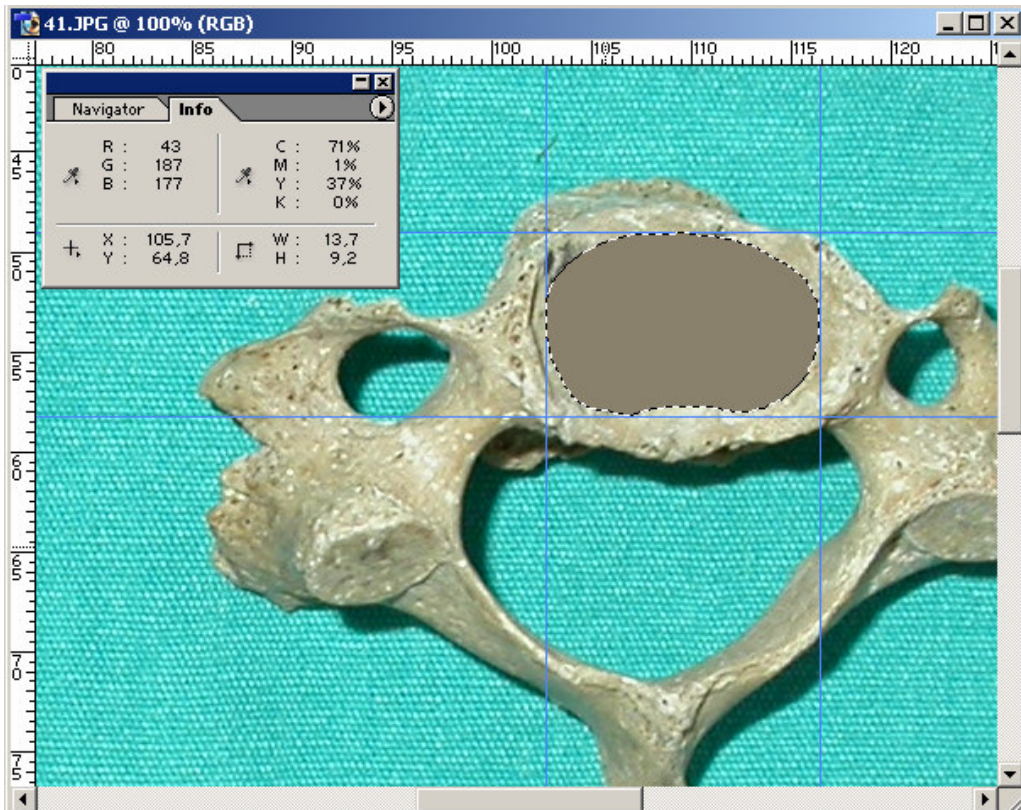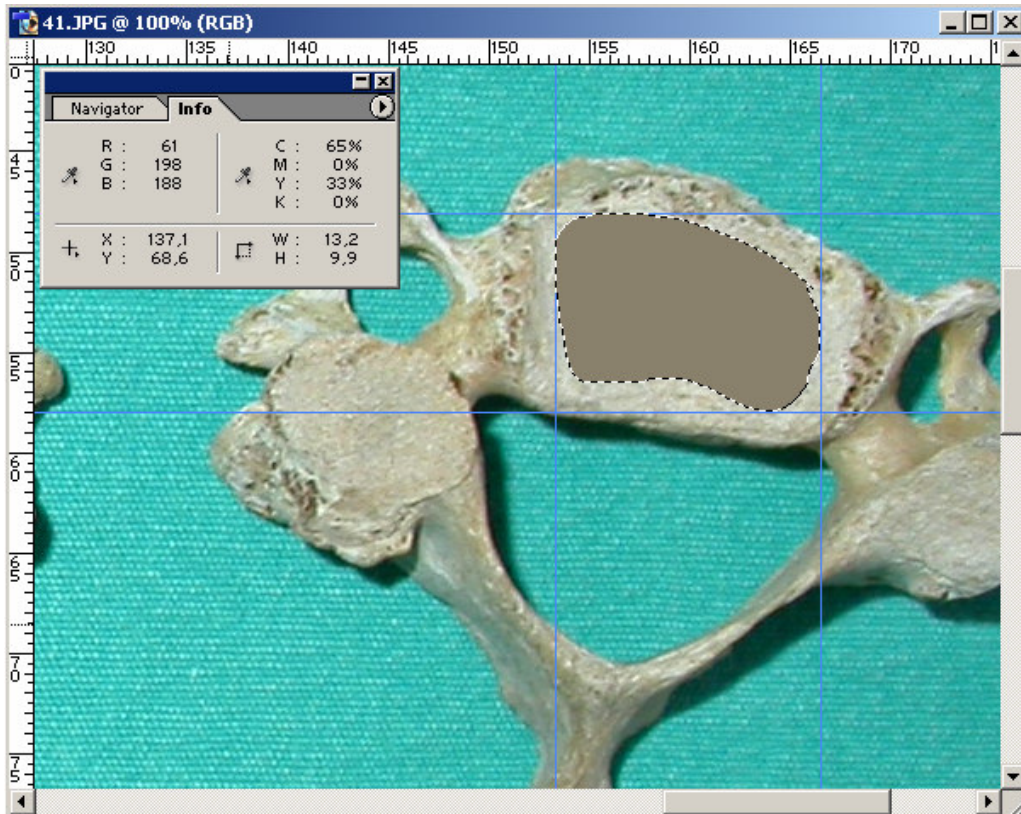

Figure A.95. Vertebra number 30-2.

Figure A.96. Vertebra number 31-1.

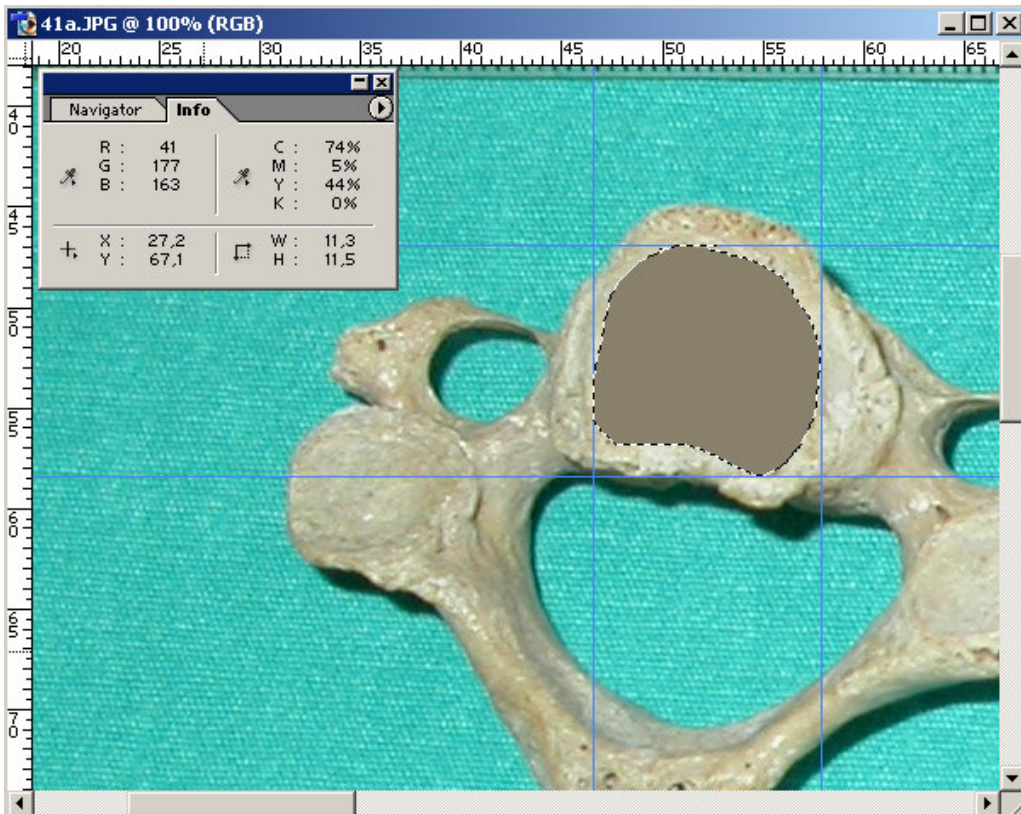
Figure A.97. Vertebra number 31-2.

Figure A.98. Vertebra number 31a-1.

Figure A.99. Vertebra number 31a-2.

Figure A.100. Vertebra number 32-1.

Figure A.101. Vertebra number 32-2.

Figure A.102. Vertebra number 32a-1.

Figure A.103. Vertebra number 32a-2.

Figure A.104. Vertebra number 33-1.

Figure A.105. Vertebra number 33-2.

Figure A.106. Vertebra number 33a-1.

Figure A.107. Vertebra number 33a-2.

136

Figure A.108. Vertebra number 34-1.
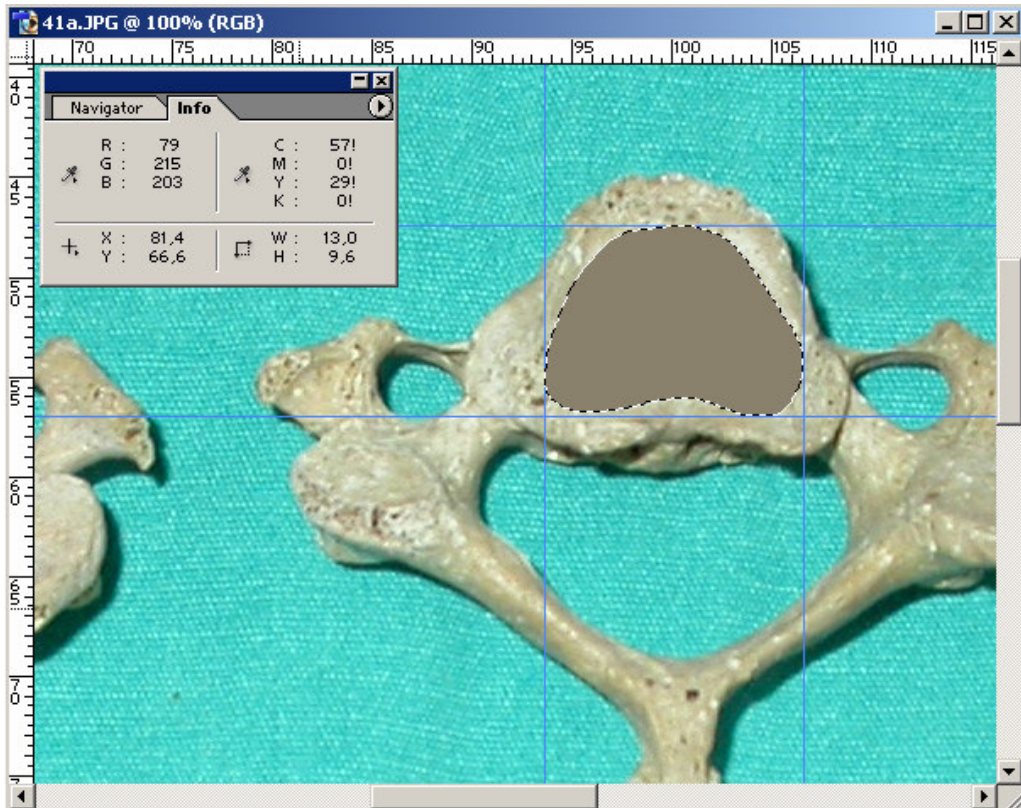

Figure A.109. Vertebra number 34-2.

Figure A.110. Vertebra number 34a-1.

Figure A.111. Vertebra number 34a-2.

Figure A.112. Vertebra number 35-1.

Figure A.113. Vertebra number 35-2.

Figure A.114. Vertebra number 35a-1.

Figure A.115. Vertebra number 35a-2.

Figure A.116. Vertebra number 36-1.

Figure A.117. Vertebra number 36-2.

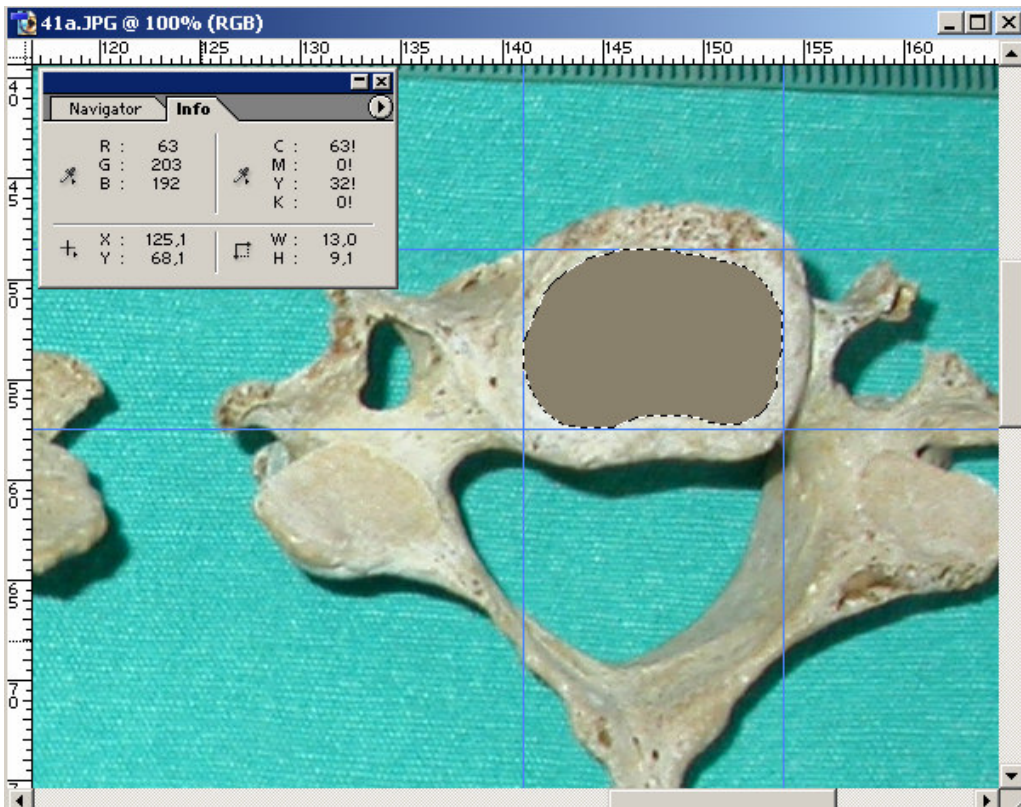Figure A.118. Vertebra number 36a-1.

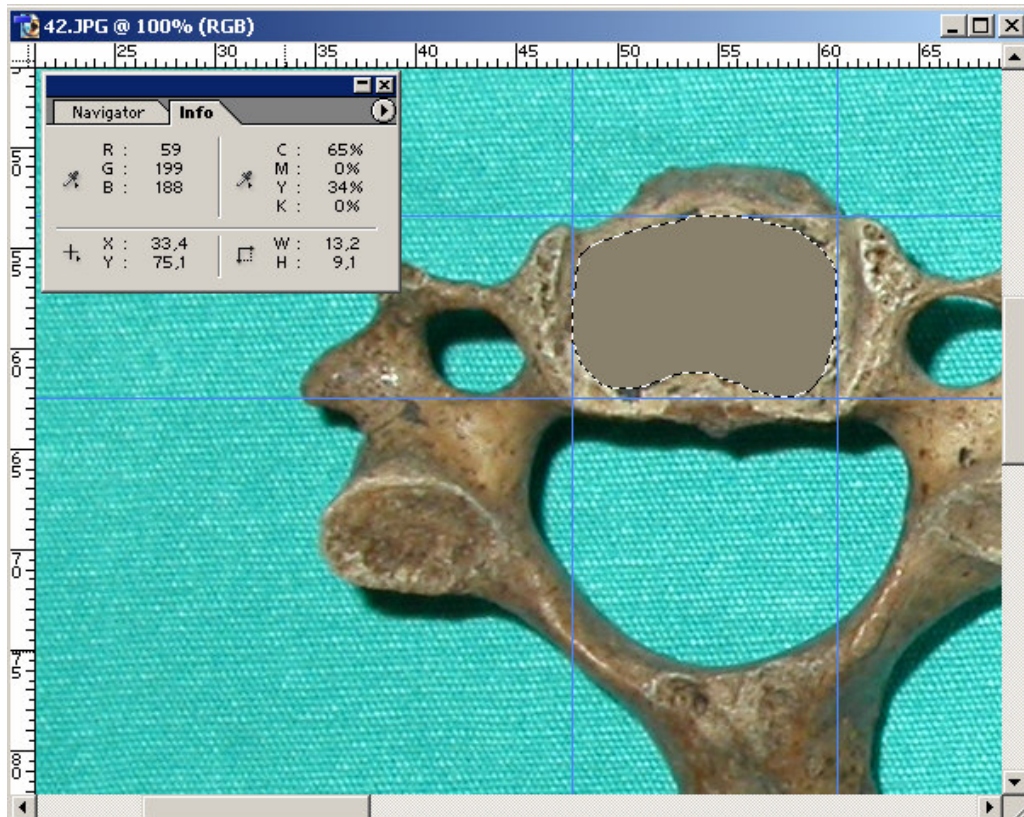Figure A.119. Vertebra number 36a-2.
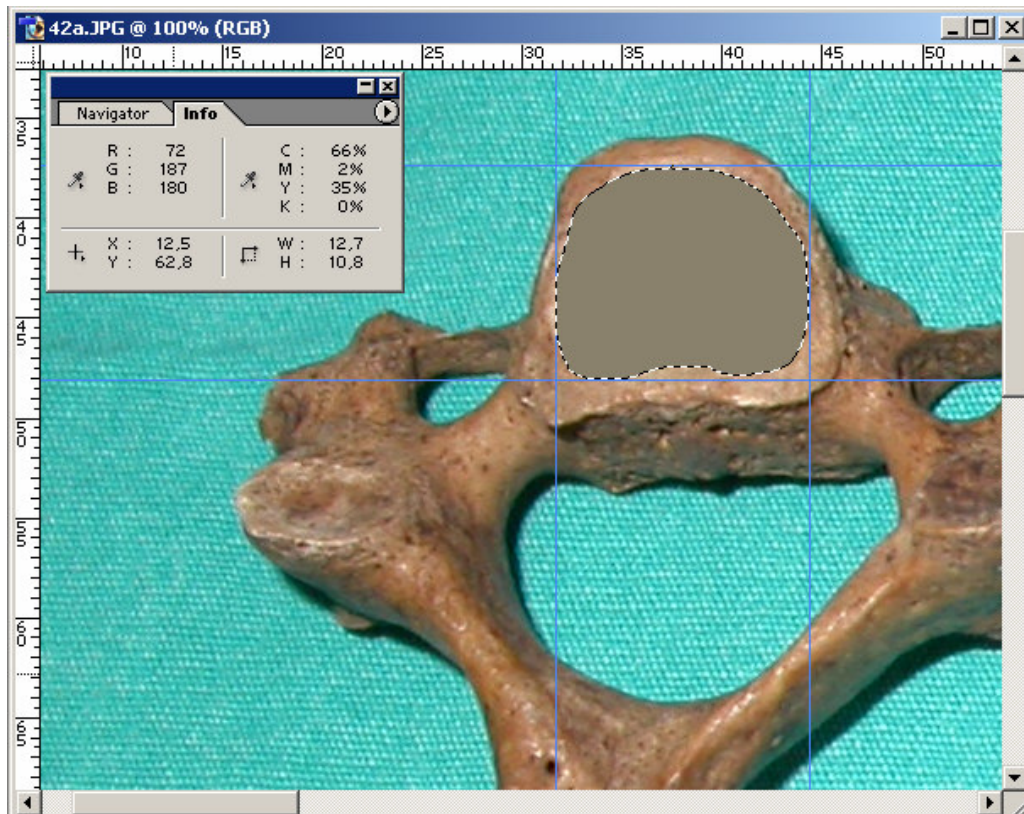
Figure A.120. Vertebra number 37-1.
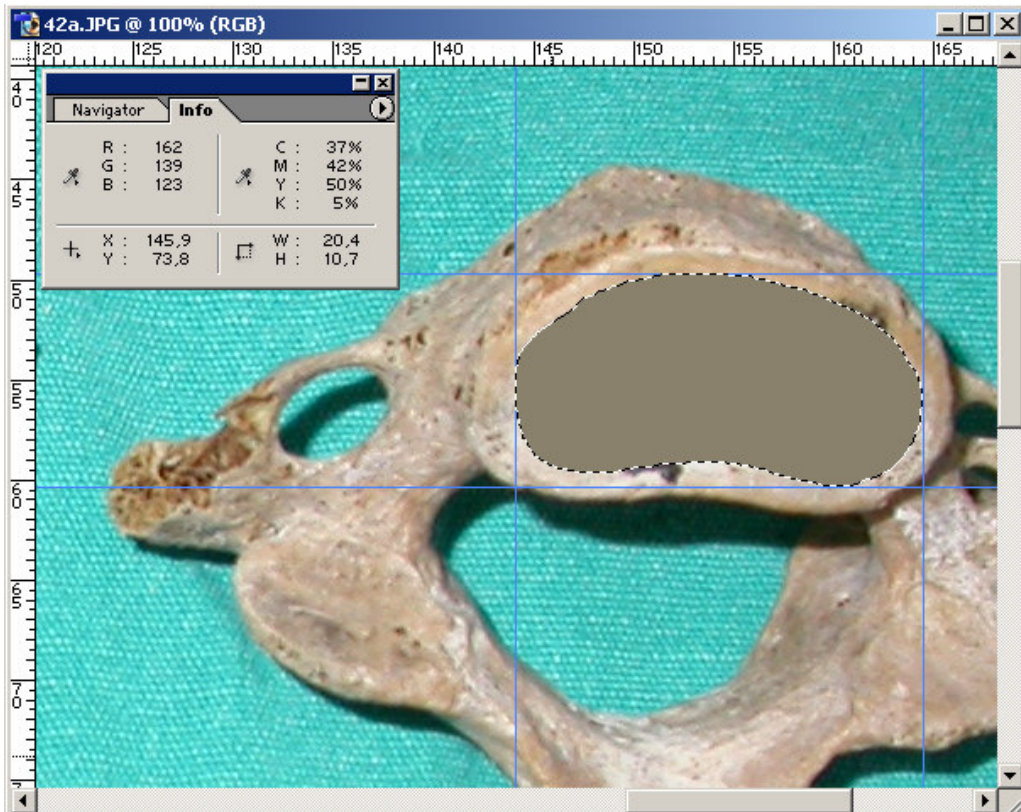

Figure A.121. Vertebra number 37-2.

Figure A.122. Vertebra number 37a-1.

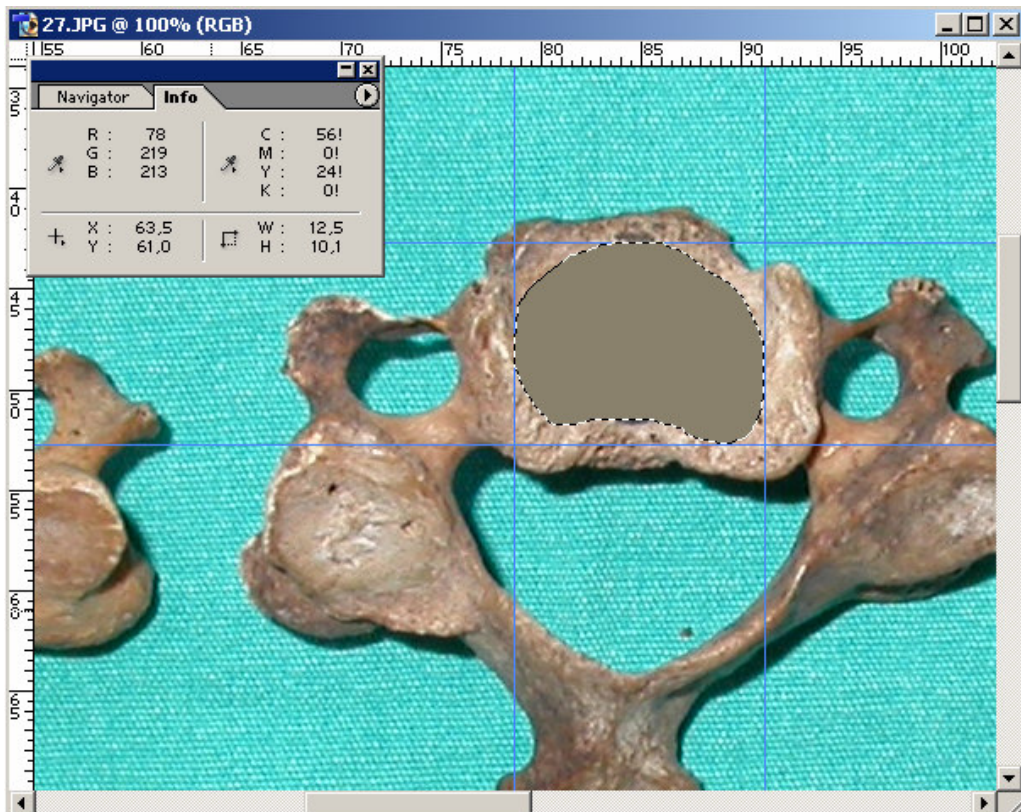
Figure A.123. Vertebra number 37a-2.

APPENDIX B

DIMENSION MEASUREMENT BEFORE AND AFTER THE SINTERING PROCESS

P	T		%50 POROSITY		P	T		%60 POROSITY	
			INITIAL (L*D)	FINAL (L*D)				INITIAL (L*D)	FINAL (L*D)
		4H	25.97X16.08	25.69*15.76			4H	24.31*16.01	24.11*15.86
	1200	6H	27.03X16.09	24.35*15.97		1200	6H	25*16.12	23.46*15.66
400 MPA					400 MPA				
	1300	4H	27.53X16.14	26.77*15.93		1300	4H	26*16.04	25.15*15.57
		6H	26.04*16.08	24.59*15.87			6H	25.02*16.08	23.27*15.69
		4H	25.70X16.12	25.44*15.76			4H	23.94*16.04	23.61*15.81
	1200	6H	24.73X16.12	26.56*15.87		1200	6H	24.81*16.10	23.46*15.84
500 MPA					500 MPA				
	1300	4H	26.45X16.18	25.73*15.62		1300	4H	25.35*16.11	24.25*15.56
		6H	25.42*16.12	24.03*15.92			6H	25.06*16.04	24.04*15.66
		4H	24.17X16.10	23.63*15.78			4H	23.65*16.08	23.24*15.88
	1200	6H	25.77X16.16	25.31*15.98		1200	6H	24.35*16.08	23.46*15.78
600 MPA					600 MPA				
	1300	4H	26.26X16.10	25.69*15.59		1300	4H	24.96*16.09	24.21*15.95
		6H	26.12*16.08	25.69*15.75			6H	24.95*16.05	25.04*15.59
		4H	24.77X16.12	24.61*15.90			4H	24*16.08	23.49*15.82
	1200	6H	24.33X16.16	23.92*15.75		1200	6H	24.25*16.17	23.41*15.97
700 MPA					700 MPA				
	1300	4H	23.48X16.14	23.09*15.66		1300	4H	24.57*16.13	23.91*15.73
		6H	24.55*16.12	26.22*15.58			6H	24.52*16.12	23.55*15.81

Figure B.1. Dimension measurement before and after the sintering process
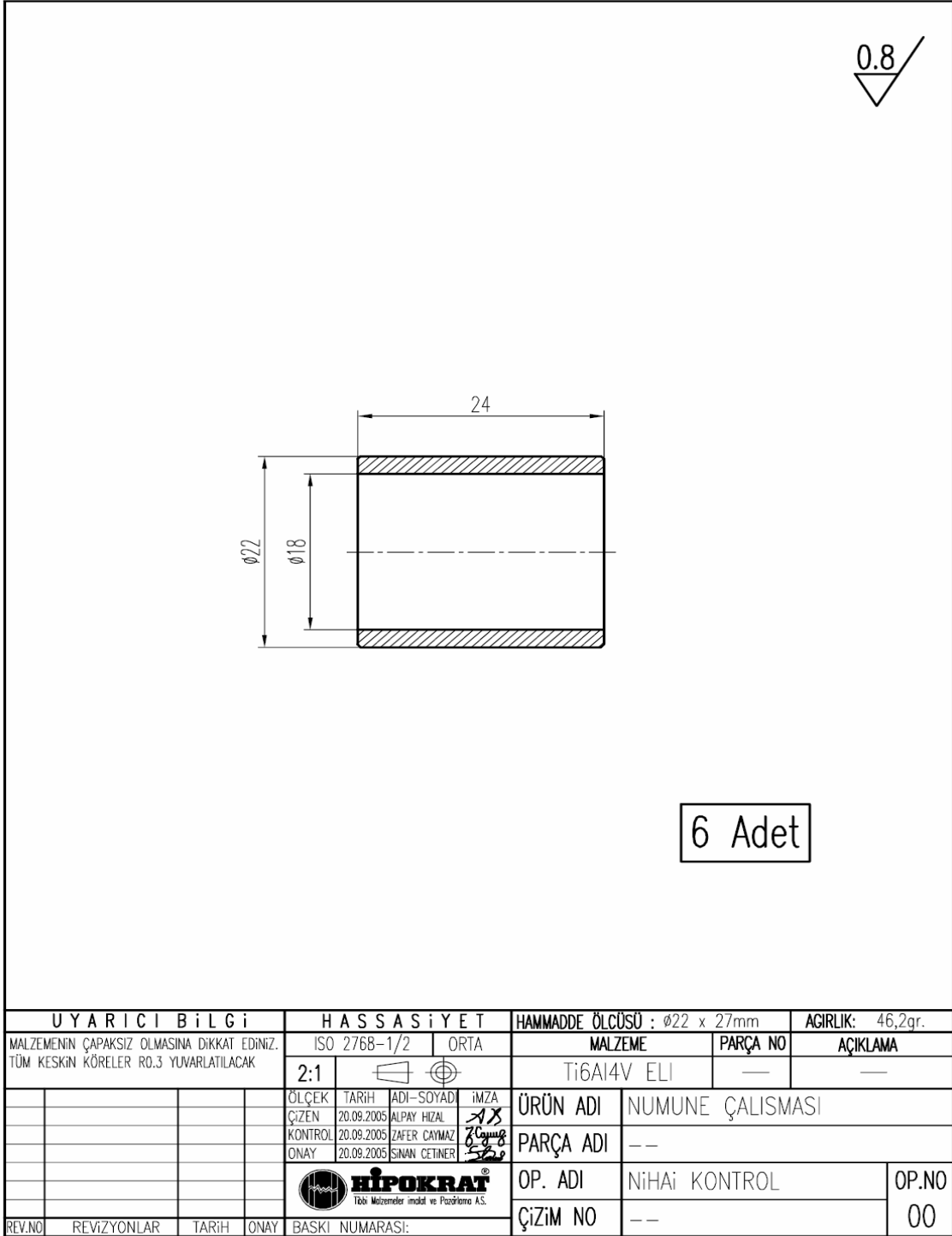
APPENDIX C

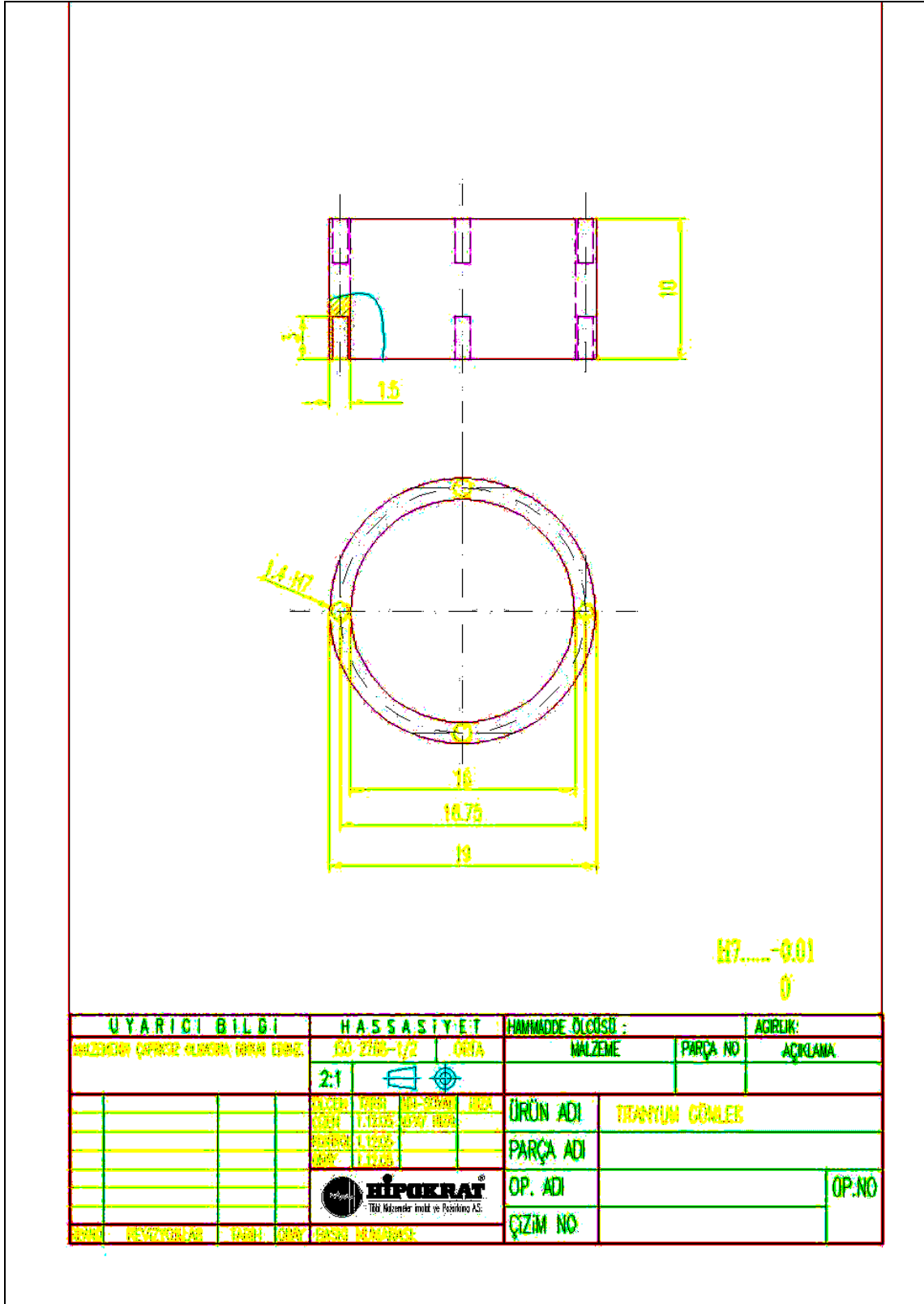# AUTOCAD DRAWINGS

Figure C.1. Protection case Autocad drawing
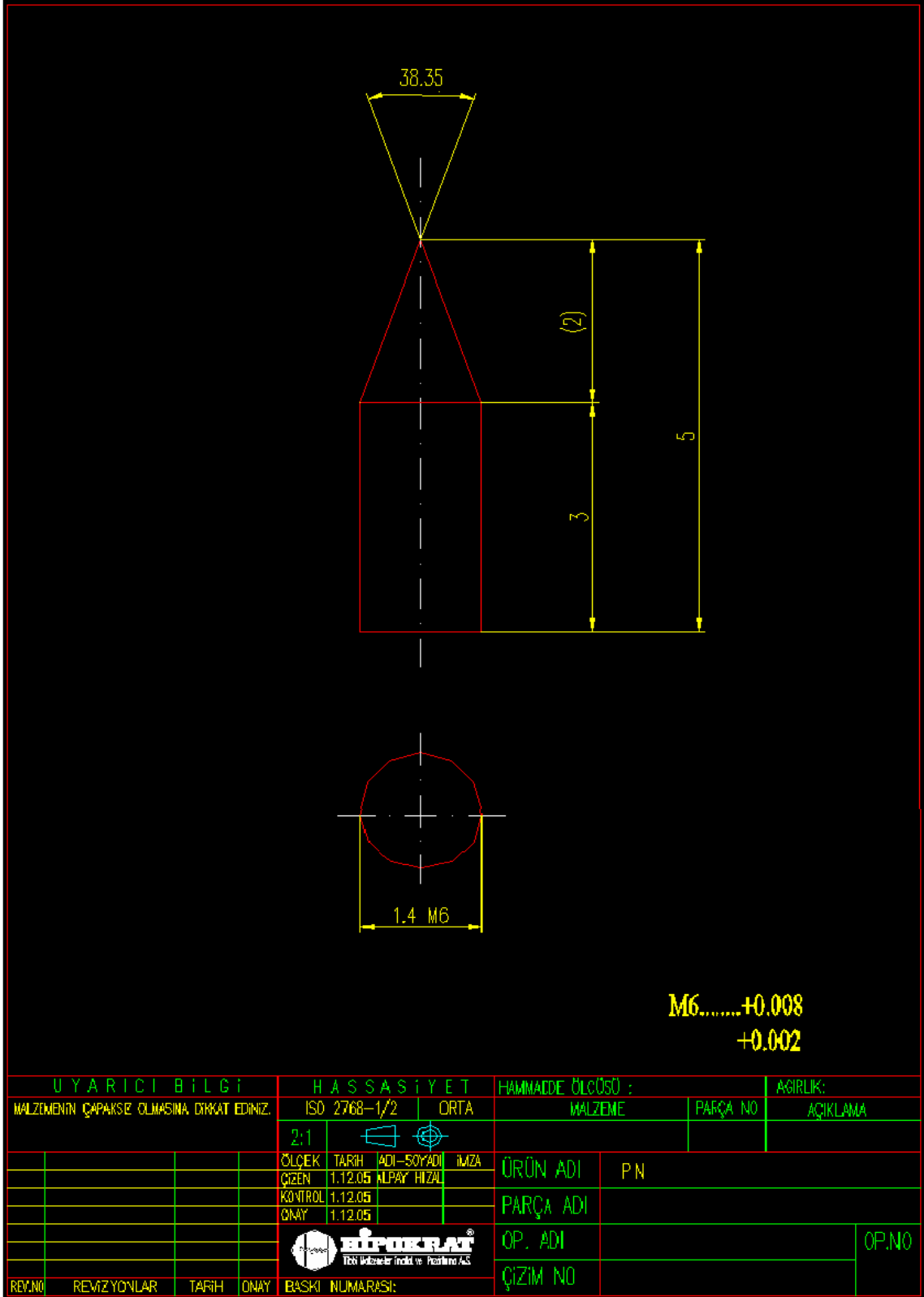
Figure C.2. Protection case Autocad drawing

Figure C.3. Supporting pim Autocad drawing

Figure C.4. Protection case Autocad drawing

APPENDIX D

CALCULATED MULTIPLICATION FACTORS

Image Number	Multiplication Factor	Image Number	Multiplication Factor
8	1.11	24a	7
8a	8.6	25	7.6
9	10.2	25a	7.2
9a	9.5	26	8.6
10	9	26a	7.7
10a	8.8	27	7.4
11	7.8	27a	7.3
11a	7.9	28	8.2
12	7.7	28a	6.6
12a	8	29	6.4
13	8.2	29a	6.6
13a	8	30	6.2
14	8.2	30a	7.1
14a	8	31	6.2
15	7.5	31a	7
15a	9	32	6
16	8.2	32a	6
16a	8	33	6.2
17	x	33a	6.7
17a	x	34	6.2
18	8	34a	6.2
18a	8.2	35	7.4
19	8	35a	7.6
19a	7	36	7.5
20	7.6	36a	6.8
20a	7	37	7.2
21	7.8	37a	7.4
21a	x		
22	x		
22a	x		
23	8		
23a	7.2		
24	8		

Figure D.1. Calculated multiplication factors